



Universiteit  
Leiden  
The Netherlands

## **Spatial and dynamic organization of molecular structures in the cell nucleus**

Brouwer, A.K.

### **Citation**

Brouwer, A. K. (2010, September 8). *Spatial and dynamic organization of molecular structures in the cell nucleus*. Retrieved from <https://hdl.handle.net/1887/15930>

Version: Corrected Publisher's Version

License: [Licence agreement concerning inclusion of doctoral thesis in the Institutional Repository of the University of Leiden](#)

Downloaded from: <https://hdl.handle.net/1887/15930>

**Note:** To cite this publication please use the final published version (if applicable).

# **Spatial and Dynamic Organization of Molecular Structures in the Cell Nucleus**

**Anne – Kee Brouwer**



# Spatial and Dynamic Organization of Molecular Structures in the Cell Nucleus

Proefschrift

ter verkrijging van  
de graad van Doctor aan de Universiteit Leiden,  
op gezag van Rector Magnificus prof. mr. P.F. van der Heijden,  
volgens besluit van het College voor Promoties  
te verdedigen op woensdag 8 september 2010  
klokke 13.45 uur

door

Anne - Kee Brouwer

geboren te Amsterdam

in 1976

## **Promotiecommissie**

Promotor: Prof. dr. H.J. Tanke

Co-promotor: Dr. R.W. Dirks

Commissieleden: Prof. dr. L.H.F. Mullenders

Dr. J.M.J.M. Zijlmans Erasmus Universiteit Rotterdam

Prof. dr. F.C.S. Ramaekers Universiteit Maastricht

The studies described in this thesis were performed at the department of Molecular Cell Biology, Leiden University Medical Center.

Printing of this thesis was financially supported by the J.E. Jurriaanse Stichting.

This thesis was printed by F&N Boekservice, Amsterdam.

# Table of contents

<b>Chapter 1</b>	Introduction and outline of the thesis	9
<b>Chapter 2</b>	STACKS: A software program for particle tracking in living cells	61
<b>Chapter 3</b>	Telomere movement is constrained by interactions with an inner nuclear lamin structure	85
<b>Chapter 4</b>	Telomeric DNA mediates de novo PML body formation	105
<b>Chapter 5</b>	Nuclear body movement is constrained by associations with chromatin	143
<b>Chapter 6</b>	Summary and discussion	165
	Nederlandse samenvatting	175
	Curriculum vitae	179



# **CHAPTER 1**

## **General introduction**





# 1. The cell nucleus

## 1.1 A concise historical perspective

The eukaryotic cell nucleus was first named in 1831 by Robert Brown when he observed an opaque structure in orchid cells. Most likely, he was not the first person who observed the cell nucleus. Already in 1802, it was Franz Bauer who described a structure in plant cells that could reflect the cell nucleus. Also, it is even possible that van Leeuwenhoek was actually the first person who observed the cell nucleus back in 1682 when he studied plant cells. These scientists, however, had no clue about the content and function of this organelle at that time. Knowledge about the constituents and function of the nucleus evolved rapidly after the first isolation of the nucleus in 1869 by Friedrich Miescher (Miescher, 1871). For this isolation he used white blood cells derived from pus, which he treated with a pig-stomach extract and acid. Miescher discovered that the nucleus contains a substance made up of large molecules containing phosphorus and nitrogen which he named 'nuclein'. When the substance was separated into protein and acid molecules it was in 1889 referred to as nucleic acid by a pupil of Miescher, Richard Altmann. It was only since the discovery of the chemical structure of DNA by James Watson and Francis Crick in 1953 that the precise role of this molecule in life became known.

## 1.2 What is inside the cell nucleus?

### 1.2.1 Chromatin

The mammalian nucleus is surrounded by a double membrane and contains sub-compartments that partition macromolecular machineries to facilitate and coordinate the various nuclear functions, including DNA replication, DNA repair, gene transcription, RNA processing, RNA transport and the transduction of intra- and extracellular signals (Stenoien, 2000; Carmo-Fonseca, 2002; Rippe, 2007). Essentially, there are two main compartments that can be distinguished in the cell nucleus, one is the chromosome territory, and the other is the remaining space, called the interchromatin domain (ICD) (Cremer, 2002). The basis for this assumption is the model (for which substantial evidence has been presented) that each chromosome forms a distinct chromosome territory that shows no or little intermingling with neighbouring chromosomes (Manuelidis, 1985). Within a chromosome territory, DNA is folded around octamers of histone proteins forming nucleosomes separated by linker DNA. The resulting "beads on a string" conformation is a platform for other proteins to bind and is collectively called chromatin. This structure is proposed to fold into 30 nm fibers that form, in turn, DNA loop domains (Cook & Brazell, 1976; Paulson & Laemmli, 1977). These DNA loops vary in size from 20 to 200 kb and contain many genes and clusters of functionally related genes. DNA loops are not only thought to be important for gene regulation, but also for the organization of replicons (a region of DNA that replicates from a single origin of replication in the genome). DNA loop anchorage sites were shown to colocalize with replication origins (van der Velden, 1984; Razin, 1986) and DNA loop sizes were shown to correlate with that of the replicons (Buongiorno-Nardelli, 1982; Marilley & Gassend-Bonnet, 1989). DNA loops are suggested to be attached to the nuclear matrix via Loop Anchorage Regions (LARs).

## Introduction

These regions have a rather complex structure and may include several elements, e.g., topoisomerase II binding sites (for review see Razin, 1996; Vassetzky, 2000b). Together, these studies suggest a strict organization principle for chromatin. The reality is, however, that we know very little about the organization of chromatin in the cell nucleus. Even there is debate whether the 30 nm fibre exists in living cells (Maeshima et al., 2010).

Typically, euchromatin is referred to as a transcriptionally active open chromosome structure having ample access to the transcription and RNA processing machinery, while heterochromatin is referred to as a transcriptionally inactive, compact chromatin structure (John, 1988; Felsenfeld & Groudine, 2003). However, these morphological terms do not provoke a very clear functional distinction, as some genes show transcriptional activity in supposed heterochromatic regions (Bühler & Moazed, 2007) and some are silenced in supposed euchromatic regions. Despite some cell type specific variation, heterochromatin is mainly positioned at the nuclear periphery and around nucleoli. It is probably also for this reason that chromatin at the nuclear periphery shows a relatively low transcriptional activity and a low gene density (Boyle, 2001; Finlan, 2008). Transcriptionally competent regions preferentially localize towards the interior of the cell nucleus and to the periphery of chromosomal territories (Verschure, 1999). The status of chromatin is characterized best by the presence or absence of specific histone and DNA modifications, rather than relying on morphological features. Histone modifications associated with transcriptional repression include methylation of histone H3 on Lysine 9 (Steward, 2005) and Lysine 36 (Strahl, 2002), and deacetylation (leading to hypoacetylation) of histone H3 (Grunstein, 1997; Turner, 2000). Histone H3 lysine 9 (H3-K9) methylation creates a specific binding site for heterochromatin protein 1 (HP1), which is targeted there by the methylating enzyme SUV39H1 (Steward, 2005; Krouwels et al., 2005). However, methylated H3-K9 is also able to suppress transcription in absence of HP1 by a mechanism involving histone deacetylation (Steward, 2005).

Methylation is the most common form of alkylation, and in biochemistry it refers to the replacement of a hydrogen atom with a methyl group (CH<sub>3</sub>). In biological systems, DNA methylation is mediated by a conserved group of proteins called DNA (cytosine-5) methyltransferases (Goll & Bestor, 2005). In vertebrates DNA base methylation typically occurs at cytosine-phosphate-guanine sites (CpG sites), DNA regions where a cytosine is directly followed by a guanine in the DNA sequence. This methylation results in the conversion of the cytosine to 5-methylcytosine, and the formation of Me-CpG is catalyzed by the enzyme DNA methyltransferase. CpG sites are uncommon in vertebrate genomes but are often found at higher density near vertebrate gene promoters where they are collectively referred to as CpG islands. The methylation state of these CpG sites can have a major impact on gene activity/expression in somatic cells. In eukaryotes, typically 2-7% of cytosines (bases that are part of the nucleotides which constitute DNA) are methylated, and this methylation is often tissue specific (Razin & Cedar, 1991). Cytosine methylation is common to all large-genome eukaryotes and present in only a few small-genome eukaryotes. Not only is there a clear correlation between gene expression and undermethylation, transfection experiments clearly demonstrated that this modification acts as a repressor of transcription (Razin & Cedar 1991). Tissue-specific genes appear to be methylated in almost all cell types and presumably undergo demethylation when expressed in a specific tissue type. In contrast, housekeeping genes contain CpG islands that are

unmethylated in all cells (Bird, 1986). Both histone and DNA methylation can act as epigenetic markers providing heritable mechanisms for gene silencing (Nakayama, 2001; Grewal & Rice, 2004).

### 1.2.2 The interchromatin domain

The interchromatin domain is inevitably a crowded space since both proteins and RNAs travel through this compartment to reach their destination or exert their function in this compartment. RNA forms together with proteins ribonucleoprotein (RNP) particles, which are thought to form a continuous nuclear network. This structure is the source of the RNP particles that are released from the nucleus by chemical or mechanical extraction (Smetana, 1963). RNA-selective staining procedures have made a complete ultrastructural characterization of the nuclear RNP network possible (Bernhard, 1969; Biggiogera & Fakan, 1998). Making use of EDTA regressive staining to localize RNA, Monneron & Bernhard were able to define, characterize and classify the interconnected nuclear RNP structures and distinguished interchromatin granule clusters, perichromatin fibrils, perichromatin granules and coiled bodies (Monneron & Bernhard, 1969). The discovery of these structures was important for our understanding of nuclear RNA metabolism (Misteli & Spector, 1998; Misteli, 2000). Perichromatin fibrils are sites of RNA transcription (Bachellerie, 1975; Cmarko, 1999), whereas interchromatin granule clusters (or speckles) play a central role in the assembly and/or modification of pre-mRNA splicing factors (Mintz, 1999; Smith, 1999; Spector, 2001).

To ensure unimpeded exchange of molecules between the nucleus and the cytoplasm, the ICD has direct access to nuclear pores. Nuclear pores are multiprotein complexes embedded in the nuclear envelope, which mediate and regulate nucleocytoplasmic transport (Vasu & Forbes, 2001; Fahrenkrog & Aebi, 2003). The 'basket' structure at the nucleoplasmic side of the nuclear pore consists of eight filaments, which attach to a distal 'ring' structure. Several reports suggest that these 'rings' connect to filaments that extend into the nucleus and facilitate nucleocytoplasmic transport (Cordes, 1993; Parfenov, 1995; Cordes, 1997).

### 1.2.3 Chromatin organization is dynamic.

It has been hypothesized that the spatial arrangement of the genome in the interphase nucleus is an important factor in the regulation of gene activity (Zink, 2004) and possibly also in orchestrating DNA replication and DNA repair. Gene loci positioned megabases apart on the same or even different chromosomes were shown to interact, suggesting that some genes are spatially positioned together in a microenvironment to coordinate their transcription and/or to facilitate the processing of their RNA transcripts (Branco & Pombo, 2006; Lonard & O'Malley, 2008). Although it is a proven fact that the cell nucleus is an ordered and structured compartment, the same structure is highly dynamic to regulate key functions such as transcriptional activity in response to signaling events and differentiation. In particular, fluorescence in situ hybridization and the application of chromosome conformation capture techniques, or a combination of both, provided important insight in the existence and dynamics of long-range

## Introduction

chromatin-chromatin interactions (Dekker, 2006). Also the positioning of specific chromatin regions at particular nuclear bodies are examples supporting the notion that the genome is not randomly organized in the cell nucleus (Smith, 1995). The challenge now is to unravel the underlying mechanisms that establish and maintain this non-random organization of chromatin in the cell nucleus.

Understanding the organization principles of the nucleus is important because rearrangements in nuclear organization have been observed in cells derived from various diseases, including cancer, and in cells with a senescent or apoptotic phenotype (Vijg & Dollé, 2002; Busuttil, 2004; Raz, 2008; Shin et al., 2010). Furthermore, a striking change in nuclear organization has been observed in embryonic stem cells at the onset of differentiation (Butler et al., 2009). Most profound rearrangements in chromatin structure have been observed when a sperm pronucleus and an egg nucleus fuse after fertilization. In many species, the size of DNA loops increases from ca. 50 kbp in early embryogenesis to 200 kbp in cells of the adult organism (Buongiorno-Nardelli, 1982). Notably, the average size of DNA loops was observed to decrease in transformed cells (Linskens, 1987). In several human cancer cell lines the DNA loop size was found to be about 50 kbp, i.e. significantly smaller than in normal cells where it varies between 70-700 kbp (Oberhammer, 1993). It is important to unravel the mechanisms that control these aspects of nuclear organization to understand their impact on the etiology, progression, and possibly treatment of human diseases. Once understood, the hope is that this new knowledge might open possibilities for treatment strategies of human disease.

### 1.3 Nuclear bodies

In addition to soluble components, the interchromatin domain (ICD) contains different kinds of subcompartments or nuclear bodies that vary in size, composition and function (Figure 3; Tsutsui, 2005). Unlike the organelles present in the cytoplasm, nuclear bodies are not surrounded by a membrane structure. Therefore, it is still an open question how these bodies assemble and maintain their unique protein constellation. It came more or less as a surprise that most if not all proteins that reside in bodies are in a dynamic equilibrium with their surroundings (Misteli, 2001). A few of these proteins have been reported to shuttle between various bodies (Snaar, 2000; Olson, 2004). Thus far, up to twelve different types of bodies have been identified, which are either permanently or temporally present in the cell nucleus depending on the physiological state of the cell (Spector, 2001). The most prominent nuclear bodies are discussed below.

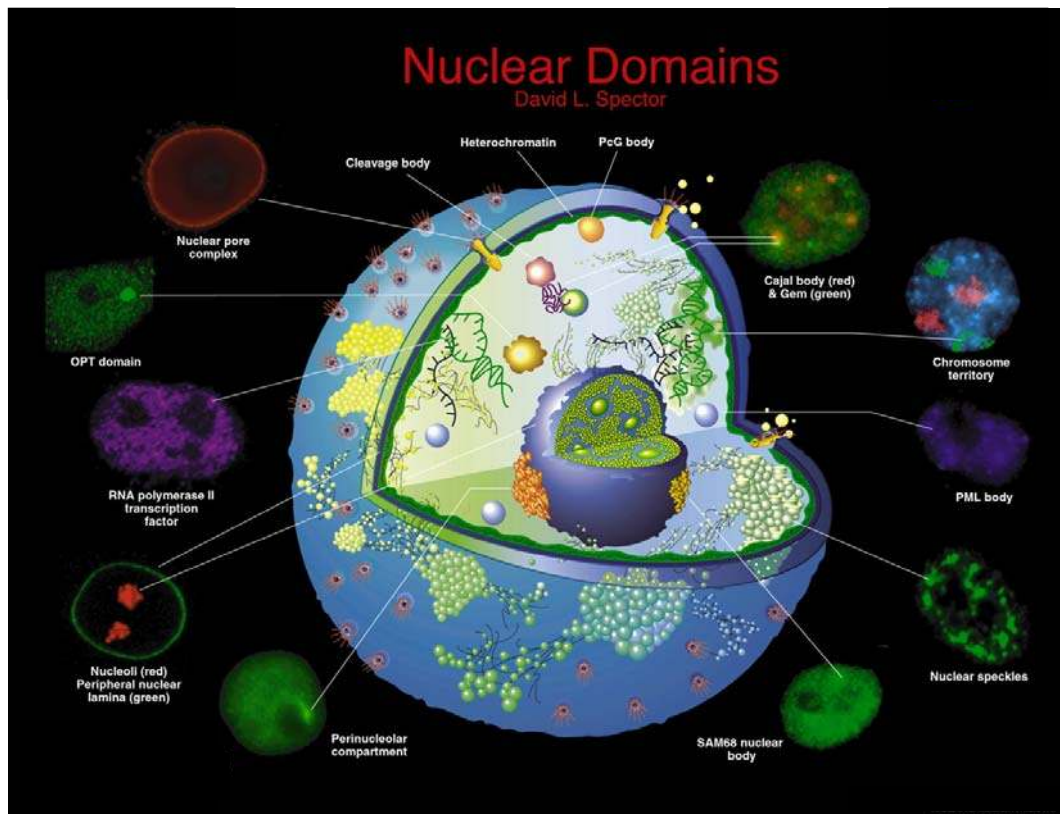


**Figure 3. Protein domains present in the mammalian cell nucleus.**

OPT domains: transcriptionally active sites that contain a specific set of transcription factors and RNA pol II, appear close to nucleoli in G1. Nuclear pore complex: multiprotein complexes where the inner and outer nuclear membranes are fused and where materials can transit between the cytoplasm and the nucleus. Cleavage body: either overlap or are localized adjacent to Cajal bodies, they consist of factors involved in the cleavage and polyadenylation steps of pre-mRNA processing. Heterochromatin: inactive chromatin. PcG body: have been found to be associated with pericentric heterochromatin (Saurin, 1998) and contain polycomb group proteins (i.e. RING1, BMI1 and hPc2). Gems: Gemini of Cajal bodies, they have been found adjacent to or coinciding with Cajal bodies. Gems are characterized by the presence of the survival of motor neurons gene product (SMN) and an associated factor, Gemin2 (Matera, 1999). SAM68 nuclear bodies/ Perinucleolar compartments (PNC): have been identified as unique structures that are associated with the surface of nucleoli and are thought to play a role in RNA metabolism (Huang, 2000). Both structures are predominantly found in cancer cells and they are rarely observed in primary cells. Other nuclear bodies are discussed in the text. (Adapted from Spector, 2001)

### 1.3.1 Nucleolus

The nucleolus was one of the first subcellular structures that were identified by early users of the light microscope (Montgomery, 1898). Nucleoli appeared as highly refractive black dots in the nucleus of cells, reflecting its dense protein content. The nucleolus is a dynamic multifunctional nuclear domain where ribosomal RNA is synthesized and the ribosomal subunits are assembled (Olson, 2002). Using mass spectrometry, up to 700 human proteins have been characterized in purified nucleoli

## Introduction

and up to 30% of these proteins are encoded by previously uncharacterized genes (Andersen, 2002; Andersen, 2005). Although it is not expected that all proteins found in nucleoli also have a function in this structure, their diversity is consistent with the idea that the nucleolus performs additional roles beyond generating ribosomal subunits (Pederson, 1998; reviewed by Olson, 2002). For example, many proteins related to cell cycle regulation (about 3.5% of the identified proteome), DNA damage repair (about 1%) and pre-mRNA processing (about 5%) have been identified in isolated nucleoli. Nucleoli have therefore been implicated in processes such as cell cycle regulation (Yamauchi, 2007), virus-replication (Jacob, 1968), regulation of tumor suppressor and oncogene activities (Itahana, 2003), DNA damage repair (van den Boom, 2004), signal recognition particle assembly (Jacobson & Pederson, 1998), RNA modification (Sansam, 2003), tRNA processing (Paushkin, 2004), aging by modulating telomerase function (Kieffer-Kwon, 2004; Zhang, 2004), regulation of protein stability (Mekhail, 2004; Rodway, 2004), senescence (reviewed by Comai, 1999; Rosete, 2007) and apoptosis (Baran, 2003). In addition, nucleoli are thought to play a role in the maturation and transport of mRNAs (Schneiter, 1995).

A possible function of the nucleolus in mRNA export was proposed 25 years ago based on observations in interspecies heterokaryons obtained from fusing chicken erythrocytes with mouse cells. It was observed that in the dormant chicken nucleus gene expression was initiated at precisely the same time when a nucleolus became detectable (Sidebottom & Harris, 1969; Deák, 1972; Harris, 1972). Furthermore, it was observed that UV irradiation of the chicken nucleolus in these heterokaryons greatly suppressed chicken-specific gene expression (Perry, 1961; Deák, 1972). Additional support for a role of nucleoli in mRNA export came by the observation that processed *myc* and *myoD* transcripts, unlike actin or lactate dehydrogenase transcripts, are present in the nucleolus of several cell types (Bond & Wold, 1993). Because *myc* intron 1-containing pre-mRNA was not detected in nucleoli but instead in the nucleoplasm, it was suggested that the nucleolar localization of Pol II transcripts is a general phenomenon for transcripts that have a rapid cytoplasmic turnover only (Bond & Wold, 1993). It should be noted, however, that these observations have thus far not been confirmed by others. In cells derived from species that vary from sea urchins to humans, nuclear poly(A)<sup>+</sup> RNA is found present primarily in discrete "transcript domains", which often concentrate around nucleoli (Carter, 1991). Thus, whether nucleoli are involved in some steps of nuclear mRNA export has yet to be confirmed.

### 1.3.2 Cajal bodies

Cajal bodies are spherical nuclear bodies that are generally present in dividing cells and in cells that show high transcriptional activity. They are prominently present in most tumor cells, which rapidly proliferate, and in neurons that are metabolically active (Cajal, 1903; Ogg & Lamond, 2002). They were first reported in 1903 by the Spanish cytologist Ramón y Cajal who named them "nucleolar accessory bodies", because of their prominent association with nucleoli in neuronal cells (Cajal, 1903). Cajal bodies were subsequently rediscovered by numerous researchers and given a variety of names in different cell types (Gall, 2000). The name "coiled body" was coined by electron microscopists, referring to their morphology in EM sections. It was not

until 1999 that Joseph Gall suggested to link Cajal's name to the nuclear body that was originally described by him in 1903 (Gall, 1999). The number and size of Cajal bodies varies among cell types (in mammalian cells typically 0–10 per nucleus, ranging 0.1–2  $\mu\text{m}$  in diameter) and they also show cell cycle variation within cell types. Cajal bodies can be discriminated in the nucleus by the presence of the protein coilin, either by immunocytochemistry or by exogenous expression of coilin-GFP (Snaar, 2000; Ogg & Lamond, 2002).

Recent studies indicated that Cajal bodies play a role in the assembly and/or modification of the transcription and RNA-processing machinery (Gall, 1999; Jády, 2003). Cajal bodies are enriched in snRNPs (small nuclear ribonucleoproteins) and snoRNPs (small nucleolar ribonucleoproteins) spliceosome subunits. Solid evidence has been provided that the final steps in snRNP maturation including snRNA base modification, U4/U6 snRNA annealing, and snRNA-protein assembly of both snoRNAs and snRNAs occur in Cajal bodies (Darzacq, 2002; Verheggen, 2002; Jady, 2003; Stanek, 2008). Despite their role in splicing factor maturation, Cajal bodies do not represent major sites of transcription *per se*, but they were observed frequently in association with a few specific genes coding for small nuclear snRNAs and histone genes in interphase cells. Because Cajal bodies do not contain either DNA (Thiry, 1994) nor non-snRNP protein splicing factors (Raska, 1991; Carmo-Fonseca, 1992) it is unlikely that these bodies are sites of transcription or pre-mRNA splicing. Thus, the current view is that Cajal bodies play a crucial role in the spliceosome cycle in which the production of new snRNPs is promoted by the import and modification of substrates (reviewed by Staněk & Neugebauer, 2006). In addition, Cajal bodies may play a role in the recycling of snRNPs from splicing complexes that are released after finishing pre-mRNA splicing. Interestingly, also the RNA subunit (hTR) of the enzyme telomerase was shown to accumulate in Cajal bodies (Jady, 2004; Zhu, 2004). During the S-phase, when telomerase is likely to act, hTR has been found to associate with a subset of telomeres while Cajal bodies are present at close distance (Jady, 2006; Tomlinson, 2006). Mutant hTR, which fails to accumulate in Cajal bodies, was fully capable of forming catalytically active telomerase *in vivo*. Telomere extension, however, turned out to be strongly impaired (Cristofari, 2007). This functional deficiency was accompanied by a decreased association of telomerase with telomeres suggesting that Cajal bodies also play an important role in telomere elongation.

### 1.3.3 Speckles

Speckles, also referred to as SC35 domains or interchromatin granule clusters (IGC), are thought to be storage sites of factors involved in mRNA synthesis, splicing, and RNA export (Dirks, 1999; reviewed by Lamond & Spector, 2003). The prevailing view is that splicing factors are recruited from speckles to sites of active transcription (Dirks, 1997; Misteli, 1997). At the electronmicroscopical level of resolution, IGCs range in size from one to several micrometers in diameter and are composed of 20–25-nm granules that are connected by thin fibrils, resulting in a beaded chain appearance (Thiry, 1995). Other splicing factor containing structures in the nucleus are perichromatin fibrils, Cajal bodies and interchromatin-granule-associated zones, also referred to as paraspeckles (Visa, 1993). Speckles, however, can be easily discriminated from these structures by their morphology and protein content and are pre-



## Introduction

sent throughout the nucleoplasm in regions that contain little or no DNA (Thiry, 1995). Furthermore, *in situ* hybridization studies revealed that speckles do not contain genes. Instead, active transcription sites were found positioned throughout the nucleoplasm and also next to speckles. Some genes have been reported to localize preferentially close to speckles (Huang, 1991; Xing, 1993; Xing, 1995; Smith, 1999; Johnson, 2000).

These observations indicate that speckles are functionally related to gene expression. Hall and coworkers proposed that speckles are hubs that spatially link the synthesis of specific pre-mRNAs to a rapid recycling of copious RNA metabolic complexes, thereby facilitating expression of many highly active genes (Hall, 2006). In addition to increasing the efficiency of each step, sequential steps in gene expression might be structurally integrated at each speckle, consistent with evidence that the biochemical machineries for transcription, splicing, and mRNA export are coupled (Hall, 2006). The observation that speckles also contain poly(A)<sup>+</sup> RNA led to the suggestion that speckles play a role in RNA metabolism and export (Carter, 1991, 1993; Molenaar, 2004). A substantial amount of mature mRNA is found to be retained in nuclear speckles until ATP is added, suggesting that speckles prevent the export of otherwise fully processed mRNAs until an energy-requiring cellular signal releases them (Schmidt, 2006).

### 1.3.4 PML bodies

The most mysterious of all nuclear bodies is the PML body, also known as ND10 (nuclear domain 10) or Kremer bodies (Kr) (Dyck, 1994; Koken, 1994; Weis, 1994). Promyelocytic leukemia bodies (PML bodies) are nuclear protein bodies, ranging in size from 0.3  $\mu\text{m}$  to 1.0  $\mu\text{m}$  in diameter and are characterized by the presence of the PML protein. Typically there are 10-20 PML nuclear bodies (PML-NB) present in the cell nucleus and they are believed to be tightly associated with nuclear matrix proteins (Stuurman, 1992). Electron microscopy studies have shown that PML-NBs are composed of a ring-like protein structure that does not contain nucleic acids in the centre of the ring (Boisvert, 2000; Dellaire & Bazett-Jones, 2004). At the periphery of the ring, however, PML-NBs are believed to make extensive contacts with chromatin fibers through protein-based threads that extend from the core of the bodies (Eskiw, 2004). These contacts have been proposed to be essential for maintaining the integrity and positional stability of PML-NBs in the nucleus.

PML bodies were originally characterized using human auto-antibodies derived from patients with primary biliary cirrhosis (Bernstein, 1984; Szostecki, 1990; Maul, 2000). Using such antibodies, Bernstein *et al.* described in 1984 the presence of certain typically speckled structures, which later came to be known as nuclear domain 10 (ND10), PML bodies, or PODs. PML bodies, however, were first named after examining cells derived from patients with acute promyelocytic leukemia (APL) (de The, 1991). Most APL patients carry the chromosomal translocation t(15,17), resulting in a fusion protein between the retinoic acid receptor- $\alpha$  (RAR) and the PML protein (de The, 1991; Melnick & Licht, 1999). The PML-RAR $\alpha$  fusion protein fails to locate to PML bodies (Melnick & Licht, 1999) and is thought to block differentiation of bone marrow cells (Naeem, 2006). In addition, the leukemic blast cells of APL patients reveal fragmented or dispersed PML bodies. Treatment of APL patients with all-trans-

retinoic acid or arsenic trioxide results in the degradation of the PML-RAR $\alpha$  fusion protein, restoration of PML bodies and remission of the disease (Koken, 1994; Weis, 1994). Recently, it has been shown that arsenic-induced degradation of PML or PML-RAR $\alpha$  is mediated by the ubiquitin ligase RNF4 (Lallemand-Breitenbach, 2008; Tatham, 2008).

In PML bodies, nearly eighty different proteins have been found present. Among them are Sp100, Sp140, SUMO-1, HAUSP (USP7), CBP and BLM, Daxx, pRB, and p53 (Hodges, 1998; LaMorte, 1998; Alcalay, 1998; Zhong, 1999; Zhang, 1999; Zhong, 2000; for a review see Salomoni & Pandolfi, 2002). Because of this variety of proteins, PML bodies have been implicated in many different functions, such as transcription regulation, protein storage, senescence and interferon-induced antiviral defense (Chelbi-Alix, 1995; Maul, 1998). Concerning transcription regulation, PML bodies have been suggested to be involved in both transcriptional activation (Maul, 1998; Zhong, 2000) and transcriptional repression (Everett, 1999). However, whether PML bodies play indeed an essential role in transcription is not clear since PML<sup>-/-</sup> mice show a very moderate phenotype. PML<sup>-/-</sup> mice are morphologically normal and do not have higher rates of spontaneous cancers than littermate controls (Wang, 1998a; Wang, 1998b). Some regions of the human genome that display high transcriptional activity do, however, associate frequently with PML NBs, although RNAi-mediated knockdown of PML did not perturb the expression of these genes (Wang, 2004).

PML bodies have also been implicated in DNA damage repair as several repair factors transit through PML bodies in a temporally regulated manner (Graham & Bazett-Jones, 2004). Furthermore, PML bodies have been shown to recruit single-stranded DNA (ssDNA) molecules in response to exogenous DNA damage (Bøe, 2006). PML bodies are also associated with the sites of initial viral DNA transcription/ replication in virus infected cells (Maul, 1996; Maul, 1998; Guldner, 1992; Stadler, 1995). PML bodies are subsequently disrupted at later stages in the infectious viral cycle (Maul, 1993). Upon treatment of cells with interferon, PML is induced and the number of nuclear bodies increases dramatically (Lavau, 1995; Gaboli, 1998). This suggests a role for PML and the nuclear bodies as part of the anti-viral defense machinery activated by interferons in viral infections. DNA and RNA viruses have a variety of effects on PML body morphology, where arenaviruses and the human immunodeficiency virus (HIV) transport PML to the cytoplasm, and herpesviruses “unwind” PML bodies (Borden, 1998; Melnick & Licht, 1999; Maul, 2000; Turelli, 2001). However, findings with HIV infected cells are somewhat controversial, since another group did not see PML NBs translocate during infection (Bell, 2001).

It has been established that PML is the primary essential component of PML NBs, and conjugation of SUMO-1 to PML is suggested to be a prerequisite for PML body formation (Ishov, 1999; Zhong, 2000). PML SUMOylation likely plays a regulatory role in the structure, composition, and function of PML bodies (Sternsdorf, 1997). Elegant studies demonstrate that the RING domain of PML directly interacts with Ubc9, an enzyme which covalently attaches the SUMO1 protein onto distal regions of PML, including one B-box and a region near the nuclear localization signal (Duprez, 1999).

## Introduction

It has been demonstrated that PML contains a SUMO binding motif that is independent of its SUMOylation sites and is required for PML-NB formation. A model for PML-NB formation was proposed in which PML SUMOylation and noncovalent binding of PML to SUMOylated PML through the SUMO binding motif constitutes the nucleation event for subsequent recruitment of SUMOylated proteins and/or proteins containing SUMO binding motifs to the PML NBs (Shen, 2006).

Alternatively, PML bodies may have the ability to self-assemble. Purified RING-domains (small zinc-binding domains) of PML and other proteins have been shown to self-assemble into supramolecular structures *in vitro* that resemble the structures they form in cells (Kentsis, 2002). Over-expression of SUMO-1 prevented the stress-mediated breakdown of PML bodies, indicating that PML body stability is partially dependent on SUMO-1 (Eskiw, 2003). Interestingly, many of the proteins found in the PML NBs have been shown to be SUMOylated (Seeler & Dejean, 2003).

Like PML bodies, also the PML protein has been implicated in different cellular functions including suppressing cell growth and cell transformation (Mu, 1994; Ahn 1995; Koken, 1995; review: Melnick & Licht 1999). Transduction of APL patient derived NB4 cells with a retrovirus harboring the coding sequence for PML suppressed the ability of these cells to form colonies in soft agar. In addition, conditioned medium from these cells suppressed colony formation of wild-type NB4 cells, suggesting the release of negative growth control factors (Mu, 1994). Furthermore, PML-overexpressing NB4 cells, when injected into nude mice, yielded smaller tumors that appeared with a longer latency than vector-expressing cells (Mu, 1994). In various human tumors, PML expression was shown to be decreased (Gurrieri, 2004a) and in some cases it was shown that low levels of PML correlated with poor disease outcome (Chang, 2007). Consistent with a role as tumor suppressor, it has been reported that overexpression of PML suppresses the growth of various cancer cells (Liu, 1995; Mu, 1997; Le, 1998). Also, PML knockout mice revealed an increased susceptibility to chemical-induced carcinogenesis (Wang, 1998a) and spontaneous tumorigenesis (Trotman, 2006).

Probably one of the most important functions of PML is to control apoptosis. The physiological relevance of this is emphasized by *in vivo* studies demonstrating that mice and cells that lack PML are resistant to a vast variety of apoptotic stimuli (Wang, 1998a). Although the molecular mechanism remains largely unknown, PML is thought to be a pivotal factor in  $\gamma$  irradiation-induced apoptosis (Wang, 1998a) and essential for the induction of programmed cell death by Fas, tumor necrosis factor  $\alpha$  (TNF), ceramide and type I and II interferons (IFNs) (Wang, 1998a; Quignon, 1998). In support of these thoughts, PML<sup>-/-</sup> mice and PML<sup>-/-</sup> cells are resistant to the lethal effects of  $\gamma$ -irradiation (Wang, 1998a; Yang, 2002).

## 2. The nuclear matrix

### 2.1 Evidence for a nuclear matrix structure?

For more than 30 years it has been hypothesized that the mammalian cell nucleus contains a filamentous framework, referred to as nuclear matrix or karyoskeleton, which provides structural support to the various nuclear components and a framework for all

nuclear activities. It is the observation that nuclei withstand strong hydrodynamic shear force, compression and friction during cell or tissue homogenization as well as extreme osmotic pressure that prompted scientists to believe in a nuclear matrix structure (Maggio, 1963a; Penman, 1966; Blobel & Potter, 1966; Dounce, 1995; Pederson 1997). The term 'nuclear matrix' was first used in 1974 to describe a filamentous structure that remained present when cell nuclei were salt extracted using 1.0- 2.0 M NaCl (Berezney & Coffey, 1974). Numerous studies followed since, using variations on extraction protocols until proteins, RNA- and DNA-sequences were all shown to be connected to the nuclear matrix (Berezny & Jeon, 1995). Interestingly, Jackson and Cook observed in 1988 an extensively anastomatized nuclear network of filaments after performing nuclear extractions of cells that were encapsulated in agarose spheres (Jackson & Cook, 1988). This network is believed to resemble the filamentous structure that remains present after a high ionic strength extraction of the nucleus (Capco, 1982). Many studies found 3-5 and 10-30 nm ribonucleoprotein elements/filaments remaining present in the nucleus after extraction using RNP-depleted and RNP-containing resinless electron microscopy (resin is an embedding material that scatters electrons in a similar way as the embedded specimen does) or whole mount electron microscopy (Monneron & Bernhard, 1969; Berezney & Coffey, 1974; Comings & Okada, 1976; Capco, 1982; Small, 1985; Fey, 1986; Jackson & Cook, 1988). RNP filament domains are thought to be very important for nuclear matrix organization and for some time it was not possible to remove chromatin from the nucleus without removing the RNP filament domains as well (Fey, 1986).

These ultrastructural studies of sectioned cell nuclei did, however, not confirm the presence of a filament system that was thought to comprise the nuclear matrix *in situ*. In fact enormous doubt was raised concerning the procedures used to extract cell nuclei could possibly reveal the nuclear matrix structure that may exist *in vivo*. All nuclear matrix preparation procedures used thus far involved harsh treatments, including the removal of nucleic acids, heat (Mirkovitch, 1984; Martelli, 1991), Cu<sup>2+</sup> (Mirkovitch, 1984; Neri, 1997), sulfhydryl cross-linking (Kaufmann & Shaper, 1984), and highly concentrated monovalent salts such as 2 M NaCl (Berezney & Coffey, 1977). Significantly, it has been noted that such treatments themselves result in protein rearrangements and protein aggregations (Palade & Siekevitz, 1956; Tashiro, 1958; Madison & Dickman, 1963; Lothstein, 1985). Also, protein-protein interactions and van der Waals forces between proteins and water change profoundly when high ionic strength is used (Kauzmann, 1959; Varshavsky & Ilyin, 1974), which is true for most standard nuclear matrix preparation procedures. Consequently, such artificially introduced protein filaments might easily be interpreted as a nuclear matrix structure (Finkelstein, 1997). The existence of a nuclear matrix still needs to be confirmed by other techniques, like for example live cell imaging and RNA interference.

Many who did not believe in the existence of the nuclear matrix became converted by the idea that ribonucleoproteins are functionally integrated elements of the nuclear architecture. Several groups reported pre-mRNA and splicing-intermediates to be retained in RNP-containing nuclear matrix preparations (Ben Ze'ev, 1982; Ciejek, 1982; Mariman, 1982; Ross, 1982; Gallinaro, 1983; Ben Ze'ev & Aloni, 1983). Also, several studies showed that the hyperphosphorylated form of the largest subunit of RNA polymerase II is associated with nuclear sites that are rich in pre-mRNA splicing factors, and importantly, are retained in nuclear matrix preparations (Mortillaro 1996, Vincent 1996). Hyperphosphorylation of RNA polymerase II is functionally linked to the most

## Introduction

active form of this enzyme (Dahmus, 1996). Taking all this evidence into account it can be concluded that it is very likely that there is a nuclear matrix, but still further research is necessary to precisely define its components.

Recent advances in the study of the protein composition of the nuclear matrix allowed the characterization of several proteins that are specifically associated with the nuclear matrix in tumor cells (Konety & Getzenberg, 1999). Some of these proteins are used for the diagnosis of cancer; e.g., NMP22 is specifically present in the nuclear matrix of bladder cancer cells (Ozen, 1999). Hence, detecting changes in the nuclear matrix structure may serve as a valuable tool in cancer diagnostics.

## 2.2 The nuclear lamina

The nuclear envelope is a double-layered membrane that encloses the contents of the nucleus during most of the cell's lifecycle and forms a boundary between chromosomes and the cytoplasm in eukaryotic cells. The main components of the nuclear envelope are the inner nuclear membrane, the outer nuclear membrane, which is continuous with the endoplasmic reticulum, and the nuclear pore complexes (Stuurman, 1998; Goldman, 2002). On the inner surface of the nuclear membrane, the nuclear lamins (type-V intermediate filaments) are polymerized to form a thin fibrous structure, 20-50 nm thick. The nuclear lamins form together with the inner nuclear membrane (INM) proteins the 'nuclear lamina', a stable yet dynamic network that maintains extensive interactions with both INM-specific integral membrane proteins and chromatin (Hutchison, 2002). There are two classes of lamins, A-type lamins (lamin A/lamin C, each alternatively spliced from the same gene) and B-type lamins which bind to the lamin B receptor (LBR). Mutations in the lamin A/C and lamin B genes result in diseases ranging from cardiac and skeletal myopathies and partial lipodystrophy to peripheral neuropathy and premature aging (Mounkes, 2003). Specifically, mutations in the genes encoding for A-type lamins and their binding partners have been associated with Emery-Dreifuss muscular dystrophy, dilated cardiomyopathy, Dunnigan-type familial partial lipodystrophy and Hutchinson-Gilford progeria syndrome (Bonne, 1999; Fatkin, 1999; Cao, 2000; Shackleton, 2000; Burke & Stewart, 2002; De Sandre-Giovannoli, 2003; Eriksson, 2003). B-type lamins are constitutively expressed in all somatic cells and contain a stable C-terminal farnesyl modification, which mediates tight association with the INM. Unlike B-type lamins, the A-type lamins are expressed only in differentiated cells (Lebel, 1987; Stuurman, 1998). They are components of the peripheral lamina and of structures in the nuclear interior (Moir, 2000). The lamina may be linked to nuclear pore baskets through Nup153 (Foisner, 2001).

The nuclear lamina is considered to be an important determinant of interphase nuclear architecture (Lenz-Bohme, 1997; Schirmer, 2001) because it plays an essential role in maintaining the integrity of the nuclear envelope and provides anchoring sites for chromatin (Moir, 1995; Gant & Wilson, 1997; Stuurman, 1998; Gant, 1999). In addition to the well-characterized peripheral location of lamins, there is considerable evidence for an intranuclear distribution of lamins. Both, localization in intranuclear spots (Goldman, 1992; Bridger, 1993; Moir, 1994) and a diffuse distribution throughout the nucleus (Hozak, 1995) have been reported. Intranuclear lamins have been shown to localize at sites of DNA replication (Jenkins, 1995; Goldman, 2002; Mar-

tins, 2003; Gruenbaum, 2003) and to support nuclear activities such as DNA replication and RNA synthesis (Nili, 2001; Spann, 2002; Wilkinson, 2003; Haraguchi, 2004). It is not yet clear whether intranuclear lamins form a network and whether such a network would be required for the activities supported by the lamins.

The nuclear lamins bind to several INM proteins, including lamina-associated polypeptides 1 and 2 $\beta$  (LAP1, LAP2 $\beta$ ), emerin and Man1, which share a common structural motif of about 40 amino acid residues, called the LEM (LAPs, emerin and Man1) domain (Lin, 2000). Although additional LEM domain proteins such as Nesprin, Otefin, and Lem-3 have been identified (Lin, 2000). All LAP1 isoforms and LAP2 $\alpha$  interact preferentially with A-type lamins, while the lamin B receptor and LAP2 $\beta$  interact with the B-type lamins and emerin interacts with both types of lamins (Foisner, 2001). Lamins can also bind to chromatin proteins (histone H2A or H2B dimers), as well as ostensibly soluble proteins including lamina-associated polypeptide-2 $\alpha$  (LAP2 $\alpha$ ), Kruppel-like protein (MOK2), actin, retinoblastoma protein (RB), barrier-to-autointegration factor (BAF), sterol-response-element-binding protein (SREBP) and one or more components of RNA-polymerase-II-dependent transcription complexes and DNA-replication complexes (Gruenbaum, 2003; Zastrow, 2004). In cells that lack A-type lamins, many of these proteins are not retained at the NE but instead drift throughout the NE/ER network (Sullivan, 1999; Lee, 2002; Liu, 2003; Muchir, 2003; Wagner, 2004). Lamins and their associated proteins are proposed to have roles in large-scale chromatin organization (Sullivan, 1999; Liu, 2000; Guillemain 2001; Liu, 2003; Raz, 2006; Raz, 2008), the spacing of nuclear pore complexes (Liu, 2000; Schirmer, 2001), the positioning of the nucleus in cells (Starr, 2001; Starr 2002) and the reassembly of the nucleus after mitosis (Lopez-Soler, 2001). Lamins have been shown to interact with chromatin at more than 1,300 sharply defined large domains, 0.1-10 megabases in size (Guelen, 2008). These lamina-associated domains are typified by low gene-expression levels, indicating that they represent a repressive chromatin environment (Guelen, 2008).

The nuclear lamina is linked to the cytoskeleton via the nesprin protein family, which include high molecular weight proteins embedded in the inner and outer nuclear membrane (Zhang, 2001; Mislow, 2002). When nesprins are associated with the outer nuclear membrane, the amino-terminus is exposed towards the cytoplasm and binds to microfilaments (Zhang, 2001; Zhen, 2002) and intermediate filaments (Wilhelmsen, 2005). As such they connect the nucleus to the cytoskeleton (Wang & Suo, 2005). This anchorage of the nuclear membrane to the cytoskeleton is essential for migration and correct localization of the nucleus inside the cell. Nesprins at the inner nuclear membrane (smaller isoforms) bind to lamin A/C and emerin (Mislow, 2002; Padmakumar, 2005) through their spectrin repeats in the carboxy-terminus, and – as such – interact closely with the nuclear lamina. In this way lamins play not only an essential role in the structural integrity of the nucleus but also in the structural integrity of the whole cell, via connections between nuclear lamina, cytoskeleton and extracellular matrix (Lammerding, 2004; Broers, 2004; Broers, 2005). Absence of the A-type lamins or mutations in these structural components of the nuclear lamina leads to an impaired cellular response to mechanical stress (Lammerding, 2004). Laminopathies show clinical phenotypes comparable to those seen for diseases resulting from genetic defects in cytoskeletal components, further indicating that lamins play a central role in maintaining the mechanical properties of the cell.

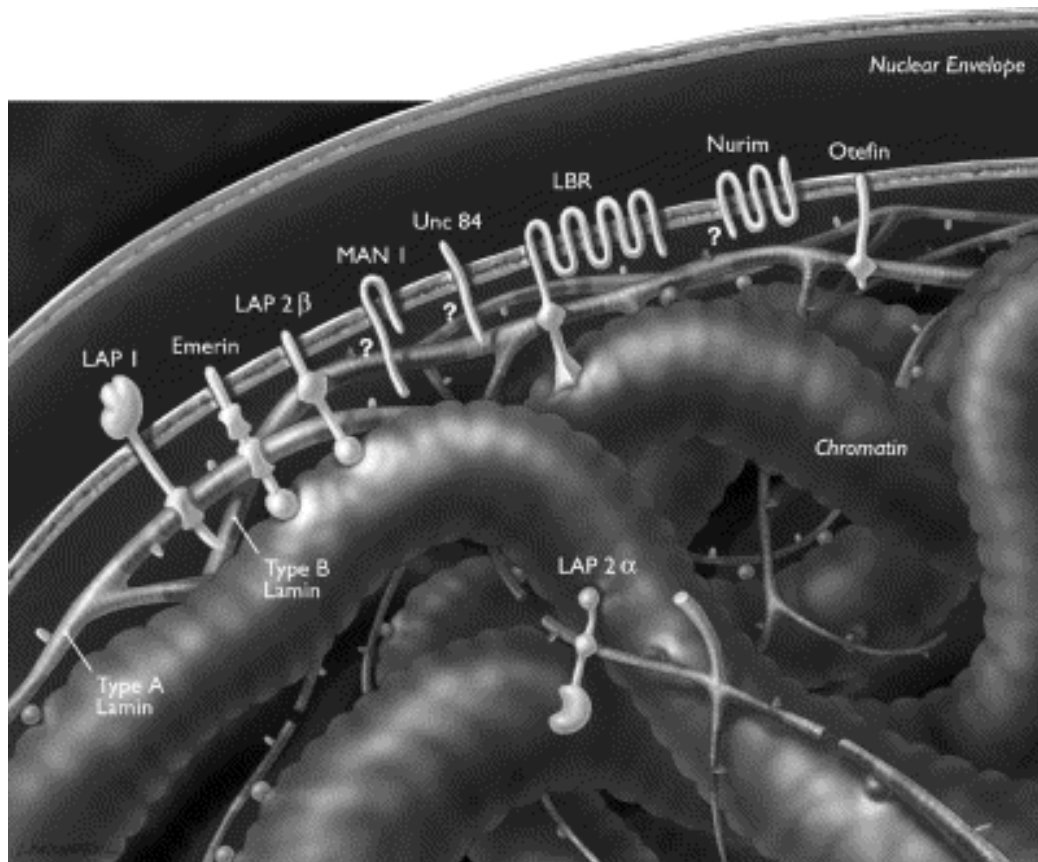


**Figure 4.** Schematic view of the nuclear envelope, lamina and chromatin. The inner and outer membranes of the nuclear envelope are shown with their enclosed lumen. Also lamin filaments and selected nuclear envelope proteins, including lamina-associated protein 1 (LAP1), emerin, LAP2 $\beta$ , MAN1, UNC-84, lamin B receptor (LBR), nurim and otefin, are shown. (Adapted from Cohen, 2001).

### 2.3 Are lamins part of the nuclear matrix?

Considering the spatial distribution of lamins in the cell nucleus, the question is raised whether lamins are part of the nuclear matrix. A large fraction of the filaments seen in resinless section images of (RNP-containing) nuclear matrix preparations are 10-11 nm in diameter (Jackson & Cook, 1988; He, 1990; Hozák, 1995; Wan, 1999), which correspond to the size of an intermediate filament. In one report, it has been described that these nuclear filaments react with a lamin A specific antibody (Hozák, 1995). Intriguingly, many different intermediate filament proteins revealed binding affinity for nucleic acids and also share some amino acid sequence homology with transcription factors (Traub & Shoeman, 1994). Other studies have also found lamins as discrete foci present in the nucleoplasm (Goldman, 1992; Bridger, 1993; Moir, 1994), and it has been shown that nucleoplasmic lamins undergo dynamic assembly-disassembly in

vivo (Goldman, 1992; Moir, 1994; Schmidt, 1994). Altogether this evidence is in favour of a role for lamins constituting part of the nuclear matrix, possibly by forming a complex network with other proteins like emerin, protein 4.1, nuclear actin and nuclear myosin (Pestic-Dragovich, 2000; Kiseleva, 2004).

## 2.4 Nuclear actin

Since one of the presumed functions of the nuclear matrix is to support and to facilitate/regulate intranuclear transport, possible nuclear matrix components may be similar to protein filament systems already characterized in the cytoplasm. Thus far, there is little if no evidence for the presence of tubulin or microtubules in the nucleus. Nuclear actin, however, is present and functional in the cell nucleus of various cell types (Clark & Merriam, 1977; Fukui, 1978; Fukui & Katsumaru, 1979; Clark & Rosenbaum, 1979; Osborn & Weber, 1980; Welch & Suhan, 1985; De Boni, 1994; Yan, 1997; Rando, 2000; Pederson and Aebi, 2002; Bettinger, 2004; Castano et al., 2010). This is also true for nuclear actin binding proteins (Ankenbauer, 1989; Rimm & Pollard, 1989) and nuclear myosin (Hauser, 1975; Berrios & Fisher, 1986; Hagen, 1986; Rimm & Pollard, 1989; Nowak, 1997). Nuclear actin has initially been suggested to play a role in transcription (Scheer, 1984) and later also in mRNA processing (Sahlas, 1993), chromatin remodelling and nuclear export (Machesky & May, 2001; Goodson & Hawse, 2002; Olave, 2002). Nuclear actin is also found present in the nucleolus (Clark & Merriam, 1977; Funaki, 1995) and TEM analysis of *Xenopus* oocyte nuclei suggested that short bundles of actin extend from nucleoli towards the nuclear envelope (Parfenov, 1995). In addition to actin, nuclei also contain a specific isoform of myosin I, nuclear myosin I (NM1), which is an actin-dependent motor. Antibodies directed against nuclear myosin I block transcription by RNA polymerase II when injected into mammalian cells and inhibit isolated transcription complexes in vitro (Pestic-Dragovich, 2000).

The most important questions about nuclear actin revolve around its polymeric state(s). Nuclear actin does not form long actin filaments ('F-actin'), it is proposed to assume shorter, potentially novel conformations (Pederson & Aebi, 2002; Bettinger, 2004). Nuclear actin 'rods,' 'bundles,' and 'tubules' have been described by a number of investigators (Fukui & Katsumaru, 1979; Iida, 1986; Iida & Yahara, 1986; Nishida, 1987; Wada, 1998), but their supramolecular organization has remained elusive except for one case (Sameshima, 2001). Sameshima *et al.* have described a new type of actin rods formed both in the nucleus and the cytoplasm of *Dictyostelium discoideum* that have been implicated in the maintenance of dormancy and viability at the spore stage of the developmental cycle. Examination of their ultrastructure has revealed these actin rods as bundles of hexagonally packed actin tubules consisting of three actin filaments each. (Interestingly, cytoplasmic actin is known to form short 'protomer' filaments (e.g. at branched intersections with protein 4.1, tropomyosin and spectrin), as well as tubes, sheets and short branched filaments (Pederson & Aebi, 2002).). Nuclear actin was shown to interact with many structural proteins in the nucleus: the intermediate filament protein lamin A (Sasseville & Langelier, 1998), membrane protein emerin (Holaska, 2004), the nesprin family of filamentous proteins (Zhang, 2002; Zhen, 2002) and nuclear-specific isoforms of protein '4.1', an actin scaffolding pro-



## Introduction

tein (Correas, 1991; Krauss, 1997; Luque & Correas, 2000). An actin network is proposed to exist at the INM and to mechanically reinforce the lamina network (Holaska, 2004). The actin-binding domain of nuclear-specific isoforms of protein 4.1 is found to be essential to reconstruct nuclei after mitosis (Krauss, 2003). In conclusion, there is ample evidence that actin is present in the cell nucleus and is involved in a variety of nuclear processes.

## 3. Telomeres & Nuclear organization

### 3.1 Telomere biology

Telomeres are structures at the ends of eukaryotic chromosomes (in greek: telo= end , mere= part). They are protein-DNA complexes that protect chromosome termini from unregulated degradation, recombination and fusion. They also serve to limit the loss of genetic material from chromosome ends that occurs during (incomplete) DNA replication. After about 60-80 cell divisions, telomere repeats are shortened from a typical initial length of 10-15 kb in human cells to ~5 kb and below, which triggers cell senescence or apoptosis (Harley, 1990; Martens, 2000; Blasco, 2007). The number of cell divisions that a normal cell can make before entering in to a state of senescence is also referred to as the 'Hayflick limit'. Leonard Hayflick demonstrated in 1965 that normal human diploid cells in a cell culture divide about 50 +/- 10 times (Hayflick, 1965).

Telomeres consist of tandemly repeated DNA sequences (TTAGGG) bound by various telomeric proteins, such as telomere repeat binding factor 1 (TRF1), telomere repeat binding factor 2 (TRF2) and protection of telomeres 1 (POT-1) (Blackburn, 2001). These proteins bind telomeric DNA directly and are interconnected by three additional proteins, TIN2, TPP1 and Rap1. Together they form a complex called the shelterin complex (figure 6) that allows cells to distinguish telomeres from sites of DNA damage (d'Adda di Fagagna, 2004; Shay & Wright, 2004; de Lange, 2005). The single stranded end-part of the telomere forms a loop structure, called the t-loop (Griffith, 1999), which is lost when TRF2 function is inhibited by expressing a dominant negative allele of TRF2 (van Steensel, 1998). Telomeres have a nonnucleosomal chromatin structure, whereas subtelomeric DNA is assembled into nucleosomes (Wright, 1992). It is possible that t-loops create an organization similar to nucleosomes that conceal the chromosome ends from the DNA damage surveillance, thus preventing telomeres from being degraded. It has been proposed that TRF2 plays an important part in protecting telomeres *in vivo* (Griffith, 1999). Most, if not all TRF2 is in a complex with human (h)Rap1, which has been identified as a direct interacting partner of TRF2 (Li, 2000). Two other telomeric proteins, TIN2 and the DNA repair protein Ku, interact with telomeres via binding to TRF1 (Kim, 1999; Hsu, 2000). TRF1 alone is insufficient to control telomere length in human cells, and the TIN2 protein is thought to be an essential mediator of TRF1 function (Kim, 1999). Moreover, TIN2 is thought to bind TRF1 and TRF2 simultaneously, stabilizing the TRF2 complex on telomeres (Ye, 2004). TPP1 was also found to interact with both TRF1 and TRF2 and to operate as a negative regulator of telomere length (Houghtaling, 2004).



## Introduction

required for DNA recombination (Lundblad, 1993). Also, individual telomeres in human ALT cells undergo steady telomere attrition upon which sudden lengthening and shortening events are superimposed in a manner that is suggestive for recombination (Murnane, 1994). Finally, functional evidence for the involvement of recombination in the ALT mechanism was provided by showing that DNA sequences are copied from telomere to telomere in ALT cells (Dunham, 2000). Telomere lengthening is also possible via intra-telomeric DNA copying (Muntoni, 2009). These observations are all consistent with a recombination-mediated DNA replication mechanism.

The hallmarks of human ALT cells include a large variance in telomere length, with telomeres that range from very short ~5kb, to very long ~50 kb (Bryan, 1995), and the presence of ALT-associated promyelocytic leukemia nuclear bodies (APBs) containing telomeric DNA and telomere binding proteins (Yeager, 1999). APBs are a subset of PML bodies that are not found in normal cells, or in tumor cells that express telomerase, and contain additional proteins involved in DNA replication, recombination and repair that are not found in normal PML bodies (Yeager, 1999; Yankiwski, 2000; Stavropoulos, 2002; Tarsounas, 2004). APBs are found in a minority of cells, approximately 5% within asynchronously dividing ALT cell populations, from which it may be concluded that their formation is cell cycle-dependent (Yeager, 1999; Grobelny, 2000; Wu, 2000). It has been suggested that APBs may have an integral role in the ALT mechanism (Yeager, 1999; Grobelny, 2000; Wu, 2000, 2003; Moleenaar, 2003). Consistent with this suggestion, inhibition of ALT in somatic cell hybrids, formed by fusing ALT and telomerase-positive cells, resulted in a substantial decrease in APBs (Perrem, 2001). It has been shown that inhibition of ALT is accompanied by a reduction of APBs, providing evidence for a direct link between APBs and ALT activity (Jiang, 2005). Furthermore, it has recently been shown that the DNA recombination endonuclease MUS81 is involved in ALT specific telomerase recombination and localizes to APBs (Zeng, 2009).

Observational and clinical studies on ALT positive tumors may help to fill the gaps in our understanding of the ALT mechanism. ALT is most commonly activated in tumors of neuroepithelial origin (astrocytomas) or mesenchymal origin, including osteosarcomas, and in soft tissue sarcomas (Henson, 2005). The reason for this is unknown, but it is possible that some mesenchymal and neuroepithelial cells repress telomerase more tightly than epithelial cells and therefore have a higher probability of activating ALT during tumorigenesis. In sarcomas, ALT is more frequently activated in subtypes that have a complex karyotype, which could be linked to chromosomal instability (Montgomery, 2004; Ulaner, 2004). It could be argued that the ALT mechanism is, in part, the cause of this instability because the critically short telomeres found in ALT cells are prone to end-to-end fusions, anaphase bridge formation, break–fusion–break events and ultimately severe chromosomal rearrangements. However, not all soft tissue sarcomas showing complex karyotypes are ALT-positive (Henson, 2005), indicating that other factors contribute to chromosomal instability as well.

Activation of the ALT pathway has been reported to be a prognostic marker for cancer progression. In case of glioblastoma, ALT correlated with a better patient prognosis, whereas no influence was detected for osteosarcomas. One of 16 non–small cell lung cancer (NSCLC) cell lines (VL-9, SK-LU-1, and VL-7) that lacked telomerase activity and displayed characteristics of an ALT mechanism showed significantly re-

duced tumorigenicity *in vitro* and *in vivo* compared to the telomerase positive NSCLC cell lines (Brachner, 2006). It can be concluded that there is some evidence indicating that the ALT mechanism is indicative for a better patient prognosis, although further research is needed to substantiate this conclusion.

### 3.3 Telomeres and the nuclear matrix

The positioning of telomeres in the cell nucleus varies among organisms (Dong & Jiang 1998). In yeast, telomeres are positioned at the nuclear periphery while in mammalian cells they seem randomly distributed in the nucleoplasm (Henderson, 1996; Bilaud, 1997; Broccoli, 1997; van Steensel, 1998). Biochemical and ultrastructural data suggest that in mammalian cells telomeric DNA and telomere binding proteins colocalize in individual condensed structures at the nuclear matrix (Ludérus, 1996). The shelterin complex component TIN2 is believed to play a dual role in tethering telomeres to the nuclear matrix (Kaminker, 2009). Consistent with this association to the nuclear matrix, telomeric TTAGGG repeats were found to contain an array of nuclear matrix attachment sites at a frequency of at least one per kb. The nuclear matrix association is supposed to involve large domains of up to 20-30 kb telomeric DNA, encompassing the entire length of most mammalian telomeres (Ludérus, 1996). Because of their association to a nuclear matrix structure, telomeres are thought to play an important role in nuclear organization (de Lange, 2002).

In situ hybridization studies revealed that in yeast telomeres are organized in clusters at the nuclear periphery (Gilson, 1993; Gotta, 1996). This organization in clusters may contribute to the repression of transcription of nearby genes, a phenomenon termed telomere position effect (TPE) (Gottschling, 1990). Telomeres in yeast have a nonnucleosomal chromatin structure, whereas subtelomeric DNA is assembled into nucleosomes (Wright, 1992). Subtelomeric chromatin in yeast has therefore many of the hallmarks of heterochromatin as present in mammalian cells: it imposes transcriptional repression (Gottschling, 1990) and late replication of nearby sequences (Ferguson, 1991).

### 3.4 Telomere and chromatin mobility in the cell nucleus

Considering the high DNA content and the large amounts of RNAs and proteins in the nucleus, one might intuitively think of the nucleus as a viscous, gel-like environment. If this were true, the movement of proteins within the organelle might be severely restricted and specific transport mechanisms would be required to deliver proteins to their destinations. Photobleaching experiments have now shown, however, that most proteins are highly mobile within the nucleus. The difference between the diffusional mobility of nonphysiological solutes in the nucleus as compared to that in an aqueous solution is only about fourfold (Fushimi & Verkman, 1991; Seksek, 1997). Thus, macromolecules such as fluorescently tagged proteins or RNAs move within the nuclear space by simple thermal diffusion at an unexpectedly high speed (Huang, 1998; Rademakers, 1999; Phair & Misteli, 2000; Pederson, 2000; Shopland & Lawrence, 2000; Snaar, 2000; Misteli, 2001). The time required for travelling from the centre to the periphery of the nucleus is in the order of several seconds for an average sized

## Introduction

monomeric protein, and only several minutes for a large complex such as a spliceosome or ribosome.

If the subnuclear positioning of any particular chromosomal locus reflects a state of transcriptional activity, then genes must be able to move from a transcriptional repressive subenvironment to a transcriptional competent environment and to obtain a tissue-specific and/or developmental-stage-specific spatial organization. In the past few years, various studies addressed the dynamic properties of chromatin in general or specific sequences in particular. Using time-lapse imaging of GFP-tagged chromosomal loci, Sedat and coworkers showed in yeast and later in flies that chromatin is engaged in a continuous random-walk-like motion (Marshall, 1997). Later, slightly less constrained random movements were described for multiple yeast loci by monitoring the movements of specific chromosomal sites fused to lac repressor binding sites that were tagged with GFP-lac repressor proteins (Heun, 2001a; Heun, 2001b). Telomeres and transcriptionally active non-telomeric loci showed clear differences in movement. Active chromosomal loci displayed a random walk movement within a radius of 0.5–0.7  $\mu\text{m}$  (Heun, 2001a; Gartenberg, 2004; Sage, 2005). This represents more than one-quarter of the nuclear diameter in yeast, but less than one-tenth of the nuclear diameter in mammalian cells. Because 50% of the yeast nuclear volume is contained within a peripheral shell that is  $<0.4 \mu\text{m}$  thick, most yeast genes have a high probability to encounter the nuclear membrane. Silent telomeres, however, moved in a highly constrained manner along the inner surface of the nuclear envelope and only rarely occupy the nuclear core (Heun, 2001a; Hediger, 2002; Gartenberg, 2004; Sage, 2005). The movement of a typical yeast telomere is restricted to an area at the inner-nuclear-envelope surface occupying  $\sim 12\%$  of the total nuclear volume (Rosa, 2006). Interestingly, a similar constraint movement was observed for a subset of active genes. Notably, galactose-induced loci were shown to associate with nuclear pores upon induction. In addition, a subtelomeric gene was shown to shift from a telomeric focus to a nuclear pore upon induction by low glucose (Cabal, 2006; Taddei, 2006). Given their lateral dynamics and striking radial confinement, it was suggested that a subset of active genes move from pore to pore (Cabal, 2006).

## Outline of this thesis

The aim of this thesis is to provide a better understanding of the principles that underlie the spatial dynamic organization of the cell nucleus. Chapter 1 reviews the current status of knowledge about the structural and functional organization of the cell nucleus. In **chapter 2**, the development of a computer program is described that has been designed to track the 2D and 3D motion of objects in the nucleus of living cells. The functionality of the program is demonstrated by tracking the movements of GFP-tagged telomeres in the nuclei of tumor cells (U2OS) and normal mouse embryonic fibroblasts (W8 MEFS). GFP-tagged proliferating cell nuclear antigen (PCNA) is used as a nuclear counterstain to correct for cell movements, and as a cell cycle marker. In **chapter 3**, evidence is provided for the existence of a nuclear matrix structure that is composed of lamin proteins, emerin and actin. By analyzing the dynamics of telomeres in nuclei of cells showing reduced levels of lamin expression, it is investigated whether telomeres anchor to an inner nuclear lamina structure. In **chapter 4** the de novo formation of PML nuclear bodies is described. Using live cell imaging and immunocytochemistry it is demonstrated that telomeres play a role in the de novo formation of PML bodies. In **chapter 5** it is investigated whether nuclear bodies are associated with chromatin in the cell nucleus. After treating cells with DNA alkylating agent MMS, the dynamics of PML bodies, Cajal bodies and speckles has been analyzed relative to chromatin in the 3D space of the cell nucleus. In chapter 6 the results of our studies and future implications are discussed.

## Introduction

## References

- Miescher F. 1871. Ueber die chemische Zusammensetzung der Eiterzellen. *Hoppe-Seyler's Med. Chem. Unters.* **4**, 441-460
- Stenoien D.L., Simeoni S., Sharp Z.D., Mancini M.A. 2000. Subnuclear dynamics and transcription factor function. *J Cell Biochem.* **3**, 99–106
- Carmo-Fonseca M. 2002. The contribution of nuclear compartmentalization to gene regulation. *Cell* **108**, 513–521
- Rippe K. 2007. Dynamic organization of the cell nucleus. *Current Opinion in Genetics & Development* **17**, 373-380
- Cremer T., Kreth G., Koester H., Fink R.H., Heintzmann R., Cremer M., Solovei I., Zink D. & Cremer C. 2002. Chromosome territories, interchromatin domain compartment, and nuclear matrix: An integrated view of the functional nuclear architecture. *Crit Rev Eukaryot Gene Expr.* **10**, 179-212
- Manuelidis L. 1985. Individual interphase chromosome domains revealed by in situ hybridization. *Hum. Genet.* **71**, 288-293
- Cook P.R. & Brazell I.A. 1976. Conformational constraints in nuclear DNA. *J Cell Sci.* **22**, 287-302
- Paulson J.R. & Laemmli U.K. 1977. The structure of histonedepleted metaphase chromosomes. *Cell* **12**, 817-825
- van der Velden H.M., van Willigen G., Wetzels R.H. & Wanka F. 1984. Attachment of Origins of Replication to the Nuclear Matrix and the Chromosomal Scaffold. *FEBS Lett.* **171**, 13–16
- Razin S.V., Kekelidze M.G., Lukanidin E.M. 1986. Replication origins are attached to the nuclear skeleton. *Nucl. Acids Res.* **14**, 8189–8207
- Buongiorno-Nardelli M., Micheli G., Carri M.T. & Marilley M. 1982. A relationship between replicon size and supercoiled loop domains in the eukaryotic genome. *Nature* **298**, 100–102
- Marilley M. & Gassend-Bonnet G. 1989. Supercoiled loop organization of genomic DNA: A close relationship between loop domains, expression units, and replicon organization in rDNA from *Xenopus laevis*. *Exp. Cell Res.* **180**, 475–489
- Razin S.V. 1996. Functional architecture of chromosomal DNA domains. *Crit. Rev. Eukaryot. Gene Expr.* **6**, 247–269
- Vassetzky Y., Lemaitre J.M. & Mechali M. 2000b. Specification of chromatin domains and regulation of replication and transcription during development. *Crit. Rev. Eukaryot. Gene Expr.* **10**, 31–38
- John B. 1988. The Biology of Heterochromatin. (ed. Verma R.S.) (Cambridge Univ. Press, Cambridge).
- Felsenfeld G. & Groudine M. 2003. Controlling the double helix. *Nature* **421**, 448–453

- Bühler M. & Moazed D. 2007. Transcription and RNAi in heterochromatic gene silencing. *Nature Structural & Molecular Biology* **14**, 1041-1048
- Boyle S., Gilchrist S., Bridger J.M., Mahy N.L., Ellis J.A. & Bickmore W.A. 2001. The spatial organization of human chromosomes within the nuclei of normal and emerin-mutant cells. *Hum. Mol. Genet.* **10**, 211–219
- Finlan L.E., Sproul D., Thomson I., Boyle S., Kerr E., Perry P., Ylstra B., Chubb J.R., Bickmore W.A. 2008. Recruitment to the Nuclear Periphery Can Alter Expression of Genes in Human Cells. *PLoS Genet.* **4**, e1000039
- Verschure P.J., van Der Kraan I., Manders E.M. & van Driel R. 1999. Spatial relationship between transcription sites and chromosome territories. *J. Cell Biol.* **147**, 13– 24
- Stewart M.D., Li J. & Wong J. 2005. Relationship between Histone H3 Lysine 9 Methylation, Transcription Repression, and Heterochromatin Protein 1 Recruitment. *Molecular and cellular biology* **25**, 2525–2538
- Strahl B.D., Grant P.A., Briggs S.D., Sun Z.W., Bone J.R., Caldwell J.A., Mollah S., Cook R.G., Shabanowitz J., Hunt D.F. & Allis C.D. 2002. Set2 is a nucleosomal histone H3-selective methyltransferase that mediates transcriptional repression. *Mol. Cell. Biol.* **22**, 1298 -1306
- Grunstein M. 1997. Histone acetylation in chromatin structure and transcription. *Nature* **389**, 349-352
- Turner B.M. 2000. Histone acetylation and an epigenetic code. *BioEssays* **450**, 1-10
- Krouwels I.M., Wiesmeijer K., Abraham T.E., Molenaar C., Verwoerd N.P., Tanke H.J., and Dirks R.W. 2005. A glue for heterochromatin maintenance: stable SUV39H1 binding to heterochromatin is reinforced by the SET domain *J. Cell Biol.* **170**, 537-549
- Goll M.G. & Bestor T.H. 2005. Eukaryotic cytosine methyltransferases. *Annual Review of Biochemistry* **74**, 481-514
- Razin A. & Cedar H. 1991. DNA methylation and gene expression. *Microbiol. Rev.* **55**, 451-458
- Bird A.P. 1986. CpG-rich islands and the function of DNA methylation. *Nature* **321**, 209-213
- Nakayama J., Rice J.C., Strahl B.D., Allis C.D., Grewal S.I. 2001. Role of histone H3 lysine 9 methylation in epigenetic control of heterochromatin assembly. *Science* **292**, 110–113
- Grewal S.I. & Rice J.C. 2004. "Regulation of heterochromatin by histone methylation and small RNAs". *Curr. Opin. Cell Biol.* **16**, 230–238
- Maeshima K., Hihara, S., and Eltsov, M. 2010. Chromatin structure: does the 30-nm fibre exist in vivo? *Curr. Opin. Cell Biol.* In press
- Smetana K., Steele W. J. & Busch H. 1963. A nuclear ribonucleoprotein network. *Exp. Cell Res.* **31**, 198-201
- Bernhard W. 1969. A new staining procedure for electron microscopical cytology. *J. Ultrastruct. Res.* **27**, 250-265



## Introduction

Biggiogera M. & Fakan S. 1998. Fine structural specific visualization of RNA on ultrathin sections. *J. Histochem. Cytochem.* **46**, 389-395

Monneron A. & Bernhard W. 1969. Fine structural organization of the interphase nucleus in some mammalian cells. *J. Ultrastruct. Res.* **27**, 266- 288

Misteli T. & Spector D.L. 1998. The cellular organization of gene expression. *Curr. Opin. Cell Biol.* **10**, 323-331

Misteli T. 2000. Cell biology of transcription and pre-mRNA splicing: nuclear architecture meets nuclear function. *J. Cell Sci.* **113**, 1841-1849

Bachelier J.P., Puvion E. & Zalta J.P. 1975. Ultrastructural organization and biochemical characterization of chromatin - RNA - protein complexes isolated from mammalian cell nuclei. *Eur. J. Biochem.* **58**, 327- 337

Cmarko D., Verschure P.J., Martin T.E., Dahmus M.E., Krause S., Fu X.D., van Driel R. & Fakan S. 1999. Ultrastructural analysis of transcription and splicing in the cell nucleus after bromo-UTP microinjection. *Mol. Biol. Cell* **10**, 211-223

Mintz P.J., Patterson S.D., Neuwald A.F., Spahr C.S. & Spector D.L. 1999. Purification and biochemical characterization of interchromatin granule clusters. *EMBO J.* **18**, 4308-4320

Smith K.P., Moen P.T., Wydner K.L., Coleman J.R. & Lawrence J.B. 1999. Processing of endogenous pre-mRNAs in association with SC-35 domains is gene specific. *J. Cell Biol.* **144**, 617-629

Spector D.L. 2001. Nuclear domains. *J. Cell Sci.* **114**, 2891–2893

Vasu S. & Forbes D.J. 2001. Nuclear pores and nuclear assembly. *Curr. Opin. Cell Biol.* **13**, 363-375

Fahrenkrog B. & Aebi U. 2003. The nuclear pore complex: nucleocytoplasmic transport and beyond. *Nat. Rev. Mol. Cell Biol.* **4**, 757- 766

Cordes V.C., Reidenbach S., Kohler A., Stuurman N., van Driel R. & Franke W.W. 1993. Intranuclear filaments containing a nuclear pore complex protein. *J. Cell Biol.* **123**, 1333-1344

Cordes V., Reidenbach S., Rackwitz H.R. & Franke W.W. 1997. Identification of protein 270/Tpr as a constitutive component of the nuclear pore complex-attached intranuclear filaments. *J. Cell Biol.* **136**, 515-529

Parfenov V.N., Davis D.S., Pochukalina G.N., Sample C.E., Bugaeva E.A. & Murti, K.G. 1995. Nuclear actin and their topological changes in frog oocytes. *Exp. Cell Res.* **217**, 385-394

Zink D., Amaral M.D., Englmann A., Lang S., L.A. Clarke L.A., Rudolph C., Alt F., Luther K., Braz C., Sadoni N., Rosenecker J. & Schindelbauer D. 2004. Transcription-dependent spatial arrangements of CFTR and adjacent genes in human cell nuclei. *J. Cell Biol.* **166**, 815–825

Branco M.R. & Pombo A. 2006. Intermingling of chromosome territories in interphase suggests role in translocations and transcription-dependent associations. *PLoS Biol.* **4**, 780-788

- Lonard D.M. & O'Malley B.W. 2008. Gene transcription: Two worlds merged. *Nature* **452**, 946-947
- Dekker J. 2006. The three 'C' s of chromosome conformation capture: controls, controls, controls. *Nature Methods* **3**, 17-21
- Smith K.P., Carter K.C., Johnson C.V., Lawrence J.B. 1995. U2 and U1 snRNA gene loci associate with coiled bodies. *J. Cell. Biochem.* **59**, 473-85
- Vijg J. & Dollé M.E.T. 2002. Large genome rearrangements as a primary cause of aging. *Mechanisms of ageing and development* **123**, 907-915
- Busuttill R.A., Dollé M.E.T., Campisi J., Vijg J. 2004. Genomic Instability, Aging, and Cellular Senescence. *Ann. N. Y. Acad. Sci.* **1019**, 245–255
- Raz V., Vermolen B.J., Garini Y., Onderwater J.J.M., Mommaas-Kienhuis M.A., Koster A.J., Young I.T., Tanke H.J. & Dirks R.W. 2008. The nuclear lamina promotes telomere aggregation and centromere peripheral localization during senescence of human mesenchymal stem cells. *Journal of Cell Science* **121**, 4018-4028
- Shin D-M., Kucia M., Ratajczak M.Z. 2010. Nuclear and chromatin reorganization during cell senescence and aging – a mini-review. *Gerontology*, in press
- Butler J.T., Hall L.L., Smith K.P. & Lawrence J.B. 2009. Changing nuclear landscape and unique PML structures during early epigenetic transitions of human embryonic stem cells. *J. Cell Biochem.* **107**, 609-621
- Buongiorno-Nardelli M., Micheli G., Carri M.T., Marilley M. 1982. A relationship between replicon size and supercoiled loop domains in the eukaryotic genome. *Nature* **298**, 100-102
- Linskens M.H., Eijssermans A., Dijkwel P.A. 1987. Comparative analysis of DNA loop length in nontransformed and transformed hamster cells. *Mutat. Res* **178**, 245-256
- Oberhammer F., Wilson J.W., Dive C., Morris I.D., Hickman J.A., Wakeling A.E., Walker P.R., Sikorska M. 1993. Apoptotic death in epithelial cells: cleavage of DNA to 300 and/or 50 kb fragments prior to or in the absence of internucleosomal fragmentation. *EMBO J* **12**, 3679-3684
- Tsutsui K.M., Sano K. & Tsutsui K. 2005. Dynamic View of the Nuclear Matrix. *Acta Med. Okayama* **59**, 113-120
- Misteli T. 2001. Protein dynamics: implications for nuclear architecture and gene expression. *Science* **291**, 843 -847
- Snaar S., Wiesmeijer K., Jochemsen A.G., Tanke H.J., Dirks R.W. 2000. Mutational analysis of fibrillarin and its mobility in living human cells. *J. Cell. Biol.* **151**, 653-662
- Olson M.O.J. 2004. Nucleolus. BookISBN-10: 0306478730 ISBN-13: 978-0306478734
- Spector D.L. 2001. Nuclear domains. *J. Cell Sci.* **114**, 2891–2893
- Saurin A.J., Shiels C., Williamson J., Satijn D.P., Otte A.P., Sheer D. & Freemont P.S. 1998. The human polycomb group complex associates with pericentromeric heterochromatin to form a novel nuclear domain. *J. Cell Biol.* **142**, 887 -898

## Introduction

- Matera A.G. 1999. Nuclear bodies: multifaceted subdomains of the interchromatin space. *Trends Cell Biol.* **9**, 302-309
- Huang, S. 2000. Review: perinucleolar structures. *J. Struct. Biol.* **129**, 233-240
- Montgomery T.H. 1898. Comparative cytological studies, with especial regard to the morphology of the nucleolus. *J. Morphol.* **15**, 265-565
- Olson M.O., Hingorani K. & Szebeni A. 2002. Conventional and nonconventional roles of the nucleolus. *Int. Rev. Cytol.* **219**, 199-266
- Andersen J.S., Lyon C.E., Fox A.H., Leung A.K., Lam Y.W., Steen H., Mann M. & Lamond A.I. 2002. Directed proteomic analysis of the human nucleolus. *Curr. Biol.* **12**, 1-11
- Andersen J.S., Lam Y.W., Leung A.K.L., Ong S.E., Lyon C.E., Lamond A.I. & Mann M. 2005. Nucleolar proteome dynamics. *Nature* **433**, 77-78
- Pederson T. 1998. The plurifunctional nucleolus. *Nucleic Acids Res.* **26**, 3871-3876
- Yamauchi K., Yang M., Hayashi K., Jiang P., Yamamoto N., Tsuchiya H., Tomita K., Moossa A.R., Bouvet M., Hoffman R.M. Imaging of nucleolar dynamics during the cell cycle of cancer cells in live mice. 2007. *Cell cycle* **6**, 2706-2708
- Jacob J. 1968. Involvement of the nucleolus in viral synthesis in the cells of primary renal tumors of leopard frogs. *Cancer Research* **28**, 2126-2136
- Itahana K., Krishna P., Jin B.A., Itahana Y., Hawke D., Kobayashi R. & Zhang Y. 2003. Tumor suppressor ARF degrades B23, a nucleolar protein involved in ribosome biogenesis and cell proliferation. *Molecular Cell* **12**, 1151-1164
- van den Boom, V., Citterio, E., Hoogstraten, D., Zotter, A., Egly, J.M., van Cappellen, W.A., Hoeijmakers, J.H., Houtsmuller, A.B. and Vermeulen, W. 2004. DNA damage stabilizes interaction of CSB with the transcription elongation machinery. *J. Cell Biol.* **166**, 27-36
- Jacobson M.R. & Pederson T. 1998. Localization of signal recognition particle RNA in the nucleolus of mammalian cells. *PNAS* **95**, 7981-7986
- Sansam C.L., Wells K S. & Emeson R.B. 2003. Modulation of RNA editing by functional nucleolar sequestration of ADAR2. *Proc. Natl. Acad. Sci. USA* **100**, 14018-14023
- Paushkin S.V., Patel M., Furia B.S., Peltz S.W. & Trotta C.R. 2004. Identification of a human endonuclease complex reveals a link between tRNA splicing and pre-mRNA 3' end formation. *Cell* **117**, 311-321
- Kieffer-Kwon P., Martianov I. & Davidson I. 2004. Cell-specific nucleolar localization of TBP-related factor 2. *Mol. Biol. Cell* **15**, 4356-4368
- Zhang S., Hemmerich P. & Grosse F. 2004. Nucleolar localization of the human telomeric repeat binding factor 2 (TRF2). *J. Cell Sci.* **117**, 3935-3945
- Mekhail K., Gunaratnam L., Bonicalzi M.E. & Lee S. 2004. HIF activation by pH-dependent nucleolar sequestration of VHL. *Nat. Cell Biol.* **6**, 642-647
- Rodway H., Llanos S., Rowe J. & Peters G. 2004. Stability of nucleolar versus non-nucleolar forms of human p14(ARF). *Oncogene* **23**, 6186-6192

- Comai L. 1999. The nucleolus: a paradigm for cell proliferation and aging. *Brazilian Journal of Medical and Biological Research* **32**, 1473-1478
- Rosete M., Padros M.R., Vindrola O. 2007. The nucleolus as a regulator of cellular senescence. **67**, 183-194
- Baran V., Fabian D., Rehak P., Koppel J. 2003. Nucleolus in apoptosis-induced mouse pre-implantation embryos. *Zygote* **11**, 271-283
- Schneiter R., Kadowaki T. & Tartakoff A.M. 1995. mRNA transport in yeast: time to reinvestigate the functions of the nucleus. *MCB* **6**, 357-370
- Sidebottom E. & Harris H. 1969. The role of the nucleolus in the transfer of RNA from nucleus to cytoplasm. *J. Cell Sci.* **5**, 351-364
- Deák I., Sidebottom E. & Harris H. 1972. Further experiments on the role of the nucleolus in the expression of structural genes. *J. Cell Sci.* **11**, 379-391
- Harris H. 1972. A new function for the nucleolus. *Aust. J. Exp. Biol. Med. Sci.* **50**, 827-832
- Perry R.P., Hell A. & Errera M. 1961. The role of the nucleolus in ribonucleic acid and protein synthesis. *Biochem. Biophys. Acta* **49**, 47-57
- Bond V.C. & Wold B. 1993. Nucleolar localization of myc transcripts. *Mol. Cell. Biol.* **13**, 3221-3230
- Carter K.C., Taneja K.L. & Lawrence J.B. 1991. Discrete nuclear domains of poly(A) RNA and their relationship to the functional organization of the nucleus. *J. Cell Biol.* **115**, 1191-1202
- Cajal S.R. 1903. Un sencillo método de coloración selectiva del retículo protoplásmico y sus efectos en los diversos órganos nerviosos de vertebrados e invertebrados. *Tra. Lab. Invest. Biol.* **2**, 129-221
- Ogg S.C. & Lamond A.I. 2002. Cajal bodies and coilin - moving towards function. *J Cell Biol.* **159**, 17-21
- Gall J.G. 2000. Cajal bodies: the first 100 years. *Annu. Rev. Cell Dev. Biol.* **16**, 273-300
- Gall J.G., Bellini M., Wu Z. & Murphy C. 1999. Assembly of the nuclear transcription and processing machinery: Cajal bodies (coiled bodies) and transcriptosomes. *Mol. Biol. Cell* **10**, 4385-4402
- Snaar S. Wiesmeijer K., Jochemsen A.G., Tanke H.J., Dirks R.W. 2000. Mutational analysis of fibrillarin and its mobility in living human cells. *J. Cell Biol.* **151**, 653-662
- Jády B.E., Darzacq X., Tucker K.E., Matera, A.G., Bertrand E. & Kiss T. 2003. Modification of Sm small nuclear RNAs occurs in the nucleoplasmic Cajal body following import from the cytoplasm. *EMBO J.* **22**, 1878-1888
- Darzacq X., Jady B.E., Verheggen C., Kiss A.M., Bertrand E. & Kiss T. 2002. Cajal body-specific small nuclear RNAs: a novel class of 2'-O-methylation and pseudouridylation guide RNAs. *EMBO J.* **21**, 2746-2756

## Introduction

Verheggen C., Lafontaine D.L., Samarsky D., Mouaikel J., Blanchard J.M., Bordonne R., & Bertrand E. 2002. Mammalian and yeast U3 snoRNPs are matured in specific and related nuclear compartments. *EMBO J.* **21**, 2736–2745

Staněk D., Pětidalová-Hnilicová J., Novotny I., Huranová M., Blažíková M., Wen X., Saprá A.K. & Neugebauer K.M. 2008. Spliceosomal snRNPs repeatedly cycle through Cajal Bodies. *Mol Biol Cell* **19**, 2534-2543

Thiry M. 1994. Cytochemical and immunocytochemical study of coiled bodies in different cultured cell lines. *Chromosoma* **103**, 268–276

Raska I., Andrade L.E., Ochs R.L., Chan E.K., Chang C.M., Roos G. & Tan E.M. 1991. Immunological and ultrastructural studies of the nuclear coiled body with autoimmune antibodies. *Exp. Cell Res.* **195**, 27–37

Carmo-Fonseca M., Pepperkok R., Carvalho M.T. & Lamond A.I. 1992. Transcription-dependent colocalization of the U1, U2, U4/U6, and U5 sn-RNPs in coiled bodies. *J. Cell Biol.* **117**, 1–14

Staněk D. & Neugebauer K.M. 2006. The Cajal body: a meeting place for spliceosomal snRNPs in the nuclear maze. *Chromosoma* **115**, 343–354

Jady B.E., Bertrand E. & Kiss T. 2004. Human telomerase RNA and box H/ACA scaRNAs share a common Cajal body-specific localization signal, *J. Cell Biol.* **164**, 647–652

Zhu Y., Tomlinson R.L., Lukowiak A.A., Terns R.M. & Terns M.P. 2004. Telomerase RNA accumulates in Cajal bodies in human cancer cells. *Mol. Biol. Cell* **15**, 81–90

Jady E., Richard P., Bertrand E. & Kiss T. 2006. Cell cycle-dependent recruitment of telomerase RNA and Cajal bodies to human telomeres. *Mol. Biol. Cell* **17**, 944–954

Tomlinson R.L., Ziegler T.D., Supakorndej T., Terns R.M. & Terns M.P. 2006. Cell cycle-regulated trafficking of human telomerase to telomeres, *Mol. Biol. Cell* **17**, 955–965

Christofari G., Adolf E., Reichenbach P., Sikora K., Terns R.M., Terns M.P. & Lingner J. 2007. Human telomerase RNA accumulation in Cajal bodies facilitates telomerase recruitment to telomeres and telomere elongation. *Molecular Cell* **27**, 882–889

Dirks R.W., Hattinger C.M., Molenaar C. & Snaar S.P. 1999. Synthesis, processing, and transport of RNA within the three-dimensional context of the cell nucleus. *Critical reviews in eukaryotic gene expression.* **9**, 191-201

Lamond A.I. & Spector D.L. 2003. Nuclear speckles: a model for nuclear organelles. *Nat. Rev. Mol. Cell. Biol.* **4**, 605-612

Dirks R.W., de Pauw E.S. & Raap A.K. 1997. Splicing factors associate with nuclear HCMV-IE transcripts after transcriptional activation of the gene, but dissociate upon transcription inhibition: evidence for a dynamic organization of splicing factors. *J. Cell Sci.* **110**, 515–522.

Misteli T., Caceres J.F. & Spector D.L. 1997. The dynamics of a pre-mRNA splicing factor in living cells. *Nature* **387**, 523-527

Thiry M. 1995. The interchromatin granules. *Histol. Histopathol.* **10**, 1035–1045

- Visa N., Puvion-Dutilleul F., Bachellerie J. P. & Puvion E. 1993. Intranuclear distribution of U1 and U2 snRNAs visualized by high resolution *in situ* hybridization: revelation of a novel compartment containing U1 but not U2 snRNA in HeLa cells. *Eur. J. Cell Biol.* **60**, 308–321
- Huang S. & Spector D.L. 1991. Nascent pre-mRNA transcripts are associated with nuclear regions enriched in splicing factors. *Genes Dev.* **5**, 2288–2302
- Xing Y., Johnson C.V., Dobner P.R. & Lawrence J.B. 1993. Higher level organization of individual gene transcription and RNA splicing. *Science* **259**, 1326–1330
- Xing, Y., Johnson, C. V., Moen, P. T., McNeil, J. A. & Lawrence, J. B. 1995. Nonrandom gene organization: structural arrangements of specific pre-mRNA transcription and splicing with SC35 domains. *J. Cell Biol.* **131**, 1635–1647
- Smith K.P., Moen P.T., Wydner K.L., Coleman J.R. & Lawrence J.B. 1999. Processing of endogenous pre-mRNAs in association with SC-35 domains is gene specific. *J. Cell Biol.* **144**, 617–629
- Johnson C., D. Primorac, M. McKinsty, J. McNeil, D. Rowe & J. Bentley Lawrence. 2000. Tracking *COL1A1* RNA in osteogenesis imperfecta. Splice-defective transcripts initiate transport from the gene but are retained within the SC35 domain. *J. Cell Biol.* **150**, 417–432
- Hall L.L., Smith K.P., Byron M., Lawrence J.B. 2006. Molecular anatomy of a speckle. *The Anatomical record part A* **288A**, 664–675
- Carter K.C., Taneja K.L., Lawrence J.B. 1991. Discrete nuclear domains of poly(A) RNA and their relationship to the functional organization of the nucleus. *J. Cell Biol.* **115**, 1191-1202
- Carter K.C., Bowman D., Carrington W, Fogarty K., McNeil J.A., Fay F.S., Lawrence J.B. 1993. A three-dimensional view of precursor messenger RNA metabolism within the mammalian nucleus. *Science* **259**, 1330–1335
- Molenaar C., Abdulle A., Gena A., Tanke H.J. & Dirks R.W. 2004. Poly(A)<sup>+</sup> RNAs roam the cell nucleus and pass through speckle domains in transcriptionally active and inactive cells. *J. Cell Biol.* **165**, 191-202
- Schmidt U., Richter K., Berger A. B. & Lichter P. 2006. In vivo BiFC analysis of Y14 and NXF1 mRNA export complexes: preferential localization within and around SC35 domains. *J. Cell Biol.* **172**, 373-381
- Dyck, J.A., Maul, G.G., Miller, W.H., Jr., Chen, J.D., Kakizuka, A. & Evans R.M. 1994. A novel macromolecular structure is a target of the promyelocyte- retinoic acid receptor oncoprotein. *Cell* **76**, 333-343
- Koken M.H.M., Puvion-Dutilleul F., Guillemin M. C., Viron A., Linares- Cruz G., Stuurman N., de Jong L., Szostecki C., Calvo F., Chomienne C. 1994. The t(15;17) translocation alters a nuclear body in a retinoic acid- reversible fashion. *EMBO J.* **13**, 1073-1083
- Weis K., Rambaud S., Lavau C., Jansen J., Carvalho T., Carmo-Fonseca M., Lamond A. & Dejean A. 1994. Retinoic acid regulates aberrant nuclear localization of PML-RAR alpha in acute promyelocytic leukemia cells. *Cell* **76**, 345-356

## Introduction

Stuurman N., De Graaf A., Floore A., Josso A., Humbel B., De Jong L., Van Driel R 1992. A monoclonal antibody recognizing nuclear matrix-associated nuclear bodies. *J Cell Sci* **101**, 773-784

Boisvert F.M., Hendzel M.J. & Bazett-Jones D.P. 2000. Promyelocytic leukemia (PML) nuclear bodies are protein structures that do not accumulate RNA. *J. Cell Biol.* **148**, 283–292

Dellaire G. & Bazett-Jones D.P. 2004. PML nuclear bodies: dynamic sensors of DNA damage and cellular stress. *Bioessays* **26**, 963–977

Eskiw C.H., Dellaire G. & Bazett-Jones D.P. 2004. Chromatin contributes to structural integrity of promyelocytic leukemia bodies through a SUMO-1-independent mechanism. *J. Biol. Chem.* **279**, 9577–9585

Bernstein R.M., Neuberger J.M., Bunn C.C., Callender M.E., Hughes G.R., Williams R. 1984. Diversity of autoantibodies in primary biliary cirrhosis and chronic active hepatitis. *Clin. Exp. Immunol.* **55**, 553-560

Szostecki C., Guldner H.H., Netter H.J., Will H. 1990. Isolation and characterization of cDNA encoding a human nuclear antigen predominantly recognized by autoantibodies from patients with primary biliary cirrhosis. *J. Immunol.* **145**, 4338-4347

Maul G.G., Negorev D., Bell P., Ishov A.M. 2000. Review: properties and assembly mechanisms of ND10, PML bodies, or PODs. *J. Struct. Biol.* **129**, 278-287

de Thé H., Lavau C., Marchio A., Chomienne C., Degos L & Dejean A. 1991. The PML-RAR $\alpha$  fusion mRNA generated by the t(15;17) translocation in acute promyelocytic leukemia encodes a functionally altered RAR. *Cell* **66**, 675-684

Melnick A. & Licht J.D. 1999. Deconstructing a disease: RAR $\alpha$ , its fusion partners, and their roles in the pathogenesis of acute promyelocytic leukemia. *Blood* **93**, 3167-3215

Naeem M., Harrison K., Barton K., Nand S. & Alkan S. 2006. A unique case of acute promyelocytic leukemia showing monocytic differentiation after ATRA (all-trans retinoic acid) therapy. *Eur. J. Hematol.* **76**, 164-166

Weis K., Rambaud S., Lavau C., Jansen J., Carvalho T., Carmo-Fonseca M., Lamond A., Dejean A. 1994. Retinoic acid regulates aberrant nuclear localization of PML-RAR $\alpha$  in acute promyelocytic leukemia. *Cell* **75**, 347-386

Lallemand-Breitenbach V., Jeanne M., Benhenda S., Nasr R., Lei M., Peres L., Zhou J., Zhu J., Raught B. & de Thé H. 2008. Arsenic degrades PML or PML—RAR $\alpha$  through a SUMO-triggered RNF4/ubiquitin-mediated pathway. *Nature Cell Biol.* **10**, 547-555

Tatham M.H., Geoffroy M.-C., Shen L., Plechanovova A., Hattersley N., Jaffray E.G., Palvimo J.J. & Hay R.T. 2008. RNF4 is a poly-SUMO-specific E3 ubiquitin ligase required for arsenic-induced PML degradation. *Nature Cell Biol.* **10**, 538-546

Hodges M., Tissot C., Howe K., Grimwade D. & Freemont P.S. 1998. Structure, organization, and dynamics of promyelocytic leukemia protein nuclear bodies, *Proc. Natl. Acad. Sci. U.S.A.* **59**, 94–101

LaMorte V.J., Dyck J.A., Ochs R.L. & Evans R.M. 1998. Localization of nascent RNA and CREB binding protein with the PML-containing nuclear body. *Proc. Natl. Acad. Sci. U.S.A.* **95**, 4991–4996

- Alcalay M., Tomassoni L., Colombo E., Stoldt S., Grignani F., Fagioli M., Szekely L., Helin K. & Pelicci P.G. 1998. The promyelocytic leukemia gene product (PML) forms stable complexes with the Retinoblastoma protein. *Mol. Cell Biol.* **18**, 1084–1093
- Zhong S., Hu P., Ye T.Z., Stan R., Ellis N.A. & Pandolfi P.P. 1999. A role for PML and the nuclear body in genomic stability. *Oncogene* **18**, 7941–7947
- Zhang T., Xiong H., Kan L.-X., Zhang C.-K., Jiao X.-F., Fu G., Zhang Q.-H., Lu L., Tong J.-H., Gu B.-W., Yu M., Liu J.-X., Licht J., Waxman S., Zelent A., Chen E., Chen S.-J. 1999. Genomic sequence, structural organization, molecular evolution, and aberrant rearrangement of promyelocytic leukemia zinc finger gene. *Proc. Natl. Acad. Sci. USA* **96**, 11422–11427
- Zhong S., Muller S., Ronchetti S., Freemont P.S., Dejean A. & Pandolfi P.P. 2000. Role of SUMO-1-modified PML in nuclear body formation. *Blood* **95**, 2748–2752
- Salomoni P. & Pandolfi P.P. 2002. The role of PML in tumor suppression. *Cell* **108**, 165–170
- Chelbi-Alix M.K., Pelicano L., Quignon F., Koken M.H., Venturini L., Stadler M., Pavlovic J., Degos L., de Thé H. 1995. Induction of the PML protein by interferons in normal and APL cells. *Leukemia* **9**, 2027–2033
- Maul G.G. 1998. Nuclear domain 10, the site of DNA virus transcription and replication. *Bioessays* **20**, 660–667
- Everett R.D., Earnshaw W.C., Pluta A.F., Sternsdorf T., Ainsztein A.M., Carmena M., Ruchaud S., Hsu W.L. & Orr A. 1999. A dynamic connection between centromeres and ND10 proteins. *J. Cell Sci.* **112**, 3443–3454
- Wang Z.G., Ruggero D., Ronchetti S., Zhong S., Gaboli M., Rivi R. & Pandolfi P.P. 1998a. PML is essential for multiple apoptotic pathways. *Nature Genet.* **20**, 266–272
- Wang Z.G., Delva L., Gaboli M., Rivi R., Giorgio M., Cordon-Cardo C., Grosveld F. & Pandolfi P.P. 1998b. Role of PML in cell growth and the retinoic acid pathway. *Science* **279**, 1547–1551
- Wang J., Shiels C., Sasieni P., Wu P.J., Islam S.A., Freemont P.S., Sheer D. 2004. Promyelocytic leukemia nuclear bodies associate with transcriptionally active genomic regions. *J. Cell Biol.* **164**, 515–526
- Graham D. & Bazett-Jones D.P. 2004. PML nuclear bodies: dynamic sensors of DNA damage and cellular stress. *Bioessays*. **26**, 963–977
- Bøe S.O., Haave M., Jul-Larsen Å., Grudic A., Bjerkvig R. & Lønning P.E. 2006. Promyelocytic leukemia nuclear bodies are predetermined processing sites for damaged DNA. *J Cell Sci* **119**, 3284–3295
- Maul G.G., Ishov A.M. & Everett R.D. 1996. Nuclear Domain 10 as Preexisting Potential Replication Start Sites of Herpes Simplex Virus Type-1. *Virology* **217**, 67–75
- Maul G.G. 1998. Nuclear domain 10, the site of DNA virus transcription and replication. *Bioessays* **20**, 660–667
- Guldner H.H., Szosteki C., Grotzinger T. & Will H. 1992. IFN enhance expression of Sp100, an autoantigen in primary biliary cirrhosis. *J. Immunol.* **149**, 4067–4073



## Introduction

Stadler M., Chelbi-Alix M.K., Koken M.H., Venturini L., Lee C., Saïb A., Quignon F., Pelicano L., Guillemain M.C. & Schindler C. 1995. Transcriptional induction of the PML growth suppressor gene by interferons is mediated through an ISRE and a GAS element. *Oncogene* **11**, 2565–2573

Maul G.G., Guldner H.H. & Spivack J.G. Modification of discrete nuclear domains induced by herpes simplex virus type 1 immediate early gene 1 product (ICP0). *J. Gen. Virol.* **74**, 2679-2690

Lavau C., Marchio A., Fagioli M., Jansen J., Falini B., Lebon P., Grosveld F., Pandolfi P.P., Pelicci P.G., Dejean A. 1995. The acute promyelocytic leukaemia-associated PML gene is induced by interferon. *Oncogene* **11**, 871–876

Gaboli M., Gandini D., Delva L., Wang Z.G. & Pandolfi P.P. 1998. Acute promyelocytic leukaemia as a model for cross-talk between interferon and retinoic acid pathways: from molecular biology to clinical applications. *Leuk. Lymph.* **30**, 11–22

Borden K.L.B., Campbell Dwyer E.J. & Salvato M.S. 1998. An arenavirus RING (zinc-binding) protein binds the oncoprotein promyelocyte leukemia protein (PML) and relocates PML nuclear bodies to the cytoplasm. *J. Virol.* **72**, 758-766

Melnick A. & Licht J.D. 1999. Deconstructing a disease: RAR $\alpha$ , its fusion partners, and their roles in the pathogenesis of acute promyelocytic leukemia. *Blood* **93**, 3167-3215

Maul G.G., Negorev D., Bell P. & Ishov A.M. 2000. Review: properties and assembly mechanisms of ND10, PML bodies, or PODs. *J. Struct. Biol.* **129**, 278-287

Turelli P., Doucas V., Craig E., Mangeat B., Klages N., Evans R., Kalpana G. & Trono D. 2001. Cytoplasmic recruitment of INI1 and PML on incoming HIV preintegration complexes: interference with early steps of viral replication. *Mol. Cell* **7**, 1245-1254

Bell P., Montaner L.J. & Maul G.G. 2001. Accumulation and intranuclear distribution of un-integrated human immunodeficiency virus type 1 DNA. *J. Virol.* **75**, 7683-7691

Ishov A.M., Sotnikov A.G., Negorev D., Vladimirova O.V., Neff N., Kamitani T., Yeh E.T., Strauss J.F. 3rd & G.G. Maul. 1999. PML is critical for ND10 formation and recruits the PML-interacting protein daxx to this nuclear structure when modified by SUMO-1. *J. Cell Biol.* **147**, 221–234

Zhong S., Müller S., Ronchetti S., Freemont P.S., Dejean A. & Pandolfi P.P. 2000. Role of SUMO-1-modified PML in nuclear body formation. *Blood* **95**, 2748-2752

Sternsdorf T., Jensen K. & Will H. 1997. Evidence for Covalent Modification of the Nuclear Dot-associated Proteins PML and Sp100 by PIC1/SUMO-1. *J. Cell Biol.* **139**, 1621–1634

Duprez E., Saurin A.J., Desterro J.M., Lallemand-Breitenbach V., Howe K., Boddy M.N., Solomon E., de Thé H., Hay R.T. & Freemont P.S. 1999. SUMO-1 modification of the acute promyelocytic leukaemia protein PML: implications for nuclear localization. *J. Cell Sci.* **112**, 381-393

Shen T.H., Lin H.-K., Scaglioni P.P., Yung T.M. & Pandolfi P.P. 2006. The Mechanisms of PML-Nuclear Body Formation. *Mol Cell.* **24**, 331-339

- Kentsis A., Gordon R.E. & Borden K.L.B. 2002. Control of biochemical reactions through supramolecular RING domain self-assembly. *PNAS* **99**, 15404–15409
- Eskiw C.H., Dellaire G., Mymryk J.S. & Bazett-Jones D.P. 2003. Size, position and dynamic behavior of PML nuclear bodies following cell stress as a paradigm for supramolecular trafficking and assembly *J. Cell Sci.* **116**, 4455–4466
- Seeler J.S. & Dejean A. 2003. Nuclear and unclear functions of SUMO. *Nat Rev Mol Cell Biol.* **4**, 690-699
- Mu Z.M., Chin K.V., Liu J.H., Lozano G. & Chang K.S. 1994. PML, a growth suppressor disrupted in acute promyelocytic leukemia. *Mol Cell Biol* **14**, 6858-6867
- Ahn M.J., Nason-Burchenal K., Moasser M.M., Dmitrovsky E. 1995. Growth suppression of acute promyelocytic leukemia cells having increased expression of the non-rearranged alleles: RAR alpha or PML. *Oncogene* **10**, 2307-2314
- Koken M.H.M., Linares-Cruz G., Quignon F., Viron A., Chelbi-Alix M.K., Sobczak-Thépot J., Juhlin L., Degos L., Calvo F. & de Thé H. 1995. The PML growth-suppressor has an altered expression in human oncogenesis. *Oncogene* **10**, 1315–1324
- Melnick A. & Licht J.D. 1999. Deconstructing a disease: RAR $\alpha$ , its fusion partners, and their roles in the pathogenesis of acute promyelocytic leukemia. *Blood* **93**, 3167-3215
- Gurrieri C., Capodiceci P., Bernardi R., Scaglioni P.P., Nafa K., Rush L.J., Verbel D.A., Cordon-Cardo C., Pandolfi P.P. 2004a. Loss of the tumor suppressor PML in human cancers of multiple histologic origins. *J Natl Cancer Inst* **96**, 269–279
- Chang H.J., Yoo B.C., Kim S.W., Lee B.L., Kim W.H. 2007. Significance of PML and p53 protein as molecular prognostic markers of gallbladder carcinomas. *Pathol Oncol Res* **13**, 326–335
- Ferbeyre G., de Stanchina E., Querido E., Baptiste N., Prives C. & Lowe S.W. 2000. PML is induced by oncogenic *ras* and promotes premature senescence. *Genes Dev.* **14**, 2015–2027
- Liu J.H., Mu Z.M., Chang K.S. 1995. PML suppresses oncogenic transformation of NIH/3T3 cells by activated neu. *J Exp Med* **181**, 1965–1973
- Mu Z.M., Le X.F., Vallian S., Glassman A.B., Chang K.S. 1997. Stable overexpression of PML alters regulation of cell cycle progression in HeLa cells. *Carcinogenesis* **18**, 2063–2069
- Le X.F., Vallian S., Mu Z.M., Hung M.C., Chang K.S. 1998. Recombinant PML adenovirus suppresses growth and tumorigenicity of human breast cancer cells by inducing G1 cell cycle arrest and apoptosis. *Oncogene* **16**, 1839–1849
- Wang Z.G., Ruggero D., Ronchetti S., Zhong S., Gaboli M., Rivi R. & Pandolfi P.P. 1998a. PML is essential for multiple apoptotic pathways. *Nat Genet* **20**, 266–272
- Trotman L.C., Alimonti A., Scaglioni P.P., Koutcher J.A., Cordon-Cardo C., Pandolfi P.P. 2006. Identification of a tumour suppressor network opposing nuclear Akt function. *Nature* **441**, 523–527
- Quignon F., De Bels F., Koken M., Feunteun J., Ameisen J.C., de Thé H. 1998. PML induces a novel caspase-independent death process. *Nature Genet.* **20**, 259–265

## Introduction

- Yang S., Kuo C., Bisi J.E. & Kim M.K. 2002. PML-dependent apoptosis after DNA damage is regulated by the checkpoint kinase hCds1/Chk2. *Nature Cell Biol.* **4**, 865-870
- Tsukamoto T., Hashiguchi N., Janicki S.M., Tumber T., Belmont A.S., Spector D.L. 2000. Visualization of gene activity in living cells. *Nature Cell Biol.* **2**, 871-878
- Maggio R., Siekevitz P. & Palade G.E. 1963a. Studies on isolated nuclei. I. Isolation and chemical composition of a nuclear fraction from guinea pig liver. *J. Cell Biol.* **18**, 267-291
- Penman S. 1966. RNA metabolism in the HeLa cell nucleus. *J. Mol. Biol.* **17**, 117-130
- Blobel G. & Potter V.R. 1966. Nuclei from rat liver: isolation method that combines purity with high yield. *Science* **154**, 1662-1665
- Dounce A.L. 1955. Isolation and composition of nuclei and nucleoli. In *The Nucleic Acids* (Chargaff E. & Davidson J.N. eds), pp. 93-153, Academic Press, New York
- Pederson T. 1997. Preparation of nuclei from tissue or suspension culture. In *Cells: A Laboratory Manual* (Spector, D. L., Goldman, R. D. & Leinwand, L. A., eds), vol. 1, Cold Spring Harbor Laboratory Press, pp. 43.7-43.11, Plainview, NY
- Berezney R. & Coffey D.S. 1974. Identification of a nuclear protein matrix. *Biochem. Biophys. Res. Comm.* **60**, 1410-1417
- Berezny R. & Jeon K. 1995. Nuclear matrix: structural and functional organization. Book.
- Jackson D.A. & Cook P.R. 1988. Visualization of a filamentous nucleoskeleton with a 23 nm axial repeat. *EMBO J.* **7**, 3667-3677
- Capco D.G., Wan K.M., Penman S. 1982. The nuclear matrix: three-dimensional architecture and protein composition. *Cell* **29**, 847-858
- Monneron A. & Bernhard W. 1969. Fine structural organization of the interphase nucleus in some mammalian cells. *J Ultrastruct Res.* **27**, 266-288
- Comings D.E. & Okada T.A. 1976. Nuclear proteins. III. The fibrillar nature of the nuclear matrix. *Exp. Cell Res.* **103**, 341-60
- Small D., Nelkin B. & Vogelstein B. 1985. The association of transcribed genes with the nuclear matrix of *Drosophila* cells during heat shock. *Nucleic Acids Research* **13**, 2413-2431
- Fey E.G., Krochmalnic G. & Penman S. 1986. The nonchromatin substructures of the nucleus: The ribonucleoprotein (RNP)-containing and RNP-depleted matrices analyzed by sequential fractionation and resinless section electron microscopy. *The J. Cell Biol.* **102**, 1654-1665
- Jackson D.A. & Cook P.R. 1988. Visualization of a filamentous nucleoskeleton with a 23 nm axial repeat. *EMBO J.* **7**, 3667-3677
- Mirkovitch J., Mirault M.E. and Laemmli U.K. 1984. Organization of the higher-order chromatin loop: Specific DNA attachment sites on nuclear scaffold. *Cell* **39**, 223-232.

- Martelli A.M., Falcieri E., Gobbi P., Manzoli L., Gilmour R.S. & Cocco L. 1991. Heat-induced stabilization of the nuclear matrix: A morphological and biochemical analysis in murine erythroleukemia cells. *Exp. Cell Res.* **19**, 216-225
- Neri L.M., Fackelmayer F.O., Zweyer M., Kohwi-Shigematsu T. & Martelli A.M. 1997. Sub-nuclear localization of s/mar-binding proteins is differently affected by in vitro stabilization with heat or  $\text{Cu}^{2+}$ . *Chromosoma* **106**, 81-93
- Kaufmann S.H. & Shaper J.H. 1984. A subset of non-histone nuclear proteins reversibly stabilized by the sulfhydryl cross-linking reagent tetrathionate. Polypeptides of the internal nuclear matrix. *Exp. Cell Res.* **155**, 477-495
- Berezney R. & Coffey D.S. 1977. Nuclear matrix. Isolation and characterization of a framework structure from rat liver nuclei. *J. Cell Biol.* **73**, 616-637
- Palade G.E. & Siekevitz P. 1956. Liver microsomes. An integrated morphological and biochemical study. *J. Biophys. Biochem. Cytol.* **2**, 171-200
- Tashiro Y. 1958. Studies on the ribonucleoprotein particles. III. Some physicochemical characteristics and the degradation with ribonuclease and trypsin of the microsomal ribonucleoprotein particles. *J. Biochem.* **45**, 803-813
- Madison J.T. & Dickman S.R. 1963. Beef pancreas ribosomes: stability. *Biochem.* **2**, 325-332
- Lothstein L., Arenstorf H.P., Chung S.-Y., Walker B.W., Wooley J.C. & LeSturgeon W.M. 1985. General organization of protein in HeLa 40 S nuclear ribonucleoprotein particles. *J. Cell Biol.* **100**, 1 1570-1581
- Kauzmann W. Some factors in the interpretation of protein denaturation. 1959. In: C.B. Anfinsen, Jr, M.L. Anson, K. Bailey & J.T. Edsall editors. *Advances in Protein Chemistry* **14**, 1-63
- Varshavsky A.J. & Ilyin Y.V. 1974. Salt treatment of chromatin induces redistribution of histones. *Biochim. Biophys. Acta* **340**, 207-217
- Finkelstein A.V., Protein structure: what is it possible to predict now? 1997. *Curr. Opin. Struct. Biol.* **7**, 60-71
- Ben-Ze'ev A., Abulafia R. & Aloni Y. SV40 virions and viral RNA metabolism are associated with subcellular structures. 1982. *EMBO J.* **1**, 1225-1231
- Ciejek E.M., Nordstrom J.L., Tsai M.-J. & O'Malley B.W. 1982. Ribonucleic acid precursors are associated with the chick oviduct nuclear matrix. *Biochemistry* **21**, 4945-4953
- Mariman E.C.M., van Eckelen C.A.G., Reinders R.J., Berns A.J.M. & van Venrooij W.J. 1982. Adenoviral heterogeneous nuclear RNA is associated with the host nuclear matrix during splicing. *J. Mol. Biol.* **154**, 103-119
- Ross D.A., Yen R.-W. & Chae C.B. 1982. Association of globin ribonucleic acid and its precursors with the chicken erythroblast nuclear matrix. *Biochemistry* **21**, 754-771
- Gallinaro H., Puvion E., Kister L. & Jacob M. 1983. Nuclear matrix and hnRNP share a common structural constituent associated with premessenger RNA. *EMBO J.* **2**, 953-960

## Introduction

Ben-Ze'ev A. & Aloni Y. 1983. Processing of SV40 RNA is associated with the nuclear matrix and is not followed by the accumulation of low-molecular-weight RNA products. *Virology* **125**, 475–479

Mortillaro M.J., Blencowe B.J., Wei X., Nakayasu H., Du H., Warren S.L., Sharp P.A. & Berezney R. 1996. A hyperphosphorylated form of the large subunit of RNA polymerase II is associated with splicing complexes and the nuclear matrix. *Proc. Natl Acad. Sci. USA* **93**, 8253–8257

Vincent M., Lauriault P., Dubois M.-F., Lavoie S., Bensaude O. & Chabot B. 1996. The nuclear matrix protein p225 is a highly phosphorylated form of RNA polymerase II largest subunit which associates with spliceosomes. *Nucl. Acids Res.* **24**, 4649–4652

Dahmus M.E. 1996. Reversible phosphorylation in the C-terminal domain of RNA polymerase II. *J. Biol. Chem.* **271**, 19009–19012

Konety B.R., Getzenberg R.H. 1999. Nuclear structural proteins as biomarkers of cancer. *J. Cell Biochem.* **32/33**, 183-191

Ozen H. 1999. Bladder cancer. *Curr. Opin. Oncol.* **11**, 207-212

Stuurman N., Heins S., Aebi U. 1998. Nuclear lamins: their structure, assembly, and interactions. *J. Struct Biol.* **122**, 42–66

Goldman R.D., Gruenbaum Y., Moir R.D., Shumaker D.K., Spann T.P. 2002. Nuclear lamins: building blocks of nuclear architecture. *Genes Dev.* **16**, 533–547

Hutchison C.J. 2002. Lamins: building blocks or regulators of gene expression? *Nat.Rev. Mol. Cell Biol.* **3**, 848–858

Mounkes L., Kozlov S., Burke B., Stewart C.L. 2003. The laminopathies: nuclear structure meets disease. *Curr. Opin. Genet. Dev.* **13**, 223–230

Bonne G., Di Barletta M.R., Varnous S., Bécane H.M., Hammouda E.H., Merlini L., Muntoni F., Greenberg C.R., Gary F., Urtizberea J.A., Duboc D., Fardeau M., Toniolo D., Schwartz K. 1999. Mutations in the gene encoding lamin A/C cause autosomal dominant Emery-Dreifuss muscular dystrophy. *Nat. Genet.* **21**, 285-288

Fatkin D., MacRae C., Sasaki T., Wolff M.R., Porcu M., Frenneaux M., Atherton J., Vidaillet H.J. Jr, Spudich S., De Girolami U., Seidman J.G., Seidman C., Muntoni F., Muehle G., Johnson W., McDonough B. 1999. Missense mutations in the rod domain of the lamin A/C gene as causes of dilated cardiomyopathy and conduction-system disease. *N. Engl. J. Med.* **341**, 1715-1724

Cao H. & Hegele R.A. 2000. Nuclear lamin A/C R482Q mutation in canadian kindreds with Dunnigan-type familial partial lipodystrophy. *Hum. Mol. Genet.* 2000. **9**, 109-112

Shackleton S., Lloyd D.J., Jackson S.N., Evans R., Niermeijer M.F., Singh B.M., Schmidt H., Brabant G., Kumar S., Durrington P.N., Gregory S., O'Rahilly S., Trembath R.C. 2000. LMNA, encoding lamin A/C, is mutated in partial lipodystrophy. *Nat. Genet.* **24**, 153-156

Burke B. & Stewart C.L. 2002. Life at the edge: the nuclear envelope and human disease. *Nat. Rev. Mol. Cell Biol.* **3**, 575-585

De Sandre-Giovannoli A., Bernard R., Cau P., Navarro C., Amiel J., Boccaccio I., Lyonnet S., Stewart C.L., Munnich A., Le Merrer M., Lévy N. 2003. Lamin A truncation in Hutchinson-Gilford progeria. *Science* **300**, 2055

Eriksson M., Brown W.T., Gordon L.B., Glynn M.W., Singer J., Scott L., Erdos M.R., Robbins C.M., Moses T.Y., Berglund P., Dutra A., Pak E., Durkin S., Csoka A.B., Boehnke M., Glover T.W. & Collins F.S. 2003. Recurrent de novo point mutations in lamin A cause Hutchinson-Gilford progeria syndrome. *Nature* **423**, 293-298

Lebel S., Lampron C., Royal A., & Raymond Y. 1987. Lamins A and C Appear during Retinoic Acid-induced Differentiation of Mouse Embryonal Carcinoma Cells. *The Journal of Cell Biology* **105**, 1099-1104

Stuurman N., Heins S., Aebi U. 1998. Nuclear lamins: their structure, assembly, and interactions. *J. Struct. Biol.* **122**, 42–66

Moir R. D., Miri Yoon, Satya Khuon & Robert D. Goldman. 2000. Nuclear Lamins A and B1: Different Pathways of Assembly during Nuclear Envelope Formation in Living Cells. *J. Cell Biol.* **151**, 1155-1168

Foisner R. 2001. Inner nuclear membrane proteins and the nuclear lamina. *J. Cell Sci.* **114**, 3791-3792

Lenz-Bohme B., Wismar J., Fuchs S., Reifegerste R., Buchner E., Betz H., Schmitt B. 1997. Insertional mutation of the *Drosophila* nuclear lamin Dm0 gene results in defective nuclear envelopes, clustering of nuclear pore complexes, and accumulation of annulate lamellae. *J. Cell Biol.* **137**, 1001–1016

Schirmer E.C., Guan T., Gerace L. 2001. Involvement of the lamin rod domain in heterotypic lamin interactions important for nuclear organization. *J. Cell Biol.* **153**, 479–489

Moir R.D., Spann T.P. & Goldman R.D. 1995. The dynamic properties and possible functions of nuclear lamins. *Int. Rev. Cytol.* **162B**, 141-182

Gant T.M. & Wilson K.L. 1997. Nuclear assembly. *Annu. Rev. Cell Dev. Biol.* **13**, 669-695

Stuurman N., Heins S. & Aebi U. 1998. Nuclear lamins: Their structure, assembly and interactions. *J. Struct. Biol.* **122**, 42-66

Gant T.M., Harris C.A., Wilson K.L. 1999. Roles of LAP2 proteins in nuclear assembly and DNA replication: truncated LAP2beta proteins alter lamina assembly, envelope formation, nuclear size, and DNA replication efficiency in *Xenopus laevis* extracts. *J. Cell Biol.* **144**, 1083–1096

Goldman A.E., Moir R.D., Montag-Lowy M., Stewert M. & Goldman R.D. 1992. Pathway of incorporation of microinjected lamin A into the nuclear envelope. *J. Cell Biol.* **119**, 725-735

Bridger J.M., Kill I.R., O'Farrell M. & Hutchison C.J. 1993. Internal lamin structures within G1 nuclei of human dermal fibroblasts. *J. Cell Sci.* **104**, 297-306

Moir R.D., Montaglowy M. & Goldman R.D. 1994. Dynamic properties of nuclear lamins: Lamin B is associated with sites of DNA replication. *J. Cell Biol.* **125**, 1201-1212

## Introduction

Hozak P., Sasseville A.M-J., Raymond Y. & Cook P.R. 1995. Lamin proteins form an internal nucleoskeleton as well as a peripheral lamina in human cells. *J. Cell Sci.* **108**, 635-644

Jenkins H., Whitfield W.G., Goldberg M.W., Allen T.D., Hutchison C.J. 1995. Evidence for the direct involvement of lamins in the assembly of a replication competent nucleus. *Acta Biochim. Pol.* **42**, 133-143

Goldman R.D., Gruenbaum Y., Moir R.D., Shumaker D.K. & Spann T.P. 2002. Nuclear lamins: building blocks of nuclear architecture. *Genes Dev.* **16**, 533-547

Martins S., Eikvar S., Furukawa K., Collas P. 2003. HA95 and LAP2 beta mediate a novel chromatin-nuclear envelope interaction implicated in initiation of DNA replication. *J. Cell Biol.* **160**, 177-188

Gruenbaum Y., Goldman R.D., Meyuhas R., Mills E., Margalit A., Fridkin A., Dayani Y., Prokocimer M., Enosh A. 2003. The nuclear lamina and its functions in the nucleus. *Int. Rev. Cyt.* **226**, 1-62

Nili E., Cojocar G.S., Kalma Y., Ginsberg D., Copeland N.G., Gilbert D.J., Jenkins N.A., Berger R., Shaklai S., Amariglio N., Brok-Simoni F., Simon A.J., Rechavi G. 2001. Nuclear membrane protein LAP2 mediates transcriptional repression alone and together with its binding partner GCL (germ-cell-less). *J. Cell Sci.* **114**, 3297-3307

Spann T.P., Goldman A.E., Wang C., Huang S., Goldman R.D. 2002. Alteration of nuclear lamin organization inhibits RNA polymerase II-dependent transcription. *J. Cell Biol.* **156**, 603-608

Wilkinson F.L., Holaska J.M., Zhang Z., Sharma A., Manilal S., Holt I., Stamm S., Wilson K.L., Morris G.E. 2003. Emerin interacts *in vitro* with the splicing-associated factor, YT521-B. *Eur. J. Biochem.* **270**, 459-2466

Haraguchi T., Holaska J.M., Yamane M., Koujin T., Hashiguchi N., Mori C., Wilson K.L., Hiraoka Y. 2004. Emerin binding to Btf, a death-promoting transcriptional repressor, is disrupted by a missense mutation that causes Emery-Dreifuss muscular dystrophy. *Eur. J. Biochem.* **271**, 1035-1045

Lin F., Blake D.L., Callebaut I., Skerjanc I.S., Holmer L., McBurney M.W., Paulin-Levasseur M., Worman H.J. 2000. MAN1, an inner nuclear membrane protein that shares the LEM domain with lamina-associated polypeptide 2 and emerin. *J. Biol. Chem.* **275**, 4840-4847

Foisner R. 2001. Inner nuclear membrane proteins and the nuclear lamina. *J. Cell Sci.* **114**, 3791-3792

Gruenbaum Y., Goldman R.D., Meyuhas R., Mills E., Margalit A., Fridkin A., Dayani Y., Prokocimer M., Enosh A. 2003. The nuclear lamina and its functions in the nucleus. *Int. Rev. Cyt.* **226**, 1-62

Zastrow, M.S., Vlcek, S. & Wilson, K.L. 2004. Proteins that bind A-type lamins: integrating isolated clues. *J. Cell Sci.* **117**, 979-987

Sullivan T., Escalante-Alcalde D., Bhatt H., Anverc M., Bhatc N., Nagashimac K., Stewart C. L. & Burked B. 1999. Loss of A-type lamin expression compromises nuclear envelope integrity leading to muscular dystrophy. *J. Cell Biol.* **147**, 913-920

- Lee K.K., Starr D., Cohen M., Liu J., Han M., Wilson K.L. & Gruenbaum Y. 2002. Lamin-dependent localization of UNC-84, a protein required for nuclear migration in *C. elegans*. *Mol. Biol. Cell* **13**, 892–901
- Liu J., Lee K.K., Segura-Totten M., Neufeld E., Wilson K.L. & Gruenbaum Y. 2003. MAN1 and emerlin have overlapping function(s) essential for chromosome segregation and cell division in *C. elegans*. *Proc. Natl Acad. Sci. USA* **100**, 4598–4603
- Muchir A., van Engelen B.G., Lammens M., Mislow J.M., McNally E., Schwartz K. & Bonne G. 2003. Nuclear envelope alterations in fibroblasts from LGMD1B patients carrying nonsense Y259X heterozygous or homozygous mutation in lamin A/C gene. *Exp. Cell Res.* **291**, 352–362
- Wagner N., Schmitt J. & Krohne G. 2004. Two novel LEM-domain proteins are splice products of the annotated *Drosophila melanogaster* gene CG9424 (*Bocksbeutel*). *Euro. J. Cell Biol.* **82**, 605–616
- Guillemin K., Williams T. & Krasnow M.A.A. 2001. Nuclear lamin is required for cytoplasmic organization and egg polarity in *Drosophila*. *Nature Cell Biol.* **3**, 848–851
- Raz V., Carlotti F., Vermolen B.J., van der Poel E., Sloos W.C.R., Knaän-Shanzer S., de Vries A.A.F., Hoeben R.C., Young I.T., Tanke H.J., Garini Y. & Dirks R.W. 2006. Changes in lamina structure are followed by spatial reorganization of heterochromatic regions in caspase-8-activated human mesenchymal stem cells. *J. Cell Sci.* **119**, 4247–4256
- Raz V., Vermolen B.J., Garini Y., Onderwater J.J.M., Mommaas-Kienhuis M.A., Koster A.J., Young I.T., Tanke H.J. & Dirks R.W. 2008. The nuclear lamina promotes telomere aggregation and centromere peripheral localization during senescence of human mesenchymal stem cells. *J. Cell Sci.* **121**, 4018–4028
- Liu J., Ben-Shahar T.R., Riemer D., Treinin M., Spann P., Weber K., Fire A. & Y.Gruenbaum. 2000. Essential roles for *Caenorhabditis elegans* lamin gene in nuclear organization, cell cycle progression, and spatial organization of nuclear pore complexes. *Mol. Biol. Cell* **11**, 3937–3947
- Schirmer E.C., Guan T. & Gerace L. 2001. Involvement of the lamin rod domain in heterotypic lamin interactions important for nuclear organization. *J. Cell Biol.* **153**, 479–490
- Starr D.A., Hermann G.J., Malone C.J., Fixsen W., Priess J.R., Horvitz H.R. & Han M. 2001. *unc-83* encodes a novel component of the nuclear envelope and is essential for proper nuclear migration. *Development* **128**, 5039–5050
- Starr D.A. & Han M. 2002. Role of ANC-1 in tethering nuclei to the actin cytoskeleton. *Science* **11**, 406–409
- Lopez-Soler R.I., Moir R.D., Spann T.P., Stick R. & Goldman R.D. 2001. A role for nuclear lamins in nuclear envelope assembly. *J. Cell Biol.* **154**, 61–70
- Guelen L., Pagie L., Brassat E., Meuleman W., Faza M.B., Talhout W., Eussen B.H., de Klein A., Wessels L., de Laat W., van Steensel B. 2008. Domain organization of human chromosomes revealed by mapping of nuclear lamina interactions. *Nature* **453**, 948–951



## Introduction

Zhang Q., Skepper J.N., Yang F., Davies J.D., Hegyi L., Roberts R.G., Weissberg P.L., Ellis J.A. & Shanahan C.M. 2001. Nesprins: a novel family of spectrin-repeat-containing proteins that localize to the nuclear membrane in multiple tissues. *J. Cell Sci.* **114**, 4485–4498

Mislow J.M., Kim M.S., Davis D.B. & McNally E.M. 2002. Myne-1, a spectrin repeat transmembrane protein of the myocyte inner nuclear membrane, interacts with lamin A/C. *J. Cell Sci.* **115**, 61–70

Zhen Y.Y., Libotte T., Munck M., Noegel A.A. & Korenbaum E. 2002. NUANCE, a giant protein connecting the nucleus and actin cytoskeleton, *J. Cell Sci.* **115**, 3207–3222

Wilhelmsen K., Litjens S.H., Kuikman I., Tshimbalanga N., Janssen H., van den Bout I., Raymond K. & Sonnenberg A. 2005. Nesprin-3, a novel outer nuclear membrane protein, associates with the cytoskeletal linker protein plectin. *J. Cell Biol.* **171**, 799–810

Wang N. & Suo Z. 2005. Long-distance propagation of forces in a cell. *Biochem. Biophys. Res. Commun.* **328**, 1133–1138

Mislow J.M., Holaska J.M., Kim M.S., Lee K.K., Segura-Totten M., Wilson K.L. & McNally E.M. 2002. Nesprin-1alpha self-associates and binds directly to emerin and lamin A in vitro. *FEBS Lett.* **525**, 135–140

Padmakumar V.C., Libotte T., Lu W., Zaim H., Abraham S., Noegel A.A., Gotzmann J., Foisner R. & Karakesisoglou I. 2005. The inner nuclear membrane protein Sun1 mediates the anchorage of Nesprin-2 to the nuclear envelope. *J. Cell Sci.* **118**, 3419–3430

Lammerding J., Schulze P.C., Takahashi T., Kozlov S., Sullivan T., Kamm R.D., Stewart C.L. & Lee R.T. 2004. Lamin A/C deficiency causes defective nuclear mechanics and mechanotransduction. *J. Clin. Invest.* **113**, 370–378

Broers J.L., Peeters E.A., Kuijpers H.J., Endert J., Bouten C.V., Oomens C.W., Baaijens F.P. & Ramaekers F.C. 2004. Decreased mechanical stiffness in LMNA<sup>-/-</sup> cells is caused by defective nucleo-cytoskeletal integrity: implications for the development of laminopathies. *Hum. Mol. Genet.* **13**, 2567–2580

Broers J.L., Kuijpers H.J., Ostlund C., Worman H.J., Endert J. & Ramaekers F.C. 2005. Both lamin A and lamin C mutations cause lamina instability as well as loss of internal nuclear lamin organization. *Exp. Cell Res.* **304**, 582–592

Cohen M., Lee K.K., Wilson K.L., Gruenbaum Y. 2001. Transcriptional repression, apoptosis, human disease and the functional evolution of the nuclear lamina. *Trends Biochem Sci.* **26**, 41–47

Jackson D.A. & Cook P.R. 1988. Visualization of a filamentous nucleoskeleton with a 23 nm axial repeat. *EMBO J.* **7**, 3667–3677

He D., Nickerson J.A. & Penman S. 1990. Core filaments of the nuclear matrix. *J. Cell Biol.* **110**, 569–580

Hozák P., Sasseville A.M.-J., Raymond Y. & Cook P.R. 1995. Lamin proteins form an internal nucleoskeleton as well as a peripheral lamina in human cells. *J. Cell Sci.* **108**, 635–644

Wan K.M., Nickerson J.A., Krockmalnic G. & Penman S. 1999. The nuclear matrix prepared by amine modification. *Proc. Natl. Acad. Sci. USA* **96**, 933–938

- Traub P. & Shoeman R.L. 1994. Intermediate filament proteins: cytoskeletal elements with gene-regulatory functions? *Int. Cytol. Rev.* **154**, 1-103
- Goldman A.E., Moir R.D., Montag-Lowy M., Stewart M. & Goldman R.D. 1992. Pathway of incorporation of microinjected lamin A into the nuclear envelope. *J. Cell Biol.* **119**, 725-735
- Bridger J.M., Kill I.R., O'Farrell M. & Hutchison C.J. 1993. Internal lamin structures within G1 nuclei of human dermal fibroblasts. *J. Cell Sci.* **104**, 297-306
- Moir R.D., Montag-Lowy M. & Goldman R.D. 1994. Dynamic properties of nuclear lamins: lamin B is associated with sites of DNA replication. *J. Cell Biol.* **125**, 1201-1212
- Schmidt M., Tschödrich-Rotter M.M., Peters R. & Krohne G. 1994. Properties of fluorescently labeled Xenopus lamin A in vivo. *Eur. J. Cell Biol.* **65**, 70-81
- Kiseleva E., Drummond S.P., Goldberg M.W., Rutherford S.A., Allen T.D. & Wilson K.L. 2004. Actin- and protein-4.1-containing filaments link nuclear pore complexes to subnuclear organelles in Xenopus oocyte nuclei. *Journal of Cell Science* **117**, 2481-2490
- Pestic-Dragovich L., Stojiljkovic L., Philimonenko A.A., Nowak G., Ke Y., Settlage R.E., Shabanowitz J., Hunt D.F., Hozak P., de Lanerolle P. 2000. A Myosin I Isoform in the Nucleus. *Science* **290**, 337-341
- Clark T.G. & Merriam R.W. 1977. Diffusible and bound actin in nuclei of *Xenopus laevis* oocytes. *Cell.* **12**, 883-891
- Fukui Y. 1978. Intranuclear actin bundles induced by dimethyl sulfoxide in interphase nucleus of Dictyostelium. *J. Cell Biol.* **76**, 146-157
- Fukui Y., Katsumaru H. 1979. Nuclear actin bundles in Amoeba, Dictyostelium and human HeLa cells induced by dimethyl sulfoxide. *Exp. Cell Res.* **120**, 451-455
- Clark T.G. & Rosenbaum J.L. 1979. An actin filament matrix in hand-isolated nuclei of *X. laevis* oocytes. *Cell* **18**, 1101-1108
- Osborn M. & Weber K. 1980. Dimethylsulfoxide and the ionophore A23187 affect the arrangement of actin and induce nuclear actin paracrystals in PtK2 cells. *Exp. Cell Res.* **129**, 103-114
- Welch W.J. & Suhan J.P. 1985. Morphological study of the mammalian stress response. characterization of changes in cytoplasmic organelles, cytoskeleton, and nucleoli, and appearance of intranuclear actin filaments in rat fibroblasts after heat-shock treatment. *J. Cell Biol.* **101**, 1198-1211
- DeBoni U. 1994. The interphase nucleus as a dynamic structure. *Int. Rev. Cytol.* **150**, 149-171
- Yan C., Leibowitz N., Mélése T. 1997. A role for the divergent actin gene, ACT2 in nuclear pore structure and function. *EMBO J.* **16**, 3572-3586
- Rando O. J., Zhao K. & Crabtree G.R. 2000. Searching for a function for nuclear actin. *Trends Cell Biol.* **10**, 92-97
- Pederson T. & Aebi U. 2002. Actin in the nucleus: what form and what for? *J. Struct. Biol.* **140**, 3-9

## Introduction

Bettinger B.T., Gilbert D.M. & Amberg D.C. 2004. Actin up in the nucleus. *Nature Reviews Molecular Cell Biology* **5**, 410-415

Ankenbauer T., Kleinschmidt J.A., Walsh M.J., Weiner O.H. & Franke W.W. 1989. Identification of a widespread nuclear actin binding protein. *Nature*, **342**, 822-825

Rimm D.L. & Pollard T.D. 1989. Purification and characterization of an *Acanthamoeba* nuclear actin-binding protein. *J. Cell Biol.* **109**, 585-591

Hauser M., Beinbrech G., Groschel-Stewart U. & Jockusch B.M. 1975. Localisation by immunological techniques of myosin in nuclei of lower eukaryotes. *Expt. Cell Res.* **95** 127-135.

Berrios M. & Fisher P.A. 1986. A myosin heavy-chain-like polypeptide is associated with the nuclear envelope in higher eukaryotic cells. *J. Cell Biol.* **103**, 711-724

Hagen S.J., Kiehart D.P., Kaiser D.A. & Pollard T.D. 1986. Characterization of monoclonal antibodies to *Acanthamoeba* myosin-I that cross react with both myosin-II and low molecular mass nuclear proteins. *J. Cell Biol.* **103**, 2121-2128

Rimm D.L. & Pollard T.D. 1989. Purification and characterization of an *Acanthamoeba* nuclear actin-binding protein. *J. Cell Biol.* **109**, 585-591

Nowak G., Pestic-Dragovich L., Hozak P., Philomenokov A., Simerly C., Schatten G. & de Lanerolle P. 1997. Evidence for the presence of myosin I in the nucleus. *J. Biol. Chem.* **272**, 17176-17181

Scheer U., Hinssen H., Franke W.W. & Jockusch B.M. 1984. Microinjection of actin-binding proteins and actin antibodies demonstrates involvement of nuclear actin in transcription of lampbrush chromosomes. *Cell* **39**, 111-122

Sahlas D.J., Milankov K., Park P.C. & De Boni U. 1993. Distribution of snRNPs, splicing factor SC-35 and actin in interphase nuclei: immunocytochemical evidence for differential distribution during changes in functional states. *J. Cell Sci.* **105**, 347-357

Machesky L.M. & May R.C. 2001. Arps: actin-related proteins. *Results Probl. Cell Diff.* **32**, 213-229

Goodson H.V. & Hawse W.F. 2002. Molecular evolution of the actin family. *J. Cell Sci.* **115**, 2619-2622

Olave I., Wang W., Xue Y., Kuo A., Crabtree G.R. 2002. Identification of a polymorphic, neuron-specific chromatin remodeling complex. *Genes Dev.* **16**, 2509-2517

Clark T.G. & Merriam R.W. 1977. Diffusible and bound actin in nuclei of *Xenopus laevis* oocytes. *Cell* **12**, 883-891

Funaki K., Katsumoto T. & Iino A. 1995. Immunocytochemical localization of actin in the nucleolus of rat oocytes. *Biol. Cell* **84**, 139-146

Parfenov V.N., Davis D.S., Pochukalina G.N., Sample C.E., Bugaeva E.A. & Murti K.G. 1995. Nuclear actin and their topological changes in frog oocytes. *Exp. Cell Res.* **217**, 385-394

- Pestic-Dragovich L., Stojiljkovic L., Philimonenko A.A., Nowak G., Ke Y., Settlage R. E., Shabanowitz J., Hunt D.F., Hozak P. & de Lanerolle P. 2000. A myosin I isoform in the nucleus. *Science* **290**, 337- 341
- Pederson T. & Aebi U. 2002. Actin in the nucleus: what form and what for? *J. Struct. Biol.* **140**, 3-9
- Bettinger B.T., Gilbert D.M. & Amberg D.C. 2004. Actin up in the nucleus. *Nature Reviews Molecular Cell Biology* **5**, 410-415
- Fukui Y. & Katsumaru H. 1979. Nuclear actin bundles in Amoeba, Dictyostelium and human HeLa cells induced by dimethyl sulfoxide. *Exp. Cell Res.* **120**, 451–455
- Iida K., Iida H. & Yahara I. 1986. Heat shock induction of intranuclear actin rods in cultured mammalian cells. *Exp. Cell Res.* **165**, 207–215
- Iida K. & Yahara I. 1986. Reversible induction of actin rods in mouse C3H–2K cells by incubation in salt buffers and by treatment with non-ionic detergents. *Exp. Cell Res.* **164**, 492–506
- Nishida E., Iida K., Yonezawa N., Koyasu S., Yahara, I. & Sakai H. 1987. Cofilin is a component of intranuclear and cytoplasmic actin rods induced in cultured cells. *Proc. Natl. Acad. Sci. USA* **84**, 5262–5266
- Wada A., Fukuda M., Mishima M. & Nishida E. 1998. Nuclear export of actin: a novel mechanism regulating the subcellular localization of a major cytoskeletal protein. *EMBO J.* **17**, 1635–1641
- Sameshima M., Kishi Y., Osumi M., Minamikawa-Tachino R., Mahadeo D. & Cotter D. A. 2001. The formation of actin rods composed of actin tubules in *Dictyostelium discoideum* spores. *J. Struct. Biol.* **136**, 7–19
- Sasseville A.M-J. & Langelier Y. 1998. *In vitro* interaction of the carboxy-terminal domain of lamin A with actin. *FEBS Lett.* **425**, 485-489
- Holaska J.M., Kowalski A.K. & Wilson K.L. 2004. Emerin caps the pointed end of actin filaments: evidence for an actin cortical network at the nuclear inner membrane. *PLoS Biol.* **2**, E231
- Zhang Q., Ragnauth C., Greener M J., Shanahan C.M. & Roberts R.G. 2002. The nesprins are giant actin-binding proteins, orthologous to *Drosophila melanogaster* muscle protein MSP-300. *Genomics* **80**, 473-481
- Zhen Y.Y., Libotte Y., Munck M., Noegel A.A. & Korenbaum E. 2002. NUANCE, a giant protein connecting the nucleus and actin cytoskeleton. *J. Cell Sci.* **115**, 3207-3222
- Correas I. 1991. Characterization of isoforms of protein 4.1 present in the nucleus. *Biochem. J.* **279**, 581-585
- Krauss S.W., Larabell C.A., Lockett S., Gascard P., Penman S., Mohandas N. & Chasis J.A. 1997. Structural protein 4.1 in the nucleus of human cells: dynamic rearrangements during cell division. *J. Cell Biol.* **137**, 275-289
- Luque C.M. & Correas I. 2000. A constitutive region is responsible for nuclear targeting of 4.1R: modulation by alternative sequences results in differential intracellular localization. *J. Cell Sci.* **113**, 2485-2495

## Introduction

Holaska J.M., Kowalski A.K. & Wilson K.L. 2004. Emerin caps the pointed end of actin filaments: evidence for an actin cortical network at the nuclear inner membrane. *PLoS Biol.* **2**, E231

Krauss S.W., Chen C., Penman S. & Heald R. 2003. Nuclear actin and protein 4.1: essential interactions during nuclear assembly *in vitro*. *Proc. Natl Acad. Sci. USA* **100**, 10752–10757

Castano E., Philimonenko V.V., Kahle M., Fukalova J., Kalendova A., Yildirim S., Dzijak R., Dingova-Krasna H., Hozak P. 2010. Actin complexes in the cell nucleus: new stones in an old field. *Histochem Cell Biol.* **133**, 607-626

Harley C.B., Futcher A.B. & Greider C.W. 1990. Telomeres shorten during ageing of human fibroblasts. *Nature* **345**, 458-460

Martens U.M., Chavez E.A., Poon S.S., Schmoor C. & Lansdorp P.M. 2000. Accumulation of short telomeres in human fibroblasts prior to replicative senescence. *Exp. Cell Res.* **256**, 291-299

Blasco M.A. 2007. Telomere length, stem cells and aging. *Nat Chem Biol* **3**, 640-649

Hayflick L. 1965. The limited in vitro lifetime of human diploid cell strains. *Experimental Cell Research* **37**, 614–636

Blackburn E.H. 2001. Switching and signaling at the telomere. *Cell* **106**, 661-73

de Lange T. 2005. Shelterin: The protein complex that shapes and safeguards human telomeres. *Genes Dev.* **19**, 2100–2110

Shay J.W. & Wright W.E. 2004. Telomeres are double-strand DNA breaks hidden from DNA damage responses. *Mol. Cell* **14**, 420–421

d'Adda di Fagagna F., Teo S.H. & Jackson S.P. 2004. Functional links between telomeres and proteins of the DNA-damage response. *Genes Dev.* **18**, 1781–1799

Griffith J.D., Comeau L., Rosenfield S., Stansel R.M., Bianchi A., Moss H., de Lange T., Karlseder J., Broccoli D., Dai Y. & Hardy S. 1999. Mammalian telomeres end in a large duplex loop. *Cell* **97**, 503-514

van Steensel B., Smogorzewska A. & de Lange T. 1998. TRF2 Protects Human Telomeres from End-to-End Fusions. *Cell* **92**, 401-413

Wright J.H., Gottschling D.E. & Zakian V.A. 1992. Saccharomyces telomeres assume a non-nucleosomal chromatin structure. *Genes Dev.* **6**, 197–210

Li B., Oestreich S. & de Lange T. 2000. Identification of human Rap1: implications for telomere evolution. *Cell* **101**, 471–483

Hsu H.L., Gilley D., Galande S.A., Hande M.P., Allen B., Kim S.H., Li G.C., Campisi J., Kohwi-Shigematsu T., Chen D.J. 2000. Ku acts in a unique way at the mammalian telomere to prevent end joining. *Genes Dev* **14**, 2807-2812

Kim S.H., Kaminker P., Campisi J. 1999. TIN2, a new regulator of telomere length in human cells. *Nat Genet* **23**, 405-412

- Ye J.Z., Donigian J.R., van Overbeek M., Loayza D., Luo Y., Krutchinsky A.N., Chait B.T., de Lange T. 2004. TIN2 binds TRF1 and TRF2 simultaneously and stabilizes the TRF2 complex on telomeres. *J. Biol. Chem.* **279**, 47264-47271
- Houghtaling B.R., Cuttonaro L., Chang W. & Smith S. 2004. A dynamic molecular link between the telomere length regulator TRF1 and the chromosome end protector TRF2. *Curr. Biol.* **14**, 1621-1631
- Greider C.W. & Blackburn E.H. 1985. Identification of a specific telomere terminal transferase activity in Tetrahymena extracts. *Cell* **43**, 405-413
- Greider C.W. 1996. Telomere Length Regulation. *Annu. Rev. Biochem.* **65**, 337-365
- Cooke H.J. & Smith B.A. 1986. Variability at the telomeres of the human X/Y pseudoautosomal region. *Cold Spring Harbor Symp. Quant. Biol.* **51**, 213-219
- de Lange T., Shiue L., Myers R.M., Cox D.R., Naylor S.L., Killery A.M. & Varmus H.E. 1990. Structure and variability of human chromosome ends. *Mol. Cell. Biol.* **10**, 518-527
- Harley C.B., Futcher A.B. & Greider C.W. 1990. Telomeres shorten during ageing of human fibroblasts. *Nature* **345**, 458-460
- Hastie N.D., Dempster M., Dunlop M.G., Thompson A.M., Green D.K. & Allshire R.C. 1990. Telomere reduction in human colorectal carcinoma and with ageing. *Nature* **346**, 866-868
- Counter C.M., Avilion A.A., LeFeuvre C.E., Stewart N.G., Greider C.W., Harley C.B. & Bacchetti S. 1992. Telomere shortening associated with chromosome instability is arrested in immortal cells which express telomerase activity. *EMBO* **11**, 1921-1929
- Kim N.W., Piatyszek M.A., Prowse K.R., Harley C.B., West M.D., Ho P.L.C., Coviello G.M., Wright W.E., Weinrich S.L. & Shay J.W. 1994. Specific association of human telomerase activity with immortal cells and cancer. *Science* **266**, 2011-2015
- Counter C.M., Botelho F.M., Wang P., Harley C.B. & Bacchetti S. 1994a. Stabilization of short telomeres and telomerase activity accompany immortalization of Epstein-Barr virus-transformed human B lymphocytes. *Z Virol.* **68**, 3410-3414
- Counter C.M., Hirte H.W., Bacchetti S. & Harley C. 1994b. Telomerase activity in human ovarian carcinoma. *Proc. Natl. Acad. Sci. USA.* **91**, 2900-2904
- Blasco M.A., Rizen M., Greider C.W. & Hanahan D. 1996. Differential regulation of telomerase activity and telomerase RNA during multi-stage tumorigenesis. *Nature Genet.* **12**, 200-204
- Broccoli D., Godley L.A., Donehower L.A., Varmus H.E. & de Lange T. 1996. Telomerase activation in mouse mammary tumors: lack of detectable telomere shortening and evidence for regulation of telomerase RNA with cell proliferation. *Mol. Cell. Biol.* **16**, 3765-3772
- Bacchetti S. 1996. Telomere maintenance in tumour cells. *Cancer Surv.* **28**, 197-216
- Svenson U. & Roos G. 2009. Telomere length as a biological marker in malignancy. *Biochim Biophys Acta.* **1792**, 317-323
- Shay J.W. & Bacchetti S. 1997. A survey of telomerase activity in human cancer. *Eur. J. Cancer* **33**, 787-791

## Introduction

Bryan T.M., Englezou A., Gupta J., Bacchetti S., Reddel R.R. 1995. Telomere elongation in immortal human cells without detectable telomerase activity. *EMBO J.* **14**, 4240–4248

Bryan T.M., Englezou A., Dalla-Pozza L., Dunham M.A., Reddel R.R. 1997. Evidence for an alternative mechanism for maintaining telomere length in human tumors and tumor-derived cell lines. *Nat. Med.* **3**, 1271–1274

Murnane J.P., Sabatier L., Marder B.A. & Morgan W.F. 1994. Telomere dynamics in an immortal human cell line. *EMBO J.* **13**, 4953–4962

Dunham M.A., Neumann A.A., Fasching C.L., Reddel R.R. 2000. Telomere maintenance by recombination in human cells. *Nat. Genet.* **26**, 447–450

Lundblad V. & Blackburn E.H. 1993. An alternative pathway for yeast telomere maintenance rescues *estI*<sup>-</sup> senescence. *Cell* **73**, 347–360

Muntoni A., Neumann A.A., Hills M. & Reddel R.R. 2009. Telomere elongation involves intra-molecular DNA replication in cells utilizing alternative lengthening of telomeres. *Hum Mol Genet.* **18**, 1017-1027

Bryan T.M., Englezou A., Gupta J., Bacchetti S., Reddel R.R. 1995. Telomere elongation in immortal human cells without detectable telomerase activity. *EMBO J* **14**, 4240–4248

Yeager T.R., Neumann A.A., Englezou A., Huschtscha L.I., Noble J.R., Reddel R.R. 1999. Telomerase-negative immortalized human cells contain a novel type of promyelocytic leukemia (PML) body. *Cancer Res.* **59**, 4175–4179

Tarsounas M., Munoz P., Claas A., Smiraldo P.G., Pittman D.L., Blasco M.A. & West S.C. 2004. Telomere maintenance requires the RAD51D recombination/repair protein. *Cell* **117**, 337–347

Yankiwski V., Marciniak R.A., Guarente L., Neff N.F. 2000. Nuclear structure in normal and Bloom syndrome cells. *Proc. Natl. Acad. Sci. USA* **97**, 5214–5219

Stavropoulos D.J., Bradshaw P.S., Li X., Pasic I., Truong K., Ikura M., Ungrin M., Meyn M.S. 2002. The Bloom syndrome helicase BLM interacts with TRF2 in ALT cells and promotes telomeric DNA synthesis. *Hum. Mol. Genet.* **11**, 3135–3144

Grobelny J.V., Godwin A.K., Broccoli D. 2000. ALT-associated PML bodies are present in viable cells and are Screen for ALT genes enriched in cells in the G2/M phase of the cell cycle. *J. Cell Sci.* **113**, 4577–4585

Wu G., Lee W.H., Chen P.L. 2000. NBS1 and TRF1 colocalize at promyelocytic leukemia bodies during late S/G2 phases in immortalized telomerase-negative cells. Implication of NBS1 in alternative lengthening of telomeres. *J. Biol. Chem.* **275**, 30618–30622

Wu G., Jiang X., Lee W.H., Chen P.L. 2003. Assembly of functional ALT-associated promyelocytic leukemia bodies requires Nijmegen breakage syndrome 1. *Cancer Res.* **63**, 2589–2595

Molenaar C., Wiesmeijer K., Verwoerd N.P., Khazen S., Eils R., Tanke H.J. & R.W. Dirks 2003. Visualizing telomere dynamics in living mammalian cells using PNA probes. *EMBO J.* **22**, 6631–6641

- Perrem K., Colgin L.M., Neumann A.A., Yeager T.R., Reddel R.R. 2001. Coexistence of alternative lengthening of telomeres and telomerase in hTERT-transfected GM847 cells. *Mol. Cell Biol.* **21**, 3862–3875
- Jiang W.Q., Zhong Z.H., Henson J.D., Neumann A.A., Chang A.C., Reddel R.R. 2005. Suppression of alternative lengthening of telomeres by Sp100-mediated sequestration of MRE11/RAD50/NBS1 complex. *Mol. Cell Biol.* **25**, 2708–2721
- Zeng S., Xiang T., Pandita T.K., Gonzalez-Suarez I., Gonzalo S., Harris C.C. & Yang Q. 2009. Telomere recombination requires the MUS81 endonuclease. *Nat Cell Biol.* **11**, 616–623
- Jeyapalan J.N., Mendez-Bermudez A., Zaffaroni N., Dubrova Y.E., Royle N.J. 2008. Evidence for alternative lengthening of telomeres in liposarcomas in the absence of ALT-associated PML bodies. *Int. J. Cancer* **122**, 2414–2421
- Henson J.D., Hannay J.A., McCarthy S.W., Royds J.A., Yeager T.R., Robinson R.A., Wharton S.B., Jellinek D.A., Arbuckle S.M., Yoo J., Robinson B.G., Learoyd D.L., Stalley P.D., Bonar S.F., Yu D., Pollock R.E., Reddel R.R. 2005. A robust assay for alternative lengthening of telomeres (ALT) in tumors demonstrates the significance of ALT in sarcomas and astrocytomas. *Clin. Cancer Res.* **11**, 217–225
- Ulaner G.A., Hoffman A.R., Otero J., Huang H.Y., Zhao Z., Mazumdar M., Gorlick R., Meyers P., Healey J.H. & Ladanyi M. 2004. Divergent patterns of telomere maintenance mechanisms among human sarcomas: sharply contrasting prevalence of the alternative lengthening of telomeres mechanism in Ewing's sarcomas and osteosarcomas. *Genes Chromosomes Cancer* **41**, 155–162
- Montgomery E., Argani P., Hicks J.L., DeMarzo A.M. & Meeker A.K. 2004. Telomere lengths of translocation-associated and nontranslocation-associated sarcomas differ dramatically. *Am. J. Pathol.* **164**, 1523–1529
- Scheel C., Schaefer K.L., Jauch A., Keller M., Wai D., Brinkschmidt C., van Valen F., Boecker W., Dockhorn-Dworniczak B. & Poremba C. 2001. Alternative lengthening of telomeres is associated with chromosomal instability in osteosarcomas. *Oncogene* **20**, 3835–3844
- Hakin-Smith V., Jellinek D.A., Levy D., Carroll T., Teo M., Timperley W.R., McKay M.J., Reddel R.R., Royds J.A. 2003. Alternative lengthening of telomeres and survival in patients with glioblastoma multiforme. *Lancet* **361**, 836–838
- Brachner A., Sasgary S., Pirker C., Rodgarkia C., Mikula M., Mikulits W., Bergmeister H., Setinek U., Wieser M., Chin S.-F., Caldas C., Micksche M., Cerni C. & Berger W. 2006. Telomerase- and alternative telomere lengthening-independent telomere stabilization in a metastasis-derived human non-small cell lung cancer cell line: effect of ectopic hTERT. *Cancer Res.* **66**, 3584–3592
- de Lange T. 2002. Protection of mammalian telomeres. *Oncogene* **21**, 532–540
- Dong F. & Jiang J. 1998. Non-Rabl patterns of centromere and telomere distribution in the interphase nuclei of plant cells. *Chromosome Res.* **6**, 551–558
- Gilson 1993; Gilson E., Laroche T. & Gasser. S.M. 1993. Telomeres and the functional architecture of the nucleus. *Trends Cell Biol.* **3**, 128–134



## Introduction

Gotta M., Laroche T., Formenton A., Maillet L., Shertan H. & Gasser S.M. 1996. Cytological evidence for the clustering of telomeres and their colocalization with Rap1, Sir3 and Sir4 proteins in wild-type *S. cerevisiae*. *J. Cell Biol.* (in press)

Gottschling D.E., Aparicio O.M., Billington B.L. & Zakian V.A. 1990. Position effect at *S. cerevisiae* telomeres: reversible repression of Pol II transcription. *Cell* **63**, 751–762

Conrad M.N., Wright J.H., Wolf A.J. & Zakian V.A. 1990. RAP1 protein interacts with yeast telomeres in vivo: overproduction alters telomere structure and decreases chromosome stability. *Cell* **63**, 739–750

Wright J.H., Gottschling D.E. & Zakian V.A. 1992. *Saccharomyces* telomeres assume a non-nucleosomal chromatin structure. *Genes Dev.* **6**, 197–210

Ferguson B.M., Brewer B.J., Reynolds A.E. & Fangman W.L. 1991. A yeast origin of replication is activated late in S phase. *Cell* **65**, 507–515

de Bruin D., Kantrow S., Liberatore R. & Zakian V.A. 2000. Telomere folding is required for the stable maintenance of telomere position effects in yeast. *Mol. Cell. Biol.* **20**, 7991–8000

Csank A.K. & Henikoff S. 1996. Genetic modification of heterochromatic association and nuclear organization in *Drosophila*. *Nature* **381**, 529–531

Dernburg A.F., Broman K.W., Fung J.C., Marshall W.F., Philips J., Agard D.A., Sedat J.W. 1996. Perturbation of nuclear architecture by long-distance chromosome interactions. *Cell* **85**, 745–759

Henderson S., Allsopp R., Spector D.L., Wang S.S. & Harley C. 1996. *In situ* analysis of changes in telomere size during replicative aging and cell transformation. *J. Cell Biol.* **134**, 1–12

Bilaud T., Brun C., Ancelin K., Koering C.E., Laroche T. & Gilson E. 1997. Telomeric localization of TRF2, a novel human telobox protein. *Nat. Genet.* **17**, 236–239

Broccoli D., Smogorzewska A., Chong L. & de Lange T. 1997. Human telomeres contain two distinct Myb-related proteins, TRF1 and TRF2. *Nat. Genet.* **17**, 231–235

van Steensel B., Smogorzewska A. & de Lange T. 1998. TRF2 protects human telomeres from end-to-end fusions. *Cell* **92**, 401–413

Ludérus M.E., van Steensel B., Chong L., Sibon O.C.M., Cremers F.F.M. & de Lange T. 1996. Structure, Subnuclear Distribution, and Nuclear Matrix Association of the Mammalian Telomeric Complex. *J. Cell Biol.* **135**, 867–881

Kaminker P.G., Kim S.-H., Desprez P.-Y. & Campisi J. 2009. A novel form of the telomere-associated protein TIN2 localizes to the nuclear matrix. *Cell Cycle* **8**, 931–939

Seksek O., Biwersi J., Verkman A. S. 1997. Translational Diffusion of Macromolecule-sized Solutes in Cytoplasm and Nucleus *J. Cell Biol.* **138**, 131–142

Fushimi K. and Verkman A. S. 1991. Low viscosity in the aqueous domain of cell cytoplasm measured by picosecond polarization microfluorimetry. *J. Cell Biol.* **112**, 719–725

Rademakers S., Nigg A. L., Hoogstraten D., Hoeijmakers J. H. J., Vermeulen W., Houtsmuller A.B. 1999. Action of DNA Repair Endonuclease ERCC1/XPF in Living Cells *Science* **284**, 958-961

Phair R. D. & Misteli T. 2000. High mobility of proteins in the mammalian cell nucleus. *Nature* **404**, 604-609

Huang S., Deerinck T. J., Ellisman M. H., Spector D. L. 1998. The Perinucleolar Compartment and Transcription. *J. Cell Biol.* **143**, 35-47

Snaar S., Wiesmeijer K., Jochemsen A. G., Tanke H. J., Dirks R. W. 2000. Mutational Analysis of Fibrillarin and Its Mobility in Living Human Cells. *J. Cell Biol.* **151**, 653-662

Pederson T. 2000. Diffusional protein transport within the nucleus: a message in the medium. *Nature Cell Biol.* **2**, E73-E74

Shopland L. S. & Lawrence J. B. 2000. Seeking Common Ground in Nuclear Complexity. *J. Cell Biol.* **150**, F1-F4

Misteli T. Protein dynamics: Implications for nuclear architecture and gene expression. 2001. *Science* **291**, 843-847

Marshall W.F., Straight A., Marko J.F., Swedlow J., Dernburg A., Belmont A., Murray A.W., Agard D.A., Sedat J.W. 1997. Interphase chromosomes undergo constrained diffusional motion in living cells. *Curr. Biol.* **7**, 930-939

Heun P., Laroche T., Shimada K., Furrer P. & Gasser S.M. 2001a. Chromosome dynamics in the yeast interphase nucleus. *Science* **294**, 2181-2186

Bystricky K., Heun P., Gehlen L., Langowski J. & Gasser S.M. 2004. Long-range compaction and flexibility of interphase chromatin in budding yeast analyzed by high-resolution imaging techniques. *Proc. Natl Acad. Sci. USA* **101**, 16495-16500

Heun P., Laroche T., Raghuraman M.K. & Gasser S.M. 2001b. The positioning and dynamics of origins of replication in the budding yeast nucleus. *J. Cell Biol.* **152**, 385-400

Jin Q., Trelles-Sticken E., Scherthan H. & Loidl J. 1998. Yeast nuclei display prominent centromere clustering that is reduced in nondividing cells and in meiotic prophase. *J. Cell Biol.* **141**, 21-29

Gartenberg M.R., Neumann F.R., Laroche T., Blaszczyk M., Gasser S.M. 2004. Sir-mediated repression can occur independently of chromosomal and subnuclear contexts. *Cell.* **119**, 955-967

Sage D., Neumann F.R., Hediger F., Gasser S.M. & Unser M. 2005. Automatic tracking of individual fluorescence particles: application to the study of chromosome dynamics. *IEEE Trans. Image Process.* **14**, 1372-1383

Hediger F., Neumann F.R., Van Houwe G., Dubrana K. & Gasser S.M. 2002. Live imaging of telomeres: yKu and Sir proteins define redundant telomere-anchoring pathways in yeast. *Curr. Biol.* **12**, 2076-2089

Rosa A., Maddocks J.H., Neumann F.R., Gasser S.M. & Stasiak A. 2006. Measuring limits of telomere movement on nuclear envelope. *Biophys. J.* **90**, L24-L26

## Introduction

Taddei A., Van Houwe G., Hediger F., Kalck V., Cubizolles F., Schober H., Gasser S.M. 2006. Nuclear pore association confers optimal expression levels for an inducible yeast gene. *Nature* **441**, 774–778

Cabal G.G., Genovesio A., Rodriguez-Navarro S., Zimmer C., Gadal O., Lesne A., Buc H., Feuerbach-Fournier F., Olivo-Marin J.C., Hurt E.C., Nehrass U. 2006. SAGA interacting factors confine sub-diffusion of transcribed genes to the nuclear envelope. *Nature* **441**, 770–773

Coué M., Brenner S.L., Spector I. & Korn E.D. 1987. Inhibition of actin polymerization by latrunculin A. *FEBS Letters* **213**, 316-318

## **CHAPTER 2**

### **STACKS:**

a software program for particle tracking  
in living cells



# STACKS: a software program for particle tracking in living cells

Vrolijk H., Brouwer A.K., Dirks R.W., Tanke H.J.

Department of Molecular Cell Biology, Leiden University Medical Center Leiden, The Netherlands

## Introduction

Many processes in the mammalian cell are dynamic. In order to obtain better understanding of these processes the dynamic properties of cellular structures have to be measured. Nowadays the commercially available fluorescence confocal and wide-field microscope workstations offer excellent facilities to visualize the three-dimensional spatial organization of the cell and to study the movement and interaction of nuclear and cytoplasmic particles. However, the software provided by the manufacturers of these workstations is more or less dedicated to the control of the microscope, the acquisition process and the visualization of the acquired 2D and 3D image series in time, while at present the analysis tools are mostly limited to simple measurements. However, dedicated image processing and image analysis software is required for more complex research questions, such as the tracking of moving structures in a cell.

Particle tracking is applied using a variety of biophysical techniques, such as microrheology (Tseng et al., 2002; Weihs et al., 2006; Waigh, 2005), magnetic tweezers (Bausch et al., 1998), optical tweezers (Ashkin, 1997) and is widely used for particle imaging velocimetry (Adrian, 2005; Grant, 1997). A wide range of methods have also been described to track particles in microscopic optical images (Bacher et al., 2004; Miura, 2005; Cheezum et al., 2001; Crocker & Grier, 1996; Sbalzarini & Koumoutsakos, 2005; Carter et al., 2005).

In this paper we describe a software package, called STACKS, that was developed to handle research questions that could not be solved with the standard software presently available on commercial systems, such as the tracking of particles in 2D and 3D time series and the measurement of the dynamic characteristics of these particles. We considered it important that STACKS should be able to operate directly on the data formats as produced by commercial microscope systems without a conversion step for the image data. Furthermore, the program should be user-friendly, provide visual feedback on each operating step and allow sufficient flexibility to cope with different cell types and images of varying quality. The software should also allow a sufficient amount of user interactivity for tuning the analysis procedure and editing the image stack, for instance for the removal of artifacts, which may disturb the analysis, or for correction of partly incorrect image segmentation. In STACKS a number of filter operations are provided to enhance the original image data. As a 4D image stack easily consists of more than 1000 images, these filter operations become time consuming when they are based on normal CPU processing. In STACKS many of these operations have been accelerated by making use of the GPU processor of the video board. In this paper we compare the two approaches with respect to the efficiency of the image operations. To illustrate the capabilities of the STACKS program determination of the dynamics of chromatin during different phases of the cell cycle was chosen as a test model. Chromosomes of eukaryotic cells have been shown to occupy discrete territories during interphase (Manuelidis, 1985; Trask et al., 1988). Transcriptionally competent regions preferentially localize to the periphery of these chromosomal

territories (Verschure et al., 1999), indicating that chromatin is dynamic. This type of organization is observed not only at the level of the chromosome, but also at the level of a single genetic locus in the total space of the nucleus (for a review, see Spector, 2003). Nuclei in higher organisms are known to undergo extensive changes in organization as they progress through the cell cycle and during development (for a review, see Francastel et al., 2000). For example, the brown<sup>Dominant</sup> ( $bw^D$ ) chromosome of *Drosophila melanogaster* contains a large block of heterochromatin near the end of chromosome 2 (2R) (Platero et al., 1998). This distal block associates with centric heterochromatin of the second chromosome (2Rh). The association between  $bw^D$  and 2Rh is not apparent until at least 5 hours into G1 (Csink & Henikoff, 1996; Dernburg et al., 1996). Also, as soon as the nuclear membrane forms in early G1, centromeres have been observed to rapidly disperse throughout the nucleus. Coalescing and dispersing of centromeres in cultured cells was observed in late G<sub>2</sub> and early G<sub>1</sub>, respectively (Manuelidis, 1985).

In this study telomeres were chosen as a marker for studying the dynamics of chromatin. Telomeres in living cells were labeled by transfecting U2OS cells with GFP fused telomere binding proteins TRF1 and TRF2. Time-lapse movies were recorded of moving telomeres during different phases of the cell cycle. GFP-tagged proliferating cell nuclear antigen (PCNA) was hereby used as a life cell marker to distinguish the different phases of the cell cycle, and as a counterstain to correct for cell movement. The movements of telomeres were quantitatively analyzed using STACKS and telomeres were found to be significantly more dynamic in the G1 phase than in other phases of the cell cycle (p-value = 0.05).

## Material and Methods

### Hardware

In our laboratory several fluorescence microscope workstations are present to perform live cell analysis: the AF6000, the SP5 (both Leica Microsystems, Wetzlar, Germany) and the LSM 710 (Carl Zeiss Microimaging, Jena, Germany). The AF6000 is a wide-field system and consists of an inverted DMI 6000B microscope equipped with a metal halide bulb, an automated motorized z-galvo stage for 3D imaging and a climate chamber for live cell imaging. The SP5 is a confocal laser scanning microscope (inverted) system, also equipped with a climate chamber, and the LSM 710 is a multiphoton confocal laser scanning (upright) system equipped with objectives with a large working distance and a special stage for intra-vital microscopy. The Leica SP5 is equipped with an Argon laser for 405-510 nm, a solid state laser and a helium-neon laser for respectively the 561 nm and 633 nm line and a two-photon laser with a spectral range of 710-990 nm. The Leica systems are controlled by the LAS AF software for image acquisition and analysis. The LSM 710 is equipped with similar lasers as the Leica SP5, a two photon laser for the range of 700 – 1060 nm and is controlled by the ZEN software system.

The software program described in this paper, STACKS, can be used on a regular personal computer running Windows XP, Vista, or Windows 7. It was tested on the 32 bit versions of these operating systems. The graphics processing unit (GPU) based image processing functions are currently only supported for Nvidia (Santa Clara, California, USA) video boards from the Geforce 7 series or higher with at least shader level 3. The PC used for image analysis was a Precision 380 system from Dell (Round Rock, Texas, USA) equipped with a GTX8800 Nvidia video display adapter.

### Software system

The program STACKS has been developed to cope with research questions, which could not be solved using the software that comes with commercial confocal systems and live cell workstations. It performs dedicated processing and analysis of time lapse 2D and 3D image stacks, although it can also handle single 2D and 3D images. Both 8 and 16 bit grey-value image stacks are supported as well as 24 bit color image stacks.

All image operations in STACKS are operated from the main menu. The source for the operation is always the top window. When additional images or parameters are required for the operation, a dialog is shown to ask the user to specify the additional input and/or output stack. Each image operation results in a new image stack. When the user selects an existing stack as being the result of an operation, it will be overwritten. The user has also control on which part of the image stack an operation is performed. There are 4 modes of operation. It is possible to process 1) the entire image stack, 2) the 3D image for the current time point, 3) the z-slice for all time points or 4) just a single image. By clicking on the corresponding icons in the toolbar the user can specify on which part of a stack an operation is performed.

### Image Visualization

An image stack is normally displayed in a re-sizable window, which maintains the original aspect ratio of the image. Two additional scrollbars can be present. The horizontal scrollbar at the top of the window allows the user to select a time point within the stack, whereas the vertical scrollbar at the left allows the selection of a certain z-slice; the traditional scrollbars of



the window are used for zooming. In case of 3D stacks one may also display the horizontal and vertical cross sections of an image stack, as shown in Figure 1. A crosshair is then shown in the original image to indicate where the cross sections are located. By moving the mouse over an image, the coordinates and grey-value information of the corresponding pixels are shown at the status bar at the bottom of the screen and optionally also as a tooltip. It is also possible to display a 3D representation of an image stack. This has been implemented using the public domain package of the visualization toolkit, VTK [<http://www.vtk.org/>].

### **Data I/O**

STACKS can import experiments of time-lapse 2D and / or 3D image data saved in the Leica LIF and the Zeiss LSM file format and can also export the resulting image sets in both formats, although the specific microscope settings of the original data files will be lost in these new data files. The data sets can be read in again by respectively the LAS software (Leica) or by the ZEN software from Zeiss. Another option in STACKS is to read a set of TIF files from a folder; the names of the TIF files should be of a special format containing time point, z-slice and channel information in order to reconstruct the time-lapse 3D image set from it. The supported filename formats are compatible with older confocal laser scanning systems from Leica and with Tikal, a software environment for the tracking of 3D microscopic particles as described by Bacher (Bacher et al., 2004). Analysis results can be exported as Excel spread sheets.

### **Management of the stacks**

In the program there is currently support for the simultaneous use of 10 4D image stacks and 10 3D image stacks. For each 8 or 16 bit grey-value stack there is also an additional 8 bit stack present, which is used for display purposes. This can for instance be obtained after contrast stretching of the 16 bit stack. In this way the original data values stay intact. Additionally the horizontal and vertical cross sections can be calculated and from each 4D stack the maximum projection can be obtained or a z-slice can be selected as being the projection stack. This would imply, that the total amount of memory used by image data would become about 11 Gbytes in case of 10 stacks of 512x512 pixels (16 bit + 8 bit, or 24 bit ) with 40 slices and 25 time points including cross sections and projections; evidently too large to handle in memory for a normal PC. Therefore we have chosen for an approach by which only the current visible images and the corresponding images holding the original data of each stack are present in memory. At the time that new image stacks are read from disk or created by image transformations, copies of the complete stacks are created in the /TEMP directory of the system disk which are accessible through fast random access. In this way access to the data is optimized for display purposes, so that scrolling through the stack appears to occur instantaneous to the user. This approach will result in extra overhead when stacks are processed and have to be written back to disk.

### **Segmentation**

In order to segment the particle images from the background various methods are present. Global thresholding based on the image background can be applied for the complete data set; the user may adjust this threshold per individual image, per slice in time or per time-point. Thresholding can be performed on the 8 bit image stack obtained by contrast stretching or directly on the 16 bit original data. However, it is often easier to segment small structures, such as centromeres or centrioles, after performing a 2D top-hat transformation on the image set in order to reduce the nonspecific fluorescence within the cell nucleus or the fluorescence fluctuations in the background. Other image transformations are provided to enhance the images

before the segmentation step, such as contrast enhancement, convolution filters, Fourier filters, median and min-max filter operations.

The 2D or 3D watershed algorithm represents a more automatic segmentation method, which will detect the particles as being local maxima in the 2D or 3D image sets and will find the borders of their domains as being the watershed lines between the individual particles. Within each domain a local threshold is automatically determined to segment the particles from the background. The advantage of the latter algorithm is that touching particles are often correctly separated. A possible disadvantage is that this operation may lead to over-segmentation.

Segmentation results in a new 8 bit image stack, from which one bit corresponds with the result of the segmentation, namely object or background. Other bits are reserved for segmentations of other image stacks, such as for a second label or for the counterstain. Binary operations between different bit-planes are provided, like logical AND, OR, or EXOR. Also, image transformations can be applied, such as erosion, dilation, and skeleton. The highest bit is reserved for human interaction, as will be discussed in the following paragraph. The user can select which bits of a binary stack will be displayed and edit the binary stack effects in the visible bit-planes.

### **Correction global cell movement**

The program also corrects for global cell movement. The orientation and translation of the cell is calculated for each time-point based on the counterstain image of a 2D image set (or on the maximal projection in case of a 3D image set). Alternatively, one may also select particles which are known to be immobile. The results are then used to perform a translation and / or rotation correction for the original image sets. Obviously, such corrections are essential, for instance the kinetic characteristics of the tracked particles in a cell nucleus are not very meaningful without a correction for global cell movement.

### **Particle tracking**

In order to track particles, such as telomeres and centrioles, at first the user has to segment the 3D or 4D stack. When thresholding is used for segmentation, object labeling is the next step of the process. Object labeling will detect separate objects based on 8-connectivity either in the 2D or 3D images of the binary stack and will create a new stack, called the label stack, where by all pixels of every individual particle obtain a unique index, that corresponds to a pseudo-color. However, when the watershed algorithm is applied for segmentation, both the binary stack and the label stack are directly created during the process.

Following object labeling position, size and total density of each particle are measured for all time-points and the tracks are determined by linking those particles between successive time points, which have the highest probability of being the same objects based on these features. Particles, which have been classified as being the same, are relabeled with the same pseudo-color in the label stack. This allows the user to easily verify by scrolling between the time points in the label stack, how successful the classification was performed. Figure 1 shows the various stacks involved in the tracking process and the 3D representation of the tracks found. Eventually tracks can be split and reconnected by the user to correct for errors made by the automatic procedure. Finally kinetic parameters such as mean squared displacement are measured to characterize the movement of each individual particle according to the following formula:

$$\text{MSD}_p(\Delta) = \frac{1}{N-n} \sum_{m=1}^{N-n} [ \text{pos}((m-1) \cdot \tau + \Delta) - (\text{pos}((m-1) \cdot \tau) ) ]^2$$

with  $\Delta = n \cdot \tau$      $\tau$  – measurement interval and  $n$  - an integer

pos            - position vector at a certain time point

$N$             - the total number of time points

Thus the mean squared displacement is averaged over all possible time intervals measured. This will inevitably result in a larger standard deviation for increasing values of  $n$ , as the number of interval pairs decreases. A similar function, called  $\text{MSD}_t$ , was also calculated; the position vector in the formula above is then replaced by the distance covered between two time intervals. This function provides additional information about the mobility of the particles over time.

### GPU programming

Nowadays, personal computers are equipped with video boards that provide high processing power for use in video games and multimedia applications. These graphics processing units (GPUs) are very efficient in parallel processing of small programs (called shaders) on sets of vertices and pixels, which makes these boards very suitable for general purpose image processing. Many papers have already been published on this subject (Moreland et al., 2003; Strzodka et al., 2003, 2004; Farrugia et al., 2006)

A number of image operations have been implemented in STACKS using the processing power of the GPU. Examples are simple mathematical operations, like adding, subtracting, multiplying and dividing of images. They are included, as they are internally used for more complex operations. Morphological operations have been added, like erosion, dilation, opening, closing and the top-hat transform. These min/max operations are implemented using the so-called “ping-pong” technique. This is caused by the fact that source and result image, which are defined as 2D textures in GPU memory, are not allowed to be the same for a shader. In the first pass the minimum or maximum is determined with the 4 closed neighbours only. In the next pass the result serves as the source while the minimum or maximum is determined with the 4 diagonal neighbours only and this is alternately repeated until the desired size of the neighbourhood is reached. By defining an extra image texture it can be prevented that the source is changed and that the result is obtained in the correct texture at the end of the operation. The access to texture memory is highly optimized by parallel processing, so that these operations are very efficiently handled by the GPU even when many passes are involved.

Also other filter and transformation operations based on the GPU have been implemented in STACKS, like Sobel, Laplace, Canny edge, Gaussian, median, Kuwahara, convolution up to a 40 x 40 neighbourhood, unsharp mask, a distance transform (Rong et al., 2006), nearest neighbour deconvolution and some specific color transformations, such as RGB to HSI and the inverse transform, component blend, component threshold, and color deconvolution (Rui-frok et al., 2001) Furthermore the 2D fast Fourier and inverse fast Fourier is supported including low-pass, band-pass and high-pass Gaussian and Butterworth filters based on the 2D fft. Most of the image operations have been implemented for 8-bit and 16-bit grey-value images and 24-bit color images and 32-bit float and complex images for the Fourier transform. Also 48-bit color images (16-bit for red, green and blue) have been programmed for the image operations on the GPU, but these images are not yet supported by STACKS.

Initially the shaders have been developed using the HLSL (high level shader language, Microsoft) DirectX and Direct3D. More recently Nvidia introduced CUDA as the new high level language for general purpose processing on GPU boards. For STACKS two equivalent libraries were developed, one based on HLSL and one on CUDA. Both languages have their advantages and disadvantages. In HLSL the result of a shader program can again be a 2D texture. Because the texture format is defined apart from the shader program, the same shader program can be applied for different image types such as 8-bit grey, 16-bit grey or 24 bit color. In CUDA only the source images can be 2D textures, while the result image of a shader program must be a 2D array, so that different shader programs are necessary for the different image types. The advantage of using 2D textures as input instead of 2D arrays, is that the structure is defined in the texture. Therefore the boundary conditions will be at the borders of the images and there is no need to test if neighbouring pixels exceed the borders of the source images in the shader programs themselves. CUDA has the advantage that also other memory compartments of the GPU board can be addressed, such as the local memory of the shaders. This can lead to more optimized implementations of the shader programs, as is described for the 2D convolution filter (Podlozhnyuk et al., 2001). Additionally there is a large community using CUDA for general purpose processing and a lot of examples are present in the Nvidia software development kit and on their website, which eases the development using CUDA.

In this paper the different implementations of the image operations in HLSL and CUDA are compared with the normal software implementation of these operations carried out by the CPU. The necessary overhead for processing images by the GPU, such as the additional transfer of images to and from GPU memory and the setup of textures on the GPU board will be taken into account. Image management was added to the GPU libraries in order to minimize the overhead for creating new 2D textures and reserving memory space on the GPU board. In this way new 2D textures are created only when they did not exist yet, but when a 2D texture with the same specifications has already been defined during a previous operation, textures can be reused for different images with the same specifications. Especially for processing 3D and 4D image stacks were all 2D images of the stack are of the same dimensions and the same image type, image management is very useful as new textures will be defined only during the processing of the first image of the stack.

### **Interactivity**

The program STACKS allows a large amount of user interaction on the image stacks. For instance one may separate touching objects or reconnect them, so that mistakes made by the segmentation process can be corrected. Other functions are included to delete objects or regions, or to select objects or regions and then erase the unselected parts. In this way further analysis can be restricted to a part of the image stack or to the objects of interest only. The actual drawing and selection is performed on the images of the binary stack, although the user can draw or point with the mouse in any of the image stacks with the same dimensions as the binary stack. Once an object is selected in the binary stack, there are also options to move, duplicate or erase the corresponding original object in the grey-value stack. This may be useful for cleaning up dirt that has moved in during the acquisition of the images. Depending on the selected mode of operation interactions are carried out on the 2D image only, on the 3D image, on all time-points of a slice, or on the complete 4D stack. User interaction is also possible on the particles after tracking. Tracks can be selected or erased or split at a certain time-point or two tracks can be connected at the end of the tracks found. However, in this case the program is aware how these tracked objects are connected through the slices and over time-points, so that the interactions on tracks are correctly handled in 3D and 4D.

### **Measurements**

The program STACKS was originally developed for the tracking of nuclear particles, but in order to extend its possibilities, the functionality to execute separate measurements on individual particles has been added. The user can select which features have to be measured, like size, density and shape. This can be applied for more than one color if required. STACKS also provides distance measurements between particles and selected objects. For instance, it may be of interest to determine how fast viral particles move through the cell. Measurements can also be performed within regions of interest (ROIs), that are drawn by the user in the form of simple mathematical shapes like squares, circles, rectangles, ellipses and lines, but also as freehand drawn closed regions. Selected objects may be converted into ROIs as well. ROIs have a constant shape, position and size for images of a stack in contrast with segmented objects. However, ROIs can be duplicated and moved through the image, so that exactly the same area's can be measured on different places within the images of a stack allowing for instance FLIP and FRAP measurements to be performed. The results of all measurements are shown in the result window and can be saved on disk as an Excel spreadsheet.

### **Macro recording**

Macro recording was added to STACKS to easily execute a sequence of instructions on different data sets. STACKS supports the use of 10 different macro's simultaneously, which is sufficient for most applications. Some operations, such as thresholding require user interaction. These operations are also recorded in the macro, but when the macro is executed the user can specify, whether he wants to be prompted to perform the interaction again on a new data set, or whether the macro should apply the same settings, as defined during the recording of the macro. Macro's can be executed once or repeatedly. The latter can be very useful especially when the image content is changed in each pass of the execution. For instance when a particular part of the nucleus is photo-activated and the user likes to study how the activated subcellular structures or particles diffuse through the nucleus. The user may select the photo-activated part at the first time-point and measure the intensity within this area as function of time. However, by dilating the region in each pass of the macro this intensity can also be calculated as function of the distance to the original region.

Macro's can be stored to disk in the so called "preferences" file, which contains also all other parameters and settings. How a given data set was analyzed can be saved in this way. The settings also specify other parameters such as predefined positions and sizes of the windows, the default lookup tables for the windows, and the parameters which are used for the analysis, such as the minimum object size for objects to be detected and the maximum distance over which objects still should be considered as being the same between two successive time points during the tracking analysis.

### **Cell Culture**

A study of the dynamics of telomeres during different phases of the cell cycle was performed in order to illustrate the possibilities of STACKS for particle tracking. Human osteosarcoma cells (U2OS) were cultured at 37°C on 3.5 cm glass-bottom culture dishes (MatTek) in Dulbecco's modified Eagle's medium (DMEM) without phenol red and containing 1.0 mg/ml glucose, 4% FBS, 2 mM glutamine, 100 U/ml penicillin, and 100 µg/ml streptomycin, pH 7.2 (all from Invitrogen).

**Plasmids and cell transfection**

The coding sequences for TRF1 and TRF2 have been cloned into the DsRedExpress vector (Clontech) according to standard procedures. The GFP-tagged proliferating cell nuclear antigen (PCNA) protein was a gift from M.C. Cardoso. Cells were transiently transfected with 0.5  $\mu\text{g}$  vector DNA using lipofectamine 2000 (Invitrogen).

**Live cell imaging**

Wide-field fluorescence microscopy was performed on the AF6000 multi-dimensional workstation for live cell imaging. 4D image stacks were collected using a 63 $\times$ NA 1.25 HCX plan Fluotar objective in combination with the automated motorized z-galvo stage. During imaging, the microscope was heated to 37  $^{\circ}\text{C}$  in a  $\text{CO}_2$  perfused and moisturized chamber. Generally, image stacks were collected every 30 seconds for 10 minutes. Image deconvolution was performed using the Leica software. For each experiment and cell type at least six image series were analyzed.

## Results

### Disk overhead

As described the program STACKS only has the current visible image of each stack present in memory. This will introduce extra overhead when a complete stack is processed, namely to fetch all images from disk and to restore the resulting images back to disk. An overview of the overhead measured is given in Table 1. The overhead was measured for 3 stacks of 25 time-points and 40 slices with varying image sizes of 256 x 256, 512 x 512 and 1024 x 1024 pixels. The following times were measured: the time to read the grey-value stack for the first time and create the random access files (8-bit for display purposes and 16-bit original data values) in the /TEMP directory, the time to only read the complete stack and the time to read and write the stack back to disk. The latter two measurements give an indication respectively for the overhead when the user scrolls through the stack and when a complete stack is processed. In Table 1 the results are given using two different disks, namely a 1TB disk, type HD103UJ, from Samsung (Seoul, Korea) and the solid state disk of 120 GB, type SSD2 from OCZ (San Jose, California, USA). If the time to read a stack is divided by 1000, the overhead for scrolling from image to image through the stack is obtained. This time is very short, so that scrolling appears to occur instantaneous to the user.

### Comparison between CPU and GPU processing

In Table 2 a comparison is shown for the various image operations using respectively shaders written in HLSL and CUDA and the software equivalent of these operations written in C++. The figures are given as the processing time per image. The time to put an image on the GPU board and the time to get an image from the GPU board are part of the processing time. It appears that image processing using the GPU is more effective when image operations become more complex or when kernel sizes increase. The GPU is for all measured image operations in Table 1 much faster than the software equivalent despite the overhead of transferring images between the GPU board and computer memory. The shader programs written in HLSL are almost always faster than those written in CUDA. The difference for processing color images is even more distinct. However, there are possibilities to improve most of the CUDA shader programs written for color images and therefore some improvement is to be expected. On the other hand the CUDA implementation of the functions based on the fast Fourier transform is significantly more efficient than the HLSL equivalent. In Figure 2 the dilatation or MAX operation is shown for a 16-bit image with varying image and kernel sizes. As expected, there is a linear relationship with increasing kernel size. An estimate for the time necessary to transfer an image between the GPU board and computer memory is obtained at the points where the lines cross the y-axis.

### Tracking

In this study the dynamics of telomeres during different phases of the cell cycle were measured during mitosis using the STACKS software. Global cell movement was first determined based on the nuclear image stained with GFP-PCNA. The translational and rotational movement from the cell was then removed from the stack containing the telomeres, after which the movement of individual telomeres was tracked. The MSD was measured for 6 cells for each cell cycle phase. Using GFP tagged PCNA we were able to discriminate the G1 and the G2 phase of the cell cycle, and also three different stages within the S-phase (Leonhardt et al., 2000). In Figure 3 the MSD is determined in two different ways, one method uses the distance that the telomeres have traveled, and is referred to as MSDp, and the other method determines the area in which the telomeres have moved, which is the MSDt. The extreme values were omitted, and in order to perform statistical analysis 142 telomeres per cell cycle phase were

randomly selected for analysis. In Figure 4 the average MSD curves are shown for the different phases of the cell cycle. First a Mixed Model analysis was performed using SPSS in order to determine whether there was a group effect of the telomeres that were measured within a cell, for both the MSDt and the MSDp values. The group-effect was not significant in both the MSDt and the MSDp measurements, so subsequently a One-Way Anova analysis was performed on both. For the MSDp (the distance travelled by a telomere) we found that telomeres travel over a significantly larger distance in the G1-, the G2- and the beginning of the S-phase (BegS) than during the middle (MidS) or late part (LateS) of the S-phase. For the MSDt, the nuclear area in which a telomere moves, telomeres were found to move in a significantly greater volume during the G1- and the G2 phase than during the entire S-phase.



## Discussion

This paper describes the basics and features of the program STACKS, which was developed for the tracking of nuclear particles. It has been shown that this program provides sufficient visual feedback of the processing steps involved. It offers the user adequate options and flexibility to analyze data sets of varying quality. There are also tools to interactively correct for improper automatic segmentation and even when particles are incorrectly tracked, the tracks can still be corrected by the user so that finally the proper measurements can be obtained. Additional features and measurements have been built in to make the program suitable for other applications as well.

An approach was chosen, where only the visible images are kept in memory, so that no special requirements are necessary to run the program on a regular PC. It is shown that this has hardly any impact on the responsiveness of displayed stacks. However, it gives some overhead (in the order of a few seconds) when a complete stack is processed, which increases to about a minute for a stack of 1000 images of 1024 x 1024 pixels. This overhead-time will be reduced with almost 50% when a SSD disk is applied, and probably similar results would be obtained when disks would be put in RAID. It should be realized that neither the PC used in this paper, nor the GPU board and the SSD drive are nowadays the fastest on the market. When a new system would have to be assembled as of today, performance would even be better.

The program provides a number of image operations based on the GPU. They were programmed using two different shader languages, namely HLSL (using DirectX) and CUDA. For most functions the HLSL implementation is somewhat more efficient, especially for the operations on color images. It appears also that the time to transfer images between the GPU board and computer memory is also faster using DirectX and HLSL. On the other hand the fft library from CUDA is more efficient than the fft functions written in HLSL and the convolution filter in CUDA, which is based on local memory, is also faster than the implementation using global texture memory in HLSL. The operations programmed in software carried out by the CPU are always slower compared to GPU processing despite the overhead of transferring images to and from the GPU board. The use of GPU programming especially for the processing of 4D stacks is extremely useful as more than thousand images have to be processed thereby reducing the total processing time from minutes to seconds.

The market for GPU boards is dominated by two contenders, namely Ati-Amd and Nvidia. Ati-Amd has also made a software development kit available for general purpose GPU processing, called Stream. Unfortunately, both CUDA and Stream are dedicated to the hardware of the specific vendor, so that the shader programs cannot be exchanged. A future choice could be to make use of OpenCL from Apple and DirectCompute from Microsoft, which will offer support for GPU boards of both vendors. Currently there is no support in STACKS for hardware acceleration using Ati boards. As all image operations in STACKS are also written in CPU based software, it is still possible to run STACKS anyway. However, it was shown that GPU based processing provides a significant speed improvement for image operations especially when the kernel size becomes larger.

STACKS can operate directly on the image files derived from commercially available Zeiss and Leica microscope systems. It is, however, also possible to read images from a folder. By renaming independent 2D images in a way that the program “thinks” that they form a 3D or

4D stack, it is possible to analyze large image sets of independent images using STACKS. In this way large image sets have already been analyzed using STACKS.

## Future Developments

The current version of STACKS supports the tracking of maximal 255 objects as object labeling was originally developed for 8 bit images only. This is sufficient for tracking telomeres in one cell at a time, but when for instance viral particles have to be tracked in larger images, this will become a bottleneck. Object labeling has already been extended to 16 bit and the tracking in 16 bit images and thus tracking more than 65000 objects will be realized in the near future.

The number of stacks that can be simultaneously handled by the program is currently fixed to 4 grey-value 4D stacks, 4 color 4D stacks, a binary and a label 4D stack with the same amount of 3D stacks, when a maximum projection is performed. This limitation is mainly caused by the fact that only those stacks are foreseen in the menus and dialogues. In a future release those limitations will be removed by making the menus dynamic and by providing facilities to create additional stacks. In this way a larger number of stacks can be opened simultaneously, as long as memory and disk space allow it.

Currently all image operations based on the GPU are 2D operations. 3D Object labeling and 3D watershed is carried out by normal CPU processing and the GPU based nearest neighbour deconvolution takes only the slice below and above into account. However, the latest release of CUDA supports 3D textures which will ease the development of 3D image operations, such as 3D Min / Max operations, 3D convolutions and 3D distance transforms. It can also help with more complex operations such as 3D deconvolution. A new library with the 3D fast Fourier is also released by Nvidia, so that 3D deconvolution based on inverse filtering should be relatively easy to implement.

Up to now only one graphic board is supported by STACKS. It is possible to have more GPU boards in a PC or additional special boards for general GPU processing like the Tesla boards from Nvidia. This can boost the performance of GPU processing even further. STACKS would be ideally suited for this approach, as the processing of different 2D or 3D images could be easily be carried out in parallel. This possibility will be explored in future. Finally it should be mentioned that the program STACKS is free of charge available on request for non-commercial use.

## Acknowledgements

We like to thank Ron Wolterbeek from the Department of Medical Statistics and Bioinformatics of the LUMC for assisting with the statistical analysis of the MSD measurements. The work for development of image processing functions using the GPU was financially supported by Genetix, New Milton, UK.

## References

- Adrian R.J. 2005. Twenty years of particle image velocimetry. *Exp. Fluids* **39**, 157-483
- Ashkin A. 1997. Optical trapping and manipulation of neutral particles using lasers. *Proc. Natl. Acad. Sci. U S A* **94**, 4853-4860
- Bacher C.P., Reichenzeller M., Athale C., Herrmann H. & Eils R. 2004. 4-D single particle tracking of synthetic and proteinaceous microspheres reveals preferential movement of nuclear particles along chromatin – poor tracks. *BMC Cell Biol.* **5**, 45
- Bausch A.R., Ziemann F., Boulbitch A.A., Jacobson K. & Sackmann E. 1998. Local measurements of viscoelastic parameters of adherent cell surfaces by magnetic bead microrheometry. *Biophys. J.* **75**, 2038-2049
- Carter B.C., Shubeita G.T. & Gross S.P. 2005. Tracking single particles: a user-friendly quantitative evaluation. *Phys. Biol.* **2**, 60-72
- Cheezum M.K., Walker W.F. & Guilford W.H. 2001. Quantitative comparison of algorithms for tracking single fluorescent particles. *Biophys. J.* **81**, 2378 – 2388
- Grant I. 1997. Particle image velocimetry: a review. *Proceedings of the Institution of Mechanical Engineers, Part C: J. Mech. Eng. Sci.* **211**, 55-76
- Crocker J.C. & Grier D.G. 1996. Methods of digital video microscopy for colloidal studies. *J. Coll. Interf. Sci.* **179**, 298-310
- Csirik A.K. & Henikoff S. 1996. Genetic modification of heterochromatic association and nuclear organization in *Drosophila*. *Nature* **381**, 529-531
- Dernburg A.F., Broman K.W., Fung J.C., Marshall W.F., Philips J., Agard D.A. & Sedat J.W. 1996. Perturbation of nuclear architecture by long-distance chromosome interactions. *Cell* **85**, 745-759
- Farrugia J-P., Horain P., Guehenneux E. & Allusse Y. 2006. GPUCV: A framework for image processing acceleration with graphics processors. *Proc. of the IEEE International Conference on Multimedia & Expo (ICME 2006), July 9-12, Toronto, Ontario, Canada.*
- Francastel C., Schubeler D., Martin D.I. & Groudine M. 2000. Nuclear compartmentalization and gene activity. *Nat. Rev. Mol. Cell Biol.* **1**, 137-143
- Leonhardt H., Rahn H.-P., Weinzier P., Sporbert A., Cremer T., Zink D. & Cardoso M.C. 2000. Dynamics of DNA Replication Factories in Living Cells. *J. Cell Biol.* **149**, 271-280
- Manuelidis L. 1985. Individual interphase chromosome domains revealed by in situ hybridization. *Hum. Genet.* **71**, 288-293
- Miura K. 2005. Tracking movement in cell biology. *Adv. Biochem. Eng. Biotechnol.* **95**, 267-295
- Moreland K., Angel E. 2003. The FFT on a GPU. *SIGGRAPH Eurographics Workshop on Graphics Hardware.* 112–119

## STACKS: A software program for particle tracking in living cells

- Platero, J., Csink, A., Quintanilla, A. & Henikoff, S. 1998. Changes in chromosomal localization of heterochromatin binding proteins during the cell cycle in *Drosophila*. *J. Cell Biol.* **140**, 1297-1306
- Podlozhnyuk V. Image Convolution with CUDA. 2001. CUDA SDK code samples. [www.nvidia.com](http://www.nvidia.com)
- Rong G. & Tan. T-S. 2006. Jump Flooding in GPU with Applications to Voronoi Diagram and Distance Transform. *ACM SIGGRAPH Symposium on Interactive 3D Graphics and Games (I3D 2006)*, Redwood city, CA, USA, March 2006. 109-116
- Ruifrok A.C. & Johnston D.A. 2001. Quantification of histochemical staining by color deconvolution. *Anal. Quant. Cytol. Histol.* **23**, 291-299
- Sbalzarini I.F. & Koumoutsakos P. 2005. Feature point tracking and trajectory analysis for video imaging in cell biology. *J. Struct. Biol.* **151**, 182-195
- Spector D.L. 2003. The dynamics of chromosome organization and gene regulation. *Annu. Rev. Biochem.* **72**, 573-608
- Strzodka R. & Ihrke I., Magnor M. 2003. A graphics hardware implementation of the Generalized Hough Transform for fast object recognition, scale, and 3d pose detection. *Proc. of IEEE Int.Conf. on Image Analysis and Processing (ICIAP'03)*, 188–193
- Strzodka R., Telea A. 2004. Generalized Distance Transforms and skeletons in graphics hardware. *Proc. of EG/IEEE TCVG Symposium on Visualization (VisSym '04)*, 221–230.
- Fung J., Mann S., Aimone C. 2005. *Openvidia: Parallel gpu computer vision*. *Proc. of the ACM Multimedia 2005, November 2005*, 849–852
- Trask B., van den Engh G., Pinkel D., Mullikin J., Waldman F., van Dekken H. & Gray J. 1988. Fluorescence in situ hybridization to interphase cell nuclei in suspension allows flow cytometric analysis of chromosome content and microscopic analysis of nuclear organization. *Hum. Genet.* **78**, 251-259
- Tseng Y., Kole T.P. & Wirtz D. 2002. Micromechanical mapping of live cells by multiple-particle-tracking microrheology. *Biophys. J.* **83**, 3162-3176
- Verschure P.J., van Der Kraan I., Manders E.M. & van Driel R. 1999. Spatial relationship between transcription sites and chromosome territories. *J. Cell Biol.* **147**, 13-24
- Waigh T.A. 2005. Microrheology of complex fluids. *Rep. Progr. Phys.* **68**, 685-742
- Walter J., Schermelleh L., Cremer M., Tashiro S. & Cremer T. 2003. Chromosome order in HeLa cells changes during mitosis and early G1, but is stably maintained during subsequent interphase stages, *J. Cell Biol.* **160**, 685–697
- Weihls D., Mason T.G. & Teitell M.A. 2006. Bio-microrheology: a frontier in microrheology. *Biophys. J.* **91**, 4296-4305

## Figures

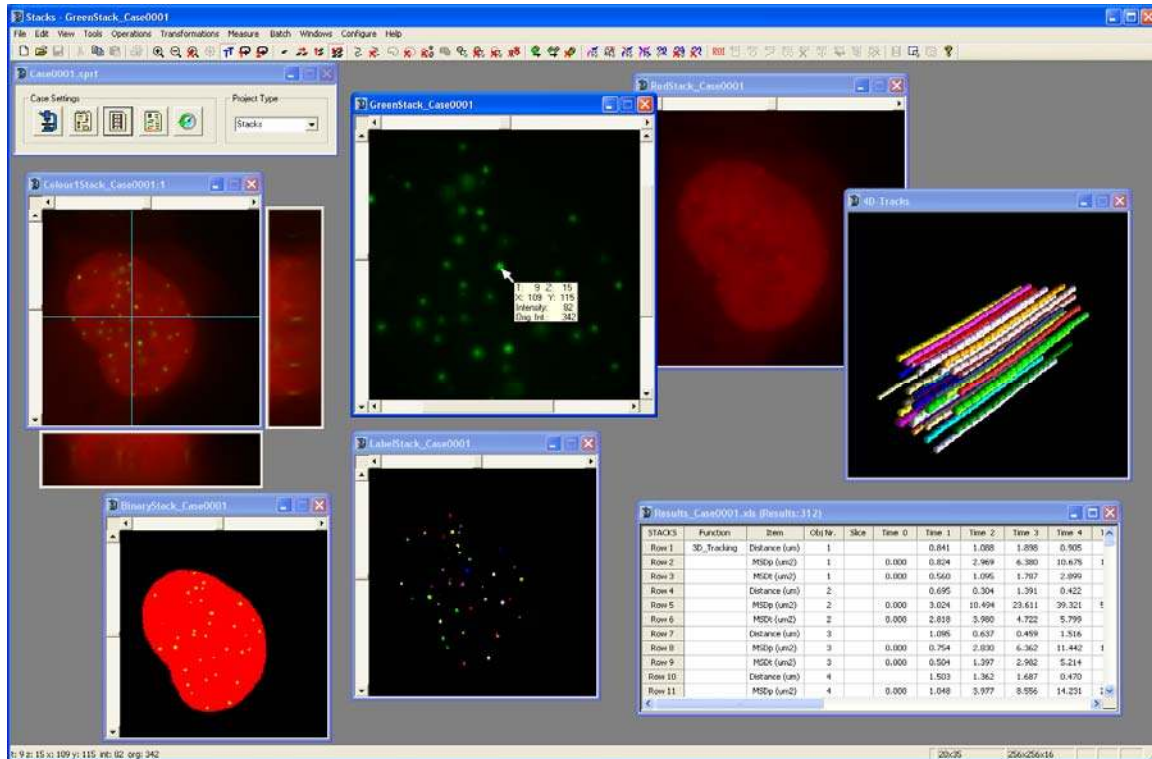


**Figure 1.** The desktop of STACKS is shown with the windows of the various stacks. Note that the window of the color stack is expanded with the cross-sections at the position of the crosshair pointer. The Green stack is displayed enlarged. This adds scroll bars to the bottom and the right for positioning the image. The scrollbar at the top is reserved for the time points and at the left for the z-slices. It is possible to show intensity information at the position of the cursor as is shown in the window of the Green stack.

Dimensions Stack	Samsung disk			OCZ SSD		
	Create stack (s)	Read stack (s)	Read / Write stack (s)	Create stack (s)	Read stack (s)	Read / Write stack (s)
25x40x256x256	5.4	0.20	3.75	4.7	0.18	2.50
25x40x512x512	25.9	1.01	14.5	16.9	0.98	8.83
25x40x1024x1024	137.1	4.19	54.80	88.7	4.10	27.83

**Table 1.** This table shows the time needed to create a new stack when it is opened for the first time, to read an existing stack only and to read an existing stack and write it back after processing. Reading the stack only occurs when the user scrolls through the stack. The last column is an indication for the disk overhead that is involved during processing. Using a solid state disk a significant improvement is obtained.

Operation	Bit Depth	HLSL (ms)	CUDA (ms)	Software CPU (ms)
Erosion (cycles: 8)	8	2.4	5.1	65.8
	16	2.8	4.9	66.1
	24	4.8	10.2	184.1
Opening (cycles: 8)	8	2.8	6.6	113.5
	16	2.9	6.9	113.8
	24	5.7	10.2	324.4
Sobel filter	8	2.0	2.7	11.4
	16	2.5	3.1	13.5
	24	4.2	8.9	30.2
LaPlace filter	8	2.0	2.7	5.3
	16	2.5	3.1	6.4
	24	4.1	8.8	13.6
Convolution (kernel:21x21)	8	6.2	4.1	118.1
	16	6.7	4.4	115.2
	24	17.2	11.5	387.9
Median (kernel: 3x3)	8	2.1	3.7	151.2
	16	2.6	4.0	153.4
	24	4.3	12.1	354.1
Kuwahara (kernel: 5x5)	8	5.8	5.4	182.7
	16	5.8	5.6	181.3
	24	7.2	16.7	533.2
Unsharp Mask (kernel: 7x7)	8	2.2	3.3	80.5
	16	2.9	3.7	78.4
	24	4.7	11.7	249.5
FFT spectrum	8	7.9	4.4	230.2
	16	8.6	4.8	228.4
Butterworth band pass (FFT)	8	11.9	8.1	not implemented
	16	13.9	8.3	not implemented
Gaussian low pass (FFT)	8	11.8	8.5	not implemented
	16	13.7	8.8	not implemented
RGB->HSI	24	4.0	8.2	43.4
Component Blend	24	4.3	8.7	13.3
Colour Deconvolution	24	4.7	8.8	127.9
Distance Transform	8	6.5	17.6	27.1
Nearest Neighbour (32 slices)	8	189.4	214.9	2772.6
	16	522.3	535.2	2798.3
	24	308.6	495.8	8597.7

**Table 2.** This table gives an overview of the time needed to process one image of 512 x 512 pixels for various image operations using the GPU and software. The overhead of transferring images to and from the GPU is included for all operations. For the nearest neighbour deconvolution the time to process 32 slices is given and the overhead to transfer the images to and from disk is included for this operation as well.

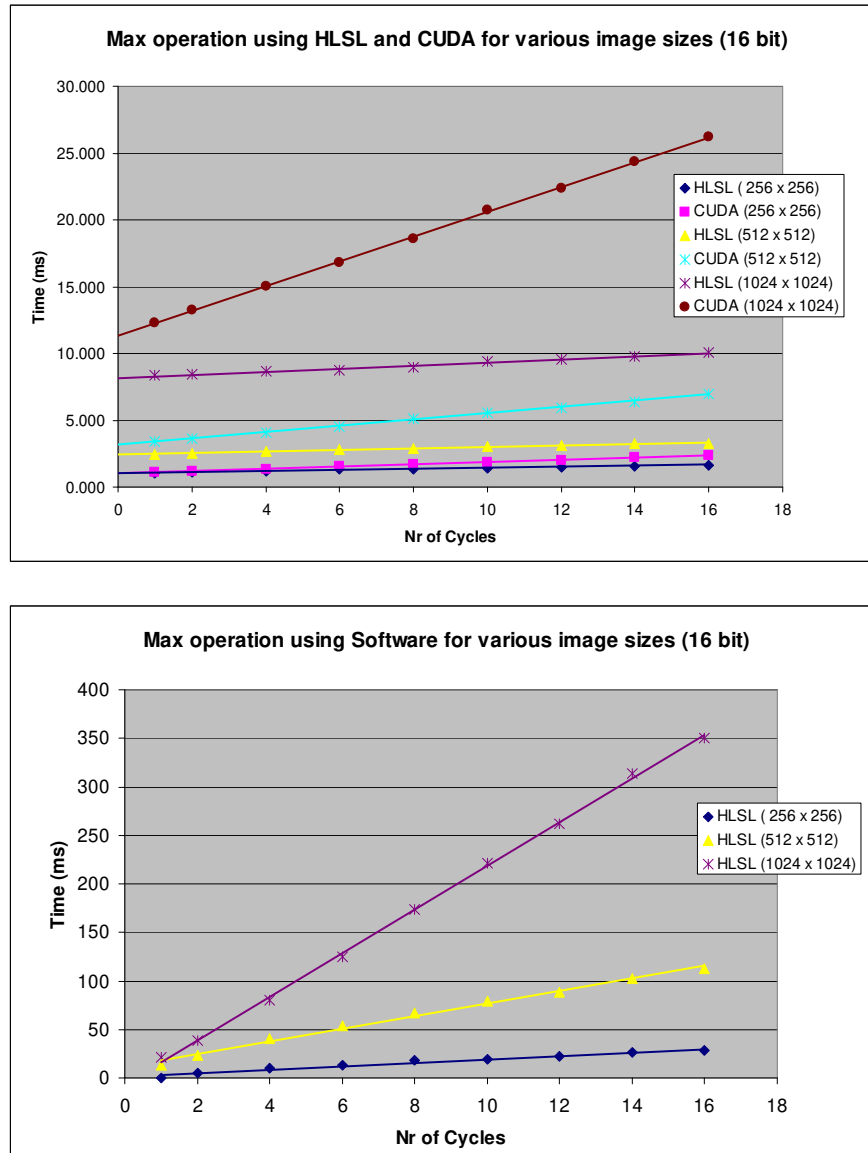


**Figure 2.** Figure 2A shows the MAX operation as function of the number of cycles for the HLSL shader and the CUDA shader program. HLSL is always faster. The time to transfer an image to/from the GPU board is included. By extrapolating the function to the y-axis the time necessary for image transfer is obtained. In figure 2B the equivalent is shown for the software implementation using the CPU.



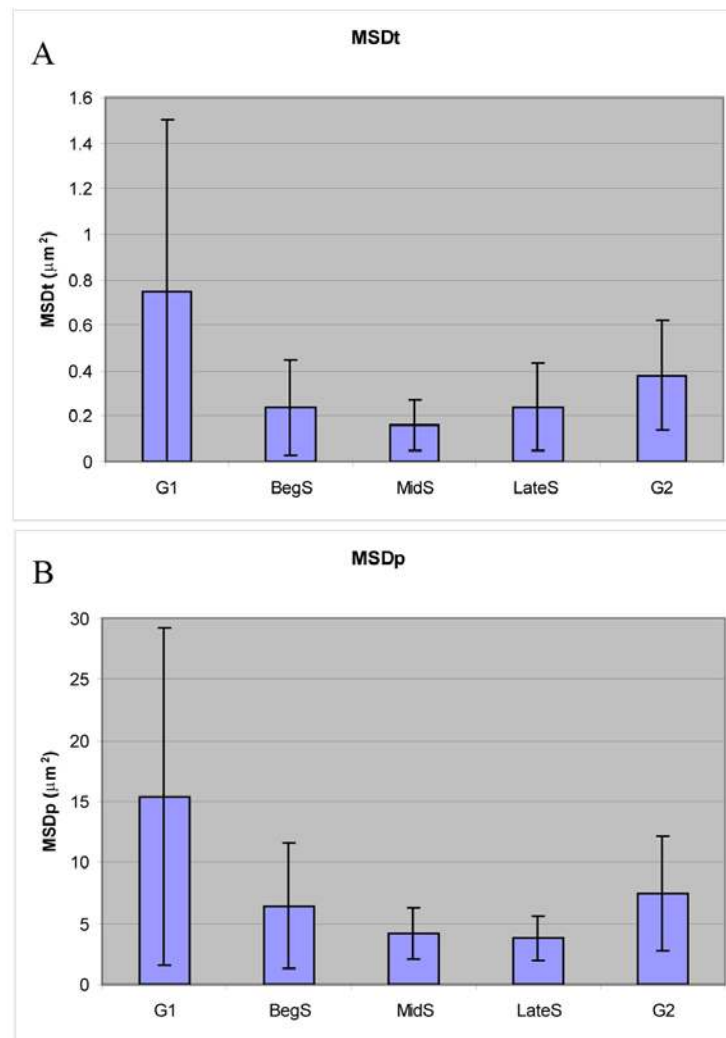


**Figure 3.** MSDt and MSDp graphs. A) The average values of the mean squared displacement (MSDt) and the standard deviation for the area in which the telomeres move in U2OS cells are shown. B) MSDp: Distance travelled by telomeres during different phases of the cell cycle.

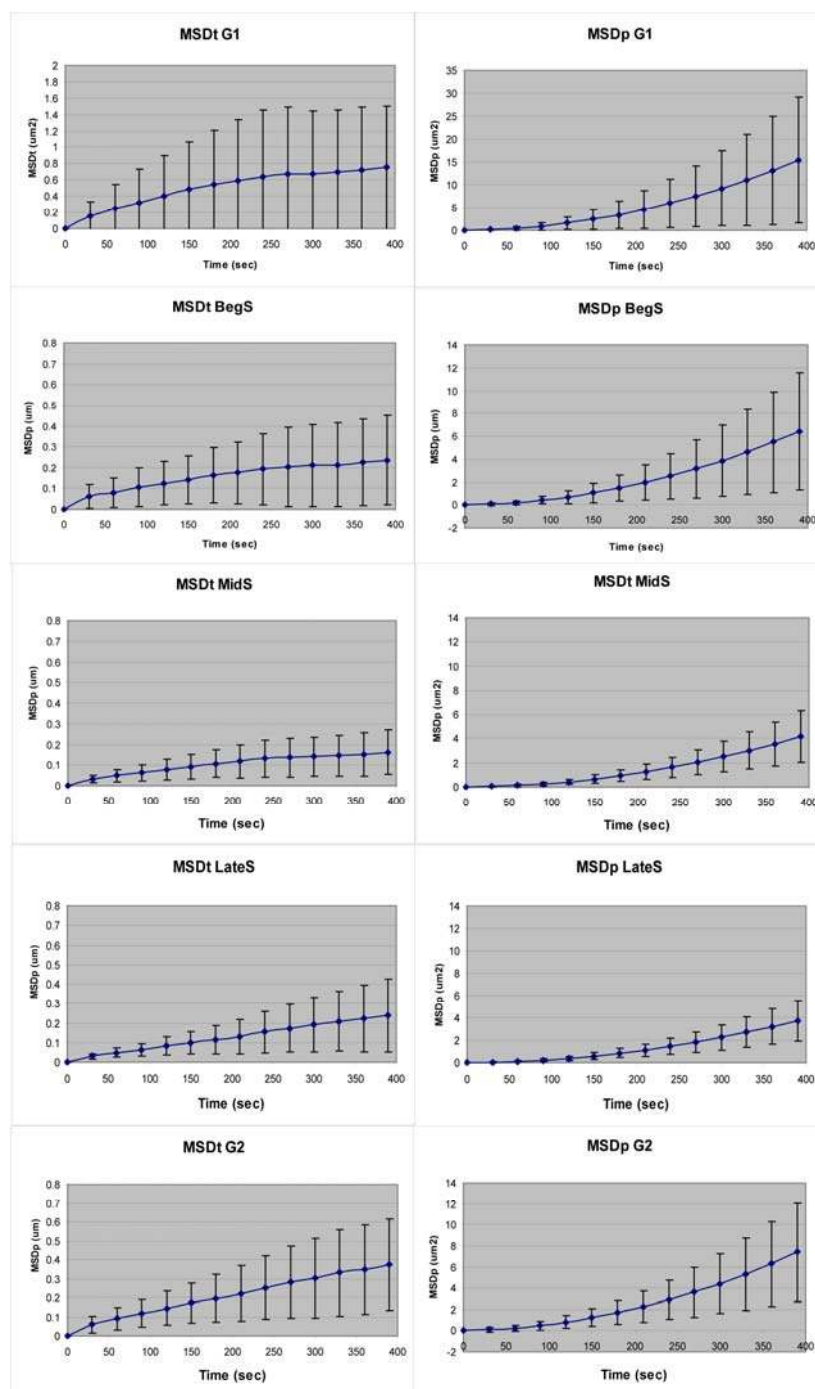


**Figure 4.** The MSDt and the MSDp curves are shown for the different phases of the cell cycle. A total of 6 cells and 142 telomeres were tracked per cell using the STACKS tracking software. Error bars represent the variance. Note that, as the telomeres become more dynamic, the error bars are also increasing. This may indicate that particularly during the G1 phase the MSD values show strong variance. This variance during the G1 phase of the cell cycle may very well be caused by a change of telomere dynamics during the G1 phase. A likely explanation could be that telomeres are very dynamic during the beginning of the G1 phase and that their dynamics decrease as they approach the end of the G1 phase. This hypothesis is in compliance with the idea that chromatin is very dynamic immediately after mitosis, because at that time many chromatin rearrangements take place (Walter et al., 2003). It is possible that for the same reason telomeres are increasingly dynamic in the G2 phase, indicating that just before mitosis also chromatin rearrangements may occur at a higher frequency.



## **CHAPTER 3**

Telomere movement is constrained by interactions with  
an inner nuclear lamin structure



## Telomere movement is constrained by interactions with an inner nuclear lamin structure

Anneke K. Brouwer, Dewi van Tol, Hans Vrolijk, Hans J. Tanke, Roeland W. Dirks

Department of Molecular Cell Biology, Leiden University Medical Center, 2300 RC Leiden, The Netherlands

### Summary

The interphase nucleus is thought to contain a three-dimensional filamentous protein network that provides structural support to chromosomes and facilitates transcription, RNA processing, DNA replication and DNA repair. The molecular composition of this network is, however, not clear. In this work we investigate whether telomeres, which are distributed throughout the nuclear interior, are attached to a nuclear matrix structure composed of lamin proteins. We used RNA interference to knockdown components of the nuclear matrix and latrunculin to depolymerize the nuclear actin network. Fluorescence time-lapse imaging revealed that telomeres become more dynamic in lamin A/C depleted cells but not in lamin B2 depleted cells. In addition, telomeres are more dynamic in emerin depleted cells and in cells that have been treated with latrunculin. These results suggest that telomeres are associated to a complex consisting of lamin A/C, emerin and actin and that the movement of telomeres is constrained by this association.

### Introduction

The cell nucleus is subdivided in distinct compartments including chromosome domains and nuclear bodies. Different types of nuclear bodies have been distinguished, each type housing a unique set of proteins that creates a specific microenvironment. The nuclear bodies are positioned in the interchromatin domain space, which separates the individual chromosome domains (Spector, 2003). The separation of chromosome domains is not absolute as some intermingling between neighbouring chromosomes has been observed (Branco & Pombo, 2006). In general, however, the spatial positioning of chromosome domains in the three-dimensional space of the interphase cell nucleus is rather fixed and non-random, though may vary among cells and change with the differentiation and proliferation state of the cell. The general concept is that gene poor chromosomes are positioned at the nuclear periphery and that gene rich chromosomes are positioned towards the nuclear interior (Croft et al., 1999). This concept is consistent with observations where the positioning of specific genes at the nuclear periphery resulted in their silencing and is explained by the predominant heterochromatic nature of chromatin at this site and by the attachment to the lamina (Finlan et al., 2008; Reddy et al., 2008). Thus, the composition of the nuclear periphery might be such that it does not favour transcriptional activity. Some genes, however, are not silenced when located at the nuclear periphery and show transcriptional activity (Kumaran & Spector, 2008). This is particularly true for genes that are positioned at nuclear pores (Casolari et al., 2004; Dieppois et al., 2006). Also, genes in

centromeric and telomeric regions, which are supposed to be heterochromatic, have been found to display transcriptional activity. Hence, additional factors are required to establish a transcriptionally competent microenvironment. These could include the spatial positioning of active genes at the periphery of compact chromatin domains facing the interchromatin domain space (Mahy et al., 2002). But also, the positioning of genes at transcription factories or at speckles (Sexton et al., 2007; Sutherland & Bickmore, 2009). These speckles are distinct nuclear bodies enriched for splicing and transcription factors. Clustering genes at transcription factories or speckles would allow for a coordinated regulation of transcription, RNA processing and RNA transport. Specific associations of genes with other nuclear bodies, like PML and Cajal bodies, have been reported as well (Trinkle-Mulcahy & Lamond, 2008). Together, these findings suggest that the spatial arrangement of genomic regions and probably also that of nuclear bodies in the cell nucleus is important to control gene activity.

One of the key questions is how the spatial organization of the cell nucleus is established and maintained during interphase, and how it reorganizes in response to external factors that may either activate or silence genes. Several lines of research suggest that the nucleus contains a rigid though dynamic nuclear skeleton or matrix structure that provides anchorage sites for chromatin and nuclear bodies. DNA loops are attached to the nuclear matrix via loop anchorage regions (LARs). These genomic regions may include matrix attachment regions (MARs), topoisomerase II binding sites and other discrete sequence motifs (Razin, 1996; Vassetzky et al., 2000). At present, a clear view about the composition and localization of the nuclear matrix does not exist. Therefore, the nuclear matrix has often been defined as a three-dimensional filamentous protein network that remains present after high-salt extractions and the removal of chromatin. Among the candidate proteins that are part of the nuclear matrix structure are the lamin proteins. The lamin proteins are encoded by three genes, the lamin A, lamin B1 and lamin B2 genes. Lamin C is a splice variant of lamin A. The lamin A and B proteins form the lamina, which is a protein filament meshwork at the nuclear periphery connected to the inner nuclear membrane (Broers et al., 2006). Lamins also exist throughout the nuclear volume and have been suggested to support transcription and DNA replication (Moir et al., 1994; Spann et al., 2002; Tang et al., 2008). Consistent with a role of lamin proteins in supporting chromatin organization are observations that the expression of mutant lamina proteins leads to nuclear reorganization (Broers et al., 2005; Taimen et al., 2009).

Previous work indicated that telomeres are firmly attached to the nuclear matrix and thereby contribute to the spatial organization of chromatin in the cell nucleus (de Lange, 1992; Luderus et al., 1996; Weipoltshammer et al., 1999). The components that mediate this interaction have, however, not been identified yet. To investigate a possible role for lamin proteins in tethering telomeres we realized a knockdown of nuclear lamin proteins by expressing specific shRNAs and measured the dynamics of telomere movement in cells by fluorescence time-lapse imaging.

## Results

### **Reduction of lamin A/C but not lamin B2 results in an increase in telomere dynamics**

To knockdown the expression of lamin A and lamin B2 we selected for each gene 5 short hairpin (sh) RNA constructs from a viral-vector-based shRNA library targeting 7100 annotated human genes. Each construct was selected to target a different region of the gene sequence and tested for its efficiency for knockdown. To this end U2OS cells were transiently transfected and cultured in the presence of puromycin for 72 hours. As a control, cells were transfected with an empty vector. Cells were lysed and subjected to Western blot analysis. Finally, we selected one shRNA construct for each target gene on the basis of most efficient knockdown of protein expression. The selected constructs were packed in lentiviral particles and used to transduce U2OS cells. At 72 hours post transduction, the knockdown of lamins was analyzed by both Western blotting and immunocytochemistry. By Western blotting we observed an almost complete reduction in expression of both lamin proteins (Fig. 1A). Next, we analyzed the efficiency of lamin protein knockdown by immunocytochemistry. As shown in Fig. 1B, the majority of cells showed an absence or strong reduction of lamin A/C staining. After counting 285 cells, we calculated an almost complete knockdown of lamin A/C in 87% of cells. For lamin B2, we calculated that 97% of cells showed a strong reduction in protein expression.

Following lentiviral transductions of U2OS cells targeting lamin A/C and lamin B2 respectively, the cells were transfected after 72 hours with TRF1-DsRed together with GFP-PCNA. As a control, cells were either not transduced or transduced with a lentivirus containing a non-silencing expression vector (SHC002). In previous studies it has been shown that TRF1-DsRed is a specific marker for telomeric DNA (Molenaar et al., 2003; Brouwer et al., 2009) and that GFP-PCNA is an efficient live cell marker to discriminate cell nuclei and cell cycle phases (Leonhardt et al., 2000). 3D time-lapse images were collected every 30 seconds for 20 minutes and the mean square displacements (MSDt) of telomeres were determined using the image analysis program STACKS. Because all MSDt curves obtained for telomere movement showed the same shape we present the MSDt values at  $\Delta t$  360 seconds in order to compare telomere movements measured under the various conditions tested in this study. STACKS first corrects for cell movements and then calculates the movements of telomeres in 2D and time. A correction has been made to compensate for the fact that a cell is a 3D object. MSDt plots representing measures for the space in which an individual dot is moving inside the cell nucleus during a given time-period. Fig. 2 shows an example of a graph representing the tracks of individual telomeres in a cell nucleus. Consistent with our previous data, we observed that the movement of telomeres in control cells is constrained (Molenaar et al., 2003) and we calculated an MSDt value of  $\sim 0.35 \mu\text{m}^2$  (at  $\Delta t$  360 seconds). All MSDt values in this study represent the total of telomeres measured in 10 individual cells. When G1 cells were excluded from the analysis on basis of PCNA staining, we calculated an MSDt value of  $\sim 0.25 \mu\text{m}^2$ , consistent with observations that telomeres are more dynamic during the G1 phase (Vrolijk et al., in preparation). Reduction of lamin A/C expression by shRNA interference resulted in an increase in telomere movement as compared to cells transduced with the SHC002 control virus, MSDt  $\sim 0.53 \mu\text{m}^2$  (stdev  $\sim 0.46 \mu\text{m}^2$ ) versus  $0.22 \mu\text{m}^2$



(stdev  $\sim 0.05 \mu\text{m}^2$ ) (Fig. 3). Surprisingly, a reduction of lamin B2 did not reveal an increase in telomere dynamics (MSDt  $\sim 0.19 \mu\text{m}^2$ , stdev  $\sim 0.12 \mu\text{m}^2$ ) (Fig. 3).

### Telomere movement in emerin depleted cells

Emerin is a nuclear membrane protein, which is missing or defective in Emery-Dreifuss muscular dystrophy (EDMD). It is a member of a family of lamina-associated proteins which includes LAP1, LAP2 and laminB receptor (LBR) (Holmer & Worman, 2001). Emerin binds directly to both A- and B-type lamins *in vitro* (Clements et al., 2000; Lee et al., 2001), colocalizes with lamins *in vivo* (Manilal, 1998), and is associated with the actin network in the nucleus (Holaska et al., 2004). Since emerin has also been identified as part of the nuclear matrix (Squarzone et al., 1998), we decided to investigate its role in telomere positioning and kinetics. From five shRNA constructs we selected one construct that when expressed in U2OS cells resulted in a 94% reduction of emerin protein as compared to endogenous levels. This construct was used to assemble lentiviral particles and then to transduce U2OS cells. Transduction resulted in a strong reduction of cells showing emerin staining. Of 452 cells that were analyzed, 85% showed absence of emerin staining (Fig. 4). Next, cells were first transduced to knockdown emerin expression and then, after 72 hours, transfected with TRF1-DsRed together with GFP-PCNA. Analysis of 3D image stacks, which were recorded every 10 seconds during 20 minutes and collected from 10 cells revealed an increase in telomere mobility (MSDt value of  $\sim 2.1 \mu\text{m}^2$ , stdev  $\sim 1.5 \mu\text{m}^2$ ) as compared to cells transduced with the control construct ( $\sim 0.35 \mu\text{m}^2$ ).

### Preventing actin polymerization causes an increase in telomere mobility

Nuclear actin has been identified as a potential nuclear matrix component (Kiseleva et al., 2004; Albrethsen et al., 2009) and as a binding partner of lamin A (Sasseville and Langelier, 1998; Zastrow et al., 2004) and emerin (Lattanzi et al., 2003). Thus telomeres could be directly or indirectly linked to a nuclear matrix by actin. To test this possibility, we treated U2OS cells expressing both TRF1-DsRed and GFP-PCNA with latrunculin A, a drug that inhibits actin polymerisation *in vitro* (Coue et al., 1987; Morton et al., 2000) and *in vivo* (Spector et al., 1983). Analysis of 3D time-lapse recordings of telomere movements in 10 cells using STACKS revealed a mean MSDt value of  $\sim 0.54 \mu\text{m}^2$  as compared to an MSDt  $\sim 0.35 \mu\text{m}^2$  that was calculated for telomeres in untreated control cells, suggesting that telomeres become more mobile in the absence of polymerized nuclear actin (Fig. 5). To confirm this finding we also treated mouse embryonic fibroblasts (W8 MEFs) expressing TRF1-DsRed together with GFP-PCNA with latrunculin A and collected 4D image stacks. Quantitative analysis of telomere movement by the program STACKS revealed a three-fold increase in MSDt value, MSDt  $\sim 1.01 \mu\text{m}^2$  as compared to MSDt  $\sim 0.35 \mu\text{m}^2$  in untreated cells (Fig. 6).

Nuclear actin has been shown to be involved in the transcription process (Zhu et al., 2004). Preventing actin polymerization by latrunculin may therefore result in global transcription inhibition, which then may result in a change in chromosome organization, leading to less constrained telomere mobility. Treatment of U2OS cells with the transcription inhibitor 5,6-dichloro-1- $\beta$ -D-ribobenzimidazole (DRB) resulted in some decrease in telomere mobility (MSDt  $\sim 0.23 \mu\text{m}^2$ ), suggesting that telomere mobility is not increased by changes in global transcriptional activity but more likely

by losing their association with an actin containing complex (Fig. 5). Also in W8 MEFs, we observed a decrease in telomere mobility, although not significant, after treatment with DRB, (MSDt  $\sim 0.32 \mu\text{m}^2$  as compared to MSDt  $\sim 0.35 \mu\text{m}^2$  in untreated cells (Fig. 6).

## Discussion

The spatial positioning and dynamic properties of telomeres in the cell nucleus have been addressed by various studies. These studies show that in yeast telomeres are positioned at the nuclear periphery and anchored to the inner nuclear membrane by Ku and Sir proteins (Hediger et al., 2002). This anchoring puts a constraint on the mobility of telomeres in yeast cells and has been functionally linked to gene regulation. Unlike in yeast, in mammalian cells telomeres are positioned throughout the nucleus (Molenaar et al., 2003; Weierich et al., 2003). Still, their mobility is not very different from that of yeast telomeres and appeared to be constrained (Molenaar et al., 2003; Jegou et al., 2009). This constrained movement can be explained by a compact organization of chromatin in the cell nucleus, but also by an association to a supporting structure like the nuclear matrix.

In this work we show that telomeres are more mobile in cells with reduced expression of lamin A/C or emerin but not in cells with reduced lamin B2 expression. These findings are consistent with the idea that lamin A/C is a component of the nuclear matrix and anchors telomeres to this structure. Patients with a 433G>A mutation in the  $\alpha$ -helical central rod domain of the A-type lamin gene show multiple nuclear alterations including mislocalization of telomeres (Taimen et al., 2009). This mutation prevents lamin A to organize in higher order structures and may thereby lose its function to anchor telomeres. Consistent with this idea, telomeres have been found to be shifted towards the nuclear periphery in MEFs devoid of A-type lamins (Gonzalez-Suarez et al., 2009). Recently, we showed that lamin redistribution in the cell nucleus is one of the first hallmarks of a senescent state of mesenchymal stem cells and that this redistribution is accompanied by a redistribution of telomeres, suggesting that telomeres are physically associated with a lamin structure (Raz et al., 2008). Previous studies suggested that telomeres are associated with a nuclear matrix structure (Gonzalez-Suarez et al., 2009). Following various nuclear extraction procedures telomeres were shown to remain attached to structures in the cell nucleus while most other DNA sequences did not (de Lange, 1992; Ludérus et al., 1996; Weipoltshammer et al., 1999). These studies, however, did not identify lamin proteins being responsible for retaining telomeric sequences. It was, however, observed that telomere binding protein TRF colocalizes with telomeric DNA in nuclear matrix preparations and that TRF was retained in the nuclear matrix even after removal of telomeric DNA, suggesting that anchoring of telomeres to the nuclear matrix is mediated by TRF (Ludérus et al., 1996). Interestingly, fluorescence recovery after photobleaching analysis showed that the association of TRF1 and TRF2 with telomeres is highly dynamic (Mattern et al., 2004). However, a fraction of TRF2 has been identified that forms more stable complexes with telomeres (Mattern et al., 2004) and might be involved in stabilizing the interaction of telomeres with a nuclear lamina structure.

One may also argue that a dynamic binding of TRF1 and TRF2 at telomeres may allow dynamic interaction with a nuclear lamina scaffold structure which may be essential for a dynamic nuclear organization. Recently, it has been shown that deletion of TRF2 in mouse cells resulted in increased telomere mobility and was dependent on 53BP1. The supposed rationale for the increased telomere mobility is to facilitate non-homologous end joining to repair DNA damage (Dimitrova et al., 2008).

A question that has not been answered yet is which factors mediate the interaction between telomeres and the nuclear matrix. Proteins in the nuclear matrix may directly interact with telomeric DNA or indirectly by association with telomere proteins. Di-

rect interactions of lamin proteins with TRF1 or TRF 2 have thus far not been observed. Recently, it has been shown that the telomere associated protein TIN2, binding both TRF1 and TRF2, associates with the nuclear matrix and thereby may mediate the binding of telomeres to the nuclear matrix (Kaminker et al., 2009).

Our observation that emerin knockdown results in an increase in telomere dynamics is consistent with a role for emerin in structuring the cell nucleus. Emerin has been shown to interact directly with A- and B-type lamins (Clements et al., 2000; Lee et al., 2001) and in patients lacking emerin lamins A, C and B2 are more soluble suggesting a disrupted lamina architecture (Markiewicz et al., 2002). Together with our observation that nuclear actin plays a role in tethering telomeres to a nuclear structure our data support a previously proposed model in which lamin A, actin and emerin form a complex which forms or is part of a network in the nucleus (Mehta et al., 2008). Telomeres could be associated with such a complex to help structuring chromosome organization in the interphase nucleus. The fact that lamin B2 knockdown does not result in increased telomere mobility suggests that telomeres are not linked to a structure composed of B type lamins. Previously, photobleaching experiments revealed that A and B type lamins show different exchange rates in the nucleoplasm, suggesting that both types are present in distinct structures (Moir et al., 2000). At the nuclear periphery, A and B type lamins were shown to be present in a separate but interconnected network (Shimi et al., 2008). This may also be true when both proteins are present in the internuclear space. Furthermore, in vitro experiments showed that lamin B does not bind to telomeric DNA while lamin A/C does (Shoeman & Traub, 1990). Thus, intranuclear B-type lamins may contribute to a stable nuclear architecture in a different fashion as compared to A-type lamins, for example by supporting a framework for RNA synthesis (Tang et al., 2008).

## Materials and Methods

### Cell Culture

Human Osteosarcoma cells (U2OS) and mouse embryonic stem cells (W8 MEFs) were cultured at 37 °C on 3.5-cm glass-bottom culture dishes (MatTek) in Dulbecco's modified Eagle's medium (DMEM) without phenol red, containing 1.0 mg/ml glucose, 4% FBS, 2 mM glutamine, 100 U/ml penicillin, and 100 µg/ml streptomycin, pH 7.2 (all from Invitrogen). Actin depolymerisation was induced by treating cells with 2 µg/ml latrunculin A for 2h. Transcription inhibition was achieved by treating cells with 30 µg/ml DRB (5,6-dichloro-1-β-D-ribozimidazole) for 2h.

### Plasmids and transfection

The cloning of TRF1 in the DsRedExpress vector (Clontech) has been described (Brouwer et al., 2009). The GFP-tagged proliferating cell nuclear antigen (PCNA) protein was a gift from M.C. Cardoso (Leonhardt et al., 2000). Cells were transiently transfected with 0.5 µg vector DNA using Lipofectamine 2000 (Invitrogen) according to instructions of the manufacturer. At 16 hours post transfection 1.5 µg/ml puromycin was added to the culture medium and cells were assayed 72 hours after transfection.

### Protein blot analysis

Cells were lysed in NuPAGE LDS sample preparation buffer (Invitrogen). Protein samples were then size fractionated on Novex 4–12% BisTris gradient gels using a MOPS buffer (Invitrogen) and were subsequently transferred onto Hybond-C extra membranes (Amersham Biosciences) using a submarine system (Invitrogen). Blots were stained for total protein using Ponceau S (Sigma-Aldrich). After blocking with PBS containing 0.1% Tween 20 and 5% milk powder, the membranes were incubated with monoclonal mouse antibodies against lamin A/C (sc-7292, Santa Cruz Biotechnology), lamin B2 (NLC-LAM-B2, Novocastra), emerin (NCL-emerin, Novocastra) and with a mouse polyclonal antibody against tubulin (1:2000; Sigma-Aldrich). The secondary antibody used was HRP-conjugated anti-mouse (1:5,000; Pierce). Bound antibodies were detected by chemiluminescence using ECL Plus (Amersham Biosciences).

### Virus production and transduction

The shRNA lentiviral plasmid vectors targeting lamin A/C, lamin B2 and emerin were selected and obtained from the Sigma human shRNA library MISSION™ TRC-Hs 1.0 (Sigma-Aldrich). The pLKO.1Puro lentiviral shRNA vectors generating an efficient knockdown of lamin A/C, lamin B2 and emerin were used to generate lentiviral particles. For this purpose 293T cells were transfected with the appropriate lentiviral shRNA vector together with the vectors pCMV-VsVG, pMDLg-RRE and pRSV-Rev using calcium phosphate precipitation. At 48 and at 72 hours after transfection the viral supernatants were harvested and filtered through a 0.45 µm pore size filter. Virus titers were determined by measuring HIV-1 p24 antigen levels by ELISA using a RETRO-TEK HIV-1 p24 antigen ELISA system (ZeptoMetrix, Buffalo, USA). Cells were transduced with lentiviral particles (MOI 3, MOI5 and MOI 10) in the presence of 8 µg/ml Polybrene (Sigma) and incubated overnight at 37 °C. Then, the cells were washed 3 times in medium and cultured in fresh culture medium until analysis.

**Live cell imaging**

Wide-field fluorescence microscopy was performed on a multi-dimensional workstation for live cell imaging (model DMI3000B; Leica Microsystems, Mannheim, Germany) equipped with a metal halide bulb and a 63× NA 1.25 HCX plan Fluotar objective. 4D image stacks, each containing 20 sections of 0.5 μm, were collected using an automated motorized z-galvo stage. During imaging, the microscope was heated to 37 °C in a CO<sub>2</sub> perfused and moisturized chamber. Image stacks were collected every 30 sec for 10 min. Image deconvolution was performed using Leica software. For each experiment and cell type at least ten movies were analyzed.

Telomere movements were quantified using an in house developed object tracking program called STACKS (Vrolijk et al., in preparation). With this program tracks of moving objects in a cell can be visualized and quantified. The movements of telomeres were quantified by measuring their mean squared displacement, or MSDt, as described in chapter 2 of this thesis.

**Immunofluorescence**

The following antibodies were used for immunofluorescence staining of cells: a mouse monoclonal antibody against lamin A/C (sc-7292, Santa Cruz Biotechnology), a mouse monoclonal antibody against lamin B2 (NLC-LAM-B2, Novocastra) and a mouse monoclonal antibody against emerin (NCL-emerin, Novocastra). Cells were grown on coverslips, washed three times in PBS and then fixed in 2% formaldehyde in PBS for 10 minutes at room temperature. After fixation, cells were washed three times in PBS, permeabilized in PBS containing 0.2% Triton X-100 for 15 min and washed once in TBS containing 0.1% Tween 20. Then, cells were incubated with primary antibody for 45 minutes at 37 °C, followed by three washes in TBS containing 0.1% Tween 20. Finally, cells were incubated with an appropriate Alexa-Fluor 488, Alexa-Fluor 594 (both Invitrogen) or Cy3 secondary antibody conjugate for 45 minutes at 37 °C, washed in TBS containing 0.1% Tween 20, and mounted in Citifluor (Agar Scientific) containing 400 μg/ml DAPI (Sigma-Aldrich).

## References

- Albrethsen J., Knol J.C. & Jimenez C.R. 2009. Unravelling the nuclear matrix proteome. *J. Proteomics* **72**, 71-81
- Branco M.R. & Pombo A. 2006. Intermingling of chromosome territories in interphase suggests role in translocations and transcription-dependent associations. *PLoS Biology* **4**, e138
- Broers J.L., Kuijpers H.J., Ostlund C., Worman H.J., Endert J. & Ramaekers F.C. 2005. Both lamin A and lamin C mutations cause lamina instability as well as loss of internal nuclear lamin organization. *Exp. Cell Res.* **304**, 582-592
- Broers J.L., Ramaekers F.C., Bonne G., Yaou R.B. & Hutchison, C.J. 2006. Nuclear lamins: laminopathies and their role in premature ageing. *Physiol. Rev.* **86**, 967-1008
- Brouwer A.K., Schimmel J., Wiegant J.C., Vertegaal A.C., Tanke H.J. & Dirks R.W. 2009. Telomeric DNA mediates de novo PML body formation. *Mol. Biol. Cell* **20**, 4804-4815
- Casolari J.M., Brown C.R., Komili S., West J., Hieronymus H., Silver P.A. 2004. Genome-wide localization of the nuclear transport machinery couples transcriptional status and nuclear organization. *Cell* **117**, 427-439
- Clements L., Manilal S., Love D.R. & Morris G.E. 2000. Direct interaction between emerin and lamin A. *Biochem. Biophys. Res. Commun.* **267**, 709-714
- Coue M., Brenner S.L., Spector I. and Korn E.D. 1987. Inhibition of actin polymerization by latrunculin A. *FEBS Lett.* **213**, 316-318
- Croft J.A., Bridger J.M, Boyle S., Perry P., Teague P. & Bickmore W.A. 1999. Differences in the localization and morphology of chromosomes in the human nucleus. *J Cell Biol.* **145**, 1119-1131
- de Lange T. 1992. Human telomeres are attached to the nuclear matrix. *EMBO J.* **11**, 717-724
- Dieppo G., Iglesias N. & Stutz F. 2006. Co-transcriptional recruitment of the mRNA export receptor Mex67p contributes to nuclear pore anchoring of activated genes. *Mol. Cell. Biol.* **21**, 7858-7870
- Dimitrova N., Chen Y-C.M., Spector D.L. & de Lange T. 2008. 53BP1 promotes non-homologous end joining of telomeres by increasing chromatin mobility. *Nature* **456**, 524-528
- Finlan L.E., Sproul D., Thomson, I., Boyle, S., Kerr, E., Perry, P., Yistra, B., Chubb, J.R., and Bickmore, W.A. 2008. Recruitment to the nuclear periphery can alter expression of genes in human cells. *PLoS Genet.* **4**, e1000039
- Gonzalez-Suarez I., Redwood A.B., Perkins S.M., Vermolen B., Lichtensztein D., Grotzky D.A., Morgado-Palacin L., Gapud E.J., Sleckman B.P., Sullivan T., Sage J., Stewart C.L., Mai S. & Gonzalo S. 2009. Novel roles for A-type lamins in telomere biology and the DNA damage response pathway. *EMBO J.* **28**, 2414-2427
- Hediger F., Neumann F.R., van Houwe G., Dubrana K. & Gasser S.M. 2002. Live imaging of telomeres: yKu and Sir proteins define redundant telomere-anchoring pathways in yeast. *Curr. Biol.* **12**, 2076-2089

- Holmer L. & Worman H.J. 2001. Inner nuclear membrane proteins: functions and targeting. *Cell. Mol. Life Sci.* **58**, 1741-1747
- Holaska J.M., Kowalski A.K. & Wilson K.L. 2004. Emerin caps the pointed end of actin filaments: evidence for an actin cortical network at the nuclear inner membrane. *PLoS Biol.* **2**, e231
- Jegou T., Chung I., Heuvelman G., Wachsmuth M., Görisch S.M., Greulich-Bode K.M., Boukamp P., Lichter P. & Rippe K. 2009. Dynamics of telomeres and promyelocytic leukemia bodies in a telomerase-negative human cell line. *Mol. Biol. Cell* **20**, 2070-2082
- Kaminker P.G., Kim S.H., Desprez P.Y. & Campisi J. 2009. A novel form of the telomere-associated protein TIN2 localizes to the nuclear matrix. *Cell Cycle* **8**, 931-939
- Kiseleva E., Drummond S.P., Goldberg M.W., Rutherford S.A., Allen T.D. & Wilson K.L. 2004. Actin- and protein-4.1-containing filaments link nuclear pore complexes to subnuclear organelles in *Xenopus* oocyte nuclei. *J. Cell Sci.* **117**, 2481-2490
- Kumaran R.I & Spector D.L. 2008. A genetic locus targeted to the nuclear periphery in living cells maintains its transcriptional competence. *J. Cell Biol.* **180**, 51-65
- Lattanzi G., Cenni V., Marmiroli S., Capanni C., Mattioli E., Merlini L., Squarzone S., & Maraldi N.M. 2003. Association of emerin with nuclear and cytoplasmic actin is regulated in differentiating myoblasts. *Biochem. Biophys. Res. Commun.* **303**, 764-770
- Lee K.K., Haraguchi T., Lee R.S., Koujin T., Hiraoka Y., Wilson K.L. 2001. Distinct functional domains in emerin bind lamin A and DNA-bridging protein BAF. *J. Cell Sci.* **114**, 4567-4573
- Leonhardt H., Rahn H.P., Weinzierl P., Sporbert A., Cremer T., Zink D. & Cardoso M.C. 2000. Dynamics of DNA replication factories in living cells. *J. Cell Biol.* **149**, 271-280
- Ludérus M.E.E., van Steensel B., Chong L., Sibon O.C.M., Cremers F.F.M. & de Lange T. 1996. Structure, subnuclear distribution, and nuclear matrix association of the mammalian telomeric complex. *J. Cell Biol.* **135**, 867-881
- Mahy N.L., Perry P.E. & Bickmore W.A. 2002. Gene density and transcription influence the localization of chromatin outside of chromosome territories detectable by FISH. *J. Cell Biol.* **159**, 753-63
- Manilal S., Nguyen T.M., Morris G.E. 1998. Colocalization of emerin and lamins in interphase nuclei and changes during mitosis. *Biochem. Biophys. Res. Commun.* **249**, 643-647
- Markiewicz E., Venables R., Mauricio-Alvarez-Revez, Quinlan R., Dorobek M., Hausmanowa-Petruciewicz I. & Hutchison C. 2002. Increased solubility of lamins and redistribution of lamin C in X-linked Emery-Dreifuss muscular dystrophy fibroblasts. *J. Struct. Biol.* **140**, 241-253
- Mattern K.A., Swiggers S.J.J., Nigg A.L., Löwenberg B., Houtsmuller A.B. & Zijlmans J.M.J.M. 2004. Dynamics of protein binding to telomeres in living cells: implications for telomere structure and function. *Mol. Cell. Biol.* **24**, 5587-5594.



## Telomere movement is constrained by interactions with a lamin structure

- Mehta I.S., Elcock L.S., Amira M., Kill I.R. & Bridger J.M. 2008. Nuclear motors and nuclear structures containing A-type lamins and emerin: is there a functional link? *Biochem. Soc. Trans.* **36**, 1384-1388
- Moir R.D., Montag-Lowy M. & Goldman R.D. 1994. Dynamic properties of nuclear lamins: lamin B is associated with sites of DNA replication. *J. Cell Biol.* **125**, 1201-1212
- Moir R.D., Yoon M., Khuon S. & Goldman R.D. 2000. Nuclear lamins A and B1: different pathways of assembly during nuclear envelope formation in living cells. *J. Cell Biol.* **151**, 1155-1168
- Molenaar C., Wiesmeijer K., Verwoerd N.P., Khazen S., Eils R., Tanke H.J. & Dirks R.W. 2003. Visualizing telomere dynamics in living mammalian cells using PNA probes. *EMBO J.* **22**, 6631-6641
- Morton W.M., Ayscough K.R. & McLaughlin P.J. 2000. Latrunculin alters the actin-monomer subunit interface to prevent polymerization. *Nature Cell Biol.* **2**, 376-378
- Raz V., Vermolen B.J., Garini Y., Onderwater J.J., Mommaas-Kleinhuis M.A., Koster A.J., Young I.T., Tanke H.J. & Dirks R.W. 2008. The nuclear lamina promotes telomere aggregation and centromere peripheral localization during senescence of human mesenchymal stem cells. *J. Cell Sci.* **121**, 4018-4028
- Razin S.V. 1996. Functional architecture of chromosomal DNA domains. *Crit. Rev. Eukaryot. Gene Expr.* **6**, 247-269
- Reddy K.L., Zullo J.M., Bertolino E. & Singh H. 2008. Transcriptional repression mediated by repositioning of genes to the nuclear lamina. *Nature* **452**, 243-247
- Sasseville A.M. & Langelier Y. 1998. In vitro interaction of the carboxy-terminal domain of lamin A with actin. *FEBS Lett.* **425**, 485-489
- Sexton T., Umlauf D., Kurukuti S. & Fraser P. 2007. The role of transcription factories in large-scale structure and dynamics of interphase chromatin. *Sem. Cell Dev. Biol.* **18**, 691-697
- Shimi T., Pflieger K., Kojima S., Pack C.G., Solovei I., Goldman A.E., Adam S.A., Shumaker D.K., Kinjo M., Cremer T. & Goldman R.D. 2008. The A- and B-type nuclear lamin networks: microdomains involved in chromatin organization and transcription. *Genes Dev.* **22**, 3409-3421
- Shoeman R.L. & Traub P. 1990. The in vitro DNA-binding properties of purified nuclear lamin proteins and vimentin. *J. Biol. Chem.* **265**, 9055-9061
- Spann T.P., Goldman A.E., Wang C., Huang S. & Goldman R.D. 2002. Alteration of nuclear lamina organization inhibits RNA polymerase II-dependent transcription. *J. Cell Biol.* **156**, 603-608
- Spector D.L. 2003. The dynamics of chromosome organization and gene regulation. *Annu. Rev. Biochem.* **72**, 573-608
- Spector I., Shochet N.R., Kashman Y. & Groweiss A. 1983. Latrunculins: novel marine toxins that disrupt microfilament organization in cultured cells. *Science* **214**, 493-495

Squarzoni S., Sabatelli P., Ognibene A., Toniolo D., Cartegni L., Cobianchi F., Petrini S., Merlini L., Maraldi N.M. 1998. Immunocytochemical detection of emerin within the nuclear matrix. *Neuromuscul. Disord.* **5**, 338-344

Sutherland H. & Bickmore W.A. 2009. Transcription factories: gene expression in unions? *Nature Rev. Genet.* **10**, 457-466

Taimen P., Pflieger K., Shimi T., Möller D., Ben-Harush K., Erdos M.R., Adam S.A., Herrmann H., Medalia O., Collins F.S., Goldman A.E. & Goldman R.D. 2009. A progeria mutation reveals functions for lamin A in nuclear assembly, architecture, and chromosome organization. *Proc. Natl. Acad. Sci. U S A.* in press.

Tang C.W., Maya-Mendoza A., Martin C., Zeng K., Chen S., Feret D., Wilson S.A., Jackson D.A. 2008. The integrity of a lamin-B1-dependent nucleoskeleton is a fundamental determinant of RNA synthesis in human cells. *J. Cell Sci.* **121**, 1014-1024

Trinkle-Mulcahy L. & Lamond A.I. 2008. Nuclear functions in space and time: Gene expression in a dynamic, constrained environment. *FEBS Lett.* **582**, 1960-1970

Vassetzky Y., Lemaitre J.M. & Mechali M. 2000. Specification of chromatin domains and regulation of replication and transcription during development. *Crit. Rev. Eukaryot. Gene Expr.* **10**, 31-38

Weierich C., Brero A., Stein S., von Hase J., Cremer C., Cremer T. & Solovei I. 2003. Three-dimensional arrangements of centromeres and telomeres in nuclei of human and murine lymphocytes. *Chromosome Res.* **11**, 485-502

Weipoltshammer K., Schöfer C., Almeder M., Philimonenko V.V., Frei K., Wachtler F. & Hozák P. 1999. Intranuclear anchoring of repetitive DNA sequences: centromeres, telomeres, and ribosomal DNA. *J. Cell Biol.* **147**, 1409-1418

Zastrow M.S., Vlcek S. & Wilson K.L. 2004. Proteins that bind A-type lamins: integrating isolated clues. *J. Cell Sci.* **117**, 979-987

Zhu X., Zeng X., Huang B. & Hao S. 2004. Actin is closely associated with RNA polymerase II and involved in activation of gene transcription. *Biochem. Biophys. Res. Commun.* **321**, 623-630

## Figures

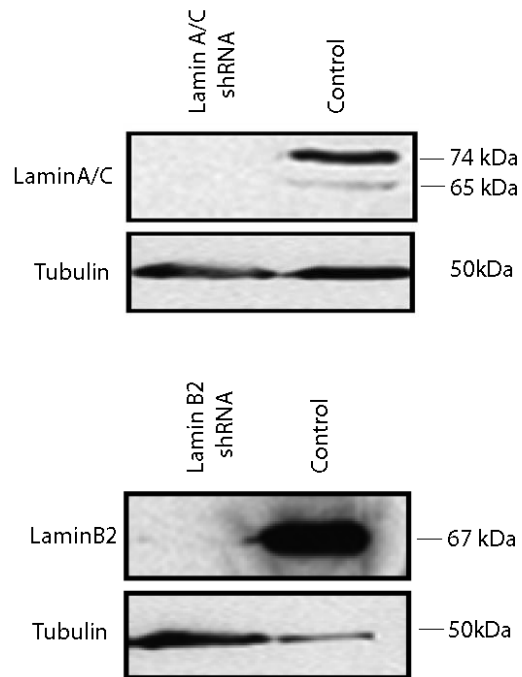


**Figure 1A** U2OS cells were transiently transfected with short hairpin (sh) RNA constructs from a viral based vector system directed against lamin A and lamin B. As a control, cells were transfected with an empty vector. Cells were lysed and subjected to Western blot analysis, 72 hours post transduction. An almost complete reduction in expression of both lamin A and lamin B proteins was achieved.

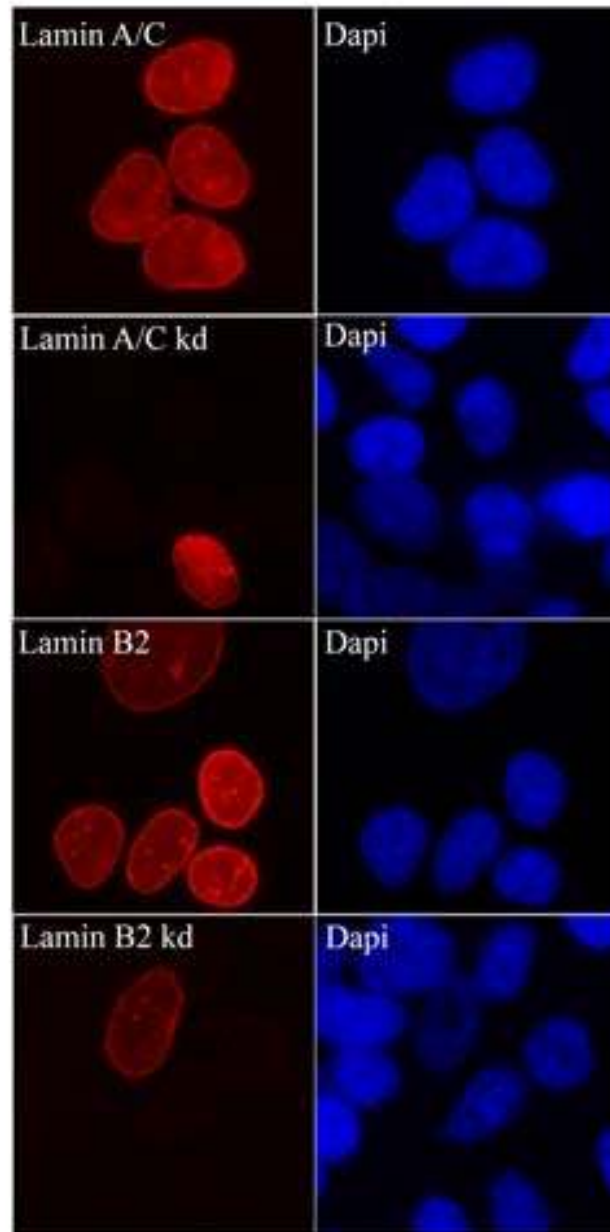


**Figure 1B.** Immunocytochemical images of U2OS cells transiently transfected with short hairpin (sh) RNA constructs from a viral based vector system directed against lamin A and lamin B. Cells were stained with anti-lamin A and anti-lamin B antibodies and showed an absence or strong reduction of lamin A/C and lamin B2 staining. Nuclei are stained with DAPI (blue).

## Telomere movement is constrained by interactions with a lamin structure

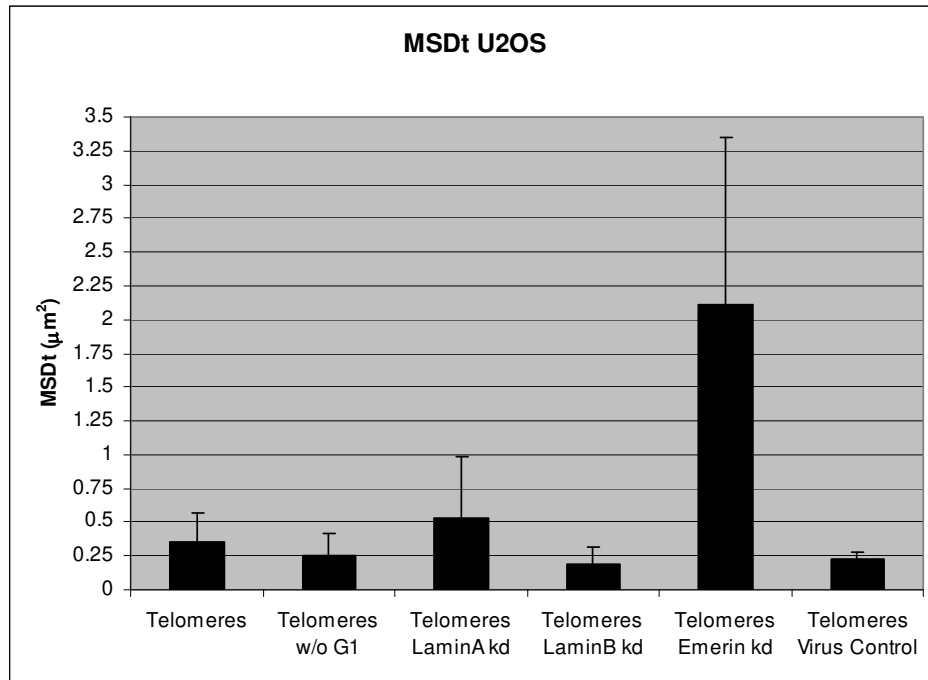


**Figure 3.** Reduction of lamin A/C expression by shRNA interference resulted in an increase in telomere movement as compared to cells transduced with the SHC002 control virus. Cells transduced with a lentiviral construct to knockdown emerin expression revealed a strong increase in telomere mobility (MSDt value of  $\sim 2.1 \mu\text{m}^2$ , stdev  $\sim 1.5 \mu\text{m}^2$ ) as compared to cells transduced with the control construct ( $\sim 0.35 \mu\text{m}^2$ ). 4D image stacks, each containing 20 sections of  $0.5 \mu\text{m}$ , were collected using an automated motorized z-galvo stage multi-dimensional workstation for live cell imaging (model DMI3000B; Leica Microsystems). MSDt values were calculated using the STACKS tracking program.

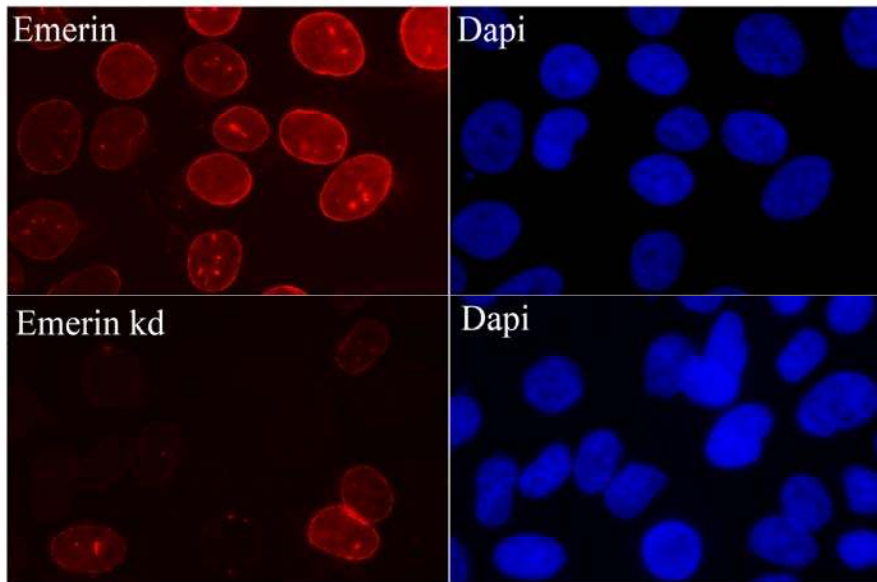


**Figure 4.** A reduction of emerin by shRNA interference in U2OS cells is shown in the lower panel, using an antibody directed against endogenous emerin. Untreated U2OS cells stained for emerin are shown in the upper panel. All cells are counterstained with DAPI (blue).

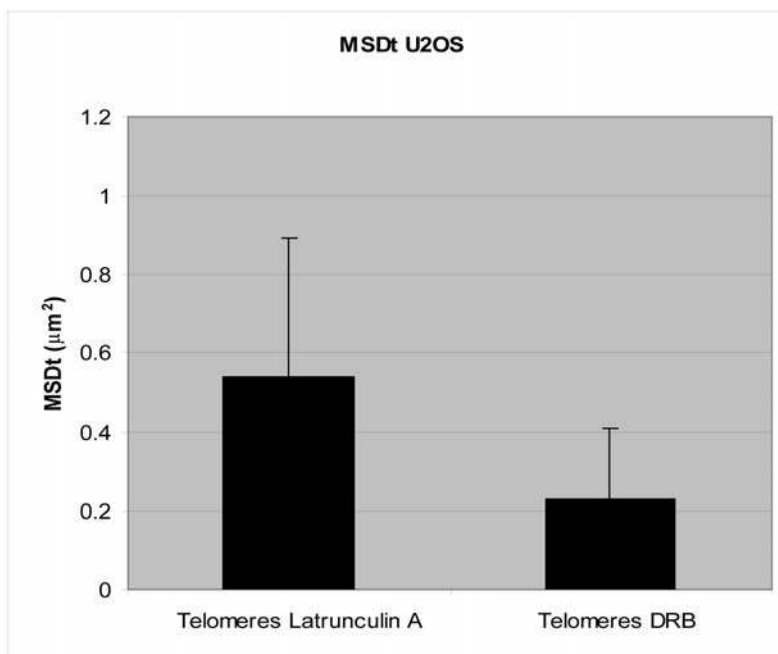


**Figure 5.** Measuring telomere mobility in U2OS cells treated with an actin depolymerizing agent latrunculin A revealed a mean MSDt value of  $\sim 0.54 \mu\text{m}^2$  as compared to a MSDt  $\sim 0.35 \mu\text{m}^2$  that was calculated for telomeres in untreated control cells. Additionally U2OS cells were treated with the transcription inhibitor 5,6-dichloro-1- $\beta$ -D-riboenzimidazole (DRB) which resulted in a slight decrease in telomere mobility (MSDt  $\sim 0.23 \mu\text{m}^2$ ). MSDt values were calculated using the STACKS tracking program.

## Telomere movement is constrained by interactions with a lamin structure

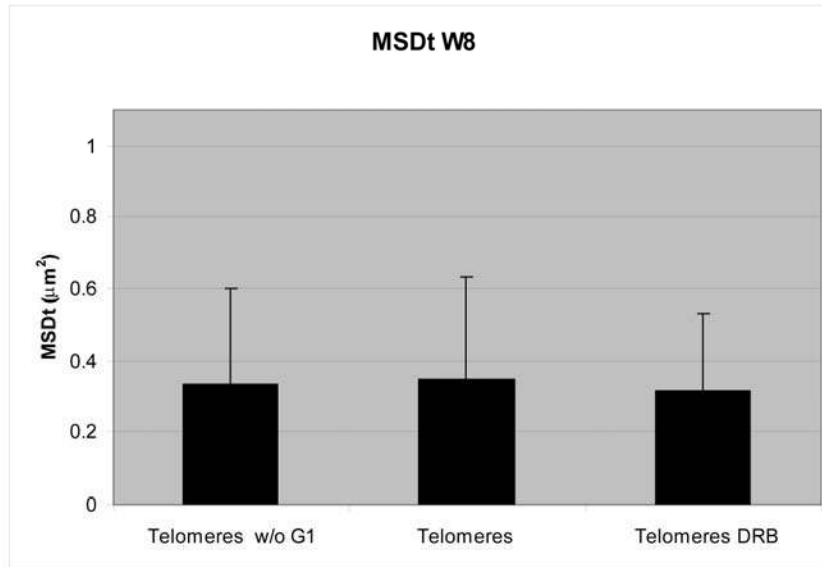


**Figure 6.** Measuring telomere mobility in mouse embryonic fibroblast cells (W8 MEFs) treated with the transcription inhibitor 5,6-dichloro-1-β-D-ribobenzimidazole (DRB) resulted in a slight decrease in telomere mobility, similar to the result in U2OS cells. MSDt values were calculated using the STACKS tracking program.

## **CHAPTER 4**

Telomeric DNA mediates de novo PML body formation

*Molecular Biology of the Cell* (2009) **20**, 4804-4815





## Telomeric DNA mediates de novo PML body formation

Anneke K. Brouwer, Joost Schimmel, Joop C.A.G. Wiegant, Alfred C.O. Vertegaal, Hans J. Tanke, Roeland W. Dirks

Department of Molecular Cell Biology, Leiden University Medical Center, 2300 RC Leiden, The Netherlands

### Abstract

The cell nucleus harbors a variety of different bodies that vary in number, composition and size. Although these bodies coordinate important nuclear processes little is known about how they are formed. Among the most intensively studied bodies in recent years is the PML body. These bodies have been implicated in gene regulation and other cellular processes and are disrupted in cells from patients suffering from acute promyelocytic leukemia. Using live cell imaging microscopy and immunofluorescence, we show in several cell types that PML bodies are formed at telomeric DNA during interphase. Recent studies revealed that both SUMO modification sites and SUMO interaction motifs in the promyelocytic leukemia (PML) protein are required for PML body formation. We show that SMC5, a component of the SUMO ligase MMS21-containing SMC5/6 complex, localizes temporarily at telomeric DNA during PML body formation, suggesting a possible role for SUMO in the formation of PML bodies at telomeric DNA. Our data identify a novel role of telomeric DNA during PML body formation.

## Introduction

The cell nucleus harbors a variety of distinct compartments and bodies, which are involved in a variety of nuclear activities, such as transcription and RNA processing. These bodies are not surrounded by membranes but accumulate specific sets of proteins by means of protein-protein interactions. Furthermore, most proteins that reside in bodies are in a dynamic equilibrium with their surroundings (Misteli, 2001) and a few of these proteins have been reported to shuttle between various bodies (Snaar et al., 2000). Typical examples of nuclear bodies are nucleoli, which are sites of rRNA synthesis and ribosome subunit assembly, speckles, sites involved in RNA splicing metabolism, and Cajal bodies, which are processing sites for several ribonucleoproteins (Spector, 2001).

The PML body has been implicated in many different cellular pathways and is characterized by the presence of the PML protein, first identified in patients with acute promyelocytic leukemia (APL) (de The et al., 1991). Virtually all APL patients carry the chromosomal translocation t(15,17), resulting in a fusion protein between the retinoic acid receptor- $\alpha$  (RAR) and the PML protein (de The et al., 1991; Melnick and Licht, 1999). The PML-RAR $\alpha$  fusion protein fails to locate to PML bodies (Melnick and Licht, 1999) and is thought to block differentiation of bone marrow cells (Naeem et al., 2006). In addition, the leukemic blast cells of APL patients reveal fragmented PML bodies. Treatment of APL patients with all-trans-retinoic acid or arsenic trioxide results in the degradation of the PML-RAR $\alpha$  fusion protein, restoration of PML bodies and remission of the disease (Koken et al., 1994; Weis et al., 1994).

Each cell nucleus contains, depending on cell type and cell cycle stage, approximately 10 to 30 PML bodies ranging in size from 0.2 to 1  $\mu$ m. In addition to PML, more than 50 PML body-associated proteins have been characterized, including Sp100, SUMO-1, Daxx, pRB, p53, HAUSP, CBP, Hp1 and BLM, which function in transcription, DNA replication, DNA repair, antiviral defense, chromatin organization, cell cycle control and apoptosis (Borden, 2002; Dellaire and Bazett-Jones, 2004; Bernardi and Pandolfi, 2007; Everett and Chelbi-Alix, 2007). Thus, PML bodies play active roles in a broad variety of nuclear processes but they also apparently function as nuclear storage depots regulating the availability of nucleoplasmic proteins in response to external stimuli (Negorev and Maul, 2001).

Most significantly, PML nuclear bodies apparently coordinate DNA repair and cell cycle checkpoint activities, as these bodies were shown to temporarily associate with sites of double strand breaks and to recruit p53 and the hMre11/Rad50/NBS1 DNA repair complex following ionizing radiation (Carbone et al., 2002). Also, PML nuclear bodies likely regulate and/or coordinate the expression of a variety of genes. Recently, it was shown that the expression of genes within the major histocompatibility class I genomic locus, which have a high degree of association with PML bodies (Shiels et al., 2001), is coordinated by the formation of higher-order chromatin-loop structures mediated by PML and SATB1 (Kumar et al., 2007). Also, it has been reported that a selection of gene rich and transcriptional active genomic loci, present on several chromosomes, reveal a non-random association with PML bodies (Wang et al., 2004). Furthermore, the observation

that a number of DNA viruses transcribe their genomes at PML bodies underscores a role of the PML body in transcription (Maul, 1998). Finally, consistent with the idea that PML bodies associate with transcriptionally active regions, newly synthesized mRNA transcripts have been found associated with the periphery of PML bodies (Boisvert et al., 2000; Kießlich et al., 2002).

Although the mechanism by which PML bodies move to and associate with specific genomic loci is not known yet, the frequency with which these associations are observed suggests that PML bodies are non-randomly organized in the cell nucleus. To address this issue, we visualized the *de novo* formation of PML bodies after the disassembly of all PML bodies in the cell nucleus and identified the sites at which they form.

## Materials and Methods

### Cell Culture

U2OS, immortalized mouse embryonic fibroblast W8 cells (gift from T. Jenuwein, Vienna, Austria), immortalized mouse embryonic PML<sup>-/-</sup> fibroblasts (gift from P.P. Pandolfi, Harvard Medical School, Boston, MA), HeLa and haematopoietic leukemia NB4 cells (gift from M. Lanotte) were cultured at 37 °C on 3.5-cm glass-bottom culture dishes (MatTek) in Dulbecco's modified Eagle's medium (DMEM) without phenol red and containing 1.0 mg/ml glucose, 4% FBS, 2 mM glutamine, 100 U/ml penicillin, and 100 µg/ml streptomycin, buffered with 25 mM Hepes, pH 7.2 (all from Invitrogen). To induce alkylating DNA damage, cells were incubated with 0.02% MMS (Sigma) for 45 minutes or 1.5 hour.

### Plasmids and cell transfection

The construction of vectors EYFP-PML I and ECFP-Sp100 is previously described (Wisemeijer et al., 2002). The coding sequence for PML III has been cloned in the pEYFP-C1 vector (Clontech) and the coding sequences for TRF1, TRF2 and ASF have been cloned into the DsRedExpress vector (Clontech) according to standard procedures. The SUMOylation-deficient YFP-tagged K65/160/490R PML mutant protein (verified by sequencing) was a gift from O.A. Vaughan. Cells were transiently transfected with 0.5 µg vector DNA using lipofectamine 2000 (Invitrogen). For the bimolecular fluorescence complementation assay, the DNA sequences for PML III and TRF1 were cloned into vectors containing YN173, corresponding to residues 1-173 of EYFP or CC155, corresponding to residues 155-238 of ECFP (Hu et al., 2002). TEL-YN was a gift from D. Baker. All protein coding sequences used in this study were of human origin. The correct localization of all expressed proteins was verified and confirmed in both U2OS and W8 MEF cells. PML-YFP expressing cells were stained with antibodies specific for endogenous Sp100, Daxx and Hausp to confirm the localization of PML-YFP in PML bodies. The localization of DsRed-TRF1 and DsRed-TRF2 at telomeric DNA was confirmed by PNA-FISH (Molenaar et al., 2003). Furthermore, it has been demonstrated before that the TTAGGG repeat binding sites in mouse and human TRF1 and TRF2 show a high level of sequence homology (Broccoli et al., 1997a) and bind to TTAGGG repeat DNA with the same preference (Broccoli et al., 1997b).

### Analysis of Fluorescence Complementation

Cells were cotransfected with combinations of the plasmids encoding PML-CC155 and YN173-TRF1 or YN173-TEL as well as YN173-PML and TRF2-CC155. The complementation assay was essentially performed as described (Hu et al., 2002). Transfected cells were first incubated for 3 hours at 37°C and then for 16 hours at 30°C to promote fluorophore maturation. Cells were monitored either alive or following fixation in 2% formaldehyde.

### Live cell imaging

Wide-field fluorescence microscopy was performed on a multi-dimensional workstation for live cell imaging (model DMIRE2; Leica Microsystems, Mannheim, Germany) equipped with a metal halide bulb and a 63× NA 1.4 PlanApo objective lens. 4D image

stacks were collected using an automated motorized piezo Z-stage. The Z-stacks were collected with 0.4- $\mu\text{m}$  steps and contained generally 20 Z-slides. During imaging, the microscope was heated to 37 °C in a CO<sub>2</sub> perfused and moisturized chamber. Image stacks were collected every 10 minutes for 1 to 4 hours and deconvolved by using the Leica software. Deconvolution is a computational algorithm that restores out-of-focus fluorescent signals resulting in a decrease of blur and an improved contrast. For each experiment and cell type at least 10 movies were analyzed.

### **Immunofluorescence**

The following antibodies were used for immunofluorescence staining: mouse monoclonal antibody 5E10 against PML (gift from R. van Driel, Amsterdam, The Netherlands), rabbit polyclonal antibody against PML (1130 directed against seq: MEPAPARSPRP-QQDP), rabbit polyclonal antibody against SP100 (ab1380, Chemicon), rabbit polyclonal antibody against Daxx (sc-7152, Santa Cruz), rabbit polyclonal antibody against Hausp (A300-033A, Bethyl Laboratories), mouse monoclonal antibody against TRF1 (ab10579-50, Abcam), mouse monoclonal antibody against TRF2 (IMG-124, Imgenex), human autoimmune serum against centromeres (Antibodies Incorporated), rabbit polyclonal antibody against  $\gamma\text{H2AX}$  (A300-081A, Bethyl Laboratories), rabbit polyclonal antibody against 53BP1 (NB100-304, Novus Biologicals) and rabbit polyclonal antibody against SMC5 (A300-236A, Bethyl Laboratories). Cells were grown on coverslips, washed three times in PBS and then fixed in 2% formaldehyde in PBS for 10 minutes at room temperature. After fixation, cells were washed three times in PBS, permeabilized in PBS containing 0.2% Triton X-100 for 15 min and washed once in TBS containing 0.1% Tween 20. Then, cells were incubated with primary antibody for 45 minutes at 37 °C, followed by three washes in TBS containing 0.1% Tween 20. Finally, cells were incubated with an appropriate Alexa-Fluor 488, Alexa-Fluor 594 (both Invitrogen) or Cy3 secondary antibody conjugate for 45 minutes at 37 °C, washed in TBS containing 0.1% Tween 20, and mounted in Citifluor (Agar Scientific) containing 400  $\mu\text{g/ml}$  DAPI (Sigma-Aldrich).

### **Fluorescence in situ hybridization**

NB4 cells were grown on coverslips, fixed in 4% formaldehyde in PBS for 10 minutes and permeabilized in PBS containing 1% Triton X-100 for 10 minutes. Then, cells were washed twice with distilled water, dehydrated in a graded series of ethanol and dried. For combined PML-immunostaining and PNA-FISH, cells were incubated with 1 ng/ $\mu\text{l}$  telomere PNA probe (DAKO) in 40% formamide/2x SSC. Cells and probe were denatured at 80°C for 3 minutes. After hybridization for 1 hour at 37°C, the cells were washed 3x5 minutes in TBS containing 0.5 % Triton X-100. Then, cells were incubated with respectively primary and secondary antibodies as described above.

### **Protein blot analysis**

Cells were lysed in NuPAGE LDS Sample Preparation Buffer (Invitrogen). Protein samples were then size fractionated on Novex 4–12% BisTris gradient gels using a MOPS buffer (Invitrogen) and were subsequently transferred onto Hybond-C extra membranes (Amersham Biosciences) using a submarine system (Invitrogen). Blots were stained for total protein using Ponceau S (Sigma-Aldrich). After blocking with PBS containing 0.1% Tween 20 and 5% milk powder, the membranes were incubated with antibody 5E10

## **Telomeric DNA mediates de novo PML body formation**

against PML or a rabbit antibody against SUMO (directed against seq: MEDEDTIDVFQQQTG) and with a mouse polyclonal antibody against tubulin (1:2000; Sigma-Aldrich). The secondary antibodies used were HRP-conjugated anti-mouse (1:5,000; Pierce) and HRP-conjugated anti-rabbit (1:2000; Pierce). Bound antibodies were detected by chemiluminescence using ECL Plus (Amersham Biosciences).

## Results

### **PML bodies do not necessarily form at previously used sites after recovery from stress**

A number of different cellular stresses have been described that induce the disassembly of PML bodies and result in the formation of PML residual bodies, PML microstructures or even in a complete disappearance of the PML body (Maul et al., 1995; Eskiw et al., 2003; Nefkens et al., 2003; Conlan et al., 2004). To examine whether PML bodies have predetermined spatial positions in the nucleus, we treated U2OS human osteosarcoma cells with the DNA methylating agent methylmethane sulfonate (MMS). This agent has previously been shown to cause a complete dispersal of PML bodies (Conlan et al., 2004). By immunofluorescence, we confirmed that PML bodies indeed disassemble completely in response to MMS treatment and that PML proteins redistribute throughout the nucleus in a diffuse manner (Fig. 1A). However, these results do not exclude the possibility that the level of PML in PML bodies is greatly reduced below the detection level or that some of the other PML body components may organize into body structures. To confirm that PML bodies indeed disassemble in response to MMS treatment, we evaluated the levels of SUMO-modified PML by immunoblot analysis. Previous studies showed that the assembly and integrity of PML bodies is dependent on post-translational modification of PML by SUMO (Zhong et al., 2000). Furthermore, it has been shown that PML is a preferential SUMO2 specific target protein (Vertegaal et al., 2006). As illustrated in Fig. 1B, the amount of SUMOylated PML was markedly reduced by MMS treatment, while the total amount of SUMO2/3 did not decrease (Fig. 1C). Also shown in Fig. 1B is that the total amount of PML protein did not significantly change by MMS treatment, which is consistent with the observed subnuclear redistribution of PML and with previous data (Conlan et al., 2004).

To image the disassembly of PML bodies in live cells, we collected 3D image stacks of U2OS cells and of mouse embryonic fibroblasts (W8 MEFs), both expressing EYFP-PML III, at 10 minute time intervals. Image collection was started immediately after MMS treatment and continued throughout the dispersal process of the PML bodies, which took on average 1 hour. Among cells there appeared to be quite some variability in the duration of the dispersal process which could possibly be due to a cell cycle dependent action of MMS. PML body dispersal was accompanied by a gradual loss of PML protein from these bodies. Some PML bodies, however, first fused into larger bodies which then rapidly dispersed (Fig. 2 and Movie 1). In a few cells some remnant PML bodies remained present after MMS treatment. Such bodies may have dispersed when cells were incubated with MMS for a longer time period. As a control, we analyzed the movement of PML bodies in untreated U2OS and W8 MEF interphase cells (10 cells each). 3D image stacks were collected every 10 minutes for 50 minutes (Supplemental Fig. 1). The 4D stacks show that fusions of PML bodies occur but at low frequencies and that PML bodies show constrained as well as dynamic movements consistent with previous observations about PML body dynamics (Muratani et al., 2002; Wiesmeijer et al., 2002; Jegou et al., 2009). In a subfraction of cells, we noticed that the number of PML bodies increased during the imaging period, which is most likely related to cell cycle phase (Dellaire et al., 2006a,b).



Interestingly, the dispersal of PML bodies proved reversible as we observed that PML bodies recover when the cells were incubated in fresh culture medium lacking MMS. Consistent with this observation, we found that the amount of SUMOylated PML increased when cells recovered from MMS treatment (Supplemental Fig. 2). All live cell experiments were performed by expressing PML isoform III and were confirmed by expressing PML isoform I. We examined whether after MMS treatment PML bodies would recover at the same spatial position in the nucleus, possibly at the same chromatin site, as they were positioned before treatment. Both, U2OS and W8 MEF cells, were transiently transfected with EYFP-PML. The 3D image stacks were collected every 10 minutes before, during, and after MMS treatment using both the YFP channel and the differential interference contrast (DIC) channel and converted to maximum projections (Fig. 3). These projections were used to denote the spatial areas occupied by PML bodies before MMS treatment by drawing 2  $\mu\text{m}$  circles around them. After analyzing the maximum projections of 10 interphase U2OS cells, collected before and 90 minutes after recovery from MMS treatment, it appeared that only 50% ( $\pm 10\%$ ) of the original number of PML bodies has been formed *de novo* after treatment. Of these bodies, 35% ( $\pm 15\%$ ) formed outside the circled areas. Because the total nuclear area occupied by circles is relatively large it is expected that a significant number of PML bodies are formed in these areas just by chance. Hence, at least 35% of the *de novo* formed PML bodies are positioned at new locations (Fig. 3A, Table 1). The analysis of the maximum projections of 4D image stacks of 10 interphase W8 MEFs taken before and 50 minutes after recovery of MMS treatment revealed that 45% ( $\pm 10\%$ ) of the original number of PML bodies has been formed *de novo* after treatment and that a median of 75% of these PML bodies formed outside the circled areas (Fig. 3B, Table 1). Whether previously used chromatin sites have moved in the intervening time to other positions in the nucleus should be addressed by additional experiments using photoactivatable GFP-tagged histone H4 (Wiesmeijer et al., 2008). Our observations suggest that a subset of PML bodies form at new locations in the cell nucleus and that this is particularly true for W8 MEFs.

### **PML bodies form *de novo* on telomeric DNA**

U2OS cells are ALT cells which contain extrachromosomal telomeric DNA and a subset of these cells contain variable numbers of PML bodies that are associated with telomeric DNA sequences (Yeager et al., 1999). Because we found in U2OS cells that about 65% of the new PML bodies formed at approximately the same positions as they were found before MMS treatment, we speculated that these positions might contain telomeric DNA. Thus, PML bodies may form *de novo* at telomeric DNA following recovery from MMS treatment. We therefore monitored PML body dispersal in interphase U2OS cells, expressing EYFP-PML together with DsRed-TRF1 or EYFP-PML together with DsRed-TRF2, during MMS treatment and then visualized the formation of PML bodies during the recovery period by capturing 3D image stacks at 10 minute time intervals. The collected 3D image data sets show that PML bodies were indeed formed at telomeric DNA foci labeled by DsRed-TRF1 or DsRed-TRF2 in U2OS cells. Approximately 1 hour after incubating the cells in fresh medium without MMS, EYFP-PML was shown to accumulate first at a few sites that are labeled by DsRed-TRF1 or DsRed-TRF2. When time proceeds, EYFP-PML was accumulating at an increasing number of telomeric sites during the time-course of the experiment (Fig. 4 and Movie 2). It should be noted, however, that

we cannot not discriminate between telomeres and extrachromosomal telomeric material, which are both present in ALT cells (Ogino et al., 1998). The amount of extrachromosomal telomeric DNA may even be increased by MMS treatment. It has been reported previously that DNA damage can lead to a 2-fold increase in extrachromosomal telomeric DNA (Fasching et al., 2007). Hence, PML bodies may form at both telomeres and extrachromosomal telomeric material in U2OS cells. The specificity of DsRed-TRF1 and DsRed-TRF2 localization at telomeric DNA was confirmed by their localization at Cy3-peptide nucleic acid -labeled telomere sequences as described previously (Molenaar et al., 2003). Both, MMS-treated and non-treated U2OS cells were stained for telomeric DNA using a PNA probe and for endogenous or exogenous TRF1 using antibodies. Double-labeled cells, both treated and non-treated, revealed 1-4 TRF1 foci that did not colocalize with telomeric DNA (Supplemental Fig. 3). Thus, a few TRF1 or TRF2 foci may label other sites in the nucleus which may represent protein aggregates formed by over expression. The presence of TRF1 or TRF2 foci that do not colocalize with telomeric DNA staining may also be explained by a poor hybridization and detection efficiency of PNA probes at short telomeres.

W8 MEFs, expressing EYFP-PML and DsRed-TRF1, were included as non-ALT control cells in live cell experiments and subjected to the same treatment as U2OS cells. W8 MEF cells contain relatively long telomeres but do not contain extrachromosomal telomeric DNA and ALT associated PML bodies. Similar to what we observed for U2OS cells, a median of 60% of EYFP-PML bodies was shown to accumulate at fluorescently-labeled telomere sequences in W8 MEFs (Movie 3). These data suggest that after dispersal, new PML bodies form and that a substantial set of these bodies use telomeric DNA as initial assembly sites.

To confirm our findings using nontransfected U2OS cells, we analyzed the formation of PML bodies in 10 U2OS cells that were allowed to recover from MMS treatment and were fixed and incubated with antibodies against PML and TRF2. Consistent with the live cell experiments, we observed that 70% ( $\pm 15\%$ ) of the newly formed PML bodies were in association with telomeric DNA (Fig. 5, A and B). As a non-ALT human control, we studied the *de novo* formation of PML bodies in telomerase expressing HeLa cells. These cells were first treated with MMS and then allowed to recover in fresh medium before they were fixed and incubated with antibodies specific for PML and TRF2. Similar to what we observed in U2OS cells, a significant number of PML bodies colocalized with telomeres (Fig. 5C).

To examine whether together with PML other typical PML body proteins are recruited to telomere sequences when PML bodies are formed, we stained cells recovering from MMS treatment for TRF2 and Sp100, Daxx or Hausp using specific antibodies. As shown in Fig. 5D, Sp100 is recruited to telomeric sites when PML bodies are formed. Before MMS treatment, no colocalization of Sp100 with TRF2 foci was observed and during MMS treatment Sp100 appeared diffuse (Supplemental Fig. 4). In addition to Sp100, both Hausp (Fig. 5E) and Daxx (not shown) were also observed to be recruited by telomeric sites in cells recovering from MMS treatment. These results suggest that together

## Telomeric DNA mediates de novo PML body formation

with PML all other major PML-body components assemble in *de novo* formed PML bodies at telomeric sites.

Because MMS is a DNA damaging agent, it could be possible that PML bodies form preferentially at damaged telomeric DNA. Therefore, we investigated the presence of DNA damage at sites of telomeric DNA before, during and after MMS treatment by staining DsRed TRF1 expressing U2OS cells for PML and  $\gamma$ H2AX. The latter is a marker for double-stranded DNA breaks. Before MMS treatment there is no significant amount of  $\gamma$ H2AX staining observed in nucleus. Small  $\gamma$ H2AX foci were observed in the nucleus of MMS treated cells showing dispersal of PML bodies. In the recovery phase when PML bodies are formed  $\gamma$ H2AX was not necessarily found present at telomeric DNA that colocalized with *de novo* formed PML bodies (Supplemental Fig. 5, A-C). Similar results were obtained when cells were stained for 53BP1, a component of DNA damage repair foci (Supplemental Fig. 5, D and E).

Next, we examined the possibility that PML bodies may form at other nuclear compartments as well. We therefore expressed the nuclear body markers EYFP-ASF, EYFP-coilin or EYFP-S5, which localize respectively at speckles, Cajal bodies and nucleoli together with DsRed-PML in U2OS cells and W8 MEFs. Following MMS treatment and PML body recovery, we observed that only 2-4 % of PML bodies colocalized with these other nuclear bodies (data not shown). Because a previous study reported a dynamic association of PML with centromeres (Everett et al., 1999a), we also wished to examine whether PML bodies could form at these chromosomal sites consisting of tandem repetitive elements. Using antibodies to the centromere protein CENPA and PML, no significant (less than 1%) colocalization of PML with centromeres was observed in both U2OS and W8 MEF cells that recovered from MMS treatment (Fig. 5F).

Together, these data suggest that at least a subset of PML bodies are formed at telomeric DNA sequences and not at any other specific nuclear structure, in both ALT and non-ALT cells. However, we cannot rule out the possibility that PML bodies may be formed at other nuclear sites as well.

### **Ectopical expression of PML in PML<sup>-/-</sup> MEFs leads to de novo PML body formation at telomeric DNA**

As PML bodies may assemble at telomeric DNA due to some effect of MMS treatment other than inducing DNA damage at telomeres, we wished to investigate whether PML bodies may also form at telomeric DNA in untreated cells. To this end we examined the formation of PML bodies in PML<sup>-/-</sup> mouse embryonic fibroblasts, which lack intact PML bodies (Wang et al., 1998). Both, EYFP-PML and DsRed-TRF1 were transiently expressed in PML<sup>-/-</sup> MEFs and 3D image stacks were captured at 3 hours after transfection. Analysis of 20 deconvolved image stacks showed a consistent colocalization of assembled PML bodies with fluorescently tagged telomeric DNA (Fig. 6A). Similar results were obtained when cells were transfected with a vector encoding EYFP-PML, incubated for 3 hours in culture medium, fixed and then stained with a TRF2 antibody or hybridized with a telomere-specific PNA probe (data not shown).

Because we observed a variable number of PML bodies that were not associated with telomeric DNA at 3 hours post transfection, we also followed the fate of PML bodies at later time points following a cotransfection of PML<sup>-/-</sup> MEFs with EYFP-PML together with DsRed-TRF1. Image stacks collected at 7 hours and 19 hours after transfection demonstrated that at 7 hours less PML bodies were associated with telomeric DNA as compared to 3 hours post transfection and that at 19 hours none or only very few PML bodies were associated with telomeric DNA (Fig. 6A). Together, these observations suggest that PML bodies dissociate from telomeric DNA after they are formed at these sites. To monitor the dissociation of *de novo* formed PML bodies from telomeric DNA sites, PML<sup>-/-</sup> MEF cells were cotransfected with EYFP-PML together with DsRed-TRF1 and at 3 hours post transfection 4D image stacks were collected every 1 minute for 30 minutes. Analysis of 10 image stacks suggests that PML bodies dissociate from telomeric DNA once they are formed at these sites (Fig. 6B and Movie 4). By analyzing single Z planes in the 3D stacks we confirmed that PML bodies are indeed associated with telomeric DNA sites before they released from these sites.

#### **Recovery of PML bodies in the APL-patient derived cell line NB4**

A characteristic morphologic feature of APL is that patient derived cells lack any intact PML bodies, however, treatment of patients with retinoic acid or arsenic trioxide results in the restoration of PML bodies. As expected, when NB4 cells (Lanotte et al., 1991) were treated with arsenic trioxide, fixed, and stained with an antibody against PML, we observed the formation of PML bodies, while untreated cells revealed a diffuse and punctate staining pattern of nuclear PML (Supplemental Fig. 6). This punctate pattern of PML staining is consistent with the observation that PML is localized in nuclear microspeckles in APL cells (Koken et al., 1994). To address whether the formation of PML bodies in APL patient derived cells also involve telomeric DNA, we examined the accumulation of PML protein at telomeric DNA following arsenic trioxide treatment for 2 to 8 hours. Combined immunofluorescence and telomere PNA FISH revealed a high extent of colocalization between newly formed PML bodies and telomeric DNA (Fig. 6C; Supplemental Fig. 6), further validating our hypothesis that non-ALT PML bodies form *de novo* at telomeric DNA. Maximum projections of image stacks collected from untreated cells revealed many PML microspeckles, some of which colocalize with telomeric DNA. Notably, this colocalization was only sporadically observed when viewing single optical sections.

#### **PML directly interacts with TRF1 and TRF2**

To further confirm that PML bodies assemble at telomeric DNA, we made use of a bimolecular fluorescence complementation assay (Hu et al., 2002). This assay is based on the reconstitution of a fluorescent protein by the close proximity of two fragments of fluorescent proteins, which are non-fluorescent themselves, when proteins fused to the fragments interact. To visualize the possible interaction of PML with TRF1 and/or TRF2 we engineered the expression constructs PML-CC155, YN173-PML, YN173-TRF1 and -TRF2-CC155, cotransfected PML<sup>-/-</sup> MEFs with the combinations PML-CC155 and YN173-TRF1 or YN173-PML and TRF2-CC155 and monitored the appearance of fluorescence signals in living cells using fluorescence microscopy. As shown for the combination PML-CC155 and YN173-TRF1, approximately 16 hours after transfection, we ob-

served the appearance of fluorescent spots in the nucleus (Fig. 7A). Similar results were obtained with the combination YN173-PML and TRF2-CC155 (data not shown). The occurrence of fluorescent spots indicates complementation and thus suggests that PML directly interacts with TRF1 as well as with TRF2. As a negative control we cotransfected PML<sup>-/-</sup> MEFs with the constructs YN173-TRF1 and TEL-CC155. TEL is a transcription repressor protein and is not expected to have an interaction with TRF1. Indeed, we observed no fluorescence appearing at 16 hours after transfection, indicating that complementation did not take place (Fig. 7B). In addition, expression of the single complementation halves did not result in any fluorescent signal (data not shown). Finally, coexpression of PML-CC155 and YN173-TRF1 in MEF W8 cells that were not treated with MMS did also not result in fluorescence complementation (data not shown). This experiment suggests that overexpressed TRF1 does not localize to already existing PML bodies. Thus, the observed complementation between PML-CC155 and YN173-TRF1 and YN173-PML and TRF2-CC155 suggest that PML bodies form at telomeric DNA, at least in part through protein-protein interactions.

### **PML body formation at telomeric DNA: a role for SUMO?**

It has recently been reported that PML requires SUMOylation sites and SUMO interaction motifs for the nucleation and formation of PML bodies (Shen et al., 2006). The SUMO interaction motifs are possibly important for the interaction of PML with other SUMOylated proteins. We therefore investigated whether SUMOylation of PML and telomere associated proteins was involved in the formation of PML bodies at telomeric DNA. Transient expression of DsRed-TRF1, ECFP-Sp100 and an YFP-tagged PML mutant that cannot be SUMOylated in PML<sup>-/-</sup> MEFs resulted in the formation of PML aggregates, which did not accumulate Sp100. Furthermore, the newly formed PML aggregates did not colocalize with telomeric DNA (Fig. 8A), suggesting that SUMOylation of PML is required for PML to localize at telomeric DNA. Similar observations were made in U2OS cells that were cotransfected with EYFP-tagged SUMOylation deficient PML and DsRed-TRF1, treated with MMS, and then incubated in fresh medium (Supplemental Fig. 7).

Because the SMC5/6 complex, containing the SUMO ligase MMS21, has recently been shown to stimulate SUMOylation of telomere binding proteins, including TRF1 and TRF2, and to be required for the recruitment of telomeres to PML bodies in ALT cells (Potts and Yu, 2007), we investigated whether the SMC5/6 complex colocalized with telomeric DNA at PML bodies. U2OS cells, recovering from MMS treatment, and PML<sup>-/-</sup> MEFs expressing EYFP-PML showed a specific staining of the SMC5/6 complex at sites of newly formed PML bodies (Fig. 8, B and C). Similar results were obtained in MMS-treated W8 MEFs (data not shown). In cells that were not treated with MMS to elicit PML body formation, the SMC5/6 complex showed both a diffuse and dot-like staining in the nucleus. As shown for non-treated and MMS-treated W8 MEFs, this pattern did clearly not colocalize with telomeric DNA (Fig. 8, D and E). Together, these results suggest a role for the SMC5/6 complex in the assembly of PML bodies at telomeric DNA, possibly by mediating SUMOylation of telomere binding proteins.

## Discussion

To date, little is known about the molecular mechanisms which drive and regulate the formation of specific bodies in the cell nucleus. Only recently it was shown that PML SUMOylation and binding of PML to SUMOylated PML through a SUMO binding motif are instrumental for PML body formation and for the recruitment of other proteins that localize at PML bodies (Shen et al., 2006). PML bodies are formed when cells progress from G1 to G2 during the cell cycle with the highest number of PML bodies found in G2 (Everett et al., 1999b; Deldaire et al., 2006a). It remained, however, unclear how PML body formation is initiated. Our results indicate for the first time an unexpected role for telomeric DNA in the formation of PML bodies.

To investigate whether PML nuclear bodies occupy preferred positions in the interphase cell nucleus, we first treated cells with the DNA demethylating agent MMS to disrupt PML bodies and then followed the reassembly of PML bodies during a recovery phase. We found that all PML bodies disassemble in response to the DNA demethylating agent MMS and that new PML bodies form during a recovery phase. Generally, the numbers of PML bodies formed are less than the original numbers of PML bodies in cells. This difference might be explained by the short time-window of recovery in which we analyze the cells. Also, cells may first have to complete a full cell cycle to obtain a full set of PML bodies. Interestingly, our data indicate that new PML bodies do not necessarily form at their original positions in the cell nucleus. Previous data, however, indicated that PML bodies are formed at pre-determined positions in the nucleus (Eskiw et al., 2003). PML bodies were shown to largely disassemble in response to heat shock, leaving behind residual PML bodies that maintain their spatial position. When cells were allowed to recover from the stress, these residual bodies were shown to recruit PML containing microbodies to form intact PML bodies. Because PML bodies were not found at new locations, it was concluded that PML bodies are formed at pre-determined positions only. Our results clearly indicate that PML bodies, after disassembly, do not necessarily recover at their original positions. Instead, we provide evidence that PML bodies nucleate at new sites, which we identified being telomeric DNA. It is probably in ALT cells only that newly formed PML bodies remain associated with telomeric DNA. In contrast to most tumor cells, ALT cells lack the enzyme telomerase for telomere maintenance and use an alternative lengthening of telomeres mechanism which is thought to involve homologous recombination (Dunham et al., 2000). A characteristic feature of ALT cells is that they contain, in addition to telomeres, extrachromosomal telomeric material and a subset of PML bodies that is in a complex with telomeric DNA. The possible function of these complexes is still not completely known (Henson et al., 2002). PML bodies that are in complex with telomeric DNA are referred to as ALT-associated PML bodies. It should be noted that the formation of ALT-associated PML bodies might be different from that of regular PML bodies that are present in both ALT and non-ALT cells. Recently, it has been described that ALT-associated PML bodies form by the binding of an existing PML body to a telomere and the subsequent recruitment of free PML protein (Jegou et al., 2009).

## Telomeric DNA mediates de novo PML body formation

While G2 cells contain the highest number of PML bodies, mitotic cells contain the fewest number. When cells enter mitosis PML bodies lose SUMO1 and Sp100 which is accompanied by a strong reduction in PML body number. However, accumulations of PML protein remained present during mitosis, some of which stably associated with chromatin (Dellaire et al., 2006). While we analyzed the formation of new PML bodies in U2OS cells following mitosis we noticed that many of the mitotic PML accumulations were associated with telomeric DNA which hampered our analysis of PML body formation at late telophase/early G1. Our analysis of the formation of new PML bodies is therefore limited to interphase cells.

Although we observed that the majority of new PML bodies are initially positioned at telomeric sites, we do not exclude the possibility that some PML bodies are formed at other loci in the nucleus. Indeed, we observed in our time-lapse recordings that a few new PML bodies did not colocalize with a telomeric site. Since PML bodies have been found in association with some specific chromatin domains, it is conceivable that these domains may function as nucleation sites as well. It may, however, also be true that some new PML bodies dissociate rapidly from telomeric sites and that some PML bodies were already dissociated before we started capturing images. We frequently observed the dissociation of new PML bodies from telomeric DNA, suggesting that most PML bodies dissociate from telomeric sites shortly after their formation. Although we observed quite some variability in the time period PML bodies remain associated with telomeric DNA, the fact that they dissociate is possibly the reason why PML-telomere associations remained thus far unnoticed except for ALT cells containing ALT associated PML bodies. As we analyzed the formation of PML bodies in a limited number of cell types, we do not exclude the possibility that other cell types support a different mechanism of PML body formation.

In addition to PML protein, we showed that newly formed PML bodies also contained Sp100, Daxx and Hausp, indicating that PML protein is not just temporarily aggregating at telomeric DNA. Whether all PML body components are recruited at the same time to the newly formed PML bodies has yet to be determined. Recent data suggest a step-wise recruitment of PML body constituents to PML bodies in early G1 cells, thereby preventing the early maturation of PML bodies at this stage (Chen et al., 2008). It can be envisaged that new, immature, PML bodies have still the ability to move to and attach to specific nuclear sites, before they recruit factors that determine their function or strengthen their interaction with chromatin. Once settled, most PML bodies reveal a constrained movement, which is consistent with their association with chromatin (Chen et al., 2008).

We propose that SUMOylation of telomere binding proteins may play an important role in the formation of PML bodies at telomeric DNA. Recent data demonstrated a role for the SMC5/6 complex in the formation of ALT-associated PML bodies by SUMOylation of six telomere-binding proteins, including TRF1 and TRF2 (Potts and Yu, 2007). Our data suggest that the SMC5/6 complex, containing the SUMO ligase MMS21, may not only fulfill a role in the telomere lengthening mechanism in ALT cells, but also in a mechanism supporting the formation of PML bodies at telomeric DNA. At present, it is unclear how and when the SMC5/6 complex is recruited to telomeric DNA and whether

this complex is essential for PML body formation. A potential mechanism could be that PML protein is recruited to SUMOylated telomere binding proteins by the SUMO binding sites present in PML. SUMOylation of PML at these sites may then lead to the recruitment of more PML protein and other PML nuclear body proteins including Sp100. Consistent with this idea is that a PML mutant that cannot be SUMOylated does not accumulate at telomeric DNA while a wild type PML protein does. However, it remains unclear whether SUMOylation of telomere associated proteins is indeed essential for PML body formation. Our initial attempts to detect SUMOylated forms of endogenous TRF1 or TRF2 in cells showing PML body formation by immunoblot analysis failed, possibly due to the rapid turnover of SUMOylated TRF1 and TRF2.

The suggestion that the telomere binding proteins TRF1 and TRF2 are likely to play a role in the formation of PML bodies is supported by our observation that both TRF1 and TRF2 interact with PML in the fluorescence complementation assay. Whether other telomere associated proteins may also be involved in PML body formation has to be investigated. Experiments aimed at reducing telomere binding protein levels by RNA interference will perhaps shed more light on the function of these proteins in PML body formation. Furthermore, it will be interesting to investigate whether each telomere has the capacity to initiate PML body formation. We cannot exclude the possibilities that the size or activity of telomeric DNA play a role in the recruitment of PML protein. This could, for example, result in the impairment of PML body formation in aged cells, which generally have short telomeres, adding another potential mechanism as to why aged cells are less responsive to stress. Studies to test these hypotheses will enrich our understanding of the biological functions of PML bodies.

In conclusion, this study provides new insights in the assembly of new PML bodies in the cell nucleus and establishes a role for telomeric foci in the recruitment of PML protein.



### **Acknowledgements**

We thank P. Pandolfi for providing PML<sup>-/-</sup> MEFs, T. Jenuwein for W8 MEFs, A.I. Lamond for the NB4 cells, R. van Driel for the 5E10 anti-PML antibody, T. Kerppola for bimolecular fluorescence complementation constructs, D. Baker for YN173-TEL and O.A. Vaughan for the SUMOylation-deficient YFP-tagged K65/160/490R PML mutant protein. Furthermore, we are grateful to L. Fradkin, D. Baker for comments on the manuscript and to M. van Hagen for his help with the immuno blots. This work was partially supported by Cyttron grant no. BSIK03036.

## References

- Bernardi R. & Pandolfi P.P. 2007. Structure, dynamics and functions of promyelocytic leukaemia nuclear bodies. *Nature Rev. Mol. Cell Biol.* **8**, 1006-1016
- Boisvert F.M., Hendzel M.J. & Bazett-Jones D.P. 2000. Promyelocytic leukemia (PML) nuclear bodies are protein structures that do not accumulate RNA. *J. Cell Biol.* **148**, 283-292
- Borden K.L.B. 2002. Pondering the promyelocytic leukemia protein (PML) puzzle: possible functions for PML nuclear bodies. *Mol. Cell. Biol.* **22**, 5259-5269
- Broccoli D., Smogorzewska A., Chong L. & de Lange T. 1997a. Human telomeres contain two distinct Myb-related proteins, TRF1 and TRF2. *Nature Genet.* **17**, 231-235
- Broccoli D., Chong L., Oelmann S., Fernald A.A., Marziliano N., van Steensel B., Kipling D., Le Beau M.M. & de Lange T. 1997b. Comparison of the human and Mouse genes encoding the telomeric protein, TRF1: chromosomal localization, expression and conserved protein domains. *Hum. Mol. Genet.* **6**, 69-76
- Carbone R., Pearson M., Minucci S. & Pelicci P.G. 2002. PML NBs associate with the hMre11 complex at sites of irradiation induced DNA damage. *Oncogene* **21**, 1633-1640
- Chen Y.C., Kappel C., Beaudouin J., Eils R. & Spector D.L. 2008. Live cell dynamics of promyelocytic leukemia nuclear bodies upon entry into and exit from mitosis. *Mol. Biol. Cell.* **19**, 3147-3162
- Conlan A.L., McNees C.J. & Heierhorst J. 2004. Proteasome-dependent dispersal of PML nuclear bodies in response to alkylating DNA damage. *Oncogene* **23**, 307-310
- de The H., Lavau C., Marchio A., Chomienne C., Degos L. & Dejean A. 1991. The PML-RAR $\alpha$  fusion mRNA generated by the t(15;17) translocation in acute promyelocytic leukemia encodes a functionally altered RAR. *Cell* **66**, 675-684
- Dellaire G. & Bazett-Jones D.P. 2004. PML nuclear bodies: dynamic sensors of DNA damage and cellular stress. *BioEssays* **26**, 963-977
- Dellaire G., Eskiw C.H., Dehghani H., Ching R.W. & Bazett-Jones D.P. 2006a. Mitotic accumulations of PML protein contribute to the re-establishment of PML nuclear bodies in G1. *J. Cell Sci.* **119**, 1034-1042
- Dellaire G., Ching R.W., Dehghani H., Ren Y. & Bazett-Jones D.P. 2006b. The number of PML nuclear bodies increases in early S phase by a fission mechanism. *J. Cell Sci.* **119**, 1026-1033
- Dunham M.A., Neumann A.A., Fasching C.L. & Reddel R.R. 2000. Telomere maintenance by recombination in human cells. *Nature Genet.* **26**, 447-450
- Eskiw C.H., Dellaire G., Mymryk J.S. & Bazett-Jones D.P. 2003. Size, position and dynamic behavior of PML nuclear bodies following cell stress as a paradigm for supramolecular trafficking and assembly. *J. Cell Sci.* **116**, 4455-4466

## Telomeric DNA mediates de novo PML body formation

Everett R.D., Earnshaw W.C., Pluta A.F., Sternsdorf T., Ainsztein A.M., Carmena M., Ruchaud S., Hsu W.L., & Orr A. 1999a. A dynamic connection between centromeres and ND10 proteins. *J. Cell Sci.* **112**, 3443-3454

Everett R.D., Lomonte P., Sternsdorf T., van Driel R. & Orr A. 1999b. Cell cycle regulation of PML modification and ND10 composition. *J. Cell Sci.* **112**, 4581-4588

Everett R.D. & Chelbi-Alix M.K. 2007. PML and PML nuclear bodies: Implications in antiviral defence. *Biochimie* **89**, 819-830

Fasching C.L., Neumann A.A., Muntoni A., Yeager T.R. & Reddel R.R. 2007. DNA damage induces alternative lengthening of telomeres (ALT)-associated promyelocytic leukemia bodies that preferentially associate with linear telomeric DNA. *Cancer Res.* **67**, 7072-7077

Henson J.D., Neumann A.A., Yeager T.R. & Reddel R.R. 2002. Alternative lengthening of telomeres in mammalian cells. *Oncogene* **21**, 598-610

Hu C.-D., Chinenov Y. & Kerppola T.K. 2002. Visualization of interactions among bZIP and Rel proteins in living cells using bimolecular fluorescence complementation. *Mol. Cell* **9**, 789-798

Jegou T., Chung I., Heuvelman G., Wachsmuth M., Görisch S.M., Greulich-Bode K.M., Boukamp P., Lichter P. & Rippe K. 2009. Dynamics of telomeres and promyelocytic leukemia nuclear bodies in a telomerase-negative human cell line. *Mol. Biol. Cell* **20**, 2070-2082

Kießlich A., von Mikecz A. & Hemmerich P. 2002. Cell cycle-dependent association of PML bodies with sites of active transcription in nuclei of mammalian cells. *J. Struct. Biol.* **140**, 167-179

Koken M.H.M., Puvion-Dutilleul F., Guillemain M.C., Viron A., Linares-Cruz G., Stuurman N., de Jong L., Szosteck C., Calvo F., Chomienne C., Degos L., Puvion E. & Dethe H. 1994. The t(15;17) translocation alters a nuclear body in a retinoic acid-reversible fashion. *EMBO J.* **13**, 1073-1079

Kumar P.P., Bischof O., Purbey P.K., Notani D., Urlaub H., Dejean A. & Galande S. 2007. Functional interaction between PML and SATB1 regulates chromatin loop architecture and transcription of the MHC class I locus. *Nature Cell Biol.* **9**, 45-56

Lanotte M., Martin-Thouvenin V., Najman S., Balerini P., Valensi F. & Berger R. 1991. NB4, a maturation inducible cell line with t(15;17) marker isolated from a human acute promyelocytic leukemia (M3). *Blood* **77**, 1080-1086

Maul G.G. 1998. Nuclear domain 10, the site of DNA virus transcription and replication. *BioEssays* **20**, 660-667

Maul G.G., Yu E., Alexander M., Ishov A.M. & Epstein A.L. 1995. Nuclear domain 10 (ND10) associated proteins are also present in nuclear bodies and redistribute to hundreds of nuclear sites after stress. *J. Cell Biochem.* **59**, 498-513

Melnick A. & Licht J.D. 1999. Deconstructing a disease: RAR $\alpha$ , its fusion partners, and their roles in the pathogenesis of acute promyelocytic leukemia. *Blood* **93**, 3167-3215

- Misteli T. 2001. Protein dynamics: Implications for nuclear architecture and gene expression. *Science* **291**, 843-847
- Molenaar C., Wiesmeijer K., Verwoerd N.P., Khazen S., Eils R., Tanke H.J. & Dirks R.W. 2003. Visualizing telomere dynamics in living mammalian cells using PNA probes. *EMBO J.* **22**, 6631-6641
- Muratani M., Gerlich D., Janicki S.M., Gebhard M., Eils R. & Spector D.L. 2002. Metabolic-energy-dependent movement of PML bodies within the mammalian cell nucleus. *Nat. Cell Biol.* **4**, 106-110
- Naeem M., Harrison K., Barton K., Nand K.S. & Alkan S. 2006. A unique case of acute promyelocytic leukemia showing monocytic differentiation after ATRA (all-trans retinoic acid) therapy. *Eur. J. Hematol.* **76**, 164-166
- Nefkens I., Negorev D.G., Ishov A.M., Michaelson J.S., Yeh E.T., Tanquay R.M., Muller W.E. & Maul G.G. 2003. Heat shock and CD(2+) exposure regulate PML and Daxx release from ND10 by independent mechanisms that modify the induction of heat-shock proteins 70 and 25 differently. *J. Cell Sci.* **116**, 513-524
- Negorev D. & Maul G.G. 2001. Cellular proteins localized at and interacting within ND10/PML nuclear bodies/PODs suggest functions of a nuclear depot. *Oncogene* **29**, 7234-7242
- Ogino H., Nakabayashi K., Suzuki M., Takahashi E., Fujii M., Suzuki T. & Ayusawa D. 1998. Release of telomeric DNA from chromosomes in immortal human cells lacking telomerase activity. *Biochem. Biophys. Res. Comm.* **248**, 223-227
- Potts P.R. & Yu H. 2007. The SMC5/6 complex maintains telomere length in ALT cancer cells through SUMOylation of telomere binding proteins. *Nature Struc. Mol. Biol.* **14**, 581-590.
- Shen T.H., Lin H.-K., Scaglioni P.P., Yung T.M. & Pandolfi P.P. 2006. The mechanisms of PML-nuclear body formation. *Mol. Cell* **24**, 331-339
- Shiels C., Islam S.A., Vatcheva R., Sasieni P., Sternberg M.J., Freemont P.S. & Sheer D. 2001. PML bodies associate specifically with the MHC gene cluster in interphase nuclei. *J. Cell Sci.* **114**, 3705-3716
- Snaar S., Wiesmeijer K., Jochemsen A.G., Tanke H.J. & Dirks R.W. 2000. Mutational analysis of fibrillarin and its mobility in living human cells. *J. Cell Biol.* **151**, 653-662
- Spector D.L. 2001. Nuclear domains. *J. Cell Sci.* **114**, 2891-2893
- Vertegaal A.C., Andersen J.S., Ogg S.C., Hay R.T., Mann M. & Lamond A.I. 2006. Distinct and overlapping sets of SUMO-1 and SUMO-2 target proteins revealed by quantitative proteomics. *Mol. Cell Proteomics* **5**, 2298-2310
- Wang Z.G., Delva L., Gaboli M., Rivi R., Giorgio M., Cordon-Cardo C., Grosveld F. & Pandolfi P.P. 1998. Role of PML in cell growth and the retinoic acid pathway. *Science* **279**, 1547-1551

## Telomeric DNA mediates de novo PML body formation

Wang J., Shiels C., Sasieni P., Wu P.J., Islam S.A., Freemont P.S. & Scheer D. 2004. Promyelocytic leukemia nuclear bodies associate with transcriptionally active genomic regions. *J. Cell Biol.* **164**, 515-526

Weis K., Ramboud S., Lavau C., Jansen J., Carvalho T., Carmo-Fonseca M., Lamond A. & Dejean A. 1994. Retinoic acid regulates aberrant nuclear localization of PML-RAR $\alpha$  in acute promyelocytic leukemia. *Cell* **75**, 347-386

Wiesmeijer K., Krouwels I.K., Tanke H.J. & Dirks R.W. 2008. Chromatin movement visualized with photoactivable GFP-labeled histone H4. *Differentiation* **76**, 83-90

Wiesmeijer K., Molenaar C., Bekeer I.M.L.A., Tanke H.J. & Dirks R.W. 2002. Mobile foci of SP100 do not contain PML: PML bodies are immobile but PML and SP100 proteins are not. *J. Struct. Biol.* **140**, 180-188

Yeager T.R., Neumann A.A., Englezou A., Huschtscha L.I., Noble J.R. & Reddel R.R. 1999. Telomerase-negative immortalized human cells contain a novel type of promyelocytic leukemia (PML) body. *Cancer Res.* **59**, 4175-4179

Zhong S., Muller S., Ronchetti S., Freemont P.S., Dejean A. & Pandolfi P.P. 2000. Role of SUMO-1-modified PML in nuclear body formation. *Blood* **95**, 2748-2752

## Tables

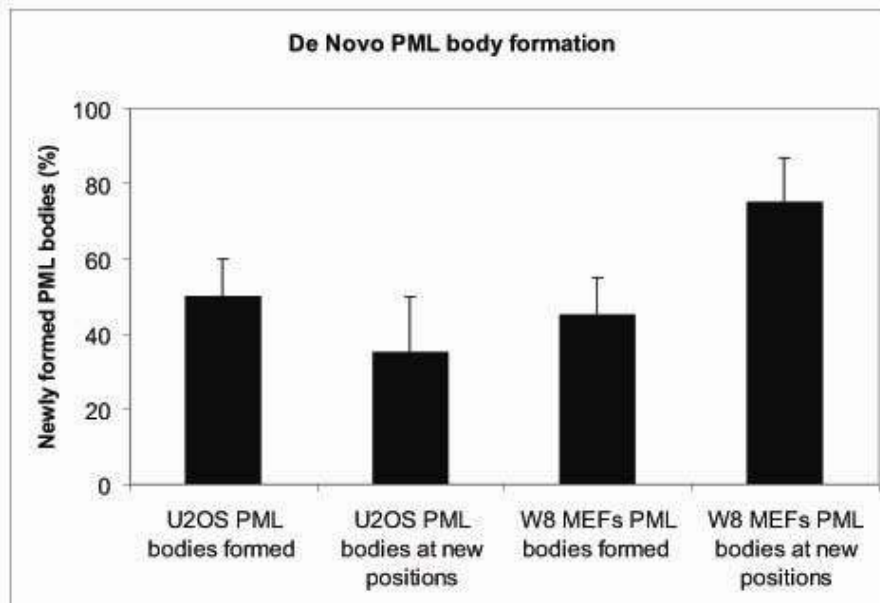
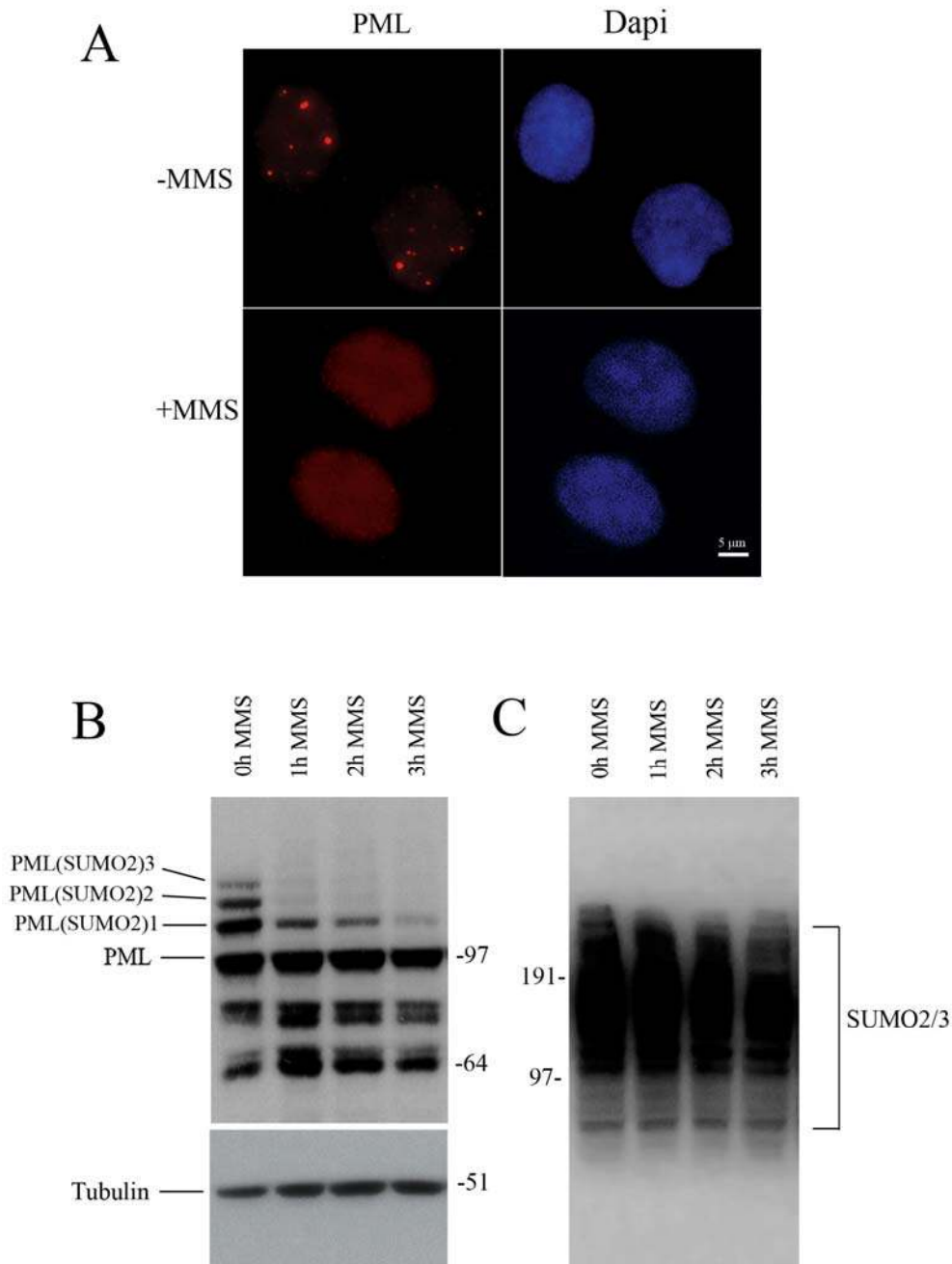


Table 1

**Table 1.** *De novo* PML body formation in U2OS and W8 MEF cells. Quantitative determination of PML bodies that form *de novo* in cells which recovered from MMS treatment as compared to the original numbers and positions of PML bodies present in the same cells before MMS treatment. The data are an average of 10 U2OS cells and 10 W8 MEF cells. Error bars, SD.

Figures



**Figure 1.** PML nuclear bodies disperse by MMS treatment. (A) U2OS cells were stained with an anti-PML antibody to detect endogenous PML and with DAPI (blue). In untreated cells, the PML protein is localized in PML nuclear bodies (upper panel) as shown by fluorescence microscopy. In cells treated with the DNA alkylating agent MMS, the PML bodies are dispersed and the PML protein is present throughout the nucleus in a diffuse and punctate pattern (lower panel). Images were not deconvolved. (B) Immunoblot analysis of PML in total lysates of U2OS cells that are treated with MMS for increasing time periods. (C) Total cell lysates from U2OS cells that are treated with MMS for increasing time periods were subjected to immunoblotting with anti-PML and anti-SUMO2/3 antibodies, respectively.

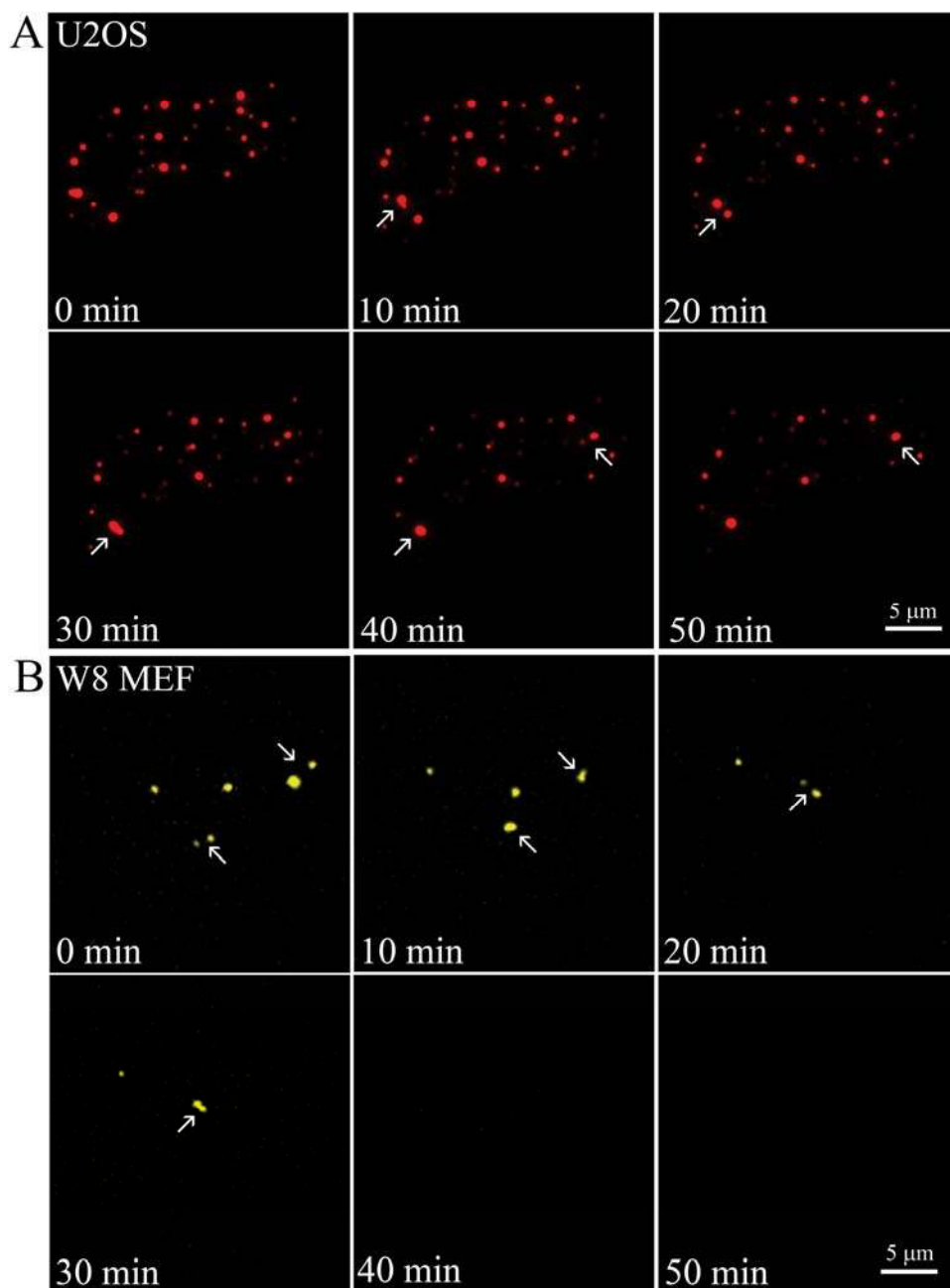


**Figure 2.** PML body dispersal is preceded by a fusion of PML bodies in MMS-treated cells. (A) U2OS cells were transiently transfected with an expression vector encoding EYFP-PML. Image acquisition of live cells was started immediately after MMS addition to the culture medium and a 3D image stack was taken every 10 minutes. Image stacks were captured using 50 millisecond exposure times and deconvolved to reduce out of focus information. Each picture shows a maximum projection of a deconvolved 3D image stack. Arrows indicate PML bodies that fuse and then disperse shortly after. (B) A similar procedure as described in (A) was used to image the disassembly of PML nuclear bodies in live W8 MEFs.



## Telomeric DNA mediates de novo PML body formation

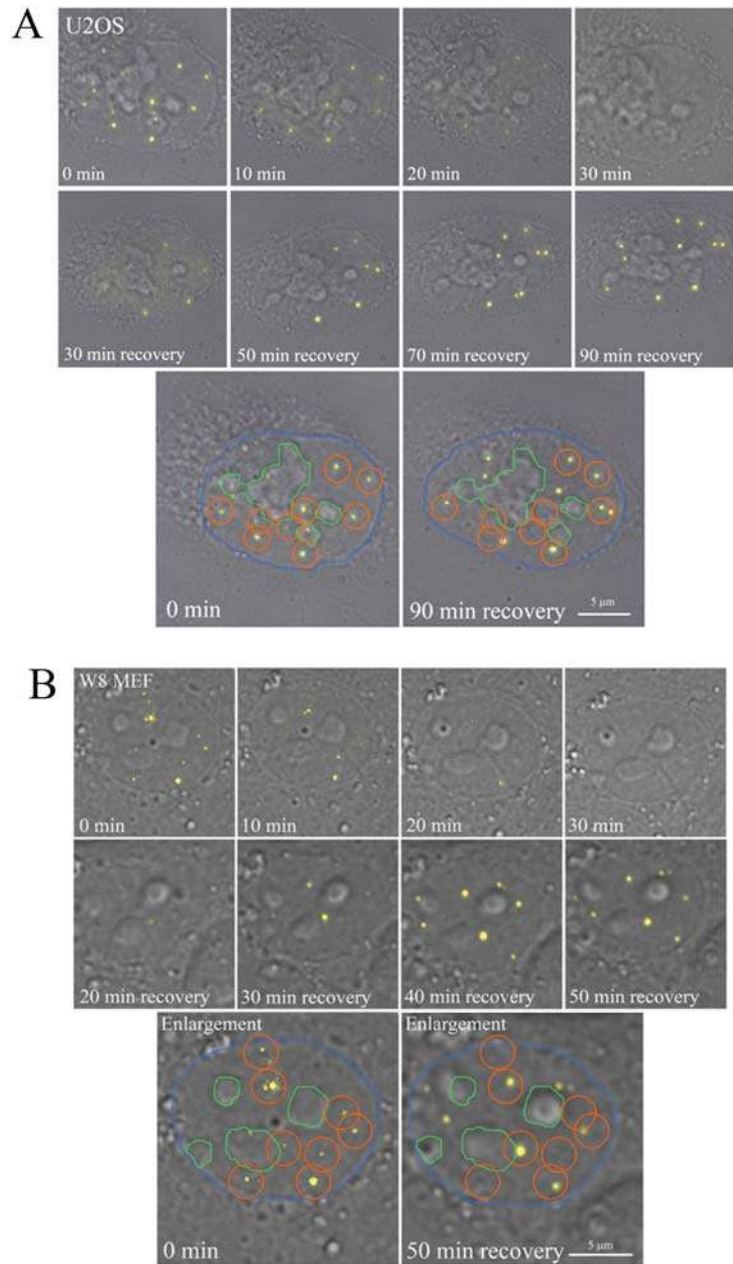


**Figure 3.** Not all PML bodies form at previously used sites in the cell nucleus. (A) Double projections of DIC and fluorescence images show the dispersal and formation of PML bodies in a U2OS cell. U2OS cells expressing EYFP-PML were treated with MMS for 40 min and then incubated in fresh medium without MMS. During the course of the experiment image stacks were taken every 10 minutes. To determine whether PML bodies recover at the same position a 2 μm orange circles are placed around the PML bodies of a cell before treatment and the nucleoli are marked by a green line (enlarged image). The orange circles were grouped together with the most nearby nucleolus (green line) and the grouped items were placed on top of the same cell after recovery. The PML bodies outside the orange circles indicate those that are formed at a different spatial position as they occupied before MMS treatment. The contour of the nucleus is indicated with a blue line. (B) Double projections of DIC and fluorescence images show the dispersal and formation of PML bodies in a W8 MEF cell. Treatment and imaging conditions were the same as for U2OS cells. The image taken after 50 minutes of recovery time shows PML bodies that are positioned both inside and outside the orange circles. The contour of the nucleus is indicated with a blue line.

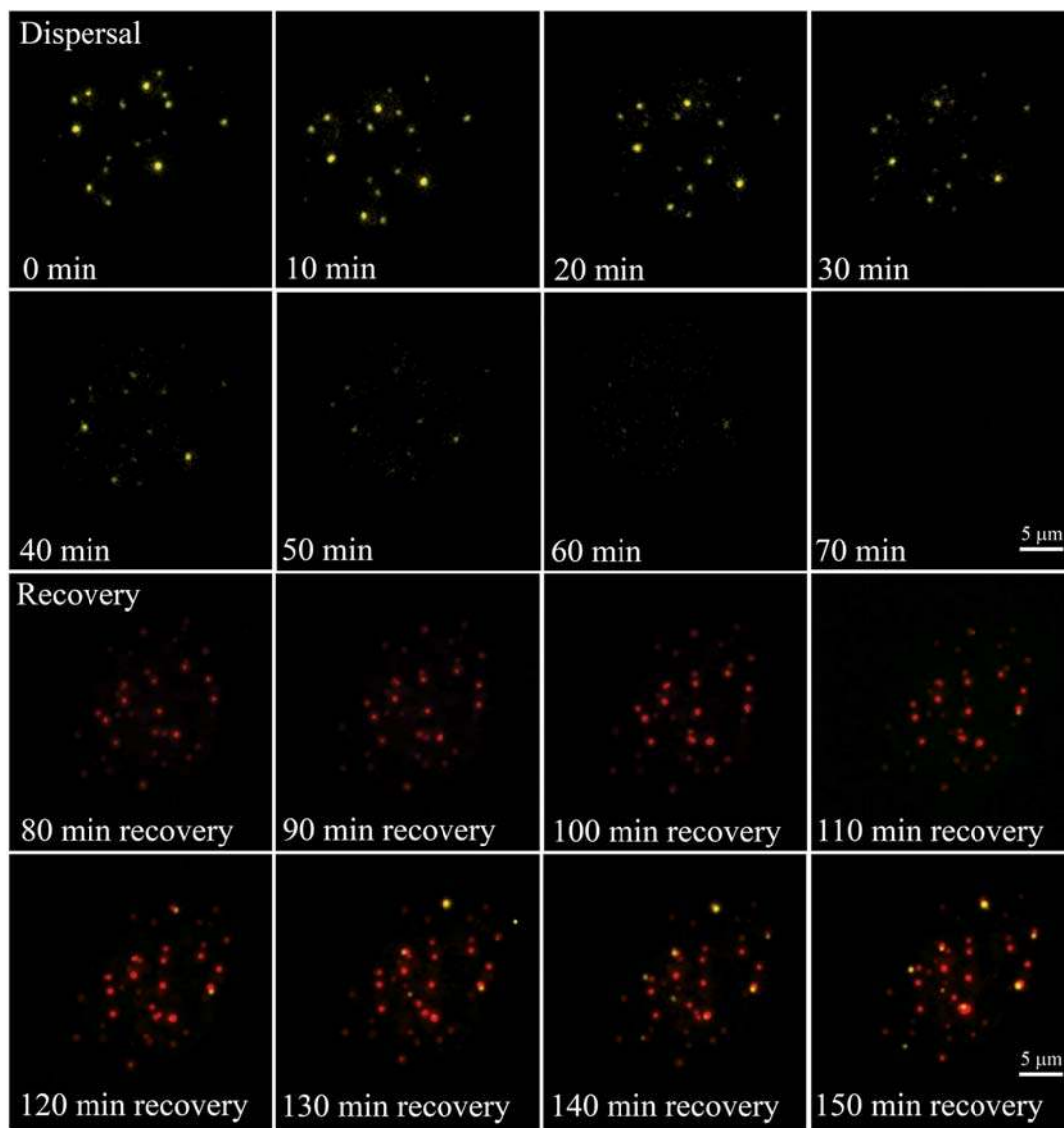


**Figure 4.** New PML bodies form on telomeric sites when U2OS cells recover from MMS treatment. U2OS cells were cotransfected with expression vectors encoding EYFP-PML and DsRed-TRF1, and 3D stacks were acquired every 10 minutes. 3D image stacks were captured using 50 millisecond exposure times and deconvolved. The images taken during the recovery phase show the spatial position of telomeric DNA in red and the accumulation of PML protein in yellow.

## Telomeric DNA mediates de novo PML body formation

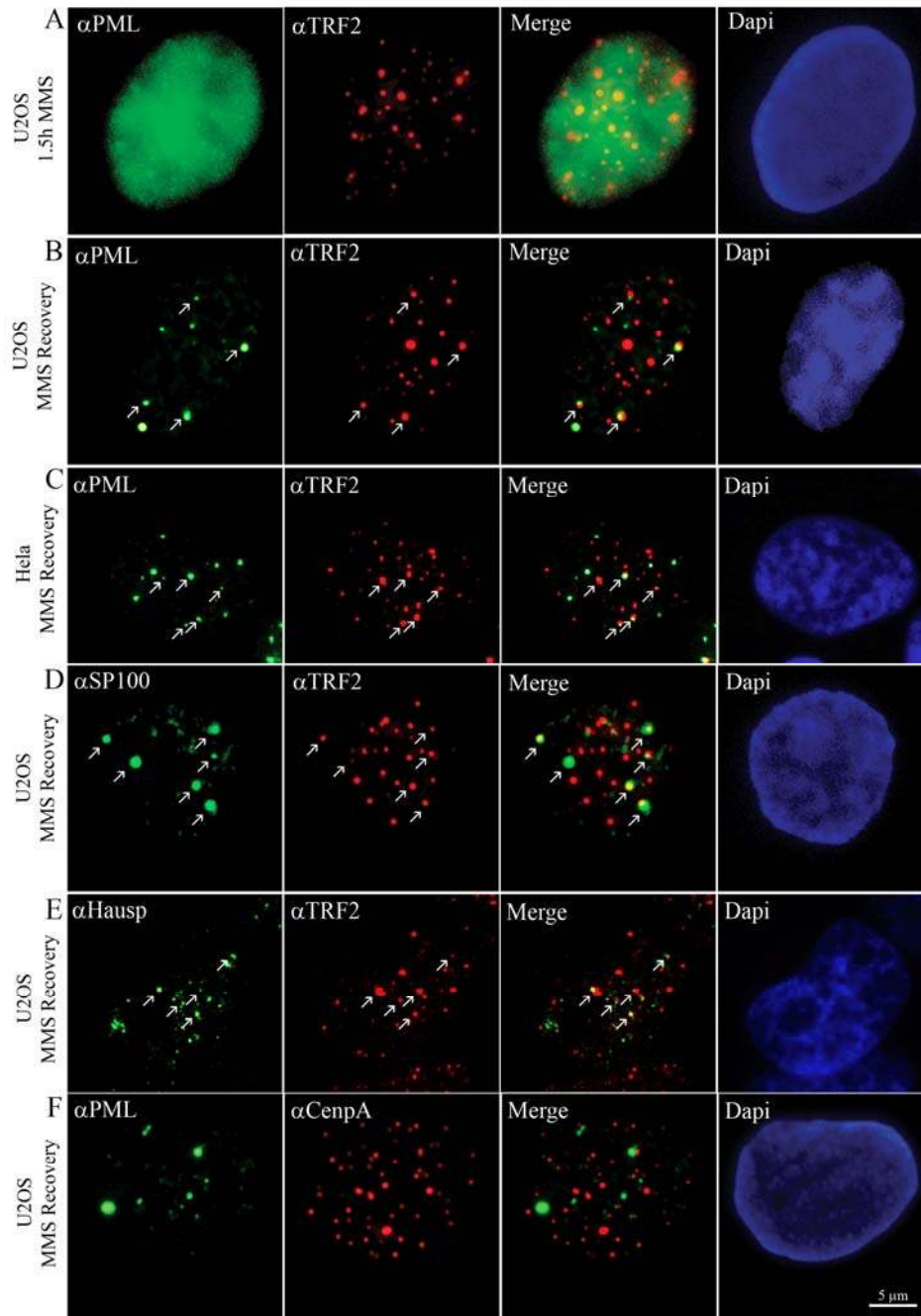


**Figure 5.** Endogenous PML, Sp100 and Hausp accumulate at telomeric sites but not at centromeres in U2OS cells recovering from MMS treatment. (A) Immunofluorescence image of a U2OS cell treated with MMS, fixed and stained with anti-PML (green) and anti-TRF2 (red) antibodies. (B) Image of a U2OS cell that recovers from MMS treatment and is stained with antibodies against PML (green) and TRF2 (red). The arrows indicate the positions where PML colocalize or associate with TRF2 foci. (C) Localization of Sp100 at telomeric sites in a U2OS cell that recovers from MMS treatment. During recovery from MMS treatment, U2OS cells were fixed and stained with anti-Sp100 and anti-TRF2 antibodies. (D) Immunofluorescence image of a U2OS cell that recovers from MMS treatment. Sites where Hausp colocalizes with telomeric DNA are indicated by arrows. (E) PML does not colocalize with centromeres in a U2OS cell that recovers from MMS treatment. Following MMS treatment, U2OS cells were incubated in fresh medium, fixed and stained with anti-PML (green) and anti-CENPA (red) antibodies. All cell nuclei are counterstained with DAPI (blue).

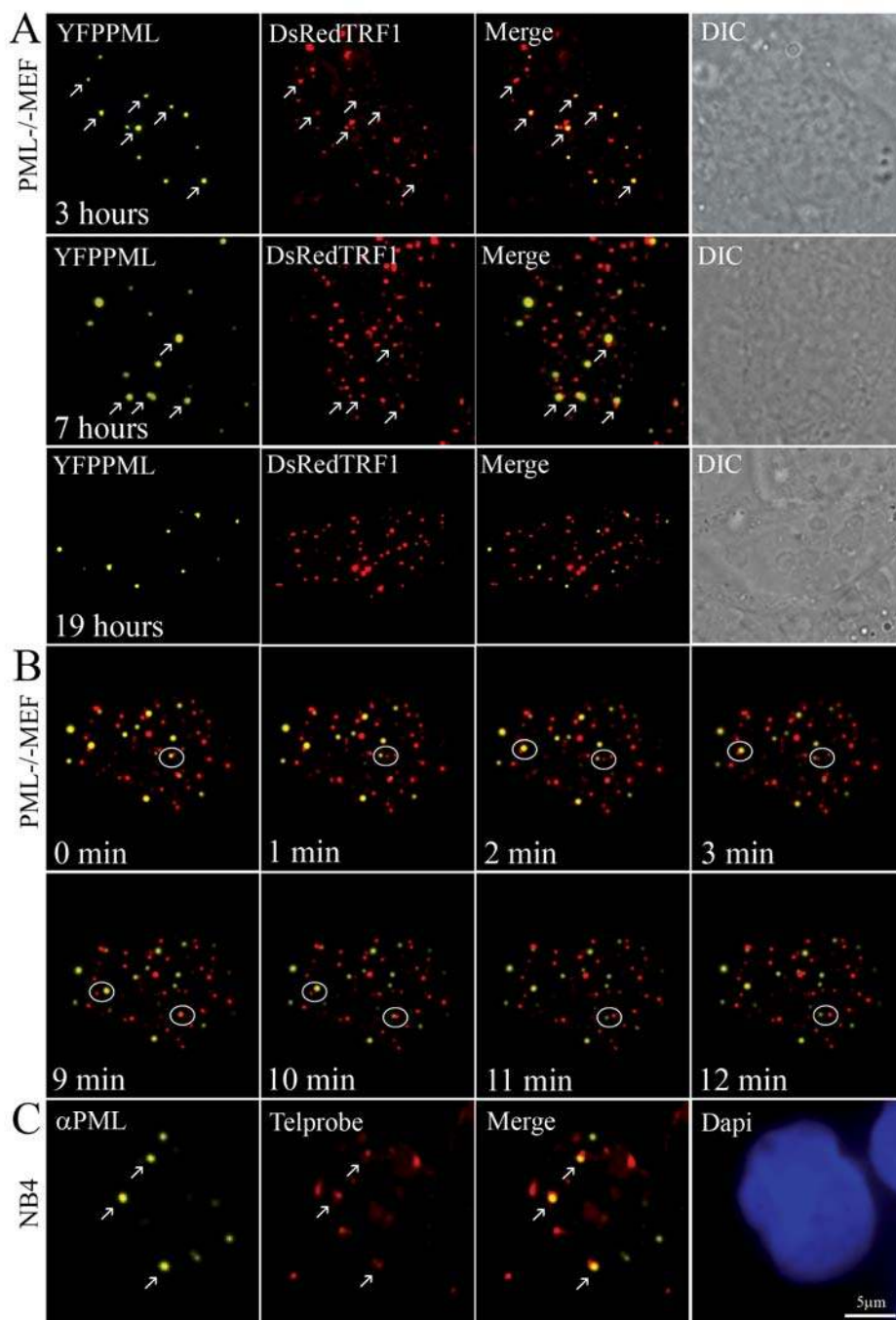


**Figure 6.** New PML bodies form on telomeric DNA in a DNA damage independent manner. (A) Ectopically expressed EYFP-PML form *de novo* PML bodies at telomeric DNA in PML<sup>-/-</sup> MEFs. PML<sup>-/-</sup> MEFs are co-transfected with EYFP-PML and DsRed-TRF1 and 3D image stacks are collected after 3 hours, 7 hours and 19 hours. Arrows indicate the positions where PML colocalize with TRF1. Note that the number of PML bodies that are associated with telomeric sites decreased at 7 and 19 hours post transfection. (B) Newly formed PML bodies dissociate from telomeric sites. PML<sup>-/-</sup> MEFs were cotransfected with EYFP-PML and DsRed-TRF1 and at 3 hours post transfection each minute a 3D image stack was taken. The area in the circle points to a PML body separating from a telomere. (C) NB4 cells were treated with Arsenic trioxide for 8 hours to initiate PML body assembly. Cells were fixed, subjected to FISH using a telomere-specific PNA probe and stained with anti-PML antibody. Arrows indicate positions where PML localize at telomeric DNA. Finally, cells were counter stained with DAPI.

## Telomeric DNA mediates de novo PML body formation

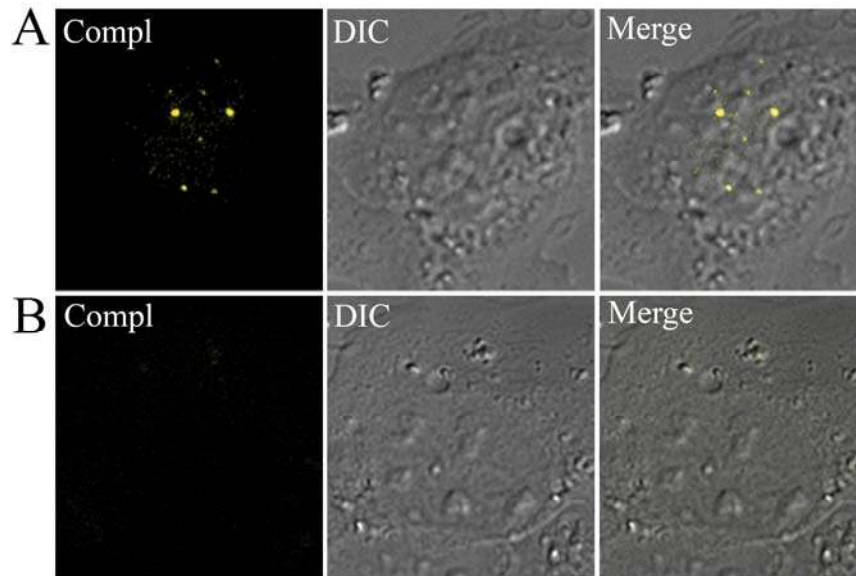


**Figure 7.** PML directly interacts with TRF at telomeric DNA. (A) Ectopically expressed PML interacts with TRF1 in the nucleus of PML<sup>-/-</sup> MEFs as shown by the appearance of yellow fluorescent signals in a combined fluorescence-DIC image. PML<sup>-/-</sup> MEFs were cotransfected with the fluorescent complementation expression vectors PML-CC155 and YN173-TRF1 and incubated at 30°C for 16 hours to allow for correct folding of fluorescent YFP. (B) Ectopically expressed YN173-TRF1 and TEL-CC155 does not interact as shown by the absence of fluorescence complementation.

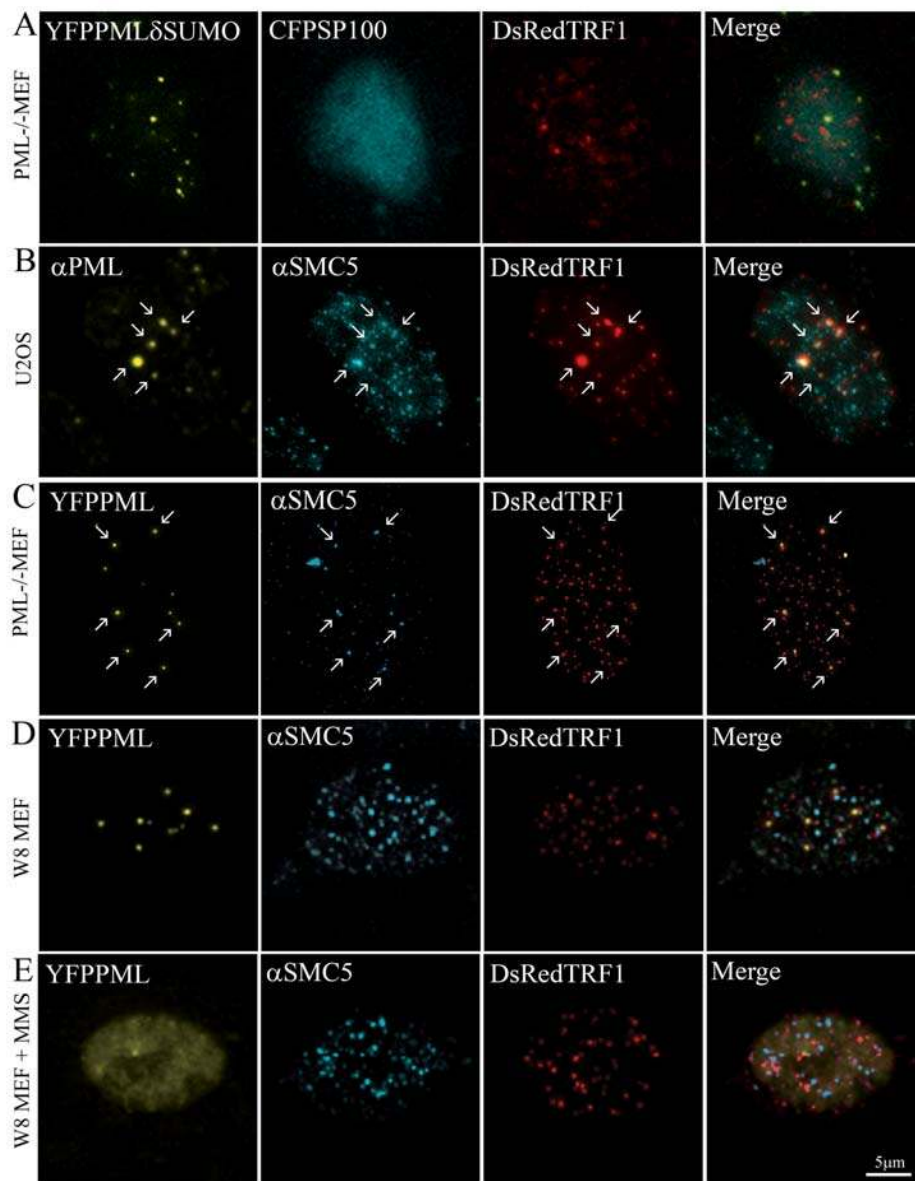
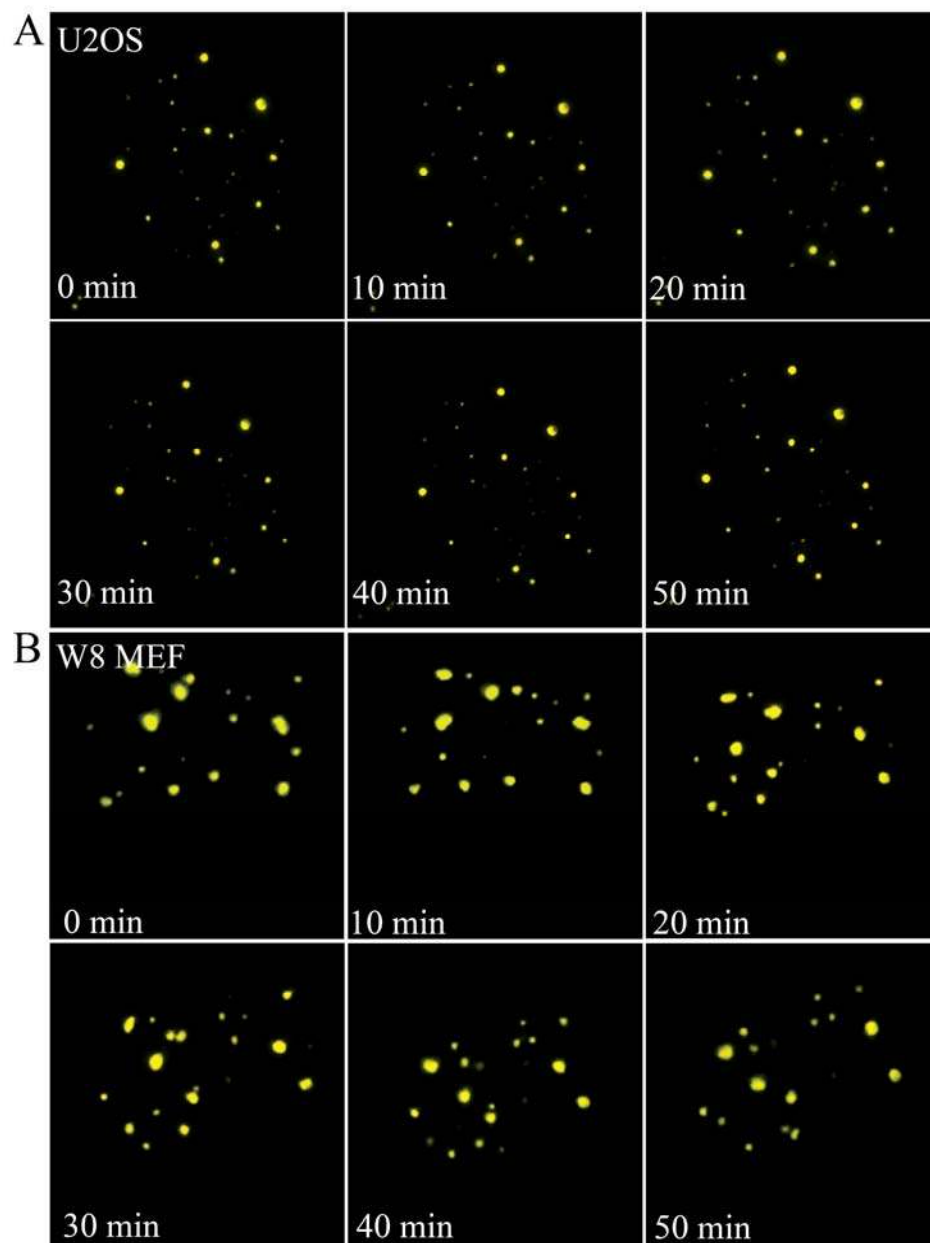


**Figure 8.** A role for SUMO in the formation of new PML bodies. (A) SUMOylation-deficient PML does not localize at telomeric DNA in PML<sup>-/-</sup> MEFs. PML<sup>-/-</sup> MEFs were cotransfected with DsRed-TRF1, ECFP-Sp100 and YFP-tagged SUMOylation-deficient PML. The image shows the formation of PML aggregates (yellow), which do not colocalize with Sp100 (cyan) and do not localize at telomeric DNA that are stained by DsRed-TRF1 (red). (B) The SMC5/6 complex is present at sites where PML bodies form at telomeric DNA. U2OS cells were transfected with DsRed-TRF1, treated with MMS, and allowed to recover in fresh medium. Cells were fixed and stained with anti-PML and anti-SMC5 antibodies. The arrows point to positions in the nucleus where PML (yellow) and SMC5 (cyan) localize at telomeric sites (red). (C) Ectopically expressed PML localizes together with SMC5 at telomeric DNA in PML<sup>-/-</sup> MEFs. PML<sup>-/-</sup> MEFs were cotransfected with EYFP-PML, to induce PML body formation, and DsRed-TRF1, fixed and stained with anti-SMC5 antibody. The arrows indicate the positions where PML (yellow) and SMC5 (cyan) localize at telomeric DNA (red). (D) PML and SMC5 do not localize at telomeric DNA in untreated and (E) MMS-treated W8 MEFs. W8 MEFs were cotransfected with YFP-PML and DsRed-TRF1 and either not treated or treated with MMS. Cells were fixed (without recovery) and stained with anti-SMC5 antibody. Both, untreated and MMS-treated cells show that the SMC5/6 complex (cyan) localize in a punctate/diffuse pattern, which does not colocalize with telomeric sites (red) or PML (yellow).



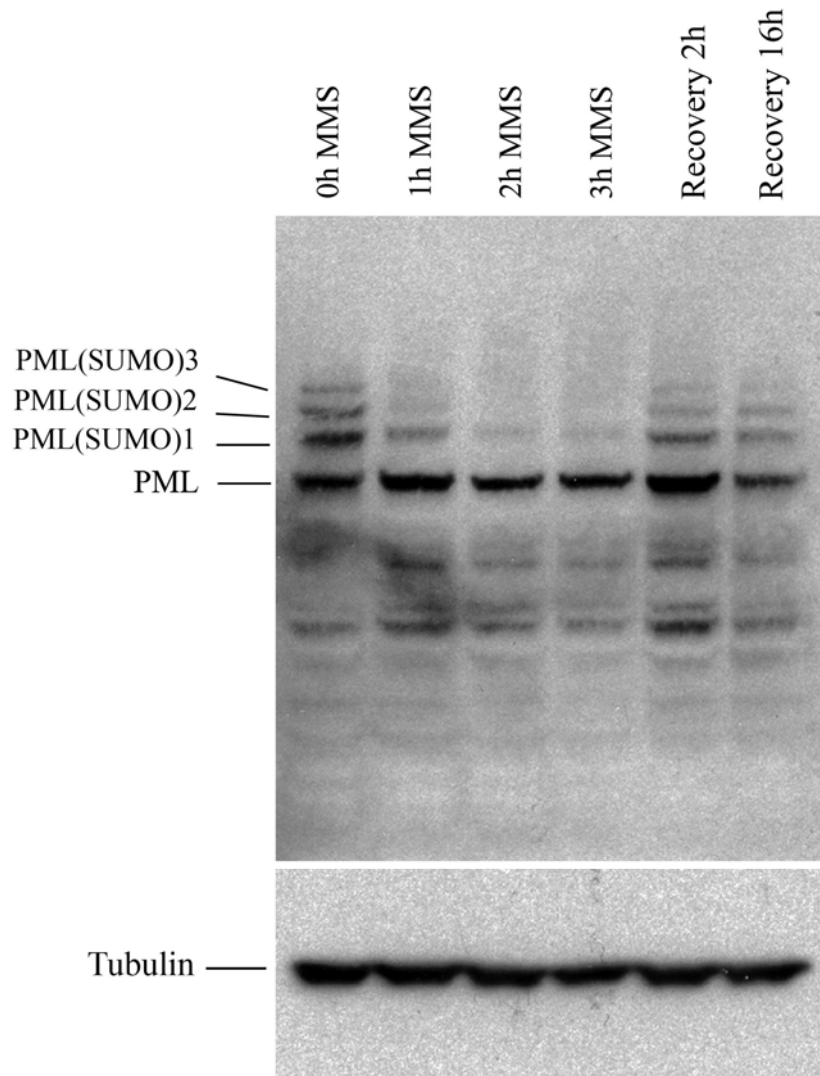
## Supplemental figures



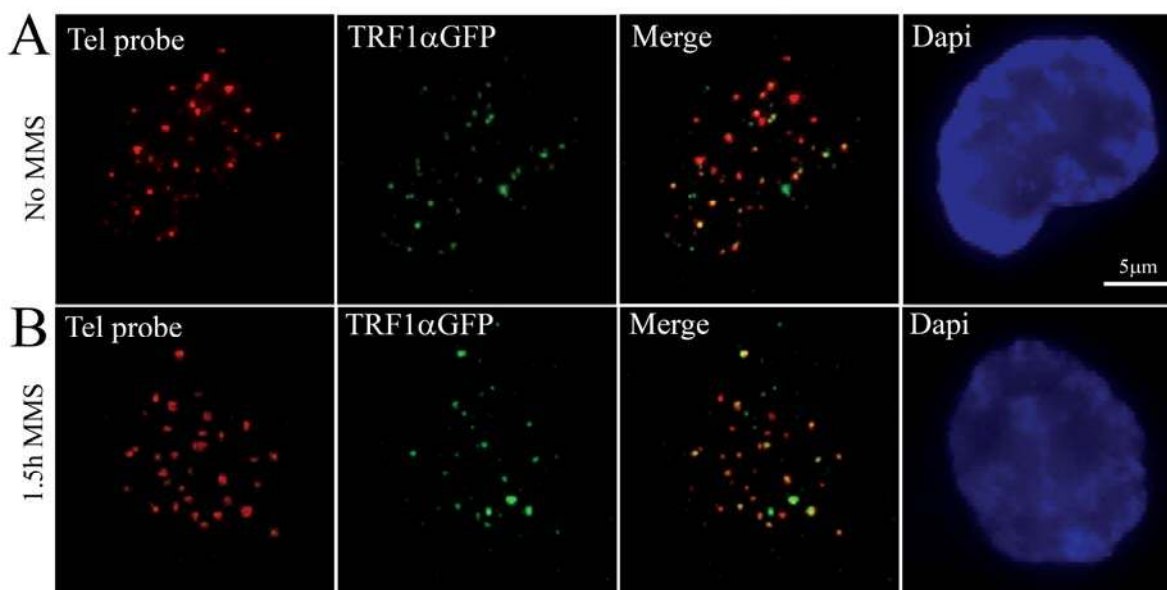
**Supplemental Figure 1.** 3D time-lapse recording of PML bodies in (A) a U2OS cell and (B) a W8 MEF, both expressing EYFP-PML. Both cells were not treated with MMS.



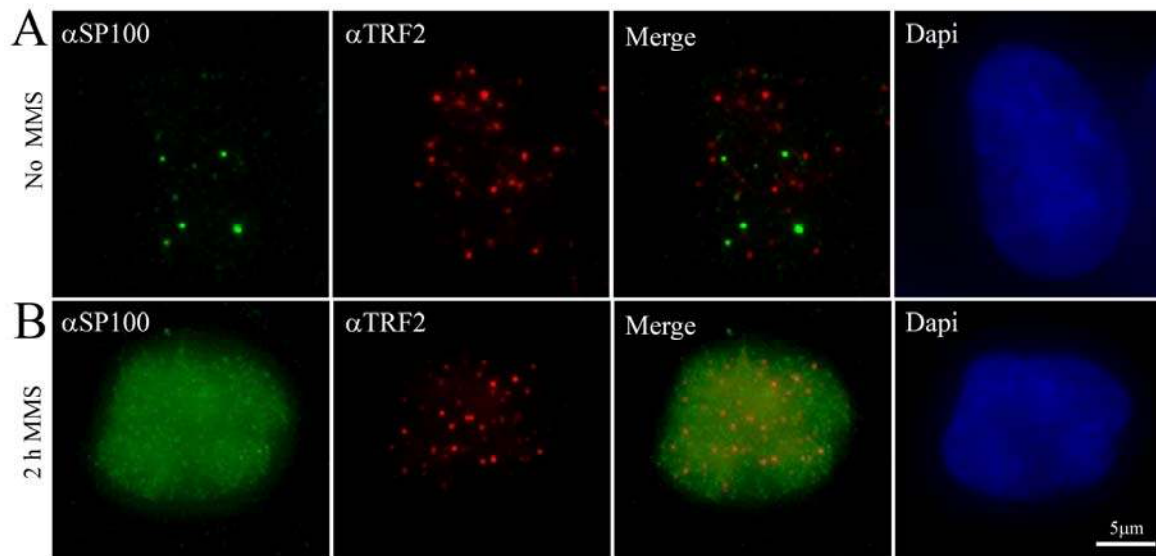
PML Body Formation – Supplemental figures



**Supplemental Figure 2.** Total cell lysates from U2OS cells that are treated with MMS for increasing time periods were subjected to immunoblotting with anti-PML and anti-SUMO2/3 antibodies, respectively. Total cell lysates from cells that were allowed to recover from the MMS treatment are shown as well. The amount of SUMOylated PML decreases during MMS treatment and returns after recovery from MMS treatment.

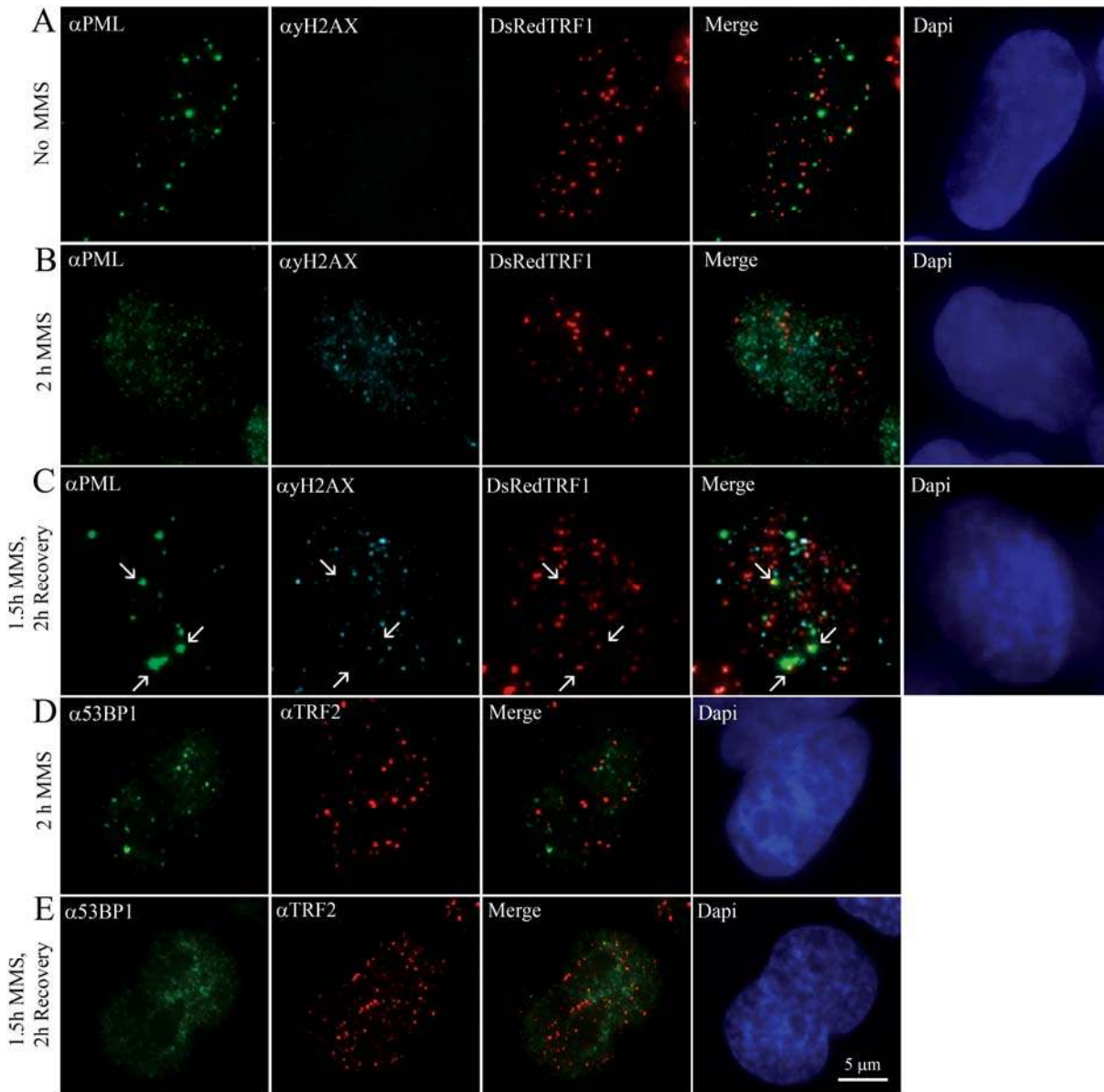


**Supplemental Figure 3.** Double labeling of exogenous TRF1 and telomeric DNA in (A) a nontreated U2OS cell and (B) an MMS treated U2OS cell. Telomeric DNA was hybridized with a telomere specific PNA probe (red) and exogenous TRF1 was labeled using an anti-GFP antibody (green). Nuclei were counterstained with DAPI (blue).

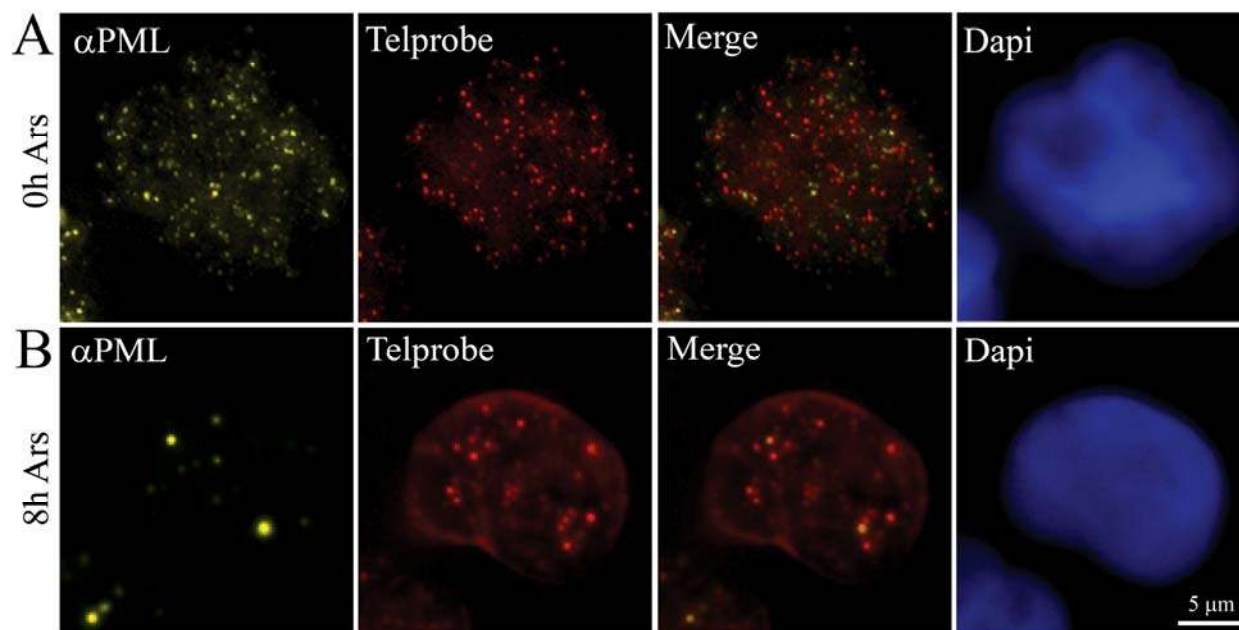


**Supplemental Figure 4.** Localization of Sp100 (green) and TRF2 (red) in a U2OS cell without (A) and with (B) MMS treatment as shown by immunofluorescence. Note that the Sp100 localization before and after treatment is similar to that observed for PML (see also figure 5). Although the cell shown in (A) does not show a colocalization of Sp100 with TRF2, a colocalization of the two is observed in U2OS cells that show in addition to regular PML bodies ALT-associated PML bodies.

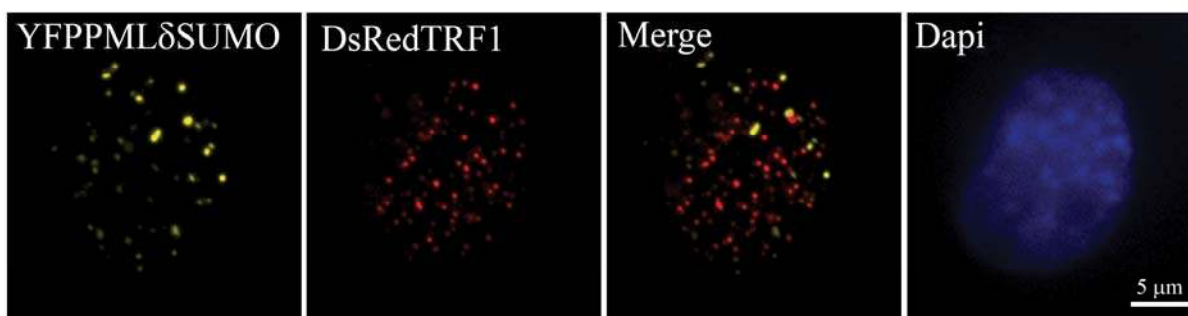
PML Body Formation – Supplemental figures



**Supplemental Figure 5.** The DNA damage markers  $\gamma$ H2AX and 53BP1 are mostly not present at telomeric DNA at which PML bodies form. (A-C) Representative immunofluorescence images of U2OS cells expressing DsRed-TRF1 and stained with antibodies directed against PML (green) and  $\gamma$ H2AX (cyan). (A) U2OS cell without treatment, (B) treated for 2 hours with MMS and (C) recovered from MMS treatment. Arrows indicate sites of newly formed PML bodies that colocalize with telomeric DNA but not with DNA damage foci. (D, E) Representative immunofluorescence images of U2OS cells stained with antibodies specific for 53BP1 (green) and TRF2 (red). (D) U2OS cell treated with MMS for 2 hours and (E) U2OS cell 2 hours after recovery from MMS treatment. Nuclei were counterstained with DAPI (blue).



**Supplemental Figure 6.** PML bodies form in NB4 cells when treated with arsenic trioxide. (A) PML does not preferentially localize at telomeric DNA in untreated NB4 cells. NB4 cells were fixed, hybridized with a telomere-specific PNA probe and stained with anti-PML antibody. PML is present in a diffuse and punctate pattern (yellow) which does not significantly overlap with the staining pattern of telomeric DNA (red). (B) Arsenic trioxide-treated NB4 cells show PML bodies that localize at telomeric DNA. NB4 cells were treated with arsenic trioxide for 8 hours, fixed, hybridized with a telomere-specific PNA probe and stained with anti-PML antibody. Nuclear DNA was counter stained with DAPI.



**Supplemental Figure 7.** SUMOylation-deficient PML does not localize at telomeric DNA in U2OS cells that recover from MMS treatment. U2OS cells were cotransfected with DsRed-TRF1 and EYFP-tagged SUMOylation-deficient PML, treated with MMS for 1.5 hours and allowed to recover in fresh medium. During the recovery phase, cells were fixed and analyzed by fluorescence microscopy. The image shows the formation of PML aggregates (yellow), which do not colocalize with telomeric DNA (red).



## **CHAPTER 5**

Nuclear body movement is constrained by associations  
with chromatin



## Nuclear body movement is constrained by associations with chromatin

Anneke K. Brouwer, Hans Vrolijk, Joop C.A.G. Wiegant, Hans J. Tanke and Roeland W. Dirks

Department of Molecular Cell Biology, Leiden University Medical Center, 2300 RC Leiden, The Netherlands

### Summary

The cell nucleus contains distinct nuclear bodies which are involved in key cellular processes. Factors that determine the integrity and spatial positioning of these bodies in the cell nucleus are unknown. Here we investigate the dynamic behavior of three prominent nuclear bodies, PML bodies, Cajal bodies and speckles relative to that of chromatin. All three bodies seem to be associated with chromatin and this association is lost in response to methylmethane sulfonate treatment. Once dissociated from chromatin, the nuclear bodies have more freedom to move in the three dimensional nuclear space. Furthermore, PML bodies will eventually disassemble but not Cajal bodies and speckles, suggesting that PML body structural integrity is dependent on its association with chromatin.

### Introduction

The cell nucleus contains various distinct nuclear compartments or bodies which differ in size, morphology, composition and function. The diversity in nuclear bodies has been explained by the various activities that are supported by the cell nucleus including transcription, RNA processing, RNA transport and DNA repair. Each of these activities requires the recruitment of multiple factors and an ordered assembly of multi-component machineries. Among the most prominent and best studied nuclear bodies are nucleoli, PML bodies, Cajal bodies and speckles. Nucleoli are sites of rRNA synthesis, rRNA processing and ribosome subunit assembly. Each of these steps is performed by different protein assemblies and takes place in three different subcompartments of the nucleolus. The functions of the other nuclear compartments are still not fully understood. Speckles have been suggested to function as storage sites of RNA processing and RNA transport factors, from which these factors are recruited to transcriptionally active genes (Misteli et al., 1997; Dirks et al., 1997; Snaar et al., 1999). Observations of active genes that are preferentially associated with speckles suggested that these domains may also function as hubs, facilitating and possibly coordinating the synthesis of mRNAs (Hall et al., 2006). In addition, speckles have also been implicated in steps of mRNA splicing control and nuclear export (Hattinger et al., 2002; Molenaar et al., 2004; Schmidt et al., 2006).



## Nuclear body movement is constrained by associations with chromatin

Functionally related to speckles are Cajal bodies, which have been identified as assembly sites of spliceosomal small nuclear ribonucleoproteins (snRNPs) and have been found present mainly in proliferating cell types (Stanek & Neugebauer, 2006).

PML bodies have been implicated in many different cellular processes such as transcription regulation, apoptosis, senescence, DNA repair, proteosomal degradation and genome stability (Bernardi & Pandolfi, 2007). Furthermore, they have been suggested to function as nuclear depots in which proteins are temporally stored (Negorev & Maul, 2001). Recent evidence suggests that PML bodies are sites at which post-translational modification of proteins by both ubiquitin and SUMO is integrated to regulate proteosomal degradation (Bailey & O'Hare, 2005; Sharma et al., 2010).

Although nuclear bodies are distinct, stable structures during interphase, their protein content is in a continuous flux with the surrounding nuclear space, allowing rapid changes in body composition. This protein flux indicates that proteins do not necessarily exert their function within or at the surface of a nuclear body but possibly elsewhere in the nucleus. Nevertheless, there is ample evidence that nuclear bodies have the ability to transiently associate with chromosomal sites. This has not only been reported for nucleoli, which associate with ribosomal DNA genes but also for PML bodies (Ching et al., 2005; Kießlich et al., 2002; Gialitakis et al., 2010), Cajal bodies (Platani et al., 2002) and speckles (Brown et al., 2008).

Live cell studies revealed that nuclear bodies generally show little movement inside the cell nucleus, which could reflect a rather stable interaction with chromatin. Alternatively, it has been suggested that nuclear body mobility is mainly determined by the poor accessibility and the slow dynamics of chromatin (Görisch et al., 2004). Also, nuclear bodies have been suggested to be connected to a nuclear matrix structure, limiting their movement. Physical associations of chromatin with immobile nuclear bodies may then restrict the movement of chromatin or even support the spatial organization of chromatin in the nucleus (Chubb et al., 2002).

A key question is whether the association of nuclear bodies with chromatin or with activities that take place at chromatin is an essential factor to ensure the stability/integrity of the bodies. Recently, we observed that the mobility of PML nuclear bodies significantly increase in cells that were treated with the DNA-methylating agent methyl methanesulfonate (MMS), before the PML bodies dispersed as a result of this treatment (Brouwer et al., 2009). Whether the increase in PML body dynamics reflects an increase in chromatin dynamics has not yet been investigated. Photoactivatable GFP (PA-GFP) Histone H4 has been used as a marker for chromatin to examine their dynamic properties in living cells (Post et al., 2005; Wiesmeijer et al., 2008). In this study, we used this marker, together with fluorescent markers for PML bodies, speckles and Cajal bodies to investigate their dynamic spatial arrangements in cells exposed to MMS treatment by fluorescence time-lapse imaging.

## Materials and Methods

### Cell culture and transfection

Human Osteosarcoma cells (U2OS) were cultured in 3.5 cm glass bottom petri dishes (MatTek Corporation, Ashland, MA) in Dulbecco's modified Eagle's medium without phenol red, containing 1.0 mg/ml glucose, 10% fetal bovine serum (FBS), 2 mM glutamine, 100 U/ml penicillin, and 100 µg/ml streptomycin (all from Invitrogen, Carlsbad, CA). Cells at 70%–80% confluency were transiently transfected with PA-GFP histone H4 (Wiesmeijer et al., 2008) together with either coilin-DsRed, SF2/ASF-DsRed or PML-DsRed by using lipofectamine 2000 (Invitrogen). Coilin, SF2/ASF and PML I were originally cloned into a GFP vector (Molenaar et al., 2004; Wiesmeijer et al., 2002) and subcloned into a DsRed vector (ClonTech, Mountain View, CA). Cells were incubated with 0.01% methyl methanesulfonate (MMS; Sigma-Aldrich, St. Louis, MO) for time periods ranging from 45 minutes to 2 hours. Cells were allowed to recover from MMS-treatment by incubating them in fresh medium containing 20% FBS for 2 to 3 hours.

### Photoactivation and microscopy

Photoactivation and subsequent time-lapse imaging were both performed using a Leica TCS SP5 confocal laser scanning microscope (Leica Microsystems, Mannheim, Germany) equipped with a climate control box. During the course of the experiments, the temperature of the cells was kept constant at 37°C and the CO<sub>2</sub> concentration at 5%. PA-GFP was activated using the 405 nm laser line at 12% laser power during a 300 ms pulse. Following photoactivation, subsequent time-lapse images were taken with a 63× NA 1.4 PlanApo oil objective lens and 488 nm and 561 nm laser lines of respectively an Argon (multi-line) and a DPSS (561nm) laser. An additional 6-fold scanning zoom was applied to collect high-resolution Z-stacks. At each time-point a two-channel Z-stack of 15-25 Z-slices (thickness 0.4 µm) was acquired using 2-5% laser power, 400 Hz scanning frequency and 512 x 512 pixels per frame. 4D image stacks were collected every 30 seconds for 10 minutes. Image acquisition and analysis were performed using the Leica SP5 software. All images and movies shown are representative of 6-10 repeats of the same experiment.

## Results

### **MMS treatment causes PML bodies to detach from chromatin**

On average, PML bodies show little movement in the cell nucleus (Wiesmeijer et al., 2002; Eskiw et al., 2003). Only a small subset of PML bodies display high mobility (Muratani et al., 2002), while directional movements of PML bodies are observed only when cells enter mitosis (Chen et al., 2008). When U2OS cells are treated with the DNA methylating agent MMS, the majority of PML bodies display a dynamic movement until they disperse (Brouwer et al., 2009). There are two possible explanations for this increase in PML body mobility. Either chromatin domains become more dynamic and accessible as a result of the DNA methylation or, alternatively, PML bodies dissociate from the chromatin to which they are bound and become dynamic.

To analyze whether the observed increase in PML body mobility after MMS treatment is related to an increase in chromatin mobility, U2OS cells were transfected with EYFP-PML-I together with DsRed-TRF2, treated with MMS, and 3D image stacks were collected at 30 second time intervals for 10 minutes. At 2 hours following MMS treatment, the majority of PML bodies moved rapidly through cell nucleus as compared to telomeres, which showed little mobility (Fig. 1 and Movie 1). Thereby, the movement of PML bodies was not limited to a confined area in the nucleus but PML bodies were shown to move over large distances. Ultimately, as indicated by arrows, PML bodies fuse with each other and disperse. As telomere movement may not be indicative for the dynamics of other chromatin regions, in particular those surrounding PML bodies, we employed a histone H4 fused at its carboxy terminus with a photoactivatable (PA) GFP, as a marker for chromatin. Incorporation of histone H4-PAGFP into chromatin allows photoactivation of selected chromatin regions in the cell nucleus using 405 nm laser light and there after their visualization using 488 nm laser light. Fluorescence 3D time lapse recordings of PML bodies containing DsRed-PML-I together with photoactivated histone H4-PAGFP surrounding these bodies showed a similar slow mobility for both compartments (Fig. 2A, Movie 2). PML bodies remained enclosed by photoactivated histone H4-PAGFP-labeled chromatin for at least 10 minutes, the maximum time-period in which we imaged cells. A time course of 10 minutes appeared optimal to obtain 3D stacks at a high temporal resolution without photobleaching of the photoactivated H4-PAGFP. A side-view of the same nucleus that is shown in Fig. 2A shows that PML bodies are evenly distributed throughout the cell nucleus (Fig. 2B). Next, U2OS cells expressing DsRed-PML-I and H4-PAGFP were incubated with MMS for 2 hours and chromatin regions directly surrounding PML bodies were photoactivated. DsRed-labeled PML bodies were observed losing contact with the fluorescently labeled chromatin and moving rapidly throughout the nucleus (Fig. 3A, B, Movie 3). The number of PML bodies that lost contact with the surrounding photoactivated chromatin varied among cells but seemed to increase when exposed to MMS for a longer time period. In some cells all PML bodies lost contact with the surrounding chromatin while in others only a few PML bodies did. Notably, during the time course in which PML bodies lose contact with chromatin, the photoactivated chromatin seemed to remain positionally stable and did not change its state of compaction in the cell nucleus. This indicates that the increase in PML body motion is not a result of an increase in chromatin mobility or a change in chromatin compaction as far it can be judged at the light microscopical level of resolution. By looking at the side-view

of cells, it appeared that the spatial distribution of PML bodies changed from being positioned throughout the 3D nuclear volume in untreated cells to a more confined localization in a Z-plane located at the centre in the 3D space of the nucleus following MMS treatment (Fig. 4). These side views in the x-z plane of cells support the conclusion that PML bodies dissociate from chromatin in response to MMS treatment.

### **Cajal bodies and speckles dissociate from chromatin in response to MMS treatment**

Next, we investigated whether the spatial positioning and dynamics of speckles and Cajal bodies in U2OS cells is also altered by MMS treatment. U2OS cells were transiently transfected with the speckle marker construct DsRed-ASF together with construct histone H4-PAGFP. Chromatin regions surrounding speckles were selected and photoactivated and cells were imaged at regular time intervals for 10 minutes. Both speckles and photoactivated chromatin showed a constrained Brownian type of movement (Fig. 5A, Movie 4). Consistent with previous data, chromatin remained associated with speckles during the 10 minutes period in which the cells were imaged (Wiesmeijer et al., 2008). In response to MMS treatment, however, speckles became more dynamic as compared to the chromatin surrounding the speckles (Fig. 5B, Movie 5). This can also be concluded from a side view of the cell (Fig. 4). Frequently, speckles were observed losing contact with the surrounding photoactivated chromatin and remaining detached from it. Probably because speckles are relatively large nuclear structures with an irregular shape, their movements are still confined to a small nuclear region as if restricted by a physical barrier. Different from what we observed for PML bodies, speckles did not disperse after they lost their association with chromatin, even after imaging the cells for another hour. In addition, we did not observe speckles to merge in larger structures. The effect of MMS on speckle behavior proved reversible as cells that were first incubated with MMS and then washed and incubated in fresh medium revealed a speckle distribution and dynamics similar to that of untreated control cells.

To analyze the movement of Cajal bodies together with that of the surrounding chromatin, U2OS cells were cotransfected with DsRed-coilin and histone H4-PAGFP. Time lapse recordings of untreated cells showed that both the Cajal bodies and the surrounding chromatin display similar slow kinetics (Fig. 6A, Movie 6). After the cells were treated with MMS a response similar to that of PML bodies and speckles was observed. The Cajal bodies moved away from the surrounding photoactivated chromatin and became more dynamic (Fig. 6B, Movie 7). Like speckles, Cajal bodies did not become dispersed when they lost contact with chromatin in response to MMS treatment.

## Discussion

Recently, it has been questioned whether nuclear bodies physically interact with chromatin foci. The interpretation of time-lapse imaging data of nuclear body and chromatin movement has led to the proposition that nuclear bodies move by diffusion in a chromatin environment. The mobility of the bodies would then be reflected by the dynamics and accessibility of the chromatin environment (Görisch et al., 2004). The time-lapse imaging data presented in this study show that PML bodies, Cajal bodies and speckles are associated with chromatin. Treatment of cells with the DNA methylating agent MMS result in the dissociation of these nuclear bodies from chromatin. Consequently, both Cajal bodies and PML bodies move through a larger area in the cell nucleus. Consistent with data showing that PML bodies, Cajal bodies and speckles associate with specific chromatin loci, our results suggest that nuclear bodies are relatively immobile in the cell nucleus because of their association with chromatin.

PML bodies have been found associated with specific, mostly transcriptionally active, chromatin loci while a subset of PML bodies have been found transiently associated with telomeric DNA in telomerase negative cells which maintain telomere length by the alternative lengthening of telomeres (ALT) mechanism (Yeager et al., 1999; Molenaar et al., 2003; Jegou et al., 2009). Furthermore, indirect evidence suggests that PML plays a role in higher-order chromatin organization (Kumar et al., 2007). Consistent with these observations, PML has been shown to physically and functionally interact with the matrix attachment region (MAR)-binding protein, a special AT-rich sequence binding protein 1 (SATB1), to organize the major histocompatibility complex (MHC) class I locus into distinct higher-order chromatin-loop structures (Kumar et al., 2007). In this and in our previous work we have shown that treatment of cells with MMS leads to an increase in PML body dynamics before they disperse (Brouwer et al., 2009). By photoactivating chromatin regions that surround PML bodies, using histone H4 fused with a photoactivatable GFP as a marker for chromatin, and subsequent fluorescence time lapse confocal imaging, we show that the increase in PML body dynamics is not accompanied by an increase in chromatin dynamics at PML bodies. This observation is consistent with our previous work showing that MMS treatment has no major impact on general chromatin dynamics (Wiesmeijer et al., 2008). Therefore, the increase in PML body movement might be explained by a retraction of chromatin from the surface of the PML bodies. At present, it is not known to what extent PML bodies interact with chromatin. Also, it is not known which proteins are involved in this interaction. Electron spectroscopic images of human neuroblastoma cells suggest that PML bodies are connected to chromatin at multiple sites (Eskiw et al., 2004).

Since MMS induces alkylating DNA damage and activates a DNA repair mechanism it is conceivable that the increase in PML body dynamics is a direct response to the DNA damage. Recently, it has been shown that following DNA damage, several repair factors transit through PML NBs in a temporally regulated manner implicating these bodies in DNA repair (Dellaire & Bazett-Jones, 2004). It is possible that PML bodies dissociate from chromatin as a result of DNA methylation and finally disassemble into large supramolecular complexes, dispersing associated repair factors to sites of damage.

In addition to PML bodies, Cajal bodies have also been reported to be associated with chromatin sites, including histone and snRNA genes. Although it is suggested that these bodies alternate between an association state with chromatin and a diffusion state in which the bodies move within the interchromatin space (Platani et al., 2002), the association state may continue as long genes are transcribed and ATP is available (Platani et al., 2002).

Compared to PML and Cajal bodies, speckles do not show a dramatic increase in mobility following MMS treatment, although various genes have been observed positioned at the periphery of speckles. Speckles have been implicated in mediating gene associations and to function as hubs (Brown et al., 2008). Most likely, it is the size of this body and its irregular shape that limits its mobility in the chromatin environment.

Methylmethane sulfonate (MMS) is a compound that methylates biologically important nucleophilic sites in DNA, through an  $S_N2$  reaction, and interacts with amino acids in proteins (Paik et al., 1984). When cells are treated with MMS, PML bodies lose their integrity and become dispersed (Conlan et al., 2004; Brouwer et al., 2009). The mechanism of their dispersal is not clear but could be a result of the applied DNA damage. However, there are other examples of cellular stress that cause PML bodies to become dispersed. Environmental stresses such as heat shock, heavy metal shock, or viral protein expression, cause the dissociation of PML bodies into many smaller punctate domains (Maul et al., 1995). MMS has been found to induce hyperacetylation of both cytoplasmic and nuclear proteins as well (Lee et al., 2007). Notably, the acetylation level upon MMS treatment was strongly correlated with the susceptibility of cancer cells, and the enhancement of MMS-induced acetylation by histone deacetylase (HDAC) inhibitors was shown to increase the cellular susceptibility to cancer.

Since PML bodies become dispersed after applying DNA damage, and Cajal bodies and speckles do not, this could implicate that regulated dispersal is an important and functional property of PML bodies. The regulated dispersal of PML bodies may facilitate the enhanced release of DNA repair proteins from NB depots, in order to respond adequately to extensive DNA damage (Conlan et al., 2004). Both speckles (Mintz et al., 1999) and Cajal bodies (Lam et al., 2002) have been isolated and this has not been achieved for PML bodies, further implying structural differences between PML bodies and other nuclear bodies. It is possible that PML body integrity depends on their interaction with chromatin, and that as soon as the interaction with chromatin is lost, PML bodies become dispersed. Further studies are necessary to investigate the effect of the association between chromatin and PML bodies on PML body stability. Also, alkylation or acetylation of the PML protein or other proteins present inside PML bodies may affect the integrity of PML bodies.

## References

- Bailey D. & O'Hare P. 2005. Comparison of the SUMO1 and ubiquitin conjugation pathways during the inhibition of proteasome activity with evidence of SUMO1 recycling. *Biochem. J.* **392**, 271-281
- Bernardi R. & Pandolfi P.P. 2007. Structure, dynamics and functions of promyelocytic leukaemia nuclear bodies. *Nat. Rev. Mol. Cell Biol.* **8**, 1006–1016
- Brouwer A.K., Schimmel J., Wiegant J.C., Vertegaal A.C., Tanke H.J. & Dirks R.W. 2009. Telomeric DNA mediates de novo PML body formation. *Mol. Biol. Cell* **20**, 4804-4815
- Brown J.M., Green J., Pires das Neves R., Wallace H.A.C., Smith A.J.H., Hughes J., Gray N., Taylor S., Wood W.G., Higgs D.R., Iborra F.J. & Buckle V.J. 2008. Association between active genes occurs at nuclear speckles and is modulated by chromatin environment. *J. Cell Biol.* **182**, 1083-1097
- Chen Y.C., Kappel C., Beaudouin J., Eils R. & Spector D.L. 2008. Live cell dynamics of promyelocytic leukemia nuclear bodies upon entry into and exit from mitosis. *Mol. Biol. Cell* **19**, 3147–3162
- Ching R.W., Dellaire G., Eskiw C.H. & Bazett-Jones D.P. 2005. PML bodies: a meeting place for genomic loci? *J. Cell Sci.* **118**, 847-854
- Chubb J.R., Boyle S., Perry P. & Bickmore W.A. 2002. Chromatin motion is constrained by association with nuclear compartments in human cells. *Curr. Biol.* **12**, 439-445
- Conlan A.L., McNeese C.J. & Heierhorst J. 2004. Proteasome-dependent dispersal of PML nuclear bodies in response to alkylating DNA damage. *Oncogene* **23**, 307–310
- Dellaire G. B & Bazett-Jones D.P. 2004. PML nuclear bodies: dynamic sensors of DNA damage and cellular stress. *Bioessays* **26**, 963-77
- Dirks R.W., de Pauw E.S. & Raap A.K. 1997. Splicing factors associate with nuclear HCMV-IE transcripts after transcriptional activation of the gene, but dissociate upon transcription inhibition: evidence for a dynamic organization of splicing factors. *J. Cell Sci.* **110**, 515–522
- Eskiw C.H., Dellaire G., Mymryk J.S. & Bazett-Jones D.P. 2003. Size, position and dynamic behavior of PML nuclear bodies following cell stress as a paradigm for supramolecular trafficking and assembly. *J. Cell Sci.* **116**, 4455-4466
- Eskiw, C.H., Dellaire, G. & Bazett-Jones, D.P. 2004. Chromatin contributes to structural integrity of promyelocytic leukemia bodies through a SUMO-1-independent mechanism. *J. Biol. Chem.* **279**, 9577-9585
- Görisch S. M., Wachsmuth M., Ittrich C., Bacher C.P., Rippe K. & Lichter P. 2004. Nuclear body movement is determined by chromatin accessibility and dynamics. *Proc. Natl. Acad. Sci. USA* **101**, 13221-13226

- Gialitakis M., Arampatzi P., Makatounakis T. & Papamatheakis J. 2010. Gamma Interferon-dependent transcriptional memory via relocalization of a gene locus to PML nuclear bodies. *Mol. Cell. Biol.* **30**, 2046-2056
- Hall L.L., Smith K.P., Byron M., Lawrence J.B. 2006. Molecular anatomy of a speckle. *The Anatomical record part A* **288A**, 664–675
- Hattinger, C.M., A.G. Jochemsen, H.J. Tanke & R.W. Dirks. 2002. Induction of p21 mRNA synthesis after short-wavelength UV light visualized in individual cells by RNA FISH. *J. Histochem. Cytochem.* **50**, 81–89
- Kieβlich A., von Mikecz A. & Hemmerich P. 2002. Cell cycle-dependent association of PML bodies with sites of active transcription in nuclei of mammalian cells. *J. Struct. Biol* **140**, 167–179
- Kumar P.P., Bischof O., Purbey P.K., Notani D., Urlaub H., Dejean A. & Galande S. 2007. Functional interaction between PML and SATB1 regulates chromatin-loop architecture and transcription of the MHC class I locus. *Nat. Cell Biol.* **9**, 45-56
- Lam Y.W., Lyon C.E. & Lamond A.I. 2002. Large-scale isolation of Cajal Bodies from HeLa cells. *Mol. Biol. Cell.* **13**, 2461-2473
- Lee M.-Y., Kim M.-A., Kim H.-J., Bae Y.-S., Park J.-I., Kwak J.-Y., Chung J.H. & Yun J. Alkylating agent methyl methanesulfonate (MMS) induces a wave of global protein hyperacetylation: Implications in cancer cell death. 2007. *Biochem. Biophys. Res. Commun.* **360**, 483-489
- Maul G.G., Yu E., Ishov A.M. & Epstein A.L. 1995. Nuclear domain 10 (ND10) associated proteins are also present in nuclear bodies and redistribute to hundreds of nuclear sites after stress. *J. Cell Biochem.* **59**, 498-513
- Mintz P.J., Patterson S.D., Neuwald A.F., Spahr C.S. & Spector D.L. 1999. Purification and biochemical characterization of interchromatin granule clusters. *EMBO J.* **18**, 4308-4320
- Misteli T., Caceres J.F. & Spector D. 1997. The dynamics of a pre-mRNA splicing factor in living cells. *Nature* **387**, 523-527
- Molenaar C., Wiesmeijer K., Verwoerd N. P., Khazen S., Eils R., Tanke H. J. & Dirks R. W. 2003. Visualizing telomere dynamics in living mammalian cells using PNA probes. *EMBO J.* **22**, 6631–6641
- Molenaar C., Abdulle A., Gena A., Tanke H.J. & Dirks R.W. 2004. Poly(A)<sup>+</sup> RNAs roam the cell nucleus and pass through speckle domains in transcriptionally active and inactive cells. *J. Cell Biol.* **165**, 191-202
- Muratani M., Gerlich D., Janicki S.M., Gebhard M., Eils R. & Spector D.L. 2002. Metabolic-energy-dependent movement of PML bodies within the mammalian cell nucleus. *Nat. Cell Biol.* **4**, 106–110
- O'Keefe R.T., Mayeda A., Sadowski C.L., Krainer A.R. & Spector D.L. 1994. Disruption of pre-mRNA splicing in vivo results in reorganization of splicing factors. *J. Cell Biol.* **124**, 249-260



## Nuclear body movement is constrained by associations with chromatin

Paik W.K., Dimaria P., Kim S., Magee P.N. & Lotlikar P.D. 1984. Alkylation of protein by methyl methanesulfonate and 1-methyl-1-nitrosourea in vitro. *Cancer Letters* **23**, 9-17

Platani M., Goldberg I., Lamond A.I. & Swedlow J.R. 2002. Cajal Body dynamics and association with chromatin are ATP-dependent. *Nat. Cell Biol.* **4**, 502-508

Post J.N., Lidke K.A., Rieger B. & Arndt-Jovin D.J. 2005. One—and two-photon photoactivation of a paGFP-fusion protein in live *Drosophila* embryos. *FEBS Lett.* **579**, 325–330

Schmidt U., Richter K., Berger A.B. & Lichter P. 2006. In vivo BiFC analysis of Y14 and NXF1 mRNA export complexes: preferential localization within and around SC35 domains. *J. Cell Biol.* **172**, 373-381

Sharma P., Murillas R., Zhang H. & Kuehn M.R. 2010. N4BP1 is a newly identified nucleolar protein that undergoes SUMO-regulated polyubiquitylation and proteasomal turnover at promyelocytic leukemia nuclear bodies. *J. Cell Sci.* **123**, 1227-1234

Snaar S., Wiesmeijer K., Jochemsen A.G., Tanke H.J. & Dirks R.W. 2000. Mutational analysis of fibrillarin and its mobility in living human cells. *J. Cell. Biol.* **151**, 653-662

Stanek D. & Neugebauer K.M. 2006. The Cajal body: a meeting place for spliceosomal snRNPs in the nuclear maze. *Chromosoma* **115**, 343–354

Wiesmeijer K., Krouwels I.K., Tanke H.J. & Dirks R.W. 2008. Chromatin movement visualized with photoactivable GFP-labeled histone H4. *Differentiation* **76**, 83–90

Wiesmeijer K., Molenaar C., Bekeer I.M.L.A., Tanke H. J. & Dirks R.W. 2002. Mobile foci of SP100 do not contain PML: PML bodies are immobile but PML and SP100 proteins are not. *J. Struct. Biol.* **140**, 180–188

Yeager T.R., Neumann A.A., Englezou A., Huschtscha L.I., Noble J.R. & Reddel R.R. 1999. Telomerase-negative immortalized human cells contain a novel type of promyelocytic leukemia (PML) body. *Cancer Res.* **59**, 4175-4179

## Figures

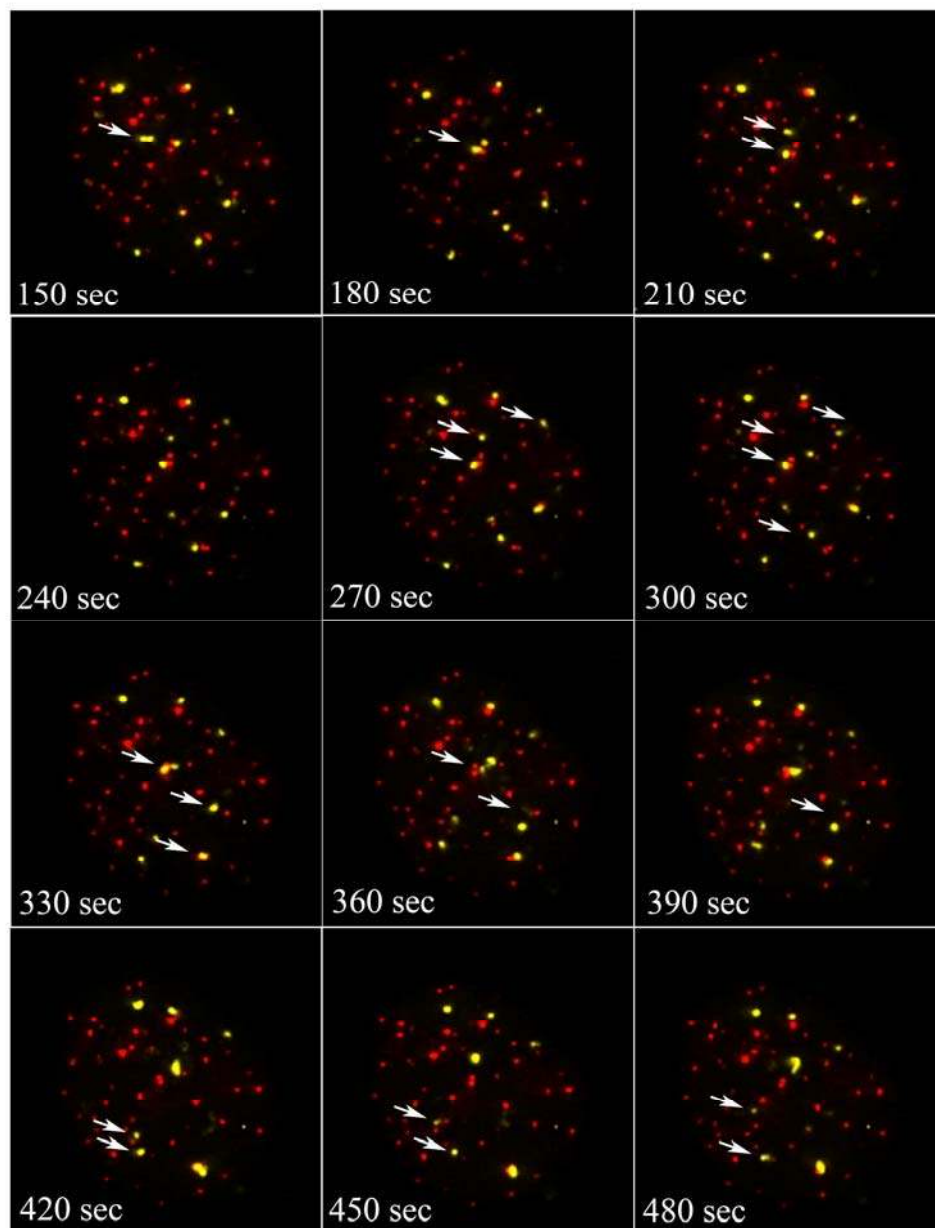


**Figure 1.** PML/TRF1 dynamics are shown in U2OS cells transfected with EYFP PML and DsRed TRF1 and subsequently treated with MMS for 2 hours. PML bodies are more dynamic than telomeres and fuse with other PML bodies and with telomeres. Dynamic or fusing PML bodies are indicated by arrows.

## Nuclear body movement is constrained by associations with chromatin

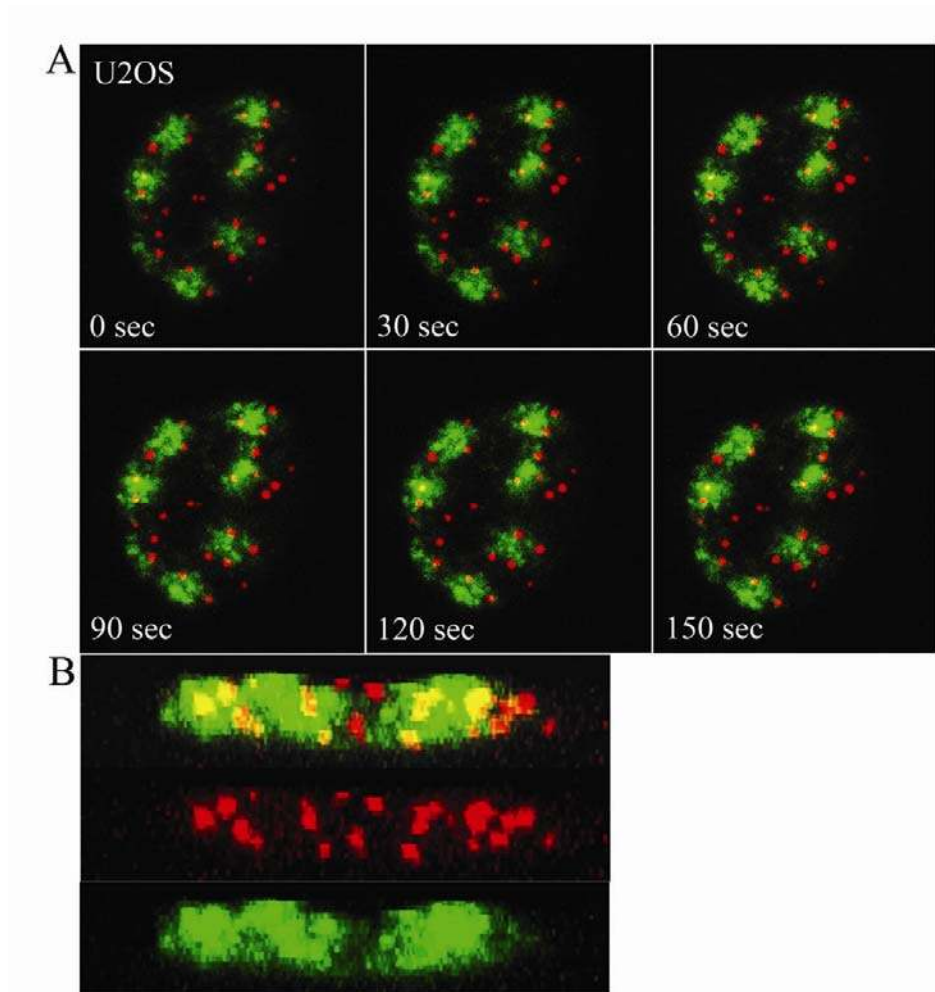


**Figure 2** A) Dynamics of PML bodies are shown in untreated U2OS cells. Photoactivatable Histone4 (H4-PAGFP) was used as a marker for chromatin and DsRed-PML-I was used as a marker for PML bodies. H4-PAGFP was photoactivated around PML bodies using the 405 nm laser on a SP5 confocal microscope. DsRed-PML-I together with photoactivated histone H4-PAGFP surrounding these bodies show a similar slow mobility. Images were acquired with 2-4% laser power, 400 Hz scanning frequency and 512 \* 512 pixels per frame. B) A side-view of the 15-25 Z-stack slices (thickness 0.4  $\mu\text{m}$ ) of the same cell is shown, time step  $t=0$  seconds.

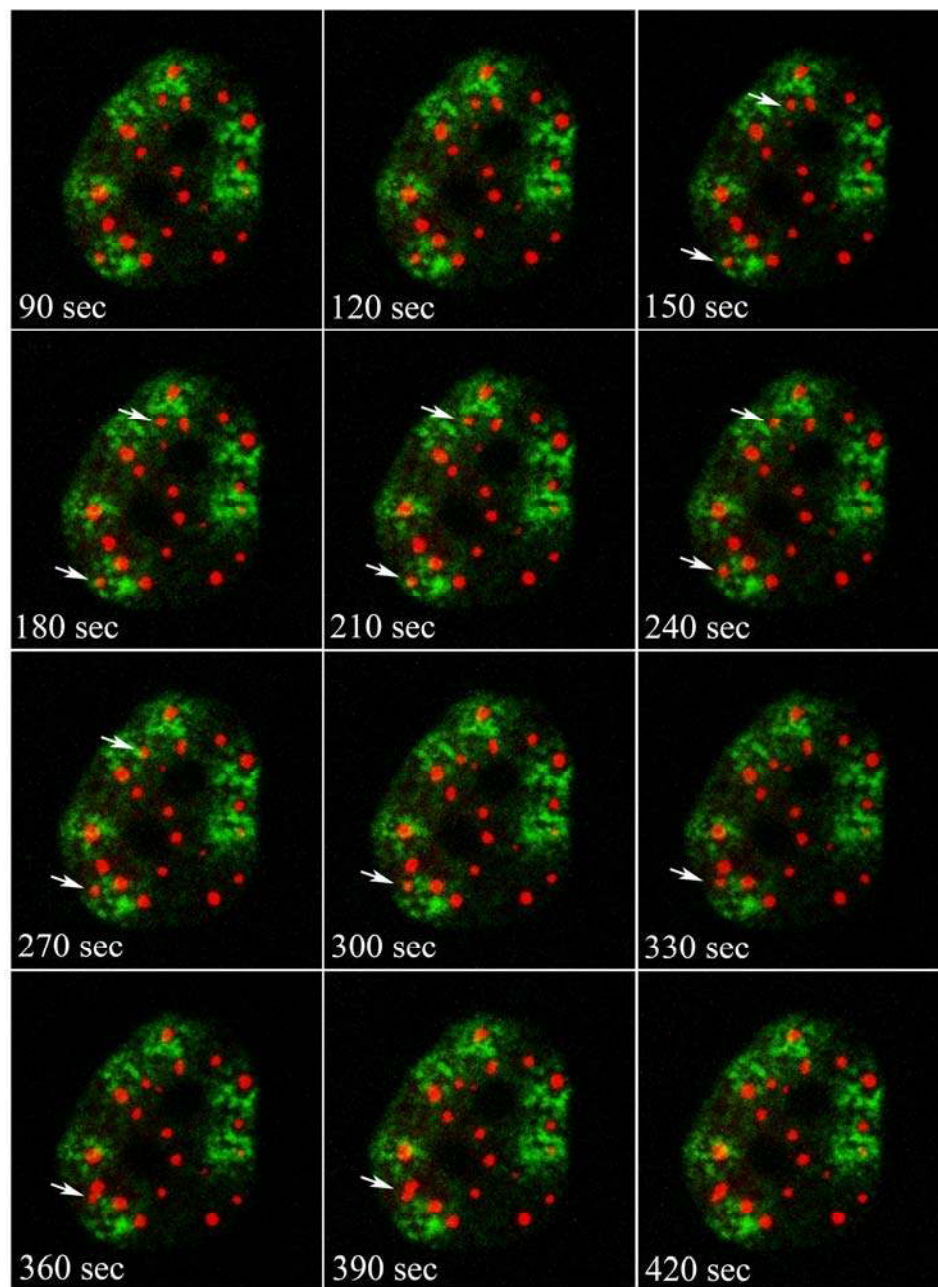


**Figure 3A.** H4-PAGFP surrounding PML bodies was photoactivated using the 405 nm laser on a SP5 confocal microscope after 2 hours of MMS treatment. Arrows indicate PML bodies that lose contact with the surrounding chromatin and move away from their original positions, displaying increased dynamics compared to the photoactivated H4-PAGFP.

## Nuclear body movement is constrained by associations with chromatin

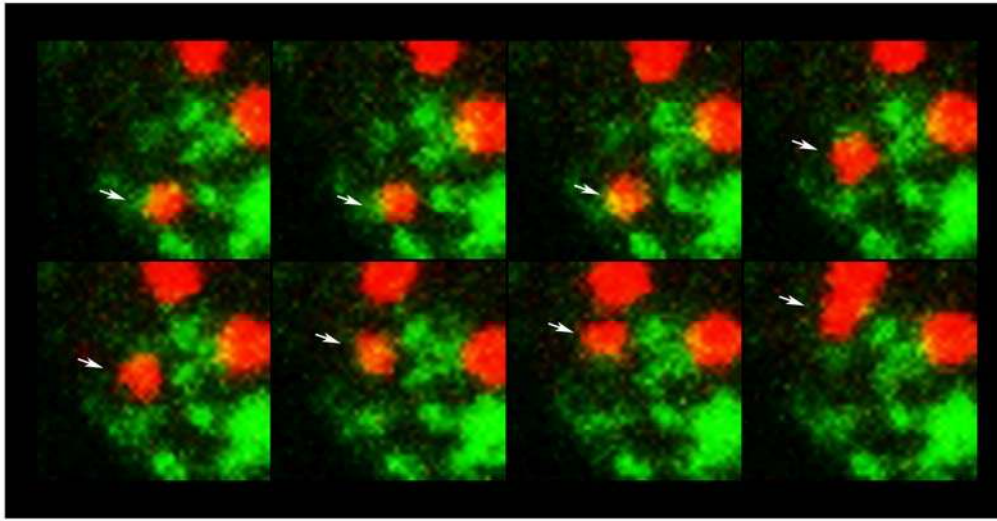


**Figure 3B.** PML bodies are dynamic after MMS treatment and lose contact with the surrounding chromatin. A section of the nucleus from figure 3A is shown at higher magnification and a PML body dissociates from the surrounding chromatin and moves away from its original position, as a result of MMS induced DNA damage.

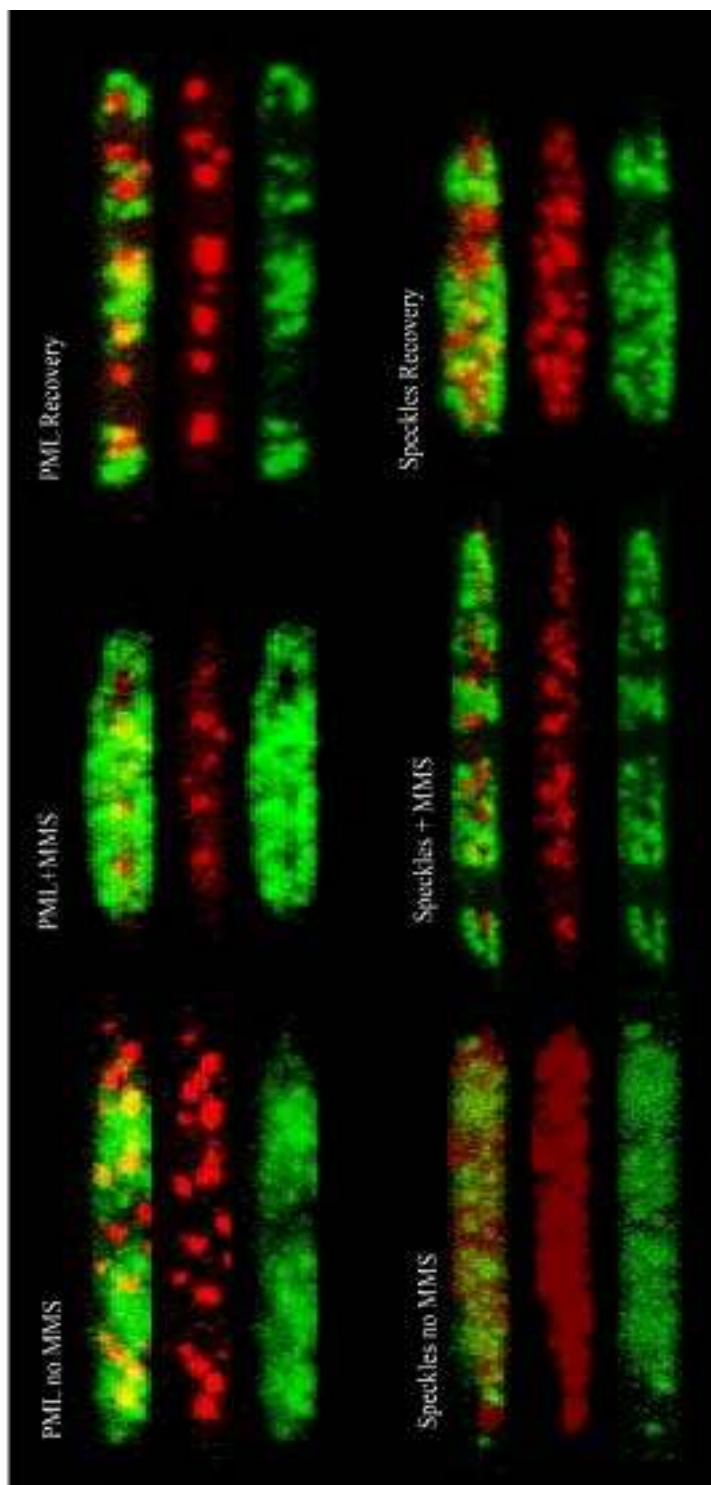


**Figure 4.** A side-view of photoactivated H4-PAGFP surrounding PML bodies, speckles and Cajal bodies using the 405 nm laser on the SP5 confocal microscope. The spatial distribution of PML bodies appears changed from being positioned throughout the 3D nuclear volume in untreated cells to a more confined localization in a Z-plane located at the centre in the 3D space of the nucleus following MMS treatment.

## Nuclear body movement is constrained by associations with chromatin

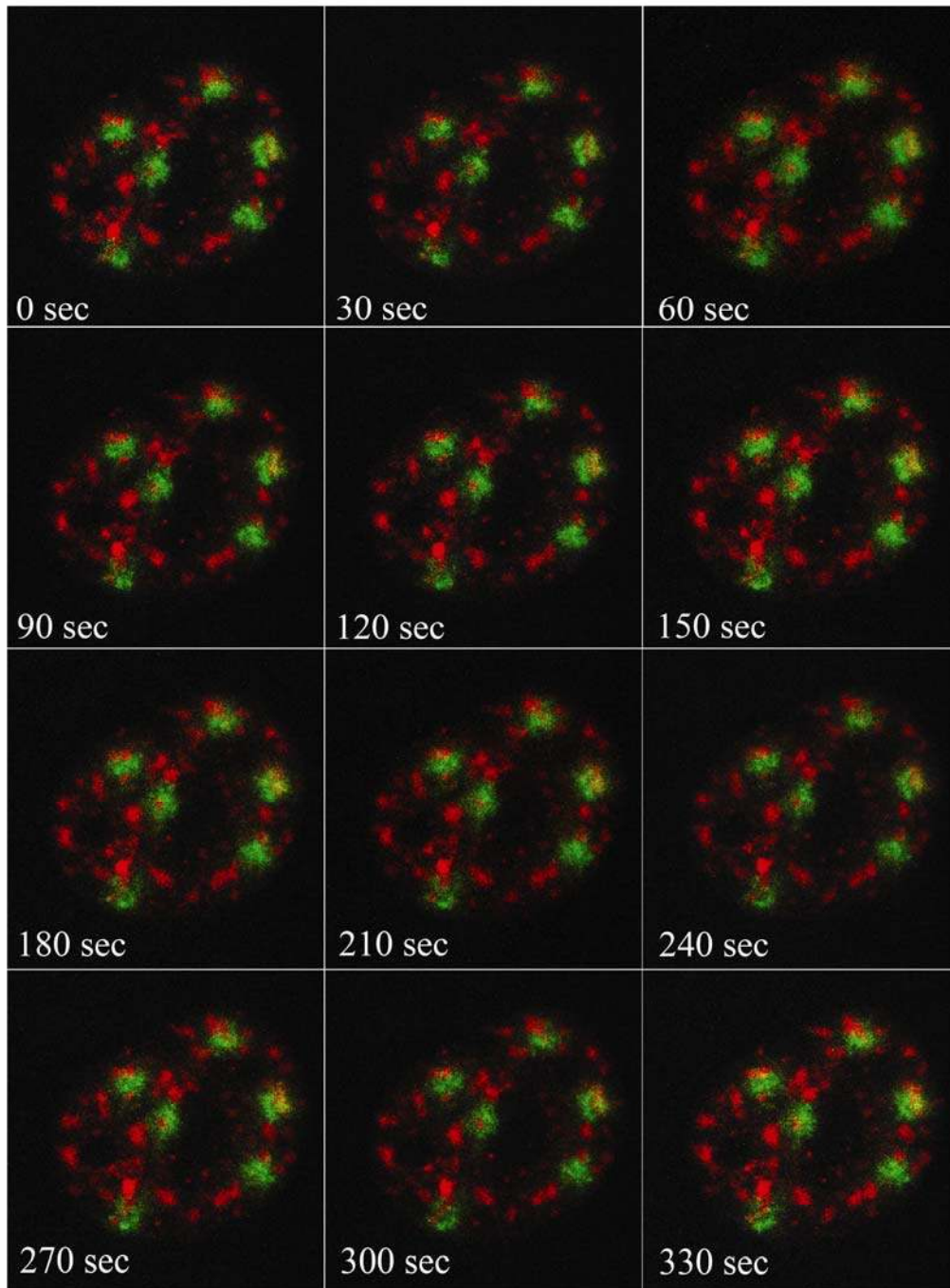


**Figure 5A.** H4-PAGFP surrounding speckles was photoactivated in U2OS cells transfected with DsRed-ASF as a marker for speckles. Chromatin regions surrounding speckles were selected and photoactivated and cells were imaged at regular time intervals for 10 minutes. Similar to PML bodies, speckles are rather immobile relative to the surrounding chromatin, suggesting that there is an interaction between speckles and the surrounding chromatin that keeps them in a fixed position.

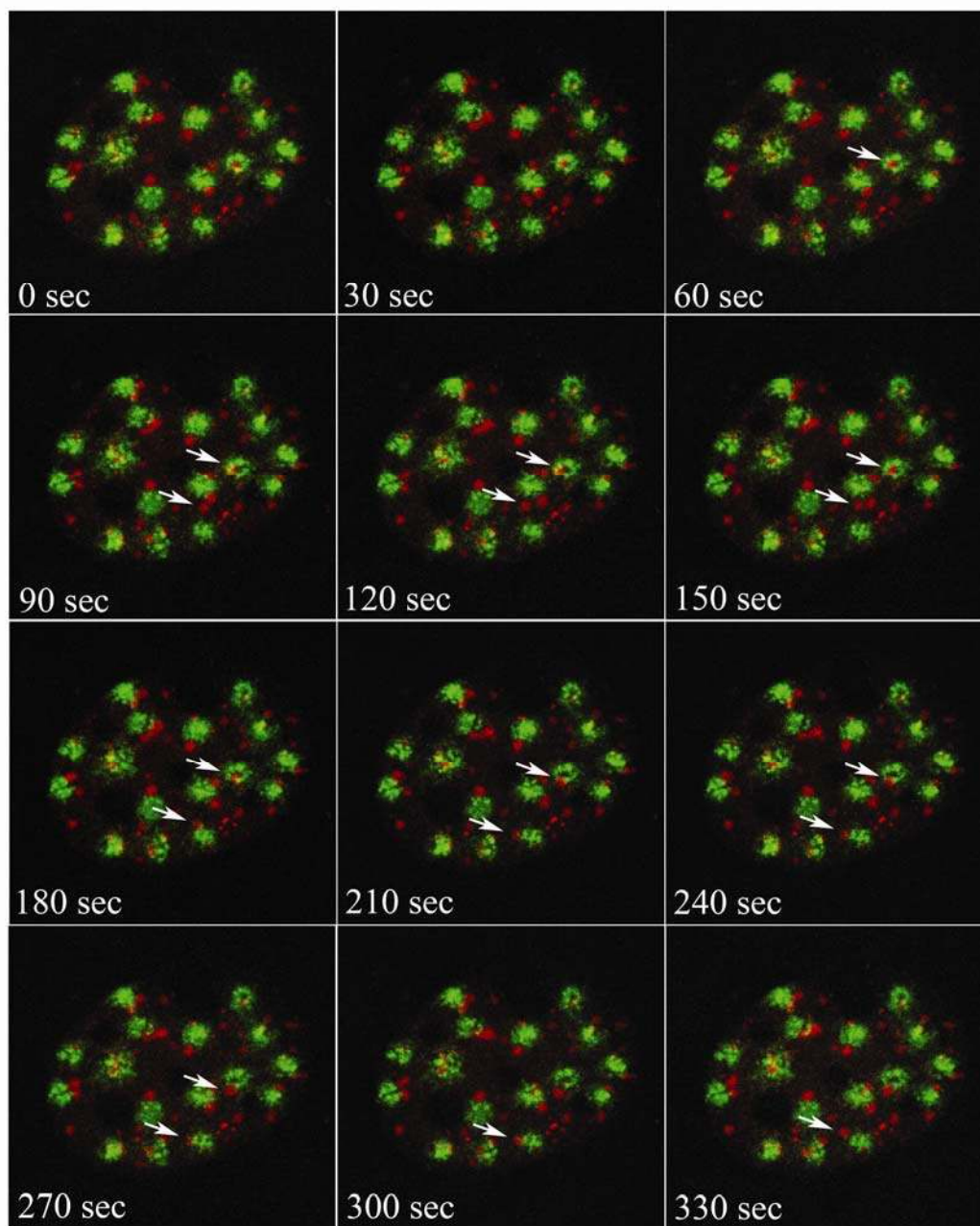


**Figure 5B.** In response to 2 hours of MMS treatment U2OS cells transfected with H4-PAGFP and DsRed-ASF show a strong increase in dynamics of speckles compared to the chromatin surrounding the speckles. Dynamic speckles that move away from their original position are indicated by arrows.



## Nuclear body movement is constrained by associations with chromatin

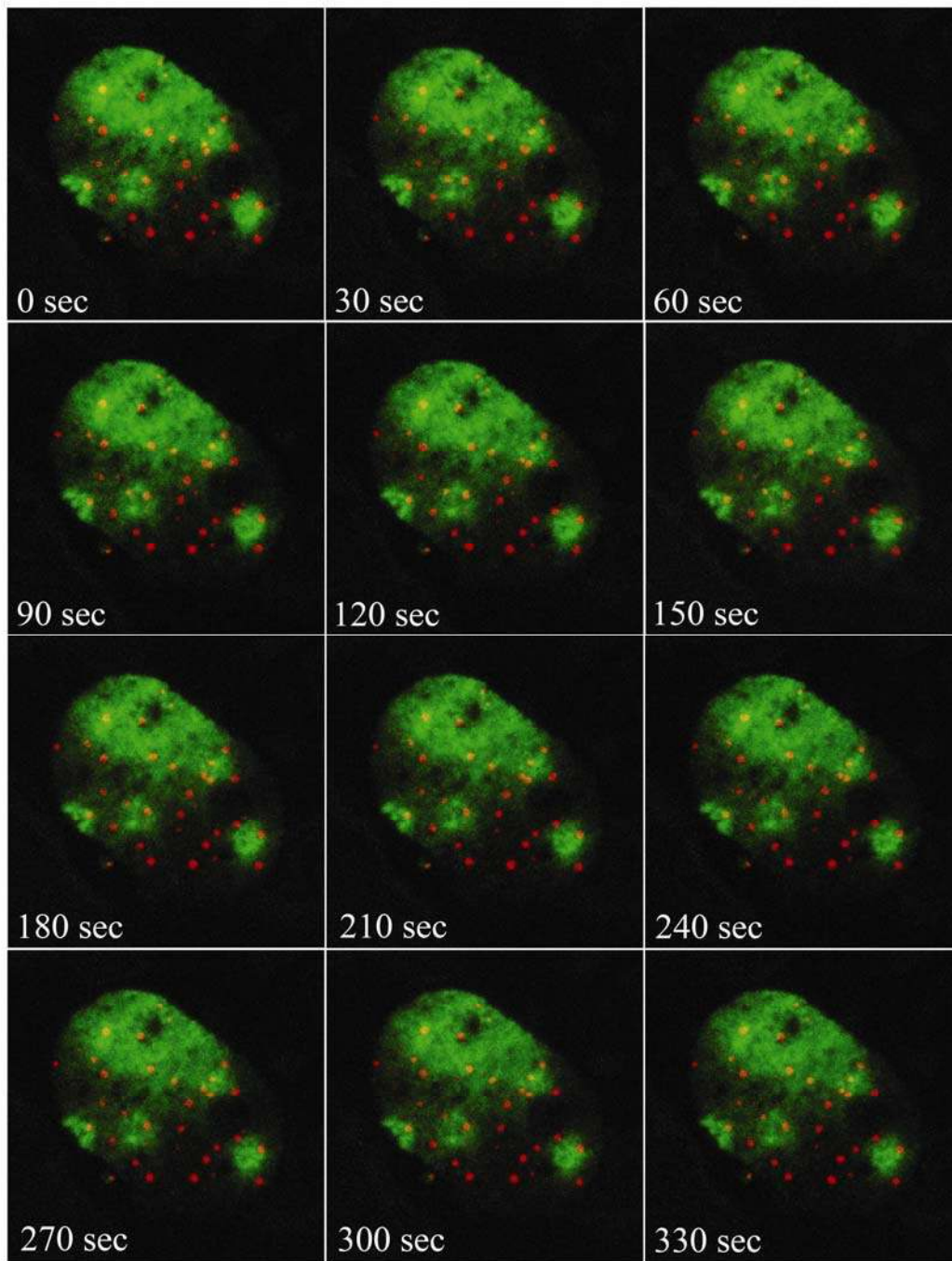


**Figure 6A.** Histon4-PA was photoactivated around Cajal bodies to study their dynamics compared to the surrounding chromatin. Similar to PML bodies and speckles, Cajal bodies are nearly immobile relative to the chromatin, suggesting that there is an interaction between the Cajal bodies and the surrounding chromatin that keeps the Cajal bodies in a fixed position.

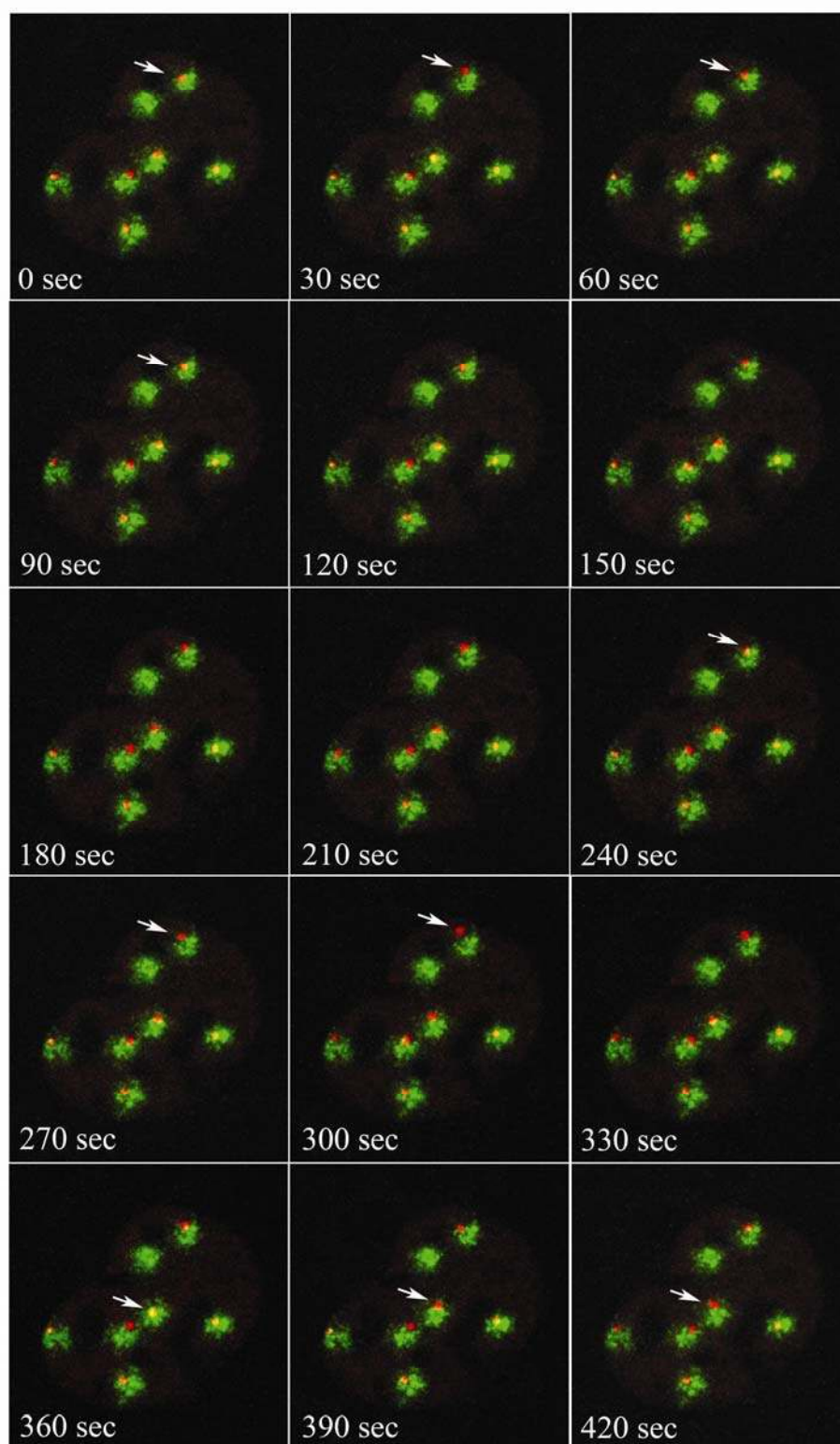


**Figure 6B.** As a response to MMS treatment Cajal bodies display increased dynamics similar to PML bodies and speckles and likewise Cajal bodies appear to lose contact with the surrounding chromatin. Dynamic Cajal bodies are indicated by arrows.



# **CHAPTER 6**

## **Summary and discussion**



## 6 Summary and discussion

The aim of this Thesis work was to gain insight into the spatio-temporal organization of the cell nucleus by using live cell imaging approaches. Chromatin domains and protein containing nuclear bodies were visualized in living cells by expressing fluorescently-tagged proteins that localize specifically to these compartments. Chromatin organization in the cell nucleus is nonrandom and its spatial organization is related to the transcriptional activity of genes. Besides chromatin, the cell nucleus contains variable numbers of different nuclear protein compartments, also referred to as nuclear bodies. These bodies are characterized by the presence of a distinct set of proteins although some proteins travel between two or more nuclear compartments. The specific protein content of nuclear bodies has linked them to various cellular activities, including transcription, RNA processing and to more general phenomena like apoptosis and senescence. Thus, the various nuclear bodies are believed to be essential in facilitating and coordinating specific nuclear activities. However, there is still a lot unknown about the underlying mechanisms that link bodies to specific nuclear activities, about the architecture of the nuclear bodies, and about the way nuclear bodies are formed. A key question is whether the spatial organization of nuclear compartments and the associated nuclear functions are supported by an underlying nuclear matrix structure. This question dominated the field of nuclear organization for many years and still remains elusive. Because the existence of a network structure resembling that of a cytoskeleton has not been demonstrated by immunocytochemistry many scientists doubt its existence in the cell nucleus. If such a structure exists it is very dynamic indeed and not comparable to the well described cytoskeleton architecture. Throughout this Thesis the term “nuclear matrix structure” has been used. By combining tools in live cell imaging, immunocytochemistry and molecular cell biology, this Thesis offers new insights in the structural organization of the cell nucleus and in the formation of one of the most intriguing nuclear bodies, the promyelocytic leukemia (PML) body.

### **Image analysis using STACKS**

In order to understand the structural organization of the cell nucleus, it is essential to study the nuclear components in living cells as these components are dynamic in nature. To describe the dynamic properties of structures that reside in the cell nucleus we developed a software program called STACKS. Despite the fact that many software packages for quantitative image analysis were already commercially or freely available, we considered it important to develop a new software program in which the possibilities for image segmentation, object tracking, distance measurement, displacement quantification and cell movement correction are all integrated. Also, the program should offer fast image processing and enable user interaction. The features of this program are described in detail in chapter 2 and illustrated by describing the dynamic behavior of telomeres in normal as well as in tumor cells in different phases of the cell cycle. In general, when studying the dynamic behavior of structures inside the cell nucleus it is important to know whether this behavior is related to a specific cell cycle stage. For example, it has been shown in yeast, in which a centromere, a telomere, and an internal chromatin site were fluorescently tagged, that the internal chromatin loci moved more rapidly and over larger distances in G<sub>1</sub>- and S-phase as compared to the other stages of the cell cycle (Heun et

## Summary and discussion

al., 2001). Smaller, saltatory movements ( $<0.2 \mu\text{m}$ ) were shown throughout interphase in both yeast and flies (Heun et al., 2001). Analysis of telomere movement by the STACKS program confirmed observations that telomeres move faster in G1 cells as compared to cells in other cell cycle stages. This was also expected because when cells exit from mitosis chromatin is unfolding and moves to its favored position in the cell nucleus.

As mentioned, the STACKS program contains various options for quantitative data processing and image transformations, which are not offered by the commercial software that comes with most wide-field and confocal microscopes. Because image analysis operations become complex and have to be performed on large data sets computation time is an issue. For this reason, the STACKS program allows GPU processing using the GPU processor of the video board. A direct comparison of image operations based on CPU and on GPU processing showed that GPU processing indeed greatly increases processing speed, which is necessary when large 4D image data sets have to be analyzed. The STACKS program is able to operate directly on data formats as produced by the commercial microscope systems, and has a convenient user interface. Furthermore, STACKS provides feedback on each operating step and offers great flexibility in order to cope with various cell types and images of varying quality or intensity. As research questions can be diverse, STACKS has been developed in a way that additional software tools can easily be added to the program, creating great flexibility for the user. In conclusion, STACKS is a major step ahead for scientists who wish to track and quantify the movements of objects in living cells or the movements of entire cells in cell or tissue cultures. In the coming years, the STACKS program will be developed further by adding specific applications to facilitate a broad spectrum of research questions.

### **Telomeres anchor at a protein complex containing lamin A/C, emerin and actin**

In chapter 3 of this thesis the program STACKS is used to answer the question whether telomeres are associated with a nuclear matrix structure. To this end, cells have been incubated with shRNAs or drugs to disturb the nuclear matrix structure and movements of fluorescently labeled telomeres have been measured. Previous studies indicated that the movement of telomeres is constrained in the cell nucleus. In yeast, this constrained movement was explained by the attachment of telomeres to the inner nuclear membrane by the Ku and Sir proteins (Hediger et al., 2002). In human cells, however, telomeres are supposed to be associated to an inner nuclear matrix structure as they are not removed from cell nuclei after extensive extraction procedures that remove all soluble proteins and most DNA. Because this retention of telomeres could be an artifact of the extraction procedure, we wished to investigate whether a selective reduction of potential nuclear matrix proteins would increase the dynamics of telomeres by a lack of anchorage sites. RNA interference and specific drugs have been used to knock down or disturb proteins that are thought to be members of the nuclear matrix structure. We quantified the dynamics of telomeres using the program STACKS and found that latrunculin A-induced depolymerization of actin filaments resulted in an increase in telomere dynamics. Also a reduction of lamin A/C or emerin expression by RNA interference was shown to increase telomere dynamics. Although lamin B2 is also a constituent of the nuclear lamina structure, a reduction of lamin B2 did not result in an increase in telomere dynamics. These observa-

tions suggest that in mammalian cells telomeres are attached to a complex containing lamin A/C, emerin and actin proteins. Although lamin A/C and actin have been found present in the nucleoplasm, these findings raise many interesting questions. More experiments are needed to determine whether the association of telomeres with this complex is direct or indirect. Also, biochemical experiments need to be performed to address the full composition of the protein complex telomeres are attached to. Furthermore, it needs to be investigated whether telomeres are the only genomic regions that are anchored to lamin A/C containing protein complexes. These are important issues because dysfunctional telomeres and mutations in lamin proteins are associated with ageing and age-related diseases (Cooke & Smith, 1986; Merideth et al., 2008). Consistent with our observations, an increase in telomere mobility has been measured recently in fibroblasts derived from a patient carrying a mutation in lamin A (Vos et al., 2010).

### **A role for telomeres in *de novo* PML body formation**

Besides chromatin, the cell nucleus contains nuclear bodies that vary in protein composition, number and shape. Knowledge about the function of these bodies is steadily increasing but still little is known about the mechanisms that lead to their formation. In chapter 4 the *de novo* formation of PML nuclear bodies is described. PML bodies disperse after treatment with the (DNA) alkylating agent methylmethane sulfonate (MMS) but reassemble when MMS is absent. Surprisingly, it was observed that PML bodies formed at telomeric DNA of U2OS cells and similar results were obtained in mouse embryonic fibroblasts. Also in cells that were derived from a patient suffering from acute promyelocytic leukemia and lack intact PML bodies we observed that expression of PML protein or treatment with arsenic trioxide resulted in the formation of PML bodies at telomeric sequences. The reason why the nucleation of PML bodies occurs at telomeres is currently not known. Initial experiments indicate that SUMO modification of telomere binding proteins might be involved. It was observed that SMC5, a component of the SUMO ligase MMS21-containing SMC5/6 complex, localizes temporarily at telomeric DNA during PML body formation. Obviously, this observation needs additional experimental support. A knockdown of SMC5/6 may confirm that the localization of this protein at telomeres is essential for PML body formation. Furthermore, it should be clarified which telomere binding proteins are sumoylated. Initial experiments were not conclusive. Knockdown of SMC5 by siRNAs prevented the formation of PML nuclear bodies after MMS treatment, but not in all cells. Furthermore, it needs to be investigated whether a reduction of SMC5 leads to a stress response preventing PML body formation. These and other experiments may unravel the mechanism by which PML bodies are formed *de novo*. This knowledge is important because PML bodies have been implicated in virus replication, monogenic transformation, cellular stress and senescence and could possibly play a role in age related disorders.

### **Chromatin is intimate with nuclear bodies**

Nuclear bodies are positioned in the interchromatin space and an intermingling of chromatin with nuclear bodies, with exception of the nucleolus, has not been reported thus far. Nevertheless, nuclear bodies show in general little movement in the nucleus which might suggest that they interact with chromatin at their surface. Indeed, specific genomic regions have been shown to be associated with PML bodies, Cajal bodies or speckles. In



## Summary and discussion

chapter 5 it is shown that during MMS treatment nuclear bodies become more dynamic in the cell nucleus while the dynamic behavior of chromatin is not altered. This suggests that due to MMS induced alkylating DNA damage, the interaction between nuclear bodies and chromatin is lost. To analyze the interaction of chromatin with nuclear bodies, cells have been cotransfected with constructs expressing different fluorescent marker proteins. One is a fluorescent fusion protein that localizes to a nuclear body and the other is a photoactivatable variant of GFP (PA-GFP) fused to a histone protein that is incorporated into chromatin. By selective activation of PA-GFP-histone proteins using 405 nm laser light the chromatin that surrounds nuclear bodies could be visualized selectively and tracked in time. The time-lapse images show clearly that nuclear bodies lose their contact with chromatin as a result of MMS treatment, suggesting that nuclear bodies are usually intimately connected with chromatin. What this means in functional terms has to be clarified yet. Recent work suggests that speckles function as nuclear hubs that connect various chromatin regions in order to facilitate and coordinate gene expression. Also, it is possible that some nuclear bodies are for their structural integrity dependent on chromatin.

### **A view of the cell nucleus at high resolution**

Important insights in the spatial-temporal organization of the cell nucleus have mainly been obtained using wide-field fluorescence microscopy and fluorescence laser scanning confocal microscopy providing a spatial resolution in xy of about 200-300 nm and in z of about 500 nm. Using these imaging systems, detailed structural information about nuclear bodies and the way they interact with chromatin cannot be obtained. Electron microscopy offers the highest spatial resolution but its application in the study of nuclear bodies has been limited. The main reason is that the bodies show little or no contrast in standard EM preparations and as such cannot be identified. Immunogold labeling techniques have been used to identify nuclear bodies but the labeling is often poor and provides little architectural detail. One exception is the nucleolus whose architecture has mainly been resolved by EM studies.

Fascinating possibilities concerning high resolution imaging lay ahead with the development of high resolution optical imaging systems. Among others, important innovations have been developed by Stefan Hell by introducing Stimulated Emission Depletion (STED) microscopy, a technique that uses the non-linear de-excitation of fluorescent dyes to overcome the resolution limit imposed by diffraction with standard confocal laser scanning microscopes and conventional far-field optical microscopes (Hell et al., 1994). The resolution of a confocal scanning microscope is limited to the spot size to which the excitation spot can be focused. STED microscopy reduces the size of the excitation spot by using a short excitation pulse that is directly followed by a doughnut-shaped depletion pulse that acts only on excited dye molecules at the periphery of a spot and quenches them. As a result the fluorescence at the center of the doughnut remains unaffected and a 12-fold increase in spatial resolution can be obtained (Donnert et al., 2006). In addition to STED, Stefan Hell also pioneered 4Pi microscopy using two objective lenses opposing each other reaching an axial resolution of about 100 nm. The impact that high resolution microscopy can have on elucidating nuclear body architecture has recently been demonstrated by elucidating the ultrastructure of PML bodies using 4Pi fluorescence laser scanning microscopy (Lang et al., 2010). It was shown that the PML bodies consist

of a sphere having a 50 – 100 nm thick shell of PML and Sp100 proteins and that telomeric repeat DNA and HP1 was found positioned inside the PML bodies.

Forthcoming high resolution microscopy techniques are photo-activated localization microscopy (PALM) (Hess et al., 2006; Egner et al., 2007), a similar technique called stochastic optical reconstruction microscopy (STORM) (Betzig et al., 2006) and structured illumination microscopy (SIM) (Gustafsson, 2005). In PALM/STORM the imaging area is filled with many dark fluorophores that can be photoactivated into a fluorescing state by a flash of light. Because photoactivation is stochastic, only a few well separated molecules will "turn on." Then Gaussians are fit to their PSFs at high precision. After the few bright dots photobleach, another flash of the photoactivating light again activates a random collection fluorophores, and the PSFs that belong to these well spaced objects are determined. This process is repeated many times, building up an image molecule-by-molecule; and because the molecules were activated at different times, the precise localization of all fluorophores can be accurately determined by calculating their centers of mass. The result is that the resolution of the final image can be much higher than that limited by diffraction. With the PALM/STORM technique a resolution of 25 nm can be reached (Betzig et al., 2006; Rust et al., 2006). The image formation in SIM is based on the illumination of samples with patterned light resulting in interference patterns from which a multicolor high 3D (100 nm) resolution image can be reconstructed (Schermetzsch et al., 2008). The main limitation of the PALM/STORM technique is that it is, like other high resolution imaging techniques, less suitable for analyzing dynamic structures in living cells. It is expected, however, that image acquisition and reconstruction will become much faster in the near future making PALM/STORM systems ideal tools for live cell imaging at high resolution. In this respect, faster image reconstruction software has been developed recently providing a 20-fold enhancement of the analysis routine (Hedde et al., 2009). The limitation that PALM/STORM imaging could be achieved in 2D only has been solved recently in a way that high resolution 3D images of cells can be obtained (Huang et al., 2008).

It should be mentioned that also correlative light-electron microscopy is a rapidly evolving field allowing the examination of fluorescently labeled objects in cells at nanometer-scale EM resolution. Currently, this approach is mainly used for analyzing complex structures in the cytoplasm of cells but it is in principle also applicable to structures that reside inside the cell nucleus (Lang et al., 2010). It is expected that with the rapid development of high, also mentioned super, resolution microscopy more detailed information about the structural organization of the cell nucleus will be obtained. This detailed knowledge about the structure of nuclear compartments is of crucial importance to understand the architecture of chromatin and nuclear bodies better, as well as the functional processes that are associated with these structures and dictate cellular function and behavior.

## References

- Heun P., Laroche T., Shimada K., Furrer P., Gasser S.M. 2001. Chromosome Dynamics in the Yeast Interphase Nucleus. *Science* **294**, 2181-2186
- Hediger F., Neumann F.R., van Houwe G., Dubrana K. & Gasser S.M. 2002. Live imaging of telomeres: Ku and Sir proteins define redundant telomere-anchoring pathways in yeast. *Curr. Biol.* **12**, 2076-2089
- Cooke H.J. & Smith B.A. 1986. Variability at the telomeres of the human X/Y pseudoautosomal region. *Cold Spring Harb. Symp. Quant. Biol.* **51**, 213–219
- Merideth M.A., Gordon L.B., Clauss S., Sachdev V., Smith A.C.M., Perry M.B., Brewer C.C., Zalewski C., Kim H.J., Solomon B., Brooks B.P., Gerber L.H., Turner M.L., Domingo D.L., Hart T.C., Graf J., Reynolds J.C., Gropman A., Yanovski J.A., Gerhard-Herman M., Collins F.S., Nabel E.G., Cannon, III, R.O., Gahl W.A. and Introne W.J. 2008. Phenotype and Course of Hutchinson–Gilford Progeria Syndrome. *N. Engl. J. Med.* **358**, 592–604
- De Vos W.H., Houben F., Hoebe R.A., Hennekam R., van Engelen B., Manders E.M.M., Ramaekers F.C.S, Broers J.L.V. and Van Oostveldt P. 2010. Increased plasticity of the nuclear envelope and hypermobility of telomeres due to the loss of A–type lamins. *Biochim. Biophys. Acta.* **4**, 448-458
- Hell S.W., Wichmann J. 1994. Breaking the diffraction resolution limit by stimulated emission: stimulated-emission-depletion fluorescence microscopy. *Opt. Lett.* **19**, 780-782
- Donnert G., Keller J., Medda R., Andrei M.A., Rizzoli S.O., Luhrmann R., Jahn R., Eggeling C., & Hell S.W. 2006. Macromolecular-scale resolution in biological fluorescence microscopy. *Proc. Natl. Acad. Sci. USA* **103**, 11440-11445
- Lang M., Jegou T., Chung I., Richter K., Munch S., Udvarhelyi A., Cremer C., Hemmerich P., Engelhardt J., Hell S.W. & Rippe K. 2010. Three-dimensional organization of promyelocytic leukemia nuclear bodies. *J. Cell Sci.* **123**, 392-400
- Hess S.T., Girirajan T.P.K. & Mason M.D. 2006. Ultra-High resolution imaging by fluorescence photoactivation localization microscopy. *Biophys. J.* **91**, 4258-4272
- Egner A., Geisler C., von Middendorff C., Bock H., Wenzel D., Medda R., Andresen M., Stiel A.C., Jakobs S., Eggeling C., Schönle A., Hell S.W. 2007. Fluorescence nanoscopy in whole cells by asynchronous localization of photoswitching emitters. *Biophys. J.* **93**, 3285–3290
- Betzig E., Patterson G.H., Sougrat R., Wolf Lindwasser O., Olenych S., Bonifacino J.S., Davidson M.W., Lippincott-Schwartz J. & Hess H.F.. 2006. Imaging intracellular fluorescent proteins at nanometer resolution. *Science* **313**, 1642 -1645
- Gustafsson M.G.L. 2005. Nonlinear structured-illumination microscopy: Wide-field fluorescence imaging with theoretically unlimited resolution. *Proc. Natl. Acad. Sci. USA* **102**, 13081-13086
- Rust M.J., Bates M. & Zhuang X. 2006. Sub-diffraction-limit imaging by stochastic optical reconstruction microscopy (STORM). *Nat. Methods* **3**, 793-796

Schermelleh L., Carlton P.M., Haase S., Shao L., Kner W.L., Burke B., Cardoso C.M., Agard D.A., Gustafsson M.G.L, Leonhardt H. & Sedat J.W. 2008. Subdiffraction multicolor imaging of the nuclear periphery with 3D structured illumination microscopy. *Science* **320**, 1332-1336

Hedde P.N., Fuchs J., Oswald F., Wiedenmann J. & Nienhaus G.U. 2009. Online image analysis software for photoactivation localization microscopy. *Nat. Methods* **6**, 689 - 690

Huang B., Wang W., Bates M. & Zhuang X. 2008. Three-dimensional super-resolution imaging by stochastic optical reconstruction microscopy. *Science* **319**, 810–813

Lang M., Jegou T., Chung I., Richter K., Münch S., Udvarhelyi A., Cremer C., Hemmerich P., Engelhardt J., Hell S.W. & Rippe K. 2010. Three-dimensional organization of promyelocytic leukemia nuclear bodies. *J. Cell Sci.* **123**, 392-400



## **Nederlandse samenvatting**



## Nederlandse samenvatting

Eukaryotische cellen bevatten een celkern welke in hoge mate georganiseerd is. De celkern bevat naast genetische informatie, in de vorm van chromatine, verschillende kernlichaampjes die in grootte, aantal, samenstelling en functie van elkaar verschillen. De ruimtelijke organisatie van chromatine en eiwitten in de celkern is van groot belang voor de regulatie en coördinatie van de verschillende processen die in de celkern plaatsvinden. Naast genexpressie gaat het hierbij om DNA replicatie, DNA schadeherstel, RNA processing en RNA transport. Chromatine, een complex van DNA en eiwitten, is in meerdere (heterochromatine) of mindere (euchromatine) mate opgevouwen in de celkern. Opmerkelijk is dat ieder chromatinemolecuul (chromosoom) een concrete plek in de celkern inneemt en dat deze chromosoomdomeinen elkaar niet of slechts in geringe mate overlappen. Het is vooral in de ruimte tussen de chromosoomdomeinen waar zich de verschillende kernlichaampjes bevinden en waar transport van grote complexen plaats kan vinden. Men denkt dat door compartimentalisatie van celkerncomponenten vooral de efficiëntie van processen die in de kern plaatsvinden verhoogd wordt. Om tijdig in te kunnen springen op veranderende omstandigheden waarin een cel zich bevindt, is de organisatie van de celkern dynamisch.

Voorbeelden van kernlichaampjes zijn Cajal lichaampjes, speckles, PML lichaampjes en nucleoli. Deze kernlichaampjes zijn gepositioneerd tussen chromatinedomeinen. In tegenstelling tot de organellen in het cytoplasma van de cel zijn kernlichaampjes, ook wel kernorganellen genoemd, niet omgeven door een celmembraan. Hoe deze kernlichaampjes in de celkern gevormd worden, in stand gehouden worden en zich verplaatsen, is grotendeels onduidelijk. Verschillende onderzoeken laten een verband zien tussen een afwijkende kernorganisatie en ziekten. Een duidelijk voorbeeld hiervan is progeria, een vervroegd verouderingsyndroom, waarbij een mutatie in het lamine A/C gen leidt tot een verstoorde kernarchitectuur wat de expressie van genen beïnvloedt. Veranderingen in kernorganisatie zijn ook gekoppeld aan verschillende vormen van kanker en aan veroudering. Dit proefschrift is gewijd aan de dynamiek van verschillende structuren in de celkern.

In **hoofdstuk 2** wordt de ontwikkeling van het computerprogramma “STACKS” beschreven. Dit programma is ontworpen om de beweging van objecten in een 2-dimensionaal vlak of in een 3-dimensionale ruimte in de tijd te analyseren en te kwantificeren. De effectiviteit van het programma wordt gedemonstreerd door de beweging van telomeren, structuren welke de uiteinden van chromosomen vormen, in verschillende fasen van de celcyclus te meten. Een belangrijk aspect hierbij is dat de metingen verricht worden aan beelden die opgenomen zijn van levende cellen, die gedurende de tijd bewegen en mogelijk van vorm veranderen. In het computerprogramma zijn mogelijkheden opgenomen om te corrigeren voor bewegingen die de cel gedurende de gehele opnameperiode maakt. Voor het zichtbaar maken van de telomeren in een levende cel is een DNA construct gemaakt dat codeert voor een fusie-eiwit dat bestaat uit een telomeer-bindend eiwit (TRF) en een fluorescerend eiwit (green fluorescent protein, GFP, en varianten daarvan). Dit DNA construct is door middel van transfectie in humane tumorcellen (U2OS) en in embryonale fibroblasten van de muis gebracht om tot expressie te komen. Om cellen in ver-



schillende fasen van de celcyclus te herkennen en om de kerncontouren duidelijk zichtbaar te maken is tevens een fusie-eiwit bestaande uit een proliferatiemarker (proliferating cell nuclear antigen, PCNA) en een fluorescerend eiwit in dezelfde cellen tot expressie gebracht. De telomeren van cellen die zich in de S- of G2-fase van de celcyclus bevinden blijken een zeer beperkte bewegingsvrijheid te vertonen. Zij veranderen nauwelijks van positie gedurende de periode dat er beelden met de fluorescentiemicroscoop zijn opgenomen. Veel dynamischer zijn telomeren in cellen die zich in de G1-fase bevinden, de fase die direct volgt op de celdeling en waarin chromatine zich positioneert. Dit verschil in dynamiek werd zowel in tumorcellen als in embryonale fibroblasten van de muis gemeten, waarbij de metingen in hoge mate reproduceerbaar bleken te zijn. Het ontwikkelde beeldbewerkingprogramma blijkt dus goed te werken, waarbij opgemerkt moet worden dat het programma gebruik maakt van snelle grafische processors (GPU) om snelle beeldbewerking te bewerkstelligen. Naast snelheid zijn de belangrijke kenmerken van het programma dat alle beeldbewerkingen en metingen binnen hetzelfde programma uitgevoerd kunnen worden, wat veel tijd bespaart, en dat op ieder gewenst moment visueel beoordeeld kan worden wat het effect van een bewerking is op een te meten object (bijvoorbeeld een telomeer). Door het toekennen van een kleur aan ieder individueel object kunnen zij eenvoudig in de tijd gevolgd worden.

In **hoofdstuk 3** wordt een onderzoek beschreven naar de mogelijke rol van een nucleaire matrix bij de positionering van telomeren in de celkern. In het verleden is vastgesteld dat telomeer DNA in de celkern achterblijft wanneer eiwitten, RNA en DNA uit kernen geëxtraheerd worden. Als verklaring hiervoor werd gegeven dat telomeren aan een nucleaire matrixstructuur vast zouden zitten en zo een rol zouden spelen bij de ruimtelijke positionering van chromosomen in de celkern. Het bestaan van een nucleaire matrix is al lange tijd controversieel en het is onduidelijk waaruit deze matrixstructuur zou moeten bestaan. Van lamine-eiwitten is bekend dat zij een netwerk vormen aan de binnenzijde van de kernmembraan, maar bovendien verspreid aanwezig zijn door de gehele kern. Om te onderzoeken of deze lamine-eiwitten mogelijk betrokken zijn bij de positionering van telomeren is RNA interferentie toegepast om de expressie van de lamine-eiwitten lamine A/C, lamine B2 en het lamine-geassocieerde eiwit emerine sterk te reduceren in U2OS cellen. Daarbij is onderzocht of een sterke afname van deze eiwitten invloed heeft op de positionering en/of dynamiek van telomeren in de levende cel. Om een eventuele rol van nucleaire actinefilamenten in de positionering van telomeren te onderzoeken zijn cellen opgegroeid in aanwezigheid van een stof welke actinepolymerisatie remt. De dynamische bewegingen van de telomeren worden gekwantificeerd met het in hoofdstuk 2 beschreven computerprogramma STACKS. De resultaten laten zien dat vermindering van lamine A/C, emerine, en gepolymeriseerd actine, maar niet van lamine B2, leidt tot een toename van mobiliteit van telomeren. Dit suggereert dat telomeren verankerd liggen aan een structuur die lamine A/C, emerine en actine bevat, maar geen lamine B2. Een eventuele rol voor het eiwit lamine B1 bij de positionering van telomeren in de celkern wordt nog onderzocht.

In **hoofdstuk 4** wordt aangetoond dat telomeren een belangrijke rol spelen bij de vorming van PML lichaampjes. In U2OS en in embryonale cellen van de muis leidt blootstelling aan de DNA methylerende stof methyl methaansulfonaat (MMS) tot het uiteenvallen van PML lichaampjes. Nadat de cellen van de DNA methylering hersteld waren, blijken de PML lichaampjes zich weer te herstellen, wat ons in staat stelde om de *de novo* vorming van PML lichaampjes te bestuderen. Na verschillende structuren in de celkern onderzocht te hebben, blijkt de vorming van PML lichaampjes plaats te vinden aan telomeer DNA.

Cellen afkomstig van leukemiepatiënten (acute promyelocytische leukemie) worden getypeerd door de afwezigheid van intacte PML lichaampjes. In deze cellen is het mogelijk om de vorming van PML lichaampjes te induceren door de cellen te behandelen met ars-eentrioxide. Toediening van ars-eentrioxide is één van de behandelmethoden voor acute promyelocytische leukemie. Bij deze leukemiecellen blijken de PML lichaampjes ook aan telomeren gevormd te worden. Bovendien blijkt tijdens de vorming van PML lichaampjes een eiwit dat betrokken is bij de sumoylering van eiwitten aanwezig te zijn op telomeren. Dit doet vermoeden dat modificatie van telomeereiwitten met SUMO de vorming van PML lichaampjes initieert.

In **hoofdstuk 5** is een onderzoek beschreven naar de associatie van kernlichaampjes met chromatine. Op basis van studies waarin de dynamiek van chromatine met die van kernlichaampjes is vergeleken is geconcludeerd dat de dynamiek van kernlichaampjes beperkt wordt door de toegankelijkheid en dynamiek van chromatine, terwijl stabiele interacties met chromatine werden uitgesloten. Deze conclusie staat haaks op studies waarin associaties van PML and Cajal lichaampjes met specifieke chromatine loci waargenomen zijn. Om te onderzoeken of de dynamiek van kernlichaampjes inderdaad beperkt wordt door de dichtheid van chromatine zijn cellen blootgesteld aan de stof MMS. Als gevolg hiervan blijkt de dynamiek van kernlichaampjes enorm toe te nemen zonder dat er aanwijzingen zijn dat de dynamiek van chromatine toeneemt. De kernlichaampjes blijken los te komen van hun chromatine omgeving en daarna door de kern te bewegen. Uit deze observaties kan geconcludeerd worden dat de kernlichaampjes door hun associatie met chromatine sterk in hun beweging beperkt worden.



## Curriculum vitae

Anneke Brouwer was born in Amsterdam on June 20<sup>th</sup>, 1976. From 1988 until 1995 she attended secondary school, VWO, Montessori Lyceum 'Herman Jordan', Zeist. In 1996 she commenced the study Chemistry at the Utrecht University. In 1998 she started the study Biology at the Utrecht University, and obtained a M.Sc. degree in Biology in 2003. Her first research internship was a psychophysics study at the Functional Neurobiology Group group at the Utrecht University, concerning the neural basis of motion detection in cats with Prof. dr. Wim A. van de Grind and Dr. Martin J.M. Lankheet. She completed her second research internship in the Cinvestav Institute in Irapuato, Mexico, investigating the synergy of two plant viruses infecting *C. papaya* at the molecular level, under the supervision of Dr. Laura S. Rosales. From Januari 2004 until Februari 2009 Anneke Brouwer was employed by the Leiden University as a PhD student at the Nuclear Organization and Gene Function group, Department of Molecular Cell Biology, Leiden University Medical Center, where the research presented in this thesis was performed.

